



# RICTA

8<sup>th</sup> Iberian Meeting on  
Aerosol Science and Technology  
*A Coruña · June 26<sup>th</sup>-28<sup>th</sup> 2024*

## ORGANIZERS:



UNIVERSIDADE DA CORUÑA



INSTITUTO UNIVERSITARIO DE  
**MEDIO AMBIENTE**  
UNIVERSIDADE DA CORUÑA



Química Analítica Aplicada Research Group  
UNIVERSIDADE DA CORUÑA

## COLLABORATORS:



Fundación  
UNIVERSIDADE DA CORUÑA



Asociación Española de  
Ciencia y Tecnología de Aerosoles

*RICTA2024*

**8<sup>th</sup> Iberian Meeting on Aerosol Science and Technology**

A Coruña

June 26<sup>th</sup>-28<sup>th</sup> 2024

Coordination:

Purificación López Mahía  
Soledad Muniategui Lorenzo

Conference co-funded by the Vice-rectorate for Research and Transference of the  
University of A Coruña (UDC)

## **RICTA2024: 8<sup>th</sup> Iberian Meeting on Aerosol Science and Technology**

ORGANIZACIÓN: Purificación López Mahía, Soledad Muniategui Lorenzo, Elia Alonso Rodríguez, María Elisa Beceiro González, Alatzne Carlosena Zubieta, Jose Manuel Andrade Garda, Rosa Soto Ferreiro, M<sup>a</sup> Isabel Turnes Carou, Jorge Moreda Piñeiro, M<sup>a</sup> José González Castro, M<sup>a</sup> del Carmen Prieto Blanco, María Piñeiro Iglesias e Javier Andrade Garda

COLECCIÓN: Cursos, congresos e simposios, CCS-162

DOI: <https://doi.org/10.17979/spudc.000035>

HANDLE (URL DO RUC): <http://hdl.handle.net/2183/36875>

EDITA: Servizo de Publicacións. Universidade da Coruña.

<<http://www.udc.gal/publicacions>>

CÓMO CITAR: López-Mahía, P., Muniategui-Lorenzo, S. (Coords.). *RICTA2024: 8th Iberian Meeting on Aerosol Science and Technology*. Book of abstracts. Universidade da Coruña. University Press, 2024

DESEÑO E MAQUETACIÓN: María Piñeiro Iglesias e Javier Andrade Garda

© do logo de RICTA2024, Javier Terán Baamonde

© dos textos, os seus autores

© das imaxes, os seus autores

© 2024 da edición, Universidade da Coruña



Esta obra publícase baixo unha licenza Creative Commons Atribución-NonComercial-Compartirlgual 4.0 Internacional (CC BY-NC-SA 4.0)

## INDEX

Organizers and Collaborators	2
Scientific Committee	3
Organizing Committee	3
Programme	4
Section 1. Plenary Speakers	10
Section 2. Invited Keynote Speakers	17
Section 3. Oral Session I. Wednesday, June 26 <sup>th</sup> 11:45-13:15	22
Section 4. Oral Session II. Wednesday, June 26 <sup>th</sup> 14:45-16:30	29
Section 5. Oral Session III. Thursday, June 27 <sup>th</sup> 10:00-11:00	35
Section 6. Oral Session IV. Thursday, June 27 <sup>th</sup> 11:45-13:15	40
Section 7. Oral Session V. Thursday, June 27 <sup>th</sup> 14:45-16:45	47
Section 8. Oral Session VI. Friday, June 28 <sup>th</sup> 10:30-11:30	53
Section 9. Oral Session VII. Friday, June 28 <sup>th</sup> 12:00-13:00	58
Section 10. Posters	61

## Organizers and Collaborators



# RICTA

8<sup>th</sup> Iberian Meeting on  
Aerosol Science and Technology  
A Coruña · June 26<sup>th</sup>-28<sup>th</sup> 2024

### VENUE:

Higher Technical University College of Maritime and Naval Machines, University of A Coruña (UDC)

### ORGANIZERS:



UNIVERSIDADE DA CORUÑA



INSTITUTO UNIVERSITARIO DE  
MEDIO AMBIENTE  
UNIVERSIDADE DA CORUÑA



Química Analítica Aplicada Research Group  
UNIVERSIDADE DA CORUÑA

### IN COOPERATION WITH:



Fundación  
UNIVERSIDADE DA CORUÑA



Asociación Española de  
Ciencia y Tecnología de los Aerosoles

### SPONSORS (alphabetical order):

Aerospec

 **Cambustion**



 Grupo Álava



**MCV**  
AIR QUALITY AND  
ATMOSPHERIC CONTROL



**SEQUOPRO**  
GRUPO DILUS



Sunset  
Laboratory Inc.



Técnicas de Control y Análisis, S.A.



© Knowledge  
Beyond  
Measure.

### COLLABORATORS (alphabetical order):



Concello da Coruña



Deputación  
DA CORUÑA



XUNTA  
DE GALICIA

## Scientific Committee

Lucas Alados, University of Granada (UGR)  
Susana Marta Almeida, Instituto Superior Técnico, Universidade de Lisboa (ULisboa)  
Andrés Alastuey, IDAEA-CSIC  
Manuel Alonso, CNIM-CSIC, Madrid  
Célia Alves, CESAM-UA  
Manuel Arias-Zugasti, UNED, Madrid  
Begoña Artiñano, CIEMAT  
Miguel A. Barrero, UPV/EHU, Donostia-San Sebastián  
Jordina Belmonte Sole, Autonomous University of Barcelona (UAB)  
Daniele Bortoli, University of Évora (UÉ-Portugal)  
Victoria E. Cachorro, University of Valladolid (UVA)  
Ana I. Calvo, University of León (ULE)  
Nuno Canha, Instituto Superior Técnico, Universidade de Lisboa (ULisboa)  
José L. Castillo, UNED  
Mário Cerqueira, CESAM-UA  
Maria João Costa, University of Évora (UÉ)  
Jesús de la Rosa, University of Huelva (UHU)  
Paulo Fialho, University of the Azores (UAc)  
José A. Garcia Orza, Miguel Hernández University of Elche (UMH)  
Pedro L. García Ybarra, UNED  
Francisco Gómez Moreno, CIEMAT  
Francisco Higuera, Polytechnic University of Madrid (UPM)  
Purificación López Mahía, University of A Coruña (UDC)  
Ignacio G. Loscertales, University of Málaga (UMA)  
Vânia Martins, Instituto Superior Técnico, Universidade de Lisboa (ULisboa)  
Luis Modesto, University of Seville (USE)  
José María Montanero, University of Extremadura (UEx)  
Teresa Moreno, IDAEA-CSIC  
Soledad Muniategui Lorenzo, University of A Coruña (UDC)  
Francisco José Olmo, University of Granada (UGR)  
Ismael K. Ortega, ONERA, Palaiseau (France)  
Casimiro Pio, CESAM-UA  
Xavier Querol, IDAEA-CSIC  
Sergio Rodríguez, IPNA-CSIC  
Jesús Rodríguez Maroto, CIEMAT  
Joan Rosell, Rovira i Virgili University (URV)  
Ana Maria Silva, University of Évora (UÉ)  
Mar Viana, IDAEA-CSIC

## Organizing Committee

Purificación López Mahía, chair  
Soledad Muniategui Lorenzo, chair  
Elia Alonso Rodríguez  
María Elisa Beceiro González  
Alatzne Carlosena Zubieta  
Jose Manuel Andrade Garda  
Rosa Soto Ferreiro  
M<sup>ª</sup> Isabel Turnes Carou  
Jorge Moreda Piñeiro  
M<sup>ª</sup> José González Castro  
M<sup>ª</sup> del Carmen Prieto Blanco  
María Piñeiro Iglesias  
Javier Andrade Garda  
In cooperation with researchers, technicians and administrative staff of QANAP research group and IUMA

# Programme

June 26<sup>th</sup>, 2024

**08:45-9:30 Registration**

**9:30-10:00 Opening Ceremony**

**10:00-11:00 Plenary Lecture.** Chair: F. J. Gómez Moreno

Electrospray Atomization and Deposition of Nanoparticle Suspensions. *J. L. Castillo*. UNED

**11:00-11:45 Coffee Break**

**11:45-13:15 Oral Session.** Chairs: F. J. Gómez Moreno, Sergio Rodríguez

11:45-12:00 Mechanisms of Aerosols Deposition in Turbulent Channel Flow. *P. L. Garcia-Ybarra*. UNED

12:00-12:15 Electrospays with Coulomb Explosions. *I. G. Loscertales*. UMA

12:15-12:30 Finite Taylor Cone: The Impact of the Electropray. *J. Rivero-Rodriguez*. UMA

12:30-12:45 Particle Charging by Electropray Nanodroplets. Measuring the Rate Constants. *F. Higuera*. UPM

12:45-13:00 Can Weekly Measurements Efficiently Identify Areas of High Concentrations of Radioactive Aerosols?. *E. Chham*. UMH

13:00-13:15 A Novel LIBS Imaging Method for the Determination of Atmospheric Particulate Matter in Remote Regions. *M. López Ochoa*. UCM

**13:15-14:45 Lunch Break**

**14:45-16:30 Invited Lecture and Oral Session.** Chairs: F. Higuera, P. L. García-Ybarra

14:45-15:15: Invited lecture: Environmental Evaluation of the Low Emissions Zone of A Coruña (ZBECOR). *G. Leira*. A Coruña Council

15:15-15:30 Analysis of Linear Regression Models to Study the Correlation Between Temperature Inversion and PM Levels in the City of Gijón (Northern Spain). *M. M. Domat Rodríguez*. UOV

15:30-15:45 Geochemical Characterization and Sources of Atmospheric Aerosols Deposited in the Ordesa y Monte Perdido National Park (PNOMP) in the Period 2016-2023, with Attention to Winter Periods. *J. Bandrés*. IPE-CSIC

15:45-16:00 Exceptional Aerosol Load Observed in the Arctic During Summer 2019. *S. Herrero-Anta*. UVA

16:00-16:15 Exploring Aerosol-Cloud-Precipitation Dynamics in the Iberian Peninsula Using the WRF-Chimere Coupled Model. *C. Gama*. CESAM-UA

16:15-16:30 Global Phenomenology of Cloud Condensation Nuclei and Particle Number Size Distribution: the DOE/ARM Network. *I. Zabala Arana*. UGR

**16:30-16:45 CAMBUSTION. Technical Tutorial**

**16:45-18:15 Coffee Break and Poster Session**

**18:15-18:45 AECyTA Meeting**

**19:30-20:15 Reception at A Coruña City Hall**

## June 27<sup>th</sup>, 2024

### 9:00-10:00 Plenary Lecture. Chair: X. Querol

What Comes In and What Goes Out: Emissions and Exposures in the Indoor Environment. *G. Bekö*. DTU (Denmark)

### 10:00-11:00 Oral Session. Chairs: X. Querol, J. A. García Orza

10:00-10:15 Exploring Gas and Particle-Phase Pollution from Rice Straw Burning in the Valencian Region. *E. Borrás García*. CEAM

10:15-10:30 On the Use of Thermodynamic Variables for Estimating Probability of African Dust Events Over Spanish Regions. *P. Salvador*. CIEMAT

10:30-10:45 Formation and Impact of a Winter Shamal Dust Storm over the Middle East. *S. Karbasi*. UMH

10:45-11:00 Emerging Extreme Dust Events Prompts Record Beating PM10 and PM2.5 Episodes in Spain. *S. Rodríguez*. IPNA-CSIC

### 11:00-11:45 Coffee Break

### 11:45-13:15 Oral Session. Chairs: A. Alastuey, J. de la Rosa

11:45-12:00 Defining the Mechanisms of Air Particles Toxicity Using In Vivo Stress Response Biomarkers. *F. Iñesta Vaquera*. UEX

12:00-12:15 Air Purification to Minimise Occupational Exposure to Incidental Nanoparticles in Industrial Settings. *V. San Félix Forner*. ITC-UJI

12:15-12:30 Indoor/Outdoor Microplastics Analysis by Thermogravimetric-Based Techniques: The Madrid's City Case of Study. *J. Cárdenas-Escudero*. UCM

12:30-12:45 Assessment of Microplastic Presence in Madrid's Atmospheric Environments: Indoor vs. Outdoor Air Samples. *S. Deylami*. UCM

12:45-13:00 Inhalation/Oral Bioaccessibility/Bioavailability of Pollutants Associated to Atmospheric Particulate Matter by Using Simulated Body Fluid. *J. Sánchez Piñero*. UDC

13:00-13:15 Structural Features and Health Effects of Water-Soluble Organic Matter from Atmospheric Fine Air Particulates. *A. S. Almeida*. CESAM-UA

### 13:15-13:30 Group Photo

### 13:30-14:45 Lunch Break

### 14:45-16:45 Invited Lecture and Oral Session. Chairs: C. Alves, M. Piñeiro-Iglesias

14:45-15:15: Invited lecture: Ionic and Mass Balance (IMB) - An Alternative Aerosol Source Apportionment Methodology. Comparative Advantages and Limitations. *C. Pio*. CESAM-UA

15:15-15:30 Sources of Deposited Aerosols over the Donaire Multi-Site Network in Spain. *J. Pey*. IPE-CSIC

15:30-15:45 Levels and Origin of Ultrafine Particles in a Complex Industrial States (La Rábida, SW SPAIN). *P. Pérez Vizcaíno*. UHU

15:45-16:00 Ultrafine Particles in Urban Europe: Results from RI-URBANS. *M. Garcia-Marlès*. IDAEA-CSIC

16:00-16:15 Biorelevant Soluble Trace Metals in the Atmospheric Aerosols Transported Observed over the Tropical North Atlantic at Cape Verde. *I. Belbachir*. IPNA-CSIC

16:15-16:30 eBC Concentration in Urban Europe: Results from RI-URBANS. *A. Alastuey*. IDAEA-CSIC

### 16:30-18:00 Coffee Break and Poster Session

### 20:30-23:30 Conference Dinner

**June 28<sup>th</sup>, 2024**

**9:30-10:30 Plenary Lecture organised by the Diputación de A Coruña (free admission for the general public).** Chair: P. López-Mahía

Advanced Air Quality Parameters in the New Air Quality Directive: The RI-URBANS/ACTRIS' View. *X. Querol*. IDAEA-CSIC

**10:30-11:30 Oral Session.** Chairs: V. Cachorro, P. López-Mahía

10:30-10:45 A Study of Black Carbon in Madrid: Sources, Trends and Characteristics. *E. Coz*. CIEMAT

10:45-11:00 Effect of Water Vapor on Pollen-Rich Atmospheric Layers Characterized by Fluorescence Raman Lidar. *F. Molero*. CIEMAT

11:00-11:15 Influence of Dust and NPF Events on CCN Concentration and Activation Properties Using Size-Resolved CCN Measurements. *A. Casans*. UGR

11:15-11:30 African Dust Ablation and Transport in the Extreme Mid-March 2022 Case. *J. A. García Orza*. UMH

**11:30-12:00 Coffee Break**

**12:00-13:00 Invited Lecture and Oral Session.** Chairs: J. Moreda, S. Muniategui

12:00-12:30: Invited lecture: How the New European Air Quality Directive affects Air Quality Assessment in Galicia. *N. Gallego*. Xunta de Galicia

12:30-12:45 Ammonia in Urban Europe: Results from RI-URBANS. *X. Querol*. IDAEA-CSIC

12:45-13:00 Multi-Instrumental Observations for the Analysis of Aerosol Optical Properties at the Cumbre Vieja Volcanic Eruption. *C. Herrero del Barrio*. UVA

**13:00-13:30 Closing and Awards Ceremony**

In the afternoon, there will be a tourist visit

## POSTERS

### 1 Aerosol Technology

1.1-1 Electro spray Deposition of Catalyst Inks on Polymer-Electrolyte Membranes for Hydrogen PEM Fuel-Cells. *P. L. Garcia-Ybarra*. UNED

1.7-1 Influence of the Air Mass Origin on Radioactivity Levels in Granada (Southern Spain). *E. Chham*. UMH

### 2 Atmospheric Aerosol Studies

2.1-1 Modelling the Secondary Particle Formation Contribution to PM<sub>10</sub> and PM<sub>2.5</sub> Concentrations at the Portuguese North Coast. *C. Gama*. CESAM-UA

2.1-2 Use of Photocatalytic Materials in an Urban Area: Analysis of Potential Impact on Mortality Attributable to NO<sub>2</sub> Pollution. *J. Fernández-Pampillón Cesteros*. CIEMAT

2.1-3 Relationship Between VOC and PM in Ambient Air at Madrid Barajas Airport. *E. Rojas*. CIEMAT

2.1-4 PM<sub>10</sub>-Bound-OCPs Evaluation in Madrid'S City: Air Quality Status and Carcinogenic Risk Assessment. *J. Cárdenas-Escudero*. UCM

2.1-5 Extreme Historic SO<sub>2</sub> Levels in an Industrial City (Huelva, SW Spain). Air Quality Implications. *J. de la Rosa*. UHU

2.1-6 2009-2023 Trend in the Chemical Composition of PM<sub>10</sub> in a Rural Area Influenced by Mine Activity in the District Mining of Riotinto, Spain. *A. M. Sánchez de la Campa Verdone*. UHU

2.1-7 The Composition of the Atmospheric Aerosols During the 2021 Eruption and Post-Eruption Periods at La Palma Island. *S. Rodríguez*. IPNA-CSIC

2.1-8 Impact of the Sierra de la Culebra Wildfire on the Air Quality of the City of León: Aerosol Characterization and Influence of Meteorological Conditions. *C. Gonçalves*. ULE

2.1-9 Published Research on Air Quality in Africa: A Result of Environmental Legislation and Research Infrastructure. *A. I. Calvo Gordaliza*. ULE

2.1-10 Real-Time Air Quality Monitoring Using RPAS. *A. I. Calvo Gordaliza*. ULE

2.1-11 Air Quality in León and Almería (Spain): Impact of Saharan Dust Intrusions in the North-South Context. *A. I. Calvo Gordaliza*. ULE

2.1-12 Saharan Dust Intrusions in Spain Between 2004 and 2023. *R. Fraile*. ULE

2.1-13 Characterization of Ultrafine Particles: Implementation of Particle Size Spectrometer at an Urban Background Station. *E. Yubero Funes*. UMH

2.1-14 Investigation on A New Biomonitor of Air PAHs. *F. de Nicola*. UniSannio (Italy)

2.1-15 PM<sub>2.5</sub> and Bioaerosols Emitted From Olive Mill Wastewater Evaporation Ponds: Assessment of Trace Elements and Microbial Diversity. *A. Rodríguez Cervantes*. UCLM

2.1-16 Indoor Air Quality in Elderly Care Centers: Chemical and Microbiological Pollutants. *S. Seseña*. UCLM

2.1-17 Analysis of Organic Pollutants Released From PM<sub>2.5</sub> in Simulated Biological Fluids: In-Vitro Inhalation Bioaccessibility and Bioavailability Estimation. *J. Sánchez Piñero*. UDC

2.1-18 In-Vitro Oral Bioavailability Method for Organic Target Pollutants in Atmospheric Particulate Matter (PM<sub>10</sub>). *N. Novo Quiza*. UDC

2.1-19 Oxidative Potential of the Inhalation Bioaccessible Fraction of PM<sub>10</sub> Samples. *N. Novo Quiza*. UDC

2.2-1 Trend Analysis of In-Situ and Column-Integrated Aerosol Radiative Properties in Spain. *E. Bazo*. UGR

2.2-2 African Desert Dust Influences on the Atlantic - Saharan Migration of the Skipjack and Other Tropical Tuna. *S. Rodríguez*. IPNA-CSIC

2.2-3 Implementation of a Synergy Strategy of Ground-Based Photometer and Spectrometer Observations Using GRASP Algorithm for Satellite Products Validation. *F. Rejano*. GRASP-SAS

2.3-1 Fluxes and Geochemical Characterisation of Saharan Dust Deposited in High-Mountain National Parks of the Iberian Peninsula. *J. Pey*. IPE-CSIC

2.3-2 The North African Regions Inducing Variability of Dust Composition in the Saharan Air Layer Identified During the Vardustsal Campaign at High Altitude in Cape Verde. *S. Rodríguez*. IPNA-CSIC

2.5-1 Development of the Granada Ice Nucleating Spectrometer Grains. *E. Bazo*. UGR

2.6-1 Study of the Effect of Synoptic Meteorological Patterns on Aerosol Concentration due to Boundary Layer Height Variations over Madrid from 2020 to 2023. *F. Molero*. CIEMAT

2.6-2 Changes in the Aerosol Optical Properties During Covid-19 Lockdown in Spain. *M. A. Obregón*. UEX

2.6-3 Is There a Relationship Between Surface and Column Aerosol Properties? *M. A. Obregón*. UEX

2.6-4 Is the Lorenz-Mie Theory Valid for Quasi-Spherical Particles? *G. Sánchez Jiménez*. UGR

2.6-5 Passive Monitoring of Airborne Microplastics in Northwest of Spain Using QC-LDIR and Comparison of Bulk Samplers. *A. López-Rosales*. UDC

2.6-6 Experimental Evidence of Inhibited Dehydration of an Inorganic Compound Caused by an Organic Coating. *G. Sánchez Jiménez*. UGR

2.6-7 Characterisation of the Wet and Dry Atmospheric Deposition Over León - NW Spain. *C. Gonçalves*. ULE

2.6-8 Assessing the Influence of Biomass Burning on Aerosol Optical Properties in a Rural Environment. *N. Galindo*. UMH

2.6-9 Methanol and Water-Soluble Organic Carbon in PM10 in the Iberian Peninsula. *E. Yubero Funes*. UMH

2.6-10 First High-Time-Resolution Carbonaceous Aerosol Speciation Using An Advanced TC-BC(II) Method In A Coruña, Spain. *M. Fernández-Amado*. UDC

2.6-11 CAECENET: Continuous and Automatic Columnar and Vertical Aerosol Properties. *C. Herrero del Barrio*. UVA

2.6-12 Analysis of Mineral Dust Episodes During A-Life Experiment in Cyprus. *D. Mateos*. UVA

2.6-13 Carbonaceous Fine Aerosol in an Urban-Industrial Site Near Lisbon, Before and After the COVID-19 Lockdown. *C. A. Gamelas*. ULisboa

2.10-1 Source Apportionment of PM2.5 at Multiple Sites in Algeria. *C. Alves*. CESAM-UA

2.10-2 Fine Aerosol European Overview in the Frame of Ri-URBANS. *M. Via*. UNG (Slovenia)

2.10-3 Spatio-Temporal Distribution of PM2.5 Emissions in Mozambique. *M. M. Correia Marques*. UTAD

2.11-1 Evolution of the Number of Nucleation Events in an Urban Background Site. *F. J. Gómez-Moreno*. CIEMAT

2.11-2 Nucleation and Ultrafine Particles Observed During the 2021 Volcanic Eruption in La Palma Island. *J. López Darias*. IPNA-CSIC

### **3 Aerosol Measurement Techniques**

3.1-1 Intercomparison Between a Low-Cost MicroStation and Reference Equipment. *C. Alves*. CESAM-UA

3.1-2 Atmospheric Monitoring with a High-Performance Raman Lidar: Alhambra. *A. Casans*. UGR

3.5-1 Evaluation of a Low-Cost Sensor for EBC Monitoring in a Suburban Area With Low Concentrations. *M. Fernández-Amado*. UDC

### **4 Aerosols and Health**

4.1-1 Trends of Airborne Pollen Concentrations in Madrid (Spain) over 2001-2020. Influence of Synoptic Meteorological Patterns. *P. Salvador*. CIEMAT

4.2-1 Inhaled Particle Dosimetry Modelling in Kindergarten And School Rooms: MPPD Versus ExDoM2. *C. Alves*. CESAM-UA

4.2-2 Statistical Quantification of PM10-Bound Polycyclic Aromatic Hydrocarbons in Ambient Air Near the Rio Tinto Mine (Southwest Spain). *E. Lorenzo*. UHU

4.2-3 PM10-Bacterial Infection Interaction in A-549 Cells: A One Health Perspective. *A. I. Calvo Gordaliza*. ULE

4.2-4 Exposure Assessment of 3D Printing of PLA with Graphene Filaments Under EN-17058:2018. *M. Domat Rodríguez*. UOV

4.2-5 Characterization of Personal Exposure to Particulate Matter Oxidative Potential in the Santander Bay (Northern Spain). *I. Fernández-Olmo*. UCN

4.3-1 The Impact of PM10 Components on the Oxidative Potential at a Rural Background Site in Southeastern Spain. *N. Galindo*. UMH

4.4-1 Chemical Profiles of PM10 in Indoor and Outdoor Air of a Charcoal-Grilled Chicken Restaurant. *C. Alves*. CESAM-UA

4.4-2 Assessment of Black Carbon Exposure and Source Apportionment in Sleeping Environments of Lisbon Dwellings. *C. A. Gamelas*. ULisboa

4.4-3 Assessment of Fine Aerosol Exposure in Sleeping Environments of Lisbon Dwellings. *S. L. Méndez Hoyos*. ULisboa

4.4-4 Levels of PM-Bound Organic Compounds from Residential Coal Combustion. *A. I. Calvo Gordaliza*. ULE

*RICTA2024*

## **8<sup>th</sup> Iberian Meeting on Aerosol Science and Technology**



## **Section 1. Plenary Speakers**

## ELECTROSPRAY ATOMIZATION AND DEPOSITION OF NANOPARTICLE SUSPENSIONS

J.L. Castillo, S. Martín, A. García-Corral and P.L. García-Ybarra

Dept. Física Matemática y de Fluidos, Facultad de Ciencias, UNED, Las Rozas, Madrid 28232, Spain

Keywords: Electrospray, Aerosol deposits, Surface coatings

Presenting author email: jcastillo@ccia.uned.es

Aerosols can be used to prepare new materials with upgraded capabilities. Thus, the controlled formation and further deposition of aerosol particles leads to the generation of granular deposits with prescribed particle sizes, porosity, distribution of pore sizes and surface roughness. These features render these layers suitable as selective coatings, gas sensors, or catalytic materials (Martín *et al.*, 2013, 2019).

Numerical simulations and experiments have been performed to study the structure of a deposit being formed by the continuous arrival of aerosol particles. The deposit morphology depends on the dynamics of the particles when approaching the deposit and on the sticking properties of the new arriving particles.

Using Monte Carlo simulations, deposits of monodisperse aerosol particles have been grown assuming perfectly sticking particles. In the simulations, the particle dynamics is characterized by a mean particle velocity,  $U$  (due to external fields or to any phoretic motion as thermophoresis or photophoresis) and a random motion (either a Brownian motion or the influence of a random field) with a characteristic diffusion coefficient  $D$ . The relative importance of these two contributions to the particle motion is given by the Peclet number,  $Pe \equiv Ua/D$ , where  $a$  is the characteristic length (the particle diameter).

Deposits formed by particles arriving with a high  $Pe$  value (ballistic deposition) are rather dense and compact whereas when the random motion dominates (diffusion limited deposition), the deposits are fractal-like with a highly branched structure and large porosity. Tuning the value of  $Pe$ , deposits with tailored morphologies (mean density and surface roughness) can be prepared (Castillo *et al.*, 2018).

Moreover, experiments have been conducted for the electrohydrodynamic atomization (electrospraying) of a liquid suspension of (50 nm Vulcan XC-72R Carbon) nanoparticles in an electrically conducting volatile liquid (ethanol). The liquid is pumped at a constant flow rate ( $Q$ ) through a metallic needle with a collector plate facing the needle. The needle and the plate separated a distance  $h$  are set to different voltages ( $V_n$  and  $V_p$ , respectively) using two different high voltage power supplies. For a given suspension composition, these parameters ( $Q$ ,  $h$ ,  $V_n$ , and  $V_p$ ) control the electrospray and thus the properties of the formed aerosol particles and their dynamics to arrive to the collector and form the deposit. To achieve a steady spray emission, the

electrospray must stay at the so-called cone-jet mode, with a Taylor cone formed at the needle exit and a thin jet emerging at the cone apex which adjust the ejected liquid rate to the prescribed flow rate. The liquid jet breaks up and forms a cloud of almost monodisperse and charged liquid droplets. These droplets driven by the externally imposed electrical field are drift towards the collector evaporating during their flight. For short needle to plate distances, the droplets do not have enough time to evaporate before reaching the collector forming an unwanted washed-like deposit. However, for a proper range of  $h$ , the solvent evaporates completely leaving a solid residue which is still charged and attach to the substrate forming the granular deposit. A stable cone-jet with a continuous generation of dry nanoparticles can be achieved by a proper selection of the electrospray working conditions.

The morphology of the deposits was examined using a scanning electron microscopy (SEM, Hitachi S-3000N). Columnar branched deposits with fractal-like structure can be formed (Figure 1). These deposits have a structure based on clusters of nanoparticles formed by the attachment at the deposit of agglomerates coming from different electrospray droplets. The agglomerate size (of the order of 10  $\mu\text{m}$ ) increases with the flow rate, while the surface roughness decreases as the agglomerate size is augmented. The mean density of these deposits also increases as the flow rate increases (as expected from the numerical simulations as larger particles and higher flow rates corresponds to higher values of the Peclet number).

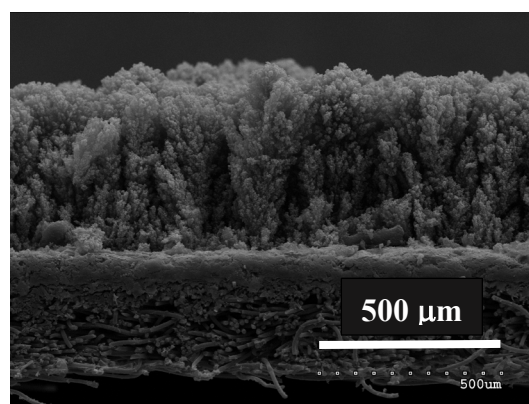


Fig. 1. SEM side view of a deposit generated by electro spraying carbon nanoparticles on a carbon cloth substrate (from Castillo *et al.*, 2018).

To test the performance of granular deposits generated by this electrospray technique, as electrodes for proton-exchange membrane fuel cells [Polymer Electrolyte Membrane (PEM) Fuel Cells (PEMFCs)], the simplest suspensions of pure carbon nanoparticles were replaced by catalytic inks of Pt/C powders (Vulcan XC-72R nanoparticles with Pt dots adhered on their surface). PEMFCs are based on two different electrodes (an anode and a cathode feed with H<sub>2</sub>/air or H<sub>2</sub>/O<sub>2</sub>, respectively) on both sides of a polymeric membrane which avoids the mixing of the electrochemically reactant gases but allows the transfer of protons across the membrane. The set of the two electrodes (with their respective gas diffusion layers to distribute the gases towards the catalytic sites in the electrodes) and the polymeric membrane is known as a MEA (Membrane Electrode Assemble). MEAs formed with different type of nanoparticles (different Pt mass percentages on the carbon support, ranging from 10% wt up to 60% wt.) were tested to analyze the fuel cell performance as a function of the Pt/C mass ratio and on the deposit growing conditions. In low temperature polymer electrolyte membrane fuel cells (LT-PEMFCs) feed with dry H<sub>2</sub> and O<sub>2</sub> on each electrode and working at 3.4 bar of gauge pressure and 70 °C, catalytic layers with Pt loadings as low as 0.01 mg<sub>Pt</sub> cm<sup>-2</sup> may achieve power densities around 600 mW cm<sup>-2</sup> that corresponds to an overall specific power of 30 kW g<sub>Pt</sub><sup>-1</sup> (Martin *et al*, 2013). These figures are indicative of the high performance of these electrosprayed electrodes.

Moreover, recent measurements for high temperature polymer electrolyte membrane fuel cells (HT-PEMFCs) have shown that when the Pt load increases (*i.e.*, the thickness of the catalytic layer increases) the fuel cell performance (measured by its power density at a fixed voltage, 0.6 V) increases initially (due to the increase in the number of active sites) up to a maximum value limited by the mass transport of oxygen and ohmic, associated to an optimum Pt-loading (different for each Pt/C ratio), Martin *et al*, 2024.

AG-C acknowledges the support by a “Margarita Salas grant” (REGAGE21e00017738309) provided by the Spanish Ministry of Universities in the framework of the Next Generation EU program. Work supported by Project PID2022-139082NB-C55 granted by MCIN/AEI/10.13039/501100011033/ FEDER, UE.

Castillo, J.L., Martín, S., Rodríguez-Pérez, D., Higuera, F.J. and García-Ybarra, P.L. (2018) *J. Aerosol Sci.* **125**, 148-163.

Martin, S., Garcia-Ybarra, P.L. and Castillo. J.L. (2024) *Int. J. of Hydrogen Energy*, submitted.

Martin, S., Jensen, J.O., Li, Q., Garcia-Ybarra, P.L. and Castillo, J.L. (2019) *Int. J. of Hydrogen Energy.* **44**, 28273-28282.

Martín, S., Martínez-Vázquez, B., García-Ybarra, P.L. and Castillo, J.L. (2013) *J. Power Sources.* **229**, 179-184.

## WHAT COMES IN AND WHAT GOES OUT: EMISSIONS AND EXPOSURES IN THE INDOOR ENVIRONMENT

G. Bekö<sup>1</sup>

<sup>1</sup>Department of Environmental and Resource Engineering, Technical University of Denmark, Kongens Lyngby, 2800, Denmark

Presenting author email: gabe@dtu.dk

### Summary

Building occupants and their activities constitute a major source of indoor air pollution. This paper and plenary talk will briefly summarize the most recent findings regarding particulate and chemical emissions in buildings, with focus on sources related to the occupant and occupant behavior. It will also elaborate the implications for exposure, associated exposure pathways and potential health effects.

### Ultrafine particles indoors

We spend most of our time in indoor environment. Our exposure to indoor and outdoor pollutants occurs primarily indoors. As outdoor particles penetrate indoors, their properties change. But indoor sources also contribute significantly to indoor exposures. For example, a study found that occupant-related source events contributed substantially to the residential daily exposure to ultrafine particles (UFP). Events contributing the most to the total residential daily exposure were candle burning and cooking. In homes where candle burning took place, more than half of the residential daily exposure was attributable to this activity. Cooking was responsible for a third of the total residential exposure in the homes where cooking occurred. Elevated particle concentrations persisted for several hours after a source event ceased (Bekö et al., 2013).

### Indoor air chemistry

Indoor air also contains a large range of chemical pollutants. Volatile organic compounds (VOC) and semivolatile organic compounds (SVOC) such as phthalates, flame retardants, pesticides can contaminate the air and indoor surfaces. Chemical transformations, such as ozone-initiated reactions occurring on surfaces, can generate reaction products that can be more harmful than their precursors. In recent years, increasing attention has been paid to indoor air chemistry, including the effect humans have on it. Primary emissions from humans, especially via exhaled breath, have been studied for a long time with the purpose to identify disease biomarkers and advance disease diagnostics. But it is only recently that the scientific community began to appreciate the significant role occupants play in indoor air chemistry. Our understanding of this field of science is now rapidly improving with the development and availability of novel measurement techniques and instrumentation. New methodologies allow us to revisit some of the research

questions that have been puzzling scientists for decades, such as the personal and environmental factors that may influence human emission (e.g., diet, stress level, hygiene habits, age, sex, health condition, activity level, personal care products, clothing, and its laundering and storage).

Human emissions can undergo chemical transformation and result in a suite of new compounds in indoor air. These reactions occur in the presence of humans as well as in previously occupied spaces, as skin oils are transferred to surfaces through touching, and via skin flakes (squames) and their constituents shed by people in a process called desquamation. Thus, humans contribute to the organic films on indoor surfaces. Settled dust in occupied settings also contains skin flakes and their associated skin oils, resulting in reactions between dust and ozone. Squalene is responsible for about 10% fraction of skin surface lipids by weight and for about 50% of the unsaturated carbon bonds in skin surface lipids. Ozonolysis of skin lipids is an important source of indoor VOCs and a sink for indoor ozone (Weschler, 2016).

Measurements of total OH reactivity (total oxidation capacity) account for all reactive organic species in the air. Comparing it to the summed reactivity anticipated from known individual trace gases reveals whether all relevant species are being measured. For breath emissions alone, the total OH reactivity without ozone is similar to that with ozone present. For dermal emissions alone, the total OH reactivity without ozone is low. It increases significantly when ozone is present (Wang et al., 2021).

Occupant related chemical reactions may contribute to indoor concentrations of ultrafine particles, as the reaction products condense on existing particles or nucleate to form new particles. As SVOCs partition between the gas-phase and airborne particles, changes in SOA levels caused by the presence of occupants alter the ratio of particle-phase to gas-phase SVOC, which has consequences for indoor air chemistry. Skin oil-ozone reactions can themselves be a source of SOA. Yang et al. (2021) detected nanocluster aerosols (NCA, particles <3 nm) in an occupied climate controlled chamber only when ozone was present. NCA emissions were dependent on clothing coverage, occupant age, air temperature, and humidity.

Submicron particles were also shown to be generated during ozone reactions with skin-oil-soiled t-shirts; higher particle production occurs at higher ozone levels and when the T-shirts are worn for a longer period of time (Rai et al. 2013).

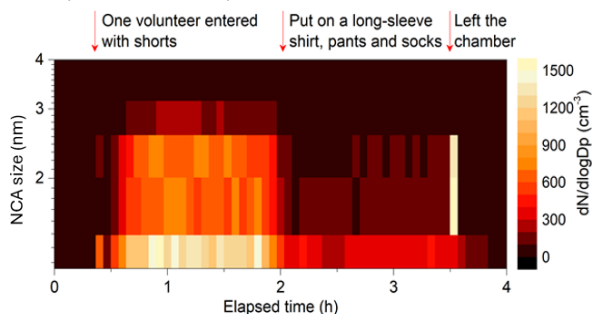


Fig. 1. Influence of clothing on NCA emissions from ozone-human chemistry (Yang et al., 2021).

### Occupants as sinks, indoor exposure

Human occupancy can also meaningfully alter the air concentrations of some volatile and semi-volatile organic compounds, for example, by removal via dust ingestion, inhalation, and dermal absorption. Some chemicals removed by the presence of occupants are known to participate in indoor chemistry, and their removal by occupancy therefore reduces product concentrations. Occupancy may reduce indoor concentrations of certain chemicals by up to 60% (Weschler, 2016). Human breath was shown to be a source for some compounds and a sink for others (He et al., 2019).

Uptake of certain chemicals through skin directly from air has been shown to be a meaningful route of exposure. The extent of dermal uptake from air has been previously studied for volatile organic compounds (VOC). This exposure pathway is often neglected in exposure assessments for SVOCs. Dermal uptake received attention with regards to contact transfer from contaminated surfaces. Modeling efforts however indicate that direct uptake of certain semivolatile organic compounds from air may occur. Experimental verification using phthalates, nicotine, and benzenophenone-3 has demonstrated that dermal uptake directly from air can be comparable to or larger than the corresponding intake from inhalation (Weschler et al., 2015; Bekö et al., 2019).

Some of the SVOCs present indoors may have adverse health effects or are categorized as potential endocrine-disrupting compounds. It has been suggested that the health effects of a chemical may depend on the pathway of exposure. Absorption, distribution, and elimination of a chemical in the body may differ between the various exposure pathways (Needham et al., 2007). Ingested compounds pass through the intestines and liver before entering the blood. Inhaled contaminants first pass through the lungs where they

may be transferred directly to capillary blood. Chemicals penetrating the skin can directly enter the blood. However, they are first absorbed at the surface of the stratum corneum, they diffuse through the cell layers, entering the viable epidermis, then the papillary dermis and then reaching the capillary. Therefore the half-life of contaminants for these routes are different. Moreover, for nominally comparable exposures, the resulting biologically effective dose to various organs can differ between exposure routes. However, studies that investigate the health consequences of SVOC uptake via a specific exposure route are lacking.

### References

- Bekö, G., Weschler, C.J., Wierzbicka, A., Karotki, D.G., Toftum, J., Loft, S., Clausen, G. (2013) Ultrafine particles: Exposure and source apportionment in 56 Danish homes. *Environmental Science and Technology*, 47, 10240-10248.
- Bekö, G., Morrison, G., Weschler, C.J., Koch, H.M., Pälme, C., Salthammer, T., Schripp, T., Eftekhari, A., Toftum, J., Clausen, G. (2018) Dermal uptake of nicotine from air and clothing: Experimental verification. *Indoor Air*, 28, 247-257.
- He, J., Sun, X., Yang, X. (2019) Human respiratory system as sink for volatile organic compounds: evidence from field measurements. *Indoor Air*, 29, 968-978.
- Needham, L.L., Calafat, A.M., Barr, D.B. (2007) Uses and issues of biomonitoring. *International Journal of Hygiene and Environmental Health*, 210, 229-238.
- Rai, A.C., Guo, B., Lin, C.H., Zhang, J., Pei, J., Chen, Q. (2013) Ozone reaction with clothing and its initiated particle generation in an environmental chamber. *Atmospheric Environment*, 77, 885-892.
- Wang, N., Zannoni, N., Ernle, L., Bekö, G., Wargocki, P., Li, M., Weschler, C.J., Williams, J. (2021) Total OH reactivity of emissions from humans: in situ measurement and budget analysis. *Environmental Science and Technology*, 55, 149-159.
- Weschler, C.J. (2016) Roles of the human occupant in indoor chemistry. *Indoor Air*, 26, 6-24.
- Weschler, C.J., Bekö, G., Koch, H.M., Salthammer, T., Schripp, T., Toftum, J., Clausen, G. (2015) Transdermal uptake of diethyl phthalate and di(n-butyl) phthalate directly from air: Experimental verification. *Environmental Health Perspectives*, 123, 10, 928-934.
- Yang, S., Licina, D., Weschler, C.J., Wang, N., Zannoni, N., Li, M., Vanhanen, J., Langer, S., Wargocki, P., Williams, J., Bekö, G. (2021) Ozone initiates human-derived emission of nanocluster aerosols. *Environmental Science and Technology*, 55, 14536-14545.

## ADVANCED AIR QUALITY PARAMETERS IN THE NEW AIR QUALITY DIRECTIVE: THE RI-URBANS/ACTRIS' VIEW

X. Querol<sup>1</sup>, A. Alastuey<sup>1</sup>, M. Pandolfi<sup>1</sup>, T. Petäjä<sup>2</sup>, M. Garcia-Marlès<sup>1,3</sup>, X. Liu<sup>1</sup>, R. Lara<sup>1</sup>, M. Savadkoobi<sup>1</sup>, T. Salameh<sup>4</sup>, M. Dufresne<sup>4</sup>, S. Sauvage<sup>4</sup>, G. Uzu<sup>5</sup>, on behalf of the RI-URBANS team

<sup>1</sup>Institute of Environmental Assessment and Water Research (IDAEA-CSIC), 08034 Barcelona, Spain

<sup>2</sup>Institute for Atmospheric and Earth System Research, Dep. Physics, 00014 University of Helsinki, Finland

<sup>3</sup>Department of Applied Physics-Meteorology, University of Barcelona, Barcelona, 08028, Spain

<sup>4</sup>Centre for Energy and Environment, Institut Mines-Télécom, Université de Lille, 59000, Lille, France

<sup>5</sup>Institut des Géosciences de l'Environnement, Université Grenoble Alpes, 38400 St Martin d'Hères, France

Keywords: Atmospheric pollutants, ultrafine particles, black carbon, ammonia

Presenting author email: xavier.querol@idaea.csic.es

The first European (air quality) AQ Daughter Directive (1999/30/CE) requested that from 01/01/2010, the 2005-inforce 40  $\mu\text{g}/\text{m}^3$  annual limit value for atmospheric particulate matter (PM) with a size equal or finer than 10  $\mu\text{m}$  (PM<sub>10</sub>) would be replaced by the existing equivalent World Health Organization (WHO) 2005 guideline value (20  $\mu\text{g}/\text{m}^3$ , WHO, 2005), following the ratification by member states (EC 1999; Annex III). The 2008/50/CE Directive derogated this part of 1999/30/EC, set an annual standard for PM equal or finer than 2.5  $\mu\text{m}$  (PM<sub>2.5</sub>) of 25  $\mu\text{g}/\text{m}^3$ , and postponed to 2013 reducing the gap between these standards and the WHO guidelines (EC 2008); and in 2014 the postponement was extended to 2020. WHO (2021) updated the AQ guidelines according the new scientific evidences and reduced the PM<sub>10</sub> and PM<sub>2.5</sub> guidelines from 20 to 15  $\mu\text{g}/\text{m}^3$  and 10 to 5  $\mu\text{g}/\text{m}^3$ , respectively. Thus, the WHO changed the AQ guidelines before the promised replacement of the AQ standards by these. In 2022, as expected for a long time, the European Commission proposed a draft for a new AQ Directive (EC, 2023) in which, for many pollutants, the 2005 WHO's AQ guidelines (WHO, 2005) are proposed as EU AQ standards, to be in force in 2030 (thus, for PM<sub>10</sub>, 20 years later than proposed by 1999/30/CE); while the ambition of the WHO (2021) guidelines is postponed for subsequent revisions.

Despite the loss of ambition in the AQ standards along the last decades, the AQ policies implemented at European, national, regional and local scales have been very positive, and levels of key AQ pollutants have been drastically reduced since late 1990s (less since 2010). In specific cases, such as benzo(a)pyrene (B(a)P), ozone (O<sub>3</sub>) and ammonia (NH<sub>3</sub>), the abatement is much lighter, or even, in some cases, increases are recorded.

Focusing on atmospheric PM (or aerosols, used as an equivalent), a major abatement of ambient concentrations has been achieved over the last decade due to the decline of primary PM emissions. This caused a relative increase in secondary components (formed into the atmosphere from gaseous precursors) in ambient PM<sub>2.5</sub> and PM<sub>10</sub>. Thus, currently around 70% of PM<sub>2.5</sub> in the European urban background is made of secondary inorganic and organic aerosols (SIA and SOA, Amato et al., 2016).

In addition to stricter AQ guideline values, WHO (2021) guidelines suggest the implementation of harmonised measurements of advanced AQ pollutants to provide data for further epidemiological analyses to obtain evidences to include some of these as criteria pollutants in further guideline revisions.

In 2021, the RI-URBANS project (Research Infrastructures Services Reinforcing Air Quality Monitoring Capacities in European Urban & Industrial AreaS, supported by EC-H2020-Green Deal) started, with a major goal of supporting the identification of major advanced AQ parameters and the implementation of their measurement across Europe. This is intended in collaboration with ACTRIS (Aerosol, Clouds and Trace Gases Research Infrastructure) and the AQ monitoring networks.

The proposal for a new AQ Directive (EC, 2023), in addition of reducing the gap between the AQ standards and the WHO guidelines, and following the recommendations by WHO (2021) requires (or recommends in some cases) the implementation of measurements of these advanced AQ measurements. The supporting documents of the EC (2023) refer to RI-URBANS and ACTRIS as relevant sources of information to include these AQ advanced parameters in the new Directive (EC, 2022, page 16). These new parameters will not only provide data for further epidemiological analyses to evaluate the implementation of AQ standards in further revisions of the legislation, but also obtain an advanced AQ assessment for the application of cost-effective AQ policies in Europe.

In addition to some criteria pollutants, such as PM<sub>10</sub>, PM<sub>2.5</sub>, NO<sub>2</sub>, O<sub>3</sub>, As, Cd, Ni, Pb, and B(a)P, the advanced parameters to be measured in AQ supersites, as included in Article 10 (and Annex VII) of the proposal for a new AQ Directive, are: Ultrafine particles (UFP) and particle number size distributions (PNSD), black carbon (BC), NH<sub>3</sub>, polycyclic aromatic hydrocarbons (PAHs), and PM<sub>2.5</sub> speciation. From these PNSD is requested for urban supersites and recommended for the rural ones, while the opposite for NH<sub>3</sub>. Moreover, for rural supersites, measurements of the total deposition fluxes of B(a)P, PAHs, As, Cd, Ni, Pb and Hg, and concentrations of ambient gaseous Hg, are also requested, and recommended for urban

supersites. Finally, measurements of oxidative potential (OP) of PM, levoglucosan concentrations in PM, ambient particulate and gaseous Hg<sup>2+</sup> and nitric acid (HNO<sub>3</sub>) are also recommended. At least 1 urban background supersite per 10 million inhabitants, and 1 rural background supersite per each 100000 km<sup>2</sup> have to be implemented by each member state.

Furthermore, Article 12 (and annex VII) of the proposed Directive recommends measuring ambient concentrations of 43 volatile organic compounds (VOCs) precursors of O<sub>3</sub> and/or SOA. These include 11 alkanes, 9 aromatic hydrocarbons, 9 alkenes, 5 terpenes, 3 ketones, 3 aldehydes, 2 alcohols, and 1 alkyne.

Article 9 also requires measuring total concentrations of UFP in locations where concentrations of these are expected to be high (hotspots, such as traffic and industrial sites, harbours, airports, among others). At least 1 measurement site per each 5 million inhabitants have to be implemented in each member state.

The RI-URBANS project (<https://riurbans.eu/>), together with ACTRIS, is producing guidelines for a number of service tools (STs) to support the AQ monitoring networks to implement the measurements of many of the above advanced parameters, until reference methods are provided. Furthermore, RI-URBANS compiled long datasets of UFP, PNSD, BC, OP, NH<sub>3</sub>, VOCs, among others, and elaborated pan-European reports showing the added value of implementing these measurements. Furthermore, epidemiological evaluations are carried out for many of these using a pan-European approach.

This presentation summarises major findings obtained for i) Time and spatial variability, source apportionment and inter-annual trends of UFP and PNSD across urban Europe; ii) Idem for BC; iii) idem for NH<sub>3</sub>; iv) measurements and source apportion of OP of PM; v) measurements of VOCs in urban Europe. Furthermore, information on the guidance for measuring each parameter is supplied.

The global results show that:

- Due to the complexity of the implementation of some of the above measurements will require of an intensive collaboration between AQ monitoring networks and research teams and research infrastructures.
- There is a need for an urgent harmonisation of some of the measurements required. The degree of evolution of the instrumentation and protocols varies widely. While for UFP, PNSD, offline NH<sub>3</sub> and BC there are CEN standards and/or ACTRIS or EMEP guidelines, for other such as OP work needs to be carried out to reach the recommendation stage.
- Major sources of UFP and BC in urban areas is road traffic, but relevant contributions from photochemical nucleation, shipping and domestic emissions, might be relevant for UFP, and from domestic biomass burning for BC.

- For both UFP and BC a clear n to S and E Europe decreasing trend is evidenced, with concentrations being higher at traffic (TR) sites > urban background (UB) > suburban background (SUB) > regional background (RB).
- For NH<sub>3</sub>, two major regions are distinguished, those being in areas considered farming/agricultural hotspots (FAHs) and those out of these areas; with the average NH<sub>3</sub> concentrations of the first being 4-fold higher than in the second. Out of the FAHs, there is an industrial (IND) = TR > UB=SUB > RB gradient showing the relevance of urban NH<sub>3</sub> emissions. However, in the FAHs, concentrations decrease as the distance to specific farming/agricultural sources increase.
- The complexity of measuring the 43 VOCs recommended by the new Directive draft is shown and the added value for O<sub>3</sub> and SOA abatement supported with specific examples.
- Finally, an overview on OP methods and relevance is provided.

This work is supported by the European Commission (RI-URBANS contract n. 101036245).

Amato F. et al. (2016) AIRUSE-LIFE+: a harmonized PM speciation and source apportionment in five southern European cities. *Atmos Chem Phys*, 16, 5, 3289-3309.

EC (1999) Council Directive 1999/30/EC of 22/04/1999 relating to limit values for sulphur dioxide, nitrogen dioxide and oxides of nitrogen, particulate matter and lead in ambient air *Off J L* 163, 29/06/1999 41-60.

EC (2008) Directive 2008/50/EC of the European Parliament and of the Council of 21/05/2008 on ambient air quality and cleaner air for Europe. *Off J L*, 152, 11/06/2008, 1–44.

EC (2022) *Systematic assessment of monitoring of other air pollutants not covered under Directives 2004/107/EC and 2008/50/EC.* <https://op.europa.eu/en/publication-detail/-/publication/1c9b2b51-54dd-11ed-92ed-01aa75ed71a1/language-en>

EC (2023) *Proposal for a Directive of The European Parliament and of The Council on ambient air quality and cleaner air for Europe.* <https://data.consilium.europa.eu/doc/document/ST-15236-2023-INIT/en/pdf>

WHO (2005) *WHO air quality guidelines: Global update 2005.* <https://www.who.int/publications/i/item/WHO-SDE-PHE-OEH-06.02>

WHO (2021) *WHO global air quality guidelines: PM<sub>2.5</sub>, PM<sub>10</sub>, O<sub>3</sub>, NO<sub>2</sub>, SO<sub>2</sub> and CO,* <https://www.who.int/publications/i/item/9789240034228>

*RICTA2024*

## **8<sup>th</sup> Iberian Meeting on Aerosol Science and Technology**



## **Section 2. Invited Keynote Speakers**

## ENVIRONMENTAL EVALUATION OF THE LOW EMISSIONS ZONE OF A CORUÑA (ZBECOR)

A. Guillermo Leira Nogales

<sup>1</sup> Environmental Quality Section. Environment Area of the City Council of A Coruña

Keywords: Air quality, Environmental modelling, L.E.Z.

Presenting author email: g.leira@coruna.gal

The declaration of Low Emission Zones, regulated by Royal Decree 1052/2022, of December 27, requires the implementation of a series of indicators linked, mainly, to air quality, climate change, sustainable mobility, the environmental noise and energy efficiency of the territory subject to this protection figure. This forces municipalities with more than 50,000 inhabitants to deploy environmental evaluation methods beyond what is determined at least by sectoral legislation, particularly air and noise legislation. This is because data is required not only at the city level, as was the case with certain agglomerations, but also with territorial disaggregation of the necessary environmental information, to be able to make comparisons between the evolution of protected and unprotected sectors.



Fig. 1. A Coruña LEZ project

In this sense, the city of A Coruña began the deployment of its air quality monitoring network in 2004, currently made up of four of its own stations, in addition to one in collaboration with a local industry and those owned by the regional government (two urban and one industrial), all for a municipality of 37.8 km<sup>2</sup>.

This path through the field of environmental assessment has been reinforced in the last two years thanks to the Next Generation and EDUSI funds. Both sources of financing have allowed the development of avant-garde projects, which in other circumstances would have been impossible to execute by a municipality of our size, trying to optimize existing resources and complement them with others of enormous potential but only economically sustainable in the future. Among these projects, a very high-resolution air quality dispersion and prediction model stands out, which allows us to generate maps of the different pollutants throughout the territory every hour, with a 10 m mesh and a prediction time horizon of 48

hours, enabling the generation of alternative scenarios in which the corrective measures to be applied are taken into account. The model used is the GRAL, which is a Lagrangian model (Microphysics Graz Lagrangian Model), developed at the Graz University of Technology (Austria), connected to a traffic demand model.

The set formed by the air quality dispersion and prediction model together with the measurement stations, makes it possible to have information at every point in the city, whether or not they have a monitoring station, with high quality data thanks to the different validation alternatives currently available.

As a complementary and pioneering pilot project in Galician territory, a continuous measurement system for vehicle exhaust gases was installed on one of the main access roads to the city, with which the emissions of more than one hundred thousand vehicles have already been analyzed, with the aim of characterizing the circulating fleet from the point of view of their real contribution to air quality, in addition to allowing other types of educational uses, such as information campaigns at the service of citizens that allow minimizing the most polluting vehicles that circulate on our roads.

These projects make it possible to have the most advanced tools in the sustainable management of environmental quality at the service and monitoring of Low Emission Zones and other environmental protection figures with similar characteristics.

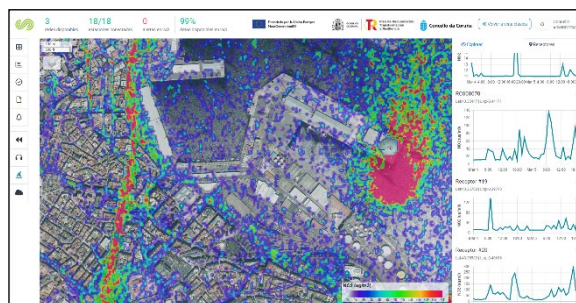


Fig. 2. GRAL high-resolution prediction model.

## IONIC AND MASS BALANCE (IMB) - AN ALTERNATIVE AEROSOL SOURCE APPORTIONMENT METHODOLOGY. COMPARATIVE ADVANTAGES AND LIMITATIONS

C. Pio<sup>1</sup>, C. A. Alves<sup>1</sup> and T.V. Nunes<sup>1</sup>

<sup>1</sup>CESAM and Department of Environment, University of Aveiro, Aveiro 3810-192 Portugal

Keywords: Ionic and Mass Balance; Source Apportionment; Methodology and applications  
casimiro@ua.pt

Source apportionment techniques, applied to analysed aerosol samples, are fundamental for the understanding and evaluation of aerosol sources and formation processes, permitting the development of correct strategies to combat and reduce atmospheric pollution.

No source apportionment technique is perfect and applicable to all environmental circumstances. Use of independent receptor models, in combination, permits more robust estimations of sources by mutually validating model's outputs.

Ionic and Mass Balance (IMB) is a source apportionment methodology independent from more common multivariate models, such as Positive Matrix Factorization (PMF). IMB is mostly based in balance comparisons between analysed compounds and total measured aerosol mass, or between analysed water-soluble anions and cations, considering that total aerosol mass is the sum of the aerosol constituents and that the aerosol anion and cation charges have to be equal for a neutralized mass. Mass balances have been frequently used in the past but mainly as a scrutinization methodology, or for partial fractions of the aerosol. Here, the IMB is developed to apportion all the aerosol mass, either, to sources, or formation processes. The method does not rely only on balance differences, but, depending on the local aerosol characteristics, also recurs to known source compositions and, or, to edge line relations between particulate components.

IMB can only be performed with success when, in the aerosol sample, water soluble inorganic ions, trace elements, organic and elementary carbon are analysed and quantified. In atmospheres with important biomass burning inputs, levoglucosan is also a necessary measurement. Considering that the method relies mostly on sequential and cumulative differentiation, analytical accuracy is fundamental for a correct predictive output.

Another essential condition for a successful application of IMB is a good understanding of aerosol processes by the user, in order to apply, adapt and interpret the partial and final results.

The sources of the aerosol are then evaluated sequentially, with an order that usually is the following:  
-Soil Dust (SD) mass is based in the analysis of Si, Al, Mn, Ti, etc., using an equation of the type:  $SD = F(2.14+Si+.89 Al+ \text{etc})$ , being the factor F dependent from the local, or regional soil composition.

-Sea Salt spray is evaluated with basis in  $Na^+$  and  $Mg^{2+}$ , after removing the ion amounts providing from soil dust. The composition of sea water and respective ratios can be used to reduce interferences from other sources such as soil or acidic attack, after emission. Unreacted (SS) and reacted ( $SIC_{ss}$ ) sea salt fractions can be then estimated.

- In urban and traffic influenced areas, with the help of edge lines, excess Fe and Ca, from soil dust and sea spray balances, can be calculated and employed to estimate non-exhaust road transport ( $N-E_{xt}$ ) emissions.

- Secondary formation of inorganic compounds ( $SIC$ ): After calculation of water-soluble ions that are associated with soil dust or sea salt, a sequentially ionic balance is applied to the remaining ions with an order that reflects the reactivity and stability of acids and salts in the atmosphere, permitting the estimation of ammonium sulphate and nitrate, and sulphuric acid in the aerosol ( $SIC_{am}$ ). Products of the reaction of atmospheric acids with soil dust can, in certain circumstances, also be estimated ( $SIC_{soil}$ ).

In anthropogenic polluted atmospheres, carbonaceous matter is frequently the dominant contributor to aerosol mass. In IMB, the source apportionment of the carbonaceous matter is done independently of the previously referred sources, with basis in OC, EC and levoglucosan.

-Carbonaceous material from biomass burning ( $OC_{bb}$  and  $EC_{bb}$ ) is estimated from edge lines relating carbon with levoglucosan and comparison with bibliographic biomass burning source composition data.

- Non-biomass burning carbon can be differentiated between fossil fuel primary EC ( $EC_{ff}$ ) and OC ( $OC_{ffp}$ ) and secondary OC ( $OC_{sec}$ ), using the edge line ratio between non-biomass burned EC and OC. This may result in the inclusion of minor amounts of non-exhaust road transport carbon from tyre wear, in the  $EC_{ff}$  and  $OC_{ff}$  estimation. Similarly, some OC from biogenic origin in pollen, etc., can be included in  $OC_{sec}$ .

The sum of source apportioned mass from previous steps constitutes, in average, only 70-80% of the total particulate mass measured, because important components, such as oxygen in Organic Matter (OM) and sorbed water, were not accounted.

-Specific ratios for  $OM_{lb}/OC_{bb}$ ,  $OM_{ffp}/OC_{ffp}$  and  $OM_{sec}/OC_{sec}$ , taken from literature, can be used to estimate the different organic matter fractions.

-Sorption of air moisture by hygroscopic aerosol and the formation of hydrates is important, because, usually, total mass is measured, in equilibrium conditions, at 50% Relative Humidity. From sea salt, secondary inorganic compounds, biomass burning, secondary organic matter, etc, above apportioned, and using bibliographic specific water sorbed data, an estimation of water content in each fraction can be obtained.

The IMB methodology was applied and tested with three data sets corresponding to a background maritime atmosphere heavily impacted by desert dust, in the western coast of Africa (Cardoso et al., 2018), a central urban area in a large city in the western coast of the Iberian Peninsula (Pio et al., 2020) and a smaller urban area largely affected by biomass burning (Pio et al., 2022). Different sampling conditions were employed at each site, which forced adaptations of the IMB method and originated specific opportunities to further detail the aerosol apportionment. PM<sub>10</sub> was measured at the first location. PM<sub>2.5</sub> and PM<sub>10</sub> were analysed at the second. Parallel measurements of PM<sub>10</sub> were made at a road side (RS) and urban background (UB), at the third site.

In the last conditions the simultaneous measurements at RS and UB, together with Cu/Fe ratios, allowed the calculation of enrichment factors for Fe and Ca with separated estimation of Road Dust (RD) and car Brake Dust (BraD) impacts. Also, from Zn concentrations, Zn/Fe edge lines and Zn emission factors from bibliography, it was possible to calculate the contribution of tyre wear (Ty) to road dust.

The IMB results were compared with PMF source estimations for the same data sets. The results were comparable for the two source apportionment methodologies, with mutual advantages in specific fractions of the aerosol. PMF could apportion better the non-measured aerosol components which are easily assigned by specific tracers, such as industrial sources in urban areas. It could also attribute the carbonaceous mass to evaluated sources, more rationally. However, some of PMF source attributions were not real and resulted from covariation of source contributions. An example is the contamination of the desert dust PMF source with covaried sea salt, during desert dust episodes, at the first site. When source contributions covaried strongly, such as in the road emissions, the PMF could not separate the individual sources, as did the IMB. The IMB gives also relevant information on source patterns, because it is able to decompose source contributions in specific sub-contributions.

The intercomparison shows that the two methods are complementary and that the application of IMB and PMF, together, allows a better insight into the contribution of sources and processes to the aerosol loading. The PMF is better in evaluating sources that contribute to various measured constituents. IMB enables identification of collinearity between aerosol

tracer concentrations and the discrimination of secondary pollutants.

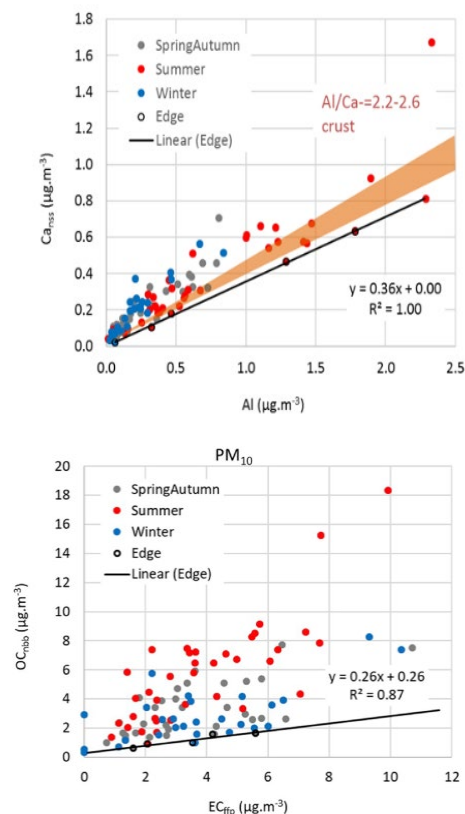


Fig. 1. Examples of edge lines for estimation of soil and secondary OC contributions, in PM<sub>10</sub>, presented together with best-fit equations. Points in grey, red and blue represent samples taken in different seasonal periods. Points with a black edge were used to estimate the edge lines. The brown area represents the range of average crustal ratios (Pio et al., 2020).

#### References:

- Cardoso J., Almeida S.M., Nunes T., Almeida-Silva M., Cerqueira M., Alves C., Rocha F., Chaves P., Reis M., Salvador P., Artiñano B., and Pio C. (2018) Source apportionment of atmospheric aerosol in a marine dusty environment by ionic/composition mass balance (IMB), *Atmos. Chem. Phys.*, 18, 13215–13230.
- Pio C., Alves C., Nunes T., Cerqueira, Lucarelli F., Nava S., Calzolari G., Gianelle V., Colombi C., Amato F., Karanasiou A., Querol X. (2020) Source apportionment of PM<sub>2.5</sub> and PM<sub>10</sub> by Ionic and Mass Balance (IMB) in a traffic-influenced urban atmosphere, in Portugal. *Atmos. Environ.*, 223, 117217.
- C. Pio, Rienda I.M., Nunes T., Gonçalves C., Tchepel O., Pina N.K., Rodrigues J., Lucarelli F., Alves C.A. (2022) Impact of biomass burning and non-exhaust vehicle emissions on PM<sub>10</sub> levels in a mid-size non-industrial western Iberian city. *Atmos. Environ.*, 289, 119293.

## HOW THE NEW EUROPEAN AIR QUALITY DIRECTIVE AFFECTS AIR QUALITY ASSESSMENT IN GALICIA

N. Gallego<sup>1</sup> and M. L. Macho<sup>2</sup>

<sup>1</sup> Air Quality Section, General Directorate of Environmental Quality, Sustainability and Climate Change, Xunta de Galicia, Santiago de Compostela, 15781 Spain

<sup>2</sup>Galician Environmental Laboratory, General Directorate of Environmental Quality, Sustainability and Climate Change, Xunta de Galicia, A Coruña, 15008 Spain

Keywords: Air Quality Assessment

Presenting author email: [nuria.gallego.fernandez@xunta.gal](mailto:nuria.gallego.fernandez@xunta.gal)

In this presentation an evaluation is made of how the new provisions included in the European Air Quality Standard review will affect the work of the team responsible for the air quality assessment and the Galician Environmental Laboratory.

The aim of this new Directive is to align EU regulations with the most recent World Health Organization (WHO) Air Quality Guidelines by setting stricter limit values and targets for several pollutants, including particulate matter (PM<sub>2.5</sub>, PM<sub>10</sub>), NO<sub>2</sub> (nitrogen dioxide), SO<sub>2</sub> (sulfur dioxide) and O<sub>3</sub> (ozone).

In addition, this new standard will bring changes in the parameters to be monitored, the monitoring methods, the requirements for control and data quality and for air quality information, as well as for air quality modelling, all with the aim of improving air quality management and prevention measures and further ensuring compliance with the standards.

In order to identify and assess the changes that this regulation will entail for the regional government of Xunta de Galicia, the first step was to evaluate the situation of the values recorded in the Galician Air Quality Network during the five-year period 2018-2022 against the values recommended by the World Health Organization (WHO). For this analysis, the stations that made up the Air Quality Network of Galicia, between 2018 and 2022 were considered, as well as the two stations of the EMEP Network (European Monitoring and Evaluation Programme) that exist in Galicia (Noia and O Saviñao).

The results obtained for the five-year period 2018-2022 show that in Galicia, in general terms, the pollutants CO, Pb, Cd and SO<sub>2</sub> are below the values recommended by the WHO in all or almost all of the monitoring stations. On the other hand, PM<sub>2.5</sub> particles, PM<sub>10</sub> particles, ozone and NO<sub>2</sub> are further away from meeting the stringent values recommended by the WHO, especially PM<sub>2.5</sub> and ozone. It should be

noted that the EMEP background stations in Galicia (O Saviñao and Noia) have exceeded these Guideline values for particulate matter and ozone.

The new Directive also introduces changes that will affect the configuration of the Galician Air Quality Network and the equipment of the fixed measurement stations that make up the network. The current zoning of Galicia is already based on modeling results, not only of measurement, but this Directive brings new changes, including the creation of the so-called "super sites", which will be representative measurement points of areas of the territory that exceed the autonomic delimitations, probably, will be part of a network managed by the Ministry for the Ecological Transition and the Demographic Challenge. The location of these points may affect the configuration of the current network of fixed stations in Galicia.

Regarding modelling, Xunta de Galicia already has experience in using this tool both as a support for air quality assessment and for prediction, since it has been running a 72-hour air quality prediction model with its own resources since 2012. This model is able to meet the demanding requirements of the new Directive with regard to the assessment of the territory. But the new Directive sets new challenges for our modelling, such as determining the representativeness of the stations.

The new Directive also addresses the monitoring of atmospheric deposition, and Galicia has a rainwater network since 1998, with collectors in the 7 cities of Galicia, managed from the Environmental Laboratory. This Laboratory also carries out determinations of the composition of particulate matter in ambient air, and one of its objectives is to include in its portfolio of services the analysis of the new parameters suggested in the proposed Directive as the test methods become clearer and standardized.

*RICTA2024*

**8<sup>th</sup> Iberian Meeting on Aerosol Science and Technology**



**Section 3. Oral Session I.**  
**Wednesday, June 26<sup>th</sup> 11:45-13:15**

**Chairs: F. J. Gómez Moreno, Sergio Rodríguez**

## MECHANISMS OF AEROSOLS DEPOSITION IN TURBULENT CHANNEL FLOW

P.L. Garcia-Ybarra<sup>1</sup> and A. Pinelli<sup>2</sup>

<sup>1</sup>Department of Física Matemática y de Fluidos, UNED, Las Rozas, 28032, Spain

<sup>2</sup>Department of Mechanical Engineering and Aeronautics, City, University of London, London, EC1V 0HB, UK

Keywords: aerosol deposition, particle laden flow, eddy diffusivity, channel flow

Presenting author email: pgybarra@ccia.uned.es

The more usual framework for aerosol deposition from a flowing carrier gas relies, in the absence of external and phoretic forces, on the interplay between particle inertia and Brownian diffusion. These are the main mechanisms that force the deposition of aerosol particles on the walls that confine a flowing carrier gas. The relative importance of each mechanism depends on the magnitude of the particle Stokes number  $Stk$  (particle relaxation time to flow characteristic time). For vanishing values of this number (*i.e.*, small particles), inertia effect is negligible, and diffusion is the mechanism responsible for deposition. On the contrary, for values larger than order unity of the Stokes number (*i.e.*, large particles), inertia takes over and becomes the main mechanism of deposition. For particle sizes between these two limit cases, deposition is usually assumed to be simply the addition of the contribution from both mechanisms (Friedlander, 2000).

In laminar flow configurations around a bluff body, particle trajectories depart from the gas streamlines with strong flow deceleration due to its inertia, *e.g.*, in the vicinity of a stagnation point flow. Particles accumulate ahead of the body near the wall, inducing a local increase in the numerical density that facilitates the deposition by Brownian diffusion, even at subcritical Stokes numbers. This effect of Brownian deposition enhancement by the inertial enrichment was stressed and revisited by Fernandez de la Mora and Rosner (2019).

In the case of turbulent flows, the same phenomenon of inertial enrichment is provided by turbophoresis (Reeks, 1983), *i.e.*, the net flux of particles due to a gradient of turbulence intensity. Particles migrate from the regions with high turbulent fluctuations and reach the near-wall regions, where they accumulate like in a particle trap because the turbulence intensity is lower and more inefficient to send particles away.

Finally, together with turbophoresis and Brownian diffusion, the third in contention is the turbulent diffusion that disperses the particles in all directions and is measured by the turbulent Schmidt number (eddy diffusivity over eddy viscosity).

In this work, the analysis of particle deposition in the range of relatively small  $Stk$  values has been performed by combining high Schmidt number asymptotics,  $Sc \equiv \text{diffusion} / \text{viscosity} \gg 1$ , (Garcia-Ybarra and Pinelli, 2004; Garcia-Ybarra, 2009), with a regular  $Stk$ -expansion. This regular expansion cannot describe inertial impaction as the particle trajectories depart only slightly from the flow streamlines by small amounts of order  $Stk$ .

Fig. 1 shows the prediction of the analysis for the deposition flux of particles, describing the combined effects of the three mechanisms: Brownian diffusion, turbulent diffusion, and small inertia. These results allow to conclude the importance of accounting for the inertial enrichment by turbophoresis to describe accurately the turbulent deposition of aerosol particles in the intermediate range of Stokes numbers.

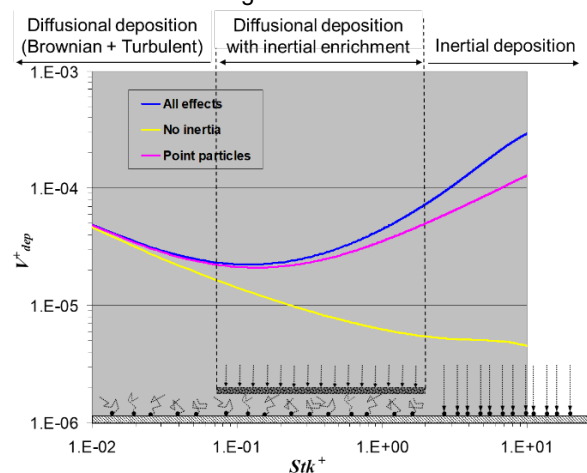


Fig. 1. Dimensionless deposition velocity of the particles in terms of the Stokes number, written in wall units.

- This work was supported by Project PID2022-139082NB-C55 granted by MCIN/AEI/10.13039/501100011033/ FEDER, UE.
- Fernandez de la Mora J., Rosner D.E. (2019) Low Reynolds number capture of small particles on cylinders by diffusion, interception, and inertia at subcritical Stokes numbers. *Aerosol Sci. Tech.* 53, 647-662.
- Friedlander, S. K. (2000) *Smoke, dust and haze. Fundamentals of aerosol dynamics*. 2<sup>nd</sup> edition, Oxford University Press, Oxford, UK.
- Garcia-Ybarra, P. L. (2009) Near-wall turbulent transport of large-Schmidt-number passive scalars. *Phys. Rev E* 79, 067302.
- Garcia-Ybarra, P. L., Pinelli, A. (2006) Turbulent channel flow concentration profile and wall deposition of a large Schmidt number passive scalar. *C. R. Mecanique* 334, 531-538.
- Reeks, M. W. (1983) The transport of discrete particles in inhomogeneous turbulence. *J. Aerosol Sci.* 14, 729-739.

## ELECTROSPRAYS WITH COULOMB EXPLOSIONS

I.G. Loscertales<sup>1</sup> and F. J. Higuera<sup>2</sup>

<sup>1</sup>Department of Mechanical, Thermal and Fluid Engineering, Universidad de Málaga, 29071 Málaga, Spain

<sup>2</sup>Department of Fluid Mechanics and Propulsion, Universidad Politécnica de Madrid, 2804 Madrid Spain

Keywords: Electrospays, evaporation of charged droplets, Coulomb fission, ion emission

Presenting author email: loscertales@uma.es

An Eulerian model is proposed to describe the structure of an electrospay of a volatile, highly conducting liquid in air, whose droplets undergo successive Coulomb explosions. They are assumed to have an initial radius  $R_1$  in the order of tens of nanometers and an initial charge  $q_1$  of the order of the Rayleigh charge. The droplets are made of an ideal solution of a fully dissociated non-volatile salt in a volatile solvent. The vaporization-induced concentration gradient in the liquid, the Stefan flow in the surrounding gas, and thermal effects are all left out; and Raoult's law is assumed to hold.

The solvent in the droplets evaporates until their radius decreases to the critical value  $R_{c1} = q_1^{2/3} / (64\pi^2 \epsilon_0 \gamma)^{1/3}$ , at which a Coulomb explosion occurs (Rayleigh, 1882). Here  $\gamma$  is the surface tension of the liquid and  $\epsilon_0$  is the permittivity of the air. The outcome of a Coulomb explosion is taken to be a single second generation droplet with a fraction  $\epsilon_m$  of the mass of the parent droplet and a fraction  $\epsilon_q$  of its charge, and a large number of much smaller progeny droplets that are assumed to evaporate instantaneously (Misra, 2023). The second generation droplet keeps evaporating until its radius decreases to the new critical value  $R_{c2} = \epsilon_q^{2/3} R_{c1}$ , at which a second explosion occurs, thus generating a third generation droplet and a large number of much smaller progeny droplets that evaporate instantaneously. This process of evaporation and explosion repeats a certain number of times ( $N$ , to be determined), leading to  $N + 1$  generations of droplets which are characterized by  $N + 1$  distribution functions  $f_i(x, R)$ .

To determine  $N$  and the fate of the small progeny droplets we consider the electric field at the surface of a droplet of radius  $R$  carrying a charge  $q$ ,  $E_s = q / 4\pi\epsilon_0 R^2$ , which increases as the droplet evaporates. Field emission of ions occurs when this field reaches a certain threshold  $E^*$  that depends on the type of ions and solvent, and is in the order of 1 V/nm (Loscertales, 1995). The surface field freezes then at  $E^*$  as the droplet evaporates, and the emission of charge prevents any further Coulomb explosion as the droplet dries and becomes a charged salt residue. We assume that the very tiny progeny droplets generated on each explosion are already in the field emission regime. This field emission mechanism may determine the maximum number of explosions,  $N$ , because a droplet of the  $N + 1$  generation will stop exploding if it enters the ion emission regime when its radius has a value  $R_{em} > R_{cN+1}$ . Assuming the evaporation and ion

emission of these small droplets are instantaneous, one may formulate the vapor generated  $w_{vd}(x)$ , the charge density generated in the form of residues  $Q_{res}(x)$  and in the form of ions  $Q_{ion}(x)$  both for the explosions (progeny) and for the last generation of droplets.

Based on these premises, we formulate conservation equations for the distribution functions,  $f_i(x, R)$ , the vapor density,  $\rho_v(x)$ , the residues charge density,  $\rho_{res}(x)$ , and the ions charge density,  $\rho_{ion}(x)$ , coupled with the Navier-Stokes for the gas and the Poisson equation for the electric potential (Loscertales, 2024). Numerical solutions of these equations will be presented for some simple cases.

This work was supported by MCIN/AEI through grants PID2020-115730GB.

- Loscertales, I. G. and Fernández de la Mora, J. (1995) Experiments on the kinetics of field evaporation of small ions from droplets. *J. Chem. Phys.* **103** (12), 5041.
- Loscertales, I. G., Rivero-Rodríguez, J., Higuera, F. J. and Hijano, A. J. (2024) Axisymmetric inertialess model for the capture of airborne microparticles using an electrospay. *J. Aerosol Sci.* **175**, 106281.
- Misra, K., Gamero-Castaño, M. (2023) Ion emission from nanodroplets undergoing Coulomb explosions: a continuum numerical study. *J. Fluid Mech.* **958**, A32.
- Rayleigh, L. (1882) On the equilibrium of liquid conducting masses charged with electricity. *Phil. Mag.* **14** (87), 184.

## FINITE TAYLOR CONE: THE IMPACT OF THE ELECTROSPRAY

J. Rivero-Rodríguez<sup>1</sup>, A. Hijano<sup>1</sup>, F. Higuera<sup>2</sup> and I.G. Loscertales<sup>1</sup>

<sup>1</sup>Department of mechanics, thermal and fluids engineering, University of Malaga, Málaga, Spain

<sup>2</sup>Department of fluid mechanics, Universidad Politécnica de Madrid, Madrid, Spain

Keywords: electrospray, Taylor cone, third, fourth

Presenting author email: jrivrod@uma.es

When a conductive liquid flows out of a needle under the effect of an electric field, a conical shape may be exhibited for a certain range of the strength of the electric field and a jet or a spray is ejected from its apex. The first attempt to model this situation was carried out by G.I. Taylor (1964), who simplified the geometry to an infinite cone and established the given value of the strength of the electric field that is in equilibrium with the surface tension and the semiangle of the cone, known as the Taylor cone angle  $\alpha$ . Later, Fernández de la Mora (1992) included in the analysis the influence of the emitted electrospray that modifies both the strength of the electric field and the cone angle, and Pantano et al. (1994) took into account the shape of the electrodes and finite value of the cone volume without the spray.

In this work, we take into consideration both (1) the influence of the finiteness of the cone and geometry of the device, and (2) the mutual impact of the electrospray.

In fig. 1, we can observe the electrode and needle (in dark blue) connected to a high voltage, the grounded counterelectrode (in dark red) and the computed shape of the cone as a result of the balance between surface tension and electrostatic stresses. The electrospray volumetric charge is also considered, although not shown.

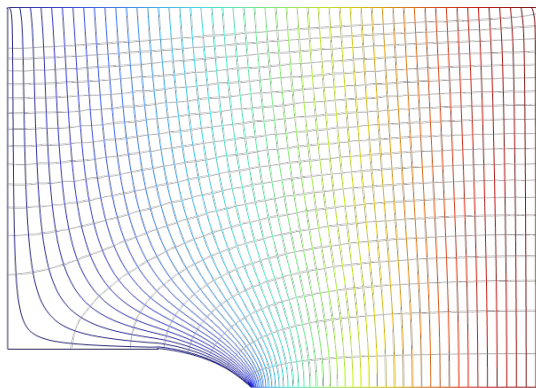


Fig. 1. Sketch of electric potential (color map) and electric field (streamlines) in an electrospray device with deformable meniscus.

In fig. 2, we have depicted the cone shape that depends on its own volume and the electric Bond number. We can observe that, the Taylor cone angle is locally reproduced at the cone apex, despite its deformation far from this region.

These simulations reproduce the results by Pantano et al. (1994) and extend it to considered the influence of the electrospray.

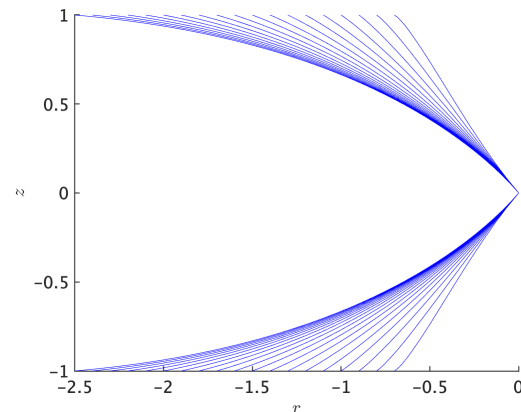


Fig. 2. Taylor cones shape for varying electric Bond number and corresponding volumes.

To do so, we have solved the Poisson equation for the electric potential, the conservation of charge for the inertialess-electrospray and the Young-Laplace stress balance for the deformable interphase in spherical coordinates formulated using the Arbitrary-Lagrangian-Eulerian (ALE) method to account for the deformation, with the help of the weak form module of Comsol Multiphysics.

As part of the results, we have obtained the range of feasible electric Bond number, based on the applied voltage and geometry of the device, while locally reproducing the one obtained by Taylor at the apex. It has been done for several values of the electric current carried by the electrospray, hence shedding light on how the electrospray influences the cone.

Taylor, G. I. (1964). Disintegration of water drops in an electric field. *Proceedings of the Royal Society of London. Series A. Mathematical and Physical Sciences*, 280(1382), 383-397.

De La Mora, J. F. (1992). The effect of charge emission from electrified liquid cones. *Journal of Fluid Mechanics*, 243, 561-574.

Pantano, C., Ganán-Calvo, A. M., & Barrero, A. (1994). Zeroth-order, electrohydrostatic solution for electrospraying in cone-jet mode. *Journal of Aerosol Science*, 25(6), 1065-1077.

## PARTICLE CHARGING BY ELECTROSPRAY NANODROPLETS. MEASURING THE RATE CONSTANTS

F. J. Higuera<sup>1</sup> and I. G. Loscertales<sup>2</sup>

<sup>1</sup>Department of Fluid Mechanics and Propulsion, Universidad Politécnica de Madrid, 28040 Madrid, Spain

<sup>2</sup>Department of Mechanical, Thermal and Fluid Engineering, Universidad de Málaga, 29071 Málaga, Spain

Keywords: Electrospays, charged droplet-particle interaction, particle removal, filtration

Presenting author email: f.higuera@upm.es

A recent attempt at modeling the charging and capture of microparticles of diameter  $d_p$  by attaching highly charged nanodroplets of diameter  $d_e \ll d_p$  from an electrospay of a high conductivity liquid in the presence of an electric field (Loscertales et al. 2024), shows that, in the absence of inertial effects, the relative velocity of a droplet to a particle is due mainly to the migration of the highly mobile droplet and is of the form  $v \approx z_e E$ , where  $z_e$  is the electrical mobility of the droplet and  $E$  is the local electric field. Calling  $n_e$  the number density of droplets, each with a charge  $q$ , and  $n_j$ , with  $j = 0, \dots, N$ , the number densities of particles that have attached  $j$  droplets and have a charge  $jq$ , the rates of attachment (numbers of droplets and particles in different states of charge generated per unit volume and time) can be written as  $w_e = -(\sum_{j=0}^{N-1} k_j n_j) E n_e$ ,  $w_0 = -k_0 E n_0 n_e$ ,  $w_j = (k_{j-1} n_{j-1} - k_j n_j) E n_e$  for  $j = 1, \dots, N-1$ , and  $w_N = k_{N-1} E n_{N-1} n_e$ . Here  $E$  is the strength of the local electric field, and the reaction constants  $k_j$  still depend on the charge of the droplets and the local field through the combination  $\tilde{q} = q/(\pi \epsilon_0 d_p^2 E)$ , where  $\epsilon_0$  is the permittivity of the gas into which the process takes place (Loscertales et al. 2024). A preliminary analysis is presented in this talk of a device intended to measure the reaction constants for large and small values of  $\tilde{q}$ . A flow rate  $Q$  of a gas carrying a number density of droplets  $n_{e0}$  and a number density of neutral particles  $n_{00}$  is fed to a grounded metallic tube of radius  $R$  and length  $L$  consisting of two electrically insulated segments. A Poiseuille velocity profile  $2U(1 - r^2/R^2)$ , with  $r$  the distance to the tube axis and  $U = (Q/\pi R^2)$ , is obtained downstream of a viscous adaptation region. The effect of the small diffusivities of the droplets and the particles is confined to a thin layer by the wall in the region of the tube of interest, and the conservation equations for the droplets and the particles in different states of charge reduce to balances of convection, migration and the attachment reactions mentioned above outside this layer. The only electric field in the tube is induced by the charges of the droplets and the particles, and is essentially radial pass the tube's entry region, of the form  $E = (q/\epsilon_0 r) \int_0^r (n_e + \sum_{j=1}^N j n_j) r dr$  from Gauss' law.

Advancing that  $n_{e_0}$  will be of the order of  $n_{0_0}$  or greater than it, the order of magnitude of the electric field is  $q n_{e_0} R / \epsilon_0$ , and  $\tilde{q} \sim 1 / (n_{e_0} R d_p^2)$ . All the reaction constants but  $k_0$  are negligible when  $\tilde{q}$  is large, because the electrostatic repulsion between droplets

and charged particles is then very strong and prevents the attachment of more than one droplet (Loscertales et al. 2024). In the opposite limit  $\tilde{q} \ll 1$ , the electrostatic repulsion is weak and all the reaction constants are nearly the same.

The radial electric field pushes the droplets toward the wall, setting a limit to the length of the tube region where droplets exist and attachment reactions occur. An order-of-magnitude balance of axial convection and radial migration of the droplets shows that the ratio of the characteristic length of this region to the tube radius is of the order of the inverse of the parameter  $\Pi = z_e q n_{e_0} R / (2 \epsilon_0 U)$ , which is taken to be small in what follows. The radial drag force of the droplets and the charged particles on the gas is balanced by a radial pressure gradient without significantly changing the Poiseuille velocity profile in this region of quasi-unidirectional flow.

The electrical mobilities of the particles are  $z_j = j z_1$ , where  $z_1 \ll z_e$  is the electrical mobility of the particles that have attached one droplet, so the charged particles migrate to the tube wall only far downstream of the region of length  $R/\Pi$  where the droplets do (the first of the two tube segments mentioned above). No droplets are left at the end of this region, while the charged particles (singly charged if  $\tilde{q} \gg 1$  or in a range of states of charge if  $\tilde{q} \ll 1$ ) reach the wall in a longer second segment of the tube. The only required value of the reaction rate in each of these limits can in principle be extracted from the conduction current generated by the charged particles in the second segment of the tube wall.

This work was supported by MCIN/AEI through grants PID2020-115730GB.

Loscertales, I. G., Rivero-Rodríguez, J., Higuera, F. J. and Hijano, A. J. (2024) J. Aerosol Sci. **175**, 106281.

## CAN WEEKLY MEASUREMENTS EFFICIENTLY IDENTIFY AREAS OF HIGH CONCENTRATIONS OF RADIOACTIVE AEROSOLS?

E. Chham<sup>1</sup> and J.A.G. Orza<sup>1</sup>

<sup>1</sup>SCOLAB, Department of Applied Physics, Universidad Miguel Hernandez, Elche, 03202, Spain

Keywords: Sampling resolution, source-receptor models, radioactive aerosols

Presenting author email: e.chham@umh.es

Accurately measuring concentrations of radioactive aerosols in the air is essential for assessing radiological risks and maintaining air quality, especially in regions prone to register high activity concentrations that could impact human health and environmental safety. In such a scenario, the temporal resolution in sampling radioactive aerosols becomes crucial for comprehending the intricate patterns of their appearance and dispersion through the atmosphere. Therefore, understanding the extent to which a change in temporal sampling resolution affects the accuracy of identifying potential sources of these aerosols is a key issue.

Typically, for radioactive aerosols, the measurements considered by radiological surveillance networks are conducted weekly. Considering that many of the air masses corresponding to the sampling period may not be related to particularly high concentration levels, the source-receptor analyses based on trajectories may inefficiently identify source areas, and a critical question can be posed: Can weekly measurements capture all the information regarding the sources of these aerosols, or is it necessary to measure with higher time resolution?

A source-receptor analysis based on back-trajectories is used to compare results with different measurement periods:

(1) The Concentration Weighted Trajectory (CWT) method has been chosen (Hopke, 2016). Applying this technique allows for a more precise analysis of the trajectory and concentration of radioactive aerosols over time. (2) Radioactivity measurements with higher than usual temporal resolution are analysed. In our case, these are more than 4800 daily measurements of <sup>7</sup>Be concentrations in Helsinki (60.210 N, 25.060 W, 26m a.s.l, Finland) over 20 years (1999-2019). (3) Weekly concentration averages are calculated to compare daily and weekly data use in identifying source regions. This comparison will determine the effectiveness of the weekly temporal resolution in assessing source regions.

The meteorological database used as input for the trajectory calculations for the CWT model is ERA-Interim, interpolated to 0.5 deg horizontal resolution, from the ECMWF. Specifically, 120 h kinematic 3D back-trajectories, were calculated 4 times per day at 150m above sea level (a.s.l.). The back-trajectories calculation used the Hybrid Single-Particle Lagrangian Integrated Trajectory (HYSPLIT) model.

**Results and discussion:** Figures 1 and 2 display the results of applying CWT models to daily data and

weekly averages, respectively. Overall, both graphs identify the same high-impact areas around latitudes and longitudes 60 over the Urals. The weekly map shows a more pronounced signal in the Atlantic, which is attributed to the scale-free transformation applied to both maps.

Considering the long study period, it can be confidently asserted that weekly sampling resolution effectively captures potential sources under diverse atmospheric conditions and can record short-duration events that characterize the vertical transport of <sup>7</sup>Be from the stratosphere to the troposphere.

This result is likely to hold for other studies where weekly sampling is needed.

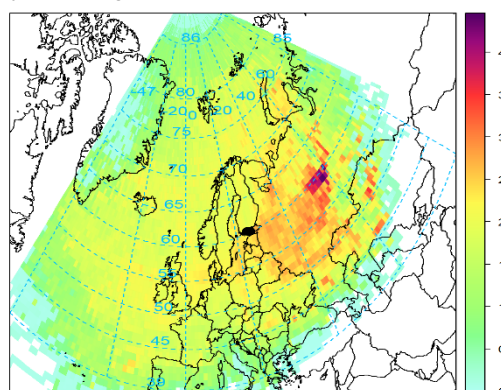


Fig. 1. CWT values of daily <sup>7</sup>Be measurements at 150 m over Helsinki during the study period.

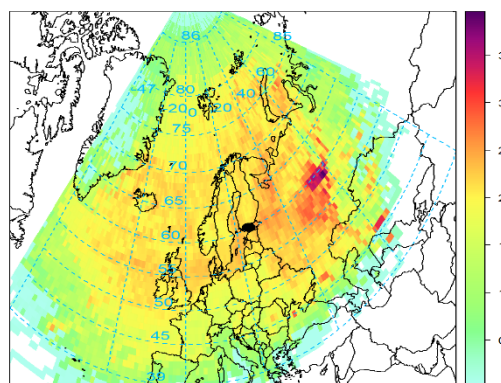


Fig. 2. As Fig 1 but for weekly averages.

### References:

Hopke, P.K. (2016) Review of receptor modeling methods for source apportionment, *Journal of the Air & Waste Management Association*, 66:3, 237-259.

## A NOVEL LIBS IMAGING METHOD FOR THE DETERMINATION OF ATMOSPHERIC PARTICULATE MATTER IN REMOTE REGIONS

M. López Ochoa, J. Cárdenas-Escudero, S. Deylami, J. Ayuso Haro, J. Urraca Ruiz, D. Galán Madruga, J.O. Cáceres

Laser Chemistry Research Group, Department of Analytical Chemistry, Faculty of Chemistry, Complutense University of Madrid, 28040 Madrid, Spain

Keywords: Laser-induced Breakdown Spectroscopy, Filter characterization, Atmospheric aerosols, Micro LIBS imaging, Antarctica

Presenting author email: marclo06@ucm.es

A better way of continuous monitoring of atmospheric aerosols (particulate matter ranging in sizes from nano to micrometers) is needed. Since traditional techniques are supposed to carry costly and complex analyses, this is why a novel method for single particle imaging using micro laser-induced breakdown spectroscopy was developed to analyze particulate matter in Antarctica.

Samples were collected in circular quartz microfiber filter papers on the deception island in austral summer. All those samples were analyzed by LIBS, and some of them were analyzed by ICP-MS as well to validate the method.

Before carrying out the LIBS analyses, the lateral resolution had to be set since (due to the violent nature of the laser ablation) using both too high and too low lateral resolution would lead to loss of information. Fig. 1 shows how the optimal distance between spots would be 40-60  $\mu\text{m}$ .

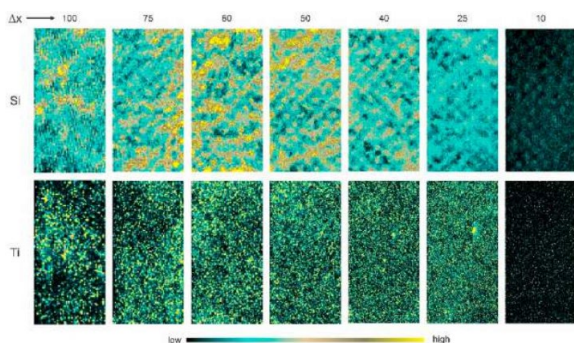


Fig 1. Elemental images of Si and Ti in the same sample, ranging from 100 to 10  $\mu\text{m}$  resolution.

The LIBS-ICP calibration curves for common elements (such as Ti and Fe, Fig. 2) had good linearity. This would mean the LIBS signal is proportional to the ICP concentration, allowing the measurement of elements with LIBS through ICP calibration. Also, the LoD values obtained for LIBS analysis were lower than those obtained for ICP.

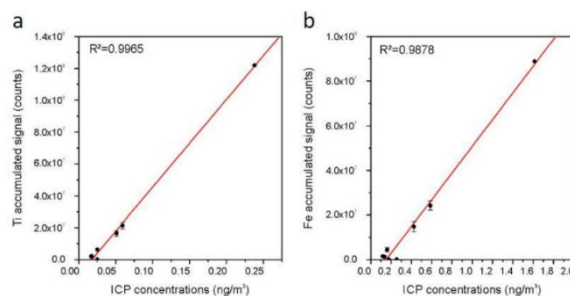


Fig. 2. LIBS-ICP calibration curves for (a) Ti and (b) Fe.

Apart from the most common metals, some other trace elements, such as Ni, Zn, Cr, or Cu, could be seen by LIBS imaging (Fig. 3). However, their quantification wasn't possible due to method limitations: not enough accuracy by ICP analysis to validate the method LIBS not being representative enough because of the low number of particles.

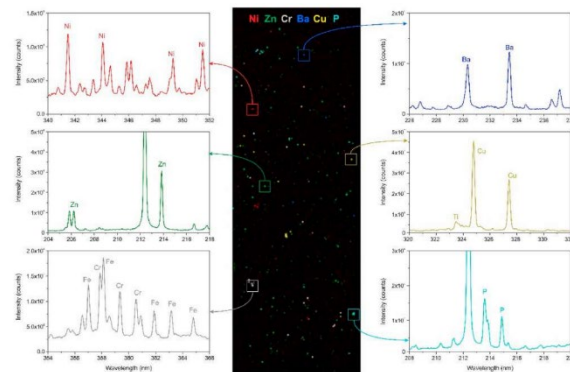


Fig. 3. Spatial distribution of different elements in a filter sample.

César Marina-Montes, Vincent Motto-Ros, Luis Vicente Pérez-Arribas, Jesús Anzano, María Millán-Martínez, Jorge O. Cáceres (2021) Aerosol analysis by micro laser-induced breakdown spectroscopy: A new protocol for particulate matter characterization in filters. In: *Analytica Chimica Acta*, 1181, 338947.

*RICTA2024*

**8<sup>th</sup> Iberian Meeting on Aerosol Science and Technology**



**Section 4. Oral Session II.**  
**Wednesday, June 26<sup>th</sup> 14:45-16:30**

**Chairs: F. Higuera, P. L. García-Ybarra**

# ANALYSIS OF LINEAR REGRESSION MODELS TO STUDY THE CORRELATION BETWEEN TEMPERATURE INVERSION AND PM LEVELS IN THE CITY OF GIJÓN (NORTHERN SPAIN)

Enrique González Plaza<sup>1</sup>, María Fernández Amor<sup>1</sup> and Maidá María Domat Rodríguez<sup>1</sup>

<sup>1</sup> Department of Physics, University of Oviedo, Oviedo, Postcode, Spain

Keywords: temperature inversion, PM concentration, linear regression

Presenting author email: domatmaida@uniovi.es

According to the study published by Glojek K. et al. in 2022, the concentration of particulate matter (PM) presents a stronger correlation with the value of temperature inversion (TI) than with any other meteorological variable. This is due to a TI being a situation in which a layer of warmer air is placed above one of colder air, creating stable atmospheric conditions that prevent the circulation between the different layers and therefore, the scattering of PM. All this should lead to higher levels of PM concentration. In this contribution, the feasibility of creating regression models that relate the concentration of PM and the value of IT is studied. To do that, the values of TI and PM between the 12<sup>th</sup> February and the 21<sup>st</sup> April of 2023 in the city of Gijón were used. The latter were obtained from the Regional Net for Air Quality Control (Red de Control de la Calidad del Aire, 2023), whereas the first ones were taken from the Spanish Meteorological Agency (AEMET open data, 2023) or measured with a homemade sensor, as presented by Fernández-Amor et al. in 2023. By applying lineal regression techniques to the data, the models in eq. (1), (2) and (3) are proposed. There  $PM_{10}(n)$  denotes the average concentration of PM under 10 microns for a given day during the morning in  $\mu\text{g}/\text{m}^3$  and  $\Gamma_n$  or  $\Gamma_{n-1}$  are the values of average temperature inversion for the given or the previous day in  $^\circ\text{C}/\text{km}$ , respectively. For all models, this value is computed as the difference between the average temperatures at a certain altitude and the one at sea level. This way, a negative value would indicate the existence of a TI. Therefore, a negative slope would point towards a correlation between the IT and a greater concentration of PM.

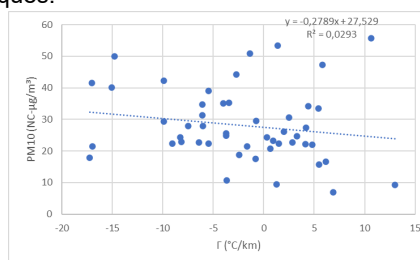
$$PM_{10}(n) = -0.2789 \Gamma_n + 27.529 \quad (1)$$

$$PM_{10}(n) = -0.6467 \Gamma_{n-1} + 26.713 \quad (2)$$

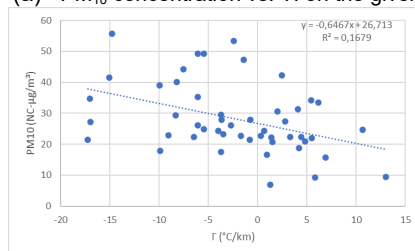
$$\text{Log}(PM_{10}(n)) = -0.0112 \Gamma_{n-1} + 1.3885 \quad (3)$$

In Fig. 1 the regression model results are depicted showing that there is some relation between the existence of TI on the previous day and the concentration of PM given the negative value of the slope. In this sense, it can also be seen, that the relation with the TI on the same day is much less clear, fig. 1a. Besides, if no IT is observed ( $\Gamma=0$   $^\circ\text{C}/\text{km}$ ) on the previous day, the PM concentration should be the expected value for the observable period. In this case, the measured average concentration during the mornings is  $28.09 \mu\text{g}/\text{m}^3$  which is a close value to the independent terms of the models. In the case of eq. (3),

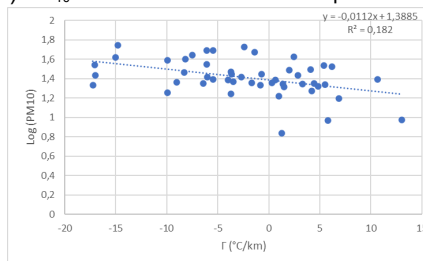
it should be the logarithm of this value. Nonetheless, despite the existence of a correlation, the relation is clearly non linear given the values of  $R^2$ . This hints at futures works regarding more complex regression models or the application of machine learning techniques.



(a)  $PM_{10}$  concentration vs. TI on the given day.



(b)  $PM_{10}$  concentration vs. TI on the previous day.



(c) Logarithm of  $PM_{10}$  concentration vs. TI on the previous day.

Fig. 1. Linear regression results for the proposed models. This work was supported by the Spanish Ministry of Education and Professional Training, under grant BDNS: 633225.

Glojek K. et al. (2022), *Atmos. Chem. Phys.*, **22**, 5577-5601

Regional Net for Air Quality Control Website, *Principality of Asturias*, [link](#).

AEMET Open Data Website, *Ministry for Ecological Transition and the Demographic Challenge*, [link](#).

Fernández-Amor et al. (2023), EAC 2023.

# GEOCHEMICAL CHARACTERIZATION AND SOURCES OF ATMOSPHERIC AEROSOLS DEPOSITED IN THE ORDESA Y MONTE PERDIDO NATIONAL PARK (PNOMP) IN THE PERIOD 2016-2023, WITH ATTENTION TO WINTER PERIODS

Javier Bandrés García<sup>1</sup>, Jorge Pey Betrán<sup>1</sup> and Juan Ignacio López Moreno<sup>1</sup>

<sup>1</sup>Instituto Pirenaico de Ecología (IPE-CSIC), Zaragoza, 50059, España

Keywords: climate change, Saharan dust, Pyrenees, receptor model, cryosphere

Presenting author email: jbandres@ipe.csic.es

Climate change and global environmental shifts are modifying conditions in the Pyrenees, potentially exacerbating the rising frequency and intensity of Saharan dust events (Salvador et al., 2022). Given this context, investigating the phenomenology of various processes affecting aerosol deposition during winter periods becomes especially crucial. These events significantly influence the regional radiative balance, the durability of snow cover, and consequently, the water balance in the area.

This study specifically delves into the geochemical characterization and identification of primary sources of atmospheric aerosols deposited in the Ordesa y Monte Perdido National Park (PNOMP) from 2016 to 2023. Emphasizing the significance of aerosols in mountainous regions like the Pyrenees, the investigation aims to shed light on their role in the PNOMP area. The primary objective is to unravel the sources of these aerosols, analyze their temporal variability, and discern the impact of certain aerosol types, especially Saharan dust, on processes affecting the surrounding cryosphere.

Methodologically, the study employs robust and established sampling and analysis techniques, including total aerosol deposition monitoring (Pey et al., 2020), widely accepted aerosol analysis methods (Querol et al., 2019), and the Positive Matrix Factorization (PMF) v5.0 source contribution model, which identifies key aerosol factors and sources.

The results exhibit variations in aerosol deposition (Fig. 1) and diverse chemical compositions among the analyzed fractions.

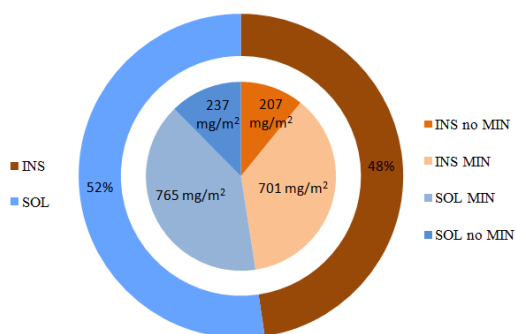


Fig. 1. Average concentration (2016-2023, in %) of insoluble (INS) vs soluble fraction (SOL), and average of the mineral part (MIN) and the non-mineral part (non MIN) (in mg/m<sup>2</sup>).

Mineral dust, in both soluble and insoluble fractions, emerges as a prominent aerosol component, often linked to intense Saharan dust deposition events. The PMF model identifies seven aerosol sources, with two associated with North African dust from distinct source regions. The slightly different composition of Saharan dust based on its source origin suggests potential modulations in cryospheric impacts. Consequently, these findings provide crucial insights that can contribute to the development of environmental management strategies and regional as well as global climate modeling, offering a perspective on atmospheric aerosol dynamics in the context of climate change.

In conclusion, this study offers a comprehensive geochemical analysis of aerosols, their sources and variability within the period 2016-2023 in the PNOMP. This analysis enhances our understanding of atmospheric aerosol dynamics in the context of climate change, emphasizing the imperative for further research on their impacts on mountain ecosystems and air quality.

The first author has an FPI predoctoral grant in the frame of MARGISNOW project (PID2021-124220OB-I00) funded by the Spanish Ministry of Science and Innovation. This research received support from POSAHPI actions (AEI, PID2019-108101RB-I00, PID2022-143146OB-I00), ASAH-AS (OAPN 2021, reference 2799/2021), and SNOWDUST (AEI, TED2021-130114B-I00).

Pey J., Larrasoaña J.C., Pérez N. *et al.* (2020). Phenomenology and geographical gradients of atmospheric deposition in southwestern Europe: results from a multi-site monitoring network. *Sci. Tot. Environ.*, 744, 140745. <https://doi.org/10.1016/j.scitotenv.2020.140745>.

Querol, X. Pérez N., Reche C. *et al.* (2019). African dust and air quality over Spain: Is it only dust that matters?. *Sci. Tot. Environ.* 686, 737-752. <https://doi.org/10.1016/j.scitotenv.2019.05.349>.

Salvador, P., Pey, J., Pérez, N. *et al.* (2022). Increasing atmospheric dust transport towards the western Mediterranean over 1948–2020. *npj Climate and Atmospheric Science* 5, 34. <https://doi.org/10.1038/s41612-022-00256-4>.

## EXCEPTIONAL AEROSOL LOAD OBSERVED IN THE ARCTIC DURING SUMMER 2019

S. Herrero-Anta<sup>1</sup>, D. Mateos<sup>1</sup>, S. Graßl<sup>2,3</sup>, C. Ritter<sup>2</sup>, S. Gilardoni<sup>4</sup>, M. Mazzola<sup>4</sup>, K. Stebel<sup>5</sup>, S. Eckhardt<sup>5</sup>, C. Herrero del Barrio<sup>1</sup>, D. González-Fernández<sup>1</sup>, R. Román<sup>1</sup> and C. Toledano<sup>1</sup>

<sup>1</sup>Group of Atmospheric Optics, University of Valladolid, 47011 Valladolid, Spain

<sup>2</sup>Alfred-Wegener-Institute Helmholtz Centre for Polar and Marine Research, 14473 Potsdam, Germany

<sup>3</sup>Institute of Physics and Astronomy, University of Potsdam, 14476 Potsdam, Germany

<sup>4</sup>Italian National Research Council, Institute of Polar Science, 40129 Bologna, Italy

<sup>5</sup>NILU, 2007 Kjeller, Norway

Keywords: Arctic, high AOD, multi-instrument

Presenting author email: sara@goa.uva.es

Polar regions represent sensitive areas where external factors can have a higher impact than in the rest of the planet. In particular, the warming in the Arctic has been much faster than the rest of the world. It has been likely caused by feedback mechanisms involving ice cover, aerosols and clouds, among others. Hence, the study of aerosols in this region is crucial because their capacity to interact with radiation and serve as cloud condensation nuclei.

One of the most northern sites in the Arctic is Ny-Ålesund (78.9°N, 11.9°E), in the Svalbard Archipelago. Different scientific instruments focused on aerosol measurements, both in-situ and remote sensing, are installed at this location. Recently, Hansen et al. (2023) integrated and analysed observations of climate-relevant aerosol parameters during 2002-2020. The analysis of that dataset has been useful to identify that in summer 2019, for many weeks the aerosol optical depth (AOD) was higher than during the 2002-2020 average (see Figure 1).

Most of the data used here were put together in the framework of the ReHearsol and the LOADRIS projects (Svalbard Science Foundation).

This work was supported by the Ministerio de Ciencia e Innovación (MICINN), with the grant no. PID2021-127588OB-I00. This work is part of the project TED2021-131211B-I00375 funded by MCIN/AEI/10.13039/501100011033 and European Union, "NextGenerationEU"/PRTR. The authors acknowledge the support of the Spanish Ministry for Science and Innovation to ACTRIS ERIC.

Hansen G, et al. (2023) Long-term observations of aerosol optical depth and their relation to in-situ aerosol properties in the Svalbard region. In: Gevers M et al. (eds) SESS report 2022, Svalbard Integrated Arctic Earth Observing System, Longyearbyen, pp 44-61, <https://doi.org/10.5281/zenodo.7376140>.

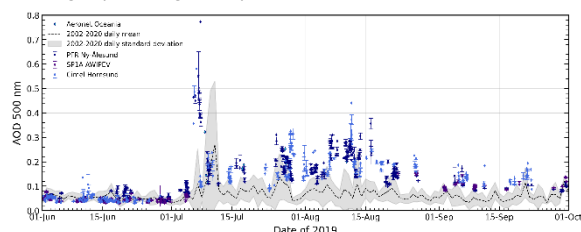


Fig. 1. Aerosol optical depth evolution from different remote sensing instruments in and around Svalbard.

Summer 2019 was an unusual year for the northern hemisphere. An increase in the background AOD was expected due to the huge wildfires happening in Siberia and Canada but also the eruptions on 21–22 June of the Raikoke volcano on the Kuril Islands in Russia. Interestingly, the observed columnar measurements did not usually correspond with in-situ measurements, highlighting an exceptional situation.

A comprehensive analysis of different parameters has been developed in the present study to understand the aerosol properties, distribution and origin during this period of exceptional aerosol loading observed in the Arctic during summer 2019.

## EXPLORING AEROSOL-CLOUD-PRECIPITATION DYNAMICS IN THE IBERIAN PENINSULA USING THE WRF-CHIMERE COUPLED MODEL

C. Gama<sup>1</sup>, D. Luís<sup>1</sup>, A. Ascenso<sup>1</sup>, C.L. Gonçalves<sup>1</sup>, Alexandra Monteiro<sup>1</sup> and I. Gorodetskaya<sup>2</sup>

<sup>1</sup>CESAM - Centre for Environmental and Marine Studies, Department of Environment and Planning, University of Aveiro, Aveiro, 3810-193, Portugal

<sup>2</sup>CIIMAR - Interdisciplinary Centre of Marine and Environmental Research, University of Porto, Matosinhos, 4450-208, Portugal

Keywords: atmospheric rivers, extreme precipitation, cloud microphysics, atmospheric aerosols  
Presenting author email: carlagama@ua.pt

In the Iberian Peninsula, extreme precipitation events are frequently associated with atmospheric rivers (ARs), which manifest as long, narrow bands of highly concentrated water vapor in the atmosphere. ARs are responsible for transporting large amounts of moisture across vast distances, often from tropical or subtropical regions to mid-latitudes or polar regions.

This study aims to better understand the processes driving the development of such events, in particular the role played by aerosols serving as ice and cloud condensation nuclei. We focus on the analysis of aerosol-cloud-precipitation interactions during two specific AR events that impacted the Iberian Peninsula: one on January 2013, associated with the explosive development of cyclone Gong, and another in December 2017, linked to storm Ana. Both events resulted in substantial rainfall and snowfall across the Northwest region of the Peninsula (see Figure 1).

Based on a modelling approach that couples the WRF meteorological model with the CHIMERE chemical transport model, we investigate aerosol-cloud interactions and their influence on cloud microphysics and precipitation formation. The modelling system provides insights into the spatial and temporal variability of emissions, transport, deposition, aerosol composition, size distribution, and simulates the two-way interaction between meteorological and chemical variables. We specifically characterize aerosol amounts and chemical properties in the North Atlantic and Iberian Peninsula, emphasizing contributions from long-range transport of desert dust, sea salt, biogenic, and anthropogenic aerosols.

Numerical simulations encompassing different aerosol types and emissions scenarios were conducted. This presentation discusses the modelled aerosol loadings and their impact on cloud microphysical properties, as well as the simulation of precipitation.

This work contributes to a better understanding of the importance of aerosols serving as ice and cloud condensation nuclei, and their contribution to generating extreme precipitation in Iberian Peninsula.

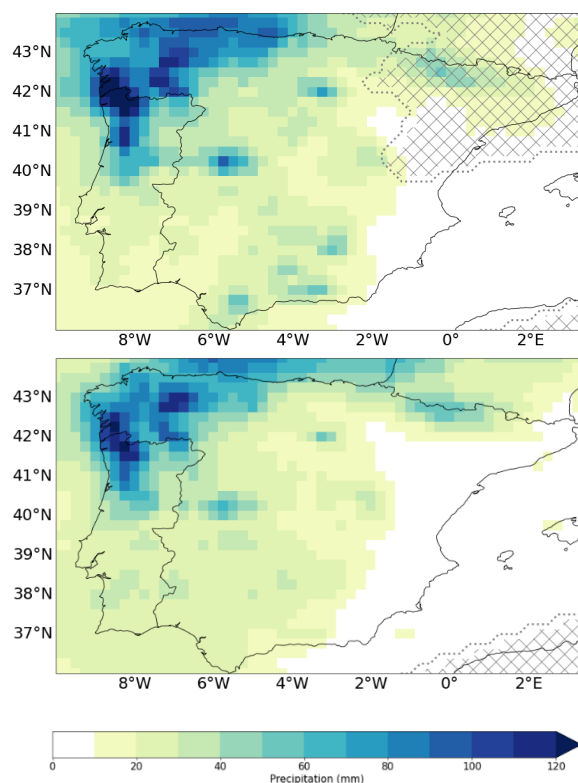


Fig. 1. Accumulated precipitation (mm) over the Iberian Peninsula from 17 to 19 January 2013 (top), and from 9 to 11 December 2017 (bottom), according to ERA5 reanalysis.

This work was supported by the ATLACE research project (CIRCNA/CAC/0273/2019), funded by the Portuguese Foundation for Science and Technology through national funds (OE).

## GLOBAL PHENOMENOLOGY OF CLOUD CONDENSATION NUCLEI AND PARTICLE NUMBER SIZE DISTRIBUTION: THE DOE/ARM NETWORK

I. Zabala<sup>1,2</sup>, J.A. Casquero-Vera<sup>1</sup>, E. Andrews<sup>3,4</sup>, G. Carrillo-Cardenas<sup>5</sup>, M. Ostlie<sup>5</sup>, S. Chu<sup>6</sup>, F. Yu<sup>6</sup>, A. G. Hallar<sup>5</sup> and G. Titos<sup>1,2</sup>

<sup>1</sup>Andalusian Institute for Earth System Research IISTA, University of Granada, 18071, Granada, Spain

<sup>2</sup>Department of Applied Physics, Faculty of Sciences, University of Granada, 18071, Granada, Spain

<sup>3</sup>CIRES, University of Colorado, Boulder, CO, 80309, United States

<sup>4</sup>Global Monitoring Laboratory, NOAA, Boulder, CO, 80305, United States

<sup>5</sup>Department of Atmospheric Sciences, Storm Peak Laboratory, University of Utah, Salt Lake City, UT 84112, United States

<sup>6</sup>Atmospheric Sciences Research Center, State University of New York, Albany, NY 12203, United States

Keywords: cloud condensation nuclei, new particle formation, particle size distribution

Presenting author email: inesabala@ugr.es

Aerosol-cloud interaction (ACI) constitutes the most significant uncertainty in anthropogenic radiative forcing (IPCC, 2021). One major source of this uncertainty is the lack of detailed knowledge about how particles evolve to become effective cloud condensation nuclei (CCN). CCN potential sources include both primary (anthropogenic and biogenic) and secondary aerosol particles. Among secondary particles, those formed by the new particle formation (NPF) process play a crucial role by forming thermodynamically stable clusters from condensable vapours that grow to sizes in the CCN range (Merikanto et al., 2009). Although modelling studies have suggested that NPF may have a strong impact on the abundance of CCN globally, the contribution of NPF to overall CCN concentration differs substantially in different models and for different environments (Yu and Luo, 2009). To reduce uncertainty in ACI, it is crucial to have a better understanding of aerosol properties on both large-scale/long-term and regional scale/short-term. Therefore, harmonized measurements of CCN concentration and particle number size distribution (PNSD) are essential (Hirshorn et al., 2022).

In order to contribute to this effort and to ensure measurement comparability on a global scale, in this work we present a quality-assured, long-term and regionally representative database of CCN concentration at different supersaturation (SS), PNSD, total particle concentration and CCN activation related parameters (critical diameter, hygroscopicity parameter and activation fraction) from multiple DOE ARM (Atmospheric Radiation Measurement facility of the US Department of Energy) sites. Figure 1 shows the location of the stations considered by indicating the instrumentation available (main and ancillary) for each site. To ensure quality of the data, a data analysis protocol has been developed and different analysis and closure studies have been carried out and included in the database. It is anticipated that this database will be useful in constraining modelling studies and may significantly enhance the accuracy of ACI simulations.

Stations are located on three continents covering a wide range of environments: coastal background, rural background, alpine sites, remote forests, urban and pristine polar locations. Here we study the spatio-temporal variability of atmospheric aerosol concentrations, CCN and the activation properties of atmospheric aerosol particles that become CCN. As expected, aerosol and CCN characteristics show a high variability among the diverse site types studied.

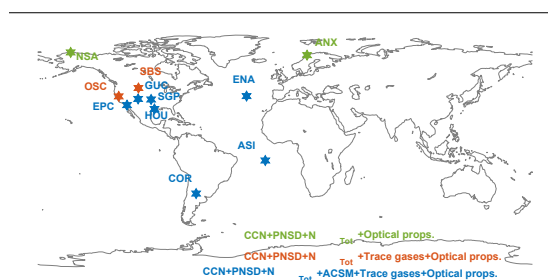


Figure 1. Map of DOE ARM surface sites and their measurements availability.

Seasonal variability of CCN concentrations and PNSD are observed at multiple stations. For example, the GUC site (high altitude) shows higher CCN concentration values in periods influenced by injections from the planetary boundary layer (predominantly in summer), the ASI site (coastal background) shows a large influence of wildfires during June–October and it is possible to distinguish between wet and dry seasons.

This work was supported by US Department of Energy under grant DE-SC0022886 and by the Scientific Unit of Excellence: Earth System (UCE-PP2017-02).

Hirshorn et al. (2022). *Atmos. Chem. Phys.*, 22, 15909-15924.

IPCC (2021). Chapter 7, Cambridge Uni. Press., 923-1054.

Merikanto et al. (2009) *Atmos. Chem. Phys.*, 9, 8601-8616.

Yu & Luo. (2009). *Atmos. Chem. Phys.*, 9, 7691-7710.

*RICTA2024*

**8<sup>th</sup> Iberian Meeting on Aerosol Science and Technology**



**Section 5. Oral Session III. Thursday,  
June 27<sup>th</sup> 10:00-11:00**

**Chairs: X. Querol, J. A. García Orza**

## EXPLORING GAS AND PARTICLE-PHASE POLLUTION FROM RICE STRAW BURNING IN THE VALENCIAN REGION

E. Borrás<sup>1</sup>, T. Vera<sup>1</sup>, T. Gómez<sup>1</sup>, M. Martínez<sup>1</sup>, R. Soler<sup>1</sup>, M. Ródenas<sup>1</sup>, E. Mantilla<sup>1</sup>, B. Domínguez<sup>1</sup>, E. Yubero<sup>2</sup>, J. Crespo<sup>2</sup>, J.F Nicolás<sup>2</sup>, N. Galindo<sup>2</sup>, M. Alfosea-Simón<sup>2</sup>, A. Muñoz<sup>\*1</sup>

<sup>1</sup>Fundación CEAM. EUPHORE Laboratories, C/ Charles R. Darwin 14, 46980, Paterna, Spain

<sup>2</sup>Miguel Hernández University, Atmospheric Pollution Laboratory, Avda. Universitat, s/n, 03202, Elche, Spain

Keywords: biomass burning, aerosol, pollutant emissions

Presenting author email: esther@ceam.es

Rice is one of the most widely cultivated cereals in the world. In Europe, rice cultivation is basically limited to Mediterranean countries, where Spain is the second largest European producer. There are some regions in Spain associated with rice production, being Levante (Valencia) the most important one, with a long cultural, social, and gastronomic tradition. The Valencian Community annually produces more than 60 kt of straw per year, and despite attempts to recycle this stubble or use it to produce building materials, a large proportion of it will be subject to a process of elimination by burning for sanitary reasons. The practice of burning it in the field has harmful effects on the environment and human health (Viana et al., 2008; Borrás et al., 2024).

The burning of rice straw, a common practice in many agricultural regions, remains a significant source of particulate and gaseous air pollution, causing frequent acute pollution episodes and exceedances of regulatory limits. However, there is a considerable lack of knowledge about the nature of these types of emissions and their potential health hazards, as well as their contribution to secondary pollution and in particular to photochemical processes.

Within this context, emissions and their chemical transformation were studied in the Valencia Region between 27/09/2023 and 02/11/2023 near a smoke-affected area. Using advanced analytical techniques to characterize the gas and the particle phase, a detailed evaluation of the components emitted during the burning of rice straw has been carried out. Various analytical instruments were used to characterize both gaseous and particle phases (PTRMS, NO<sub>x</sub>, O<sub>3</sub>, SO<sub>2</sub>, CO, CO<sub>2</sub> monitors, discrete cartridge sampling, aethalometers, nephelometer, PM low-cost sensors and PM<sub>10</sub> and PM<sub>2.5</sub> filters for offline analysis).

Throughout this period (26 days of permitted activity and prior authorization) a total of 750 burnings were carried out on 673 plots, affecting 16 municipalities, including the city of Valencia and its metropolitan area. The first results obtained show that particulate matter levels were strongly affected by the burning of nearby plots, with the maximum values obtained from 16 to 20 October, coinciding with the period when more plots and more hectares of stubble were burned (see Figure 1 and Table 1). These levels exceeded the permitted PM<sub>10</sub> daily limit values of 50 µg m<sup>-3</sup> and were well above the levels recommended by the WHO.

Table 1. Average aerosol mass concentrations (µg m<sup>-3</sup>).

	PM10 filter	PM2.5 filter	Grim-10	Grim-2.5	Grim-1
average	19.5	14.3	10.6	8.0	7.0
max	53.4	42.8	30.3	21.3	19.7
min	4.7	0.7	1.7	1.1	0.8

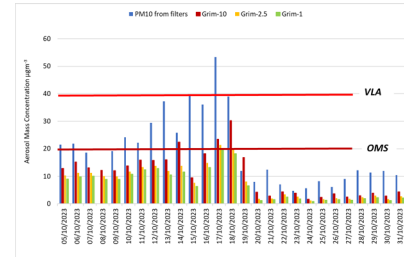


Fig. 1. Daily mean aerosol mass concentrations.

In addition, an exhaustive characterization of the aerosols generated has been carried out, highlighting the presence of fine particulate matter with potential impact on air quality and human health. The preliminary results show high levels of VOCs, PM<sub>10</sub>, PM<sub>2.5</sub> and PM<sub>1</sub> in the populated areas close to the burned plots. These emissions also caused elevated ozone levels up to 120 µg·m<sup>-3</sup> in the interior areas of the region, associated with high PM levels. These findings provide a deeper understanding of the complexity of emissions from rice straw burning and provide a solid foundation for future mitigation strategies and environmental policy development in the affected regions.

This work is part of a project that is supported by ATMOBE PID2022-1423660B-100 funded by MCIN/AEI/ 10.13039/501100011033 and, by "ERDF A way of making Europe" and by PROMETEO (EVER project) CIPROM/20200/372/.

Viana et al., 2008. Tracers and impact of open burning of rice straw residues on PM in Eastern Spain. *Atmos. Environ*, 42, 1941-1957.

Borrás et al., 2024. Analysis of combustion by-products of a construction material made with rice straw. In preparation.

## ON THE USE OF THERMODYNAMIC VARIABLES FOR ESTIMATING PROBABILITY OF AFRICAN DUST EVENTS OVER SPANISH REGIONS

P. Salvador<sup>1</sup>, J. Pey<sup>2</sup>, N. Pérez<sup>3</sup>, A. Alastuey<sup>3</sup>, X. Querol<sup>3</sup> and B. Artíñano<sup>1</sup>

<sup>1</sup>Department of Environment - Joint Research Unit Atmospheric Pollution CIEMAT-CSIC, CIEMAT, Madrid, 28040, Spain

<sup>2</sup>Instituto Pirenaico de Ecología, CSIC, Zaragoza, 50059, Spain

<sup>3</sup>Institute of of Environmental Assessment and Water Research, CSIC, Barcelona, 08034, Spain

Keywords: Desert dust, Atmospheric thermodynamics, Multilinear statistical models, Risk analysis

Presenting author email: pedro.salvador@ciemat.es

In the context of increasing dust transport towards southern Europe (Salvador et al. 2022), this study proposes a methodology for estimating the probability of occurrence of African dust events, over eight regions of the Iberian Peninsula (IP) and the Balearic Islands (BI) (SE-IP, SW-IP, E-IP, central-IP, NE-IP, N-IP, NW-IP and BI areas). In each region, a multilinear regression model was created to obtain daily probabilities of dust events using 3 thermodynamic variables (GT: geopotential thickness in the 1000 – 500 hPa layer; TPOT: mean potential temperature between 925 and 700 hPa; TANOM: temperature anomalies at 850 hPa) as assessing parameters.

First, all days with African dust transport over each region of study, were identified in the period 2001–2021 with a tried-and-true procedure (Pey et al., 2013). This information was used to obtain a functional relationship between the values of the thermodynamic parameters and the development of the dust events. The daily African dust contribution to PM<sub>10</sub> regional background levels in each region was also estimated for each episodic day (Pey et al., 2013). Then, the daily probability with which dust events happened was determined over each region when different threshold values of the parameters were exceeded. Finally, multilinear regression techniques were applied to create a statistical prediction model for daily probability of dust events as a function of the daily average values of the assessing parameters. The Box-Cox and the Cochrane-Orcutt procedures were applied to improve the linear fit of the initial models and to avoid autocorrelation between the error terms. Final models were valid in all study regions. No autocorrelation between the residuals or heteroscedasticity in the data were detected in any of them and the R<sup>2</sup> values ranged from 83.7% in the SE-IP zone to 87.5% in the NW-IP zone (Fig. 1). Moreover, a very well-defined seasonal evolution of the probability values was obtained in all regions, with the highest values in the summer months and the lowest in the winter period. The study further established that days with higher probabilities of occurrence also exhibit elevated dust contributions, indicating a direct relationship between the thermodynamic properties of allochthonous air masses and the transported dust load to the surface. Importantly, each region has a probability threshold value above which the median daily dust contribution surpasses zero, signifying an increased likelihood of

impactful African dust events. They can serve as warning indicators, effectively alerting sensitive populations to the potential occurrence of such events. This methodology aligns with the WHO Air Quality Guidelines requirements, regarding the creation of early warning systems for dust storms (WHO, 2021).

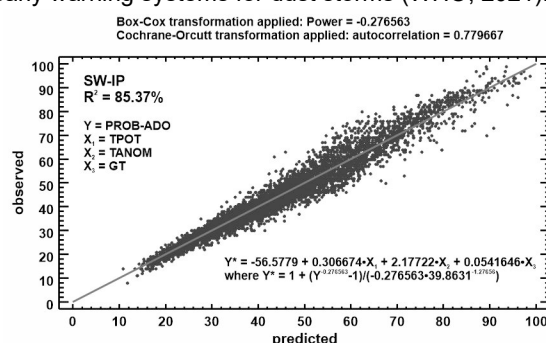


Fig. 1. Comparison of observed probability of occurrence of African dust outbreaks (PROB-ADO) in the SW region of the Iberian Peninsula (SW-IP) and predicted with the multilinear regression model in 2001–2021.

This work was supported by POSAHPI-2 (State Research Agency, grant PID2022-143146OB-I00), and ASAH-AS (Grants for scientific research projects in the National Parks Network for the year 2021, Spanish Ministry for the Ecological Transition and the Demographic Challenge, ref. 2799/2021) projects.

Pey J., Querol X., Alastuey A., Forastiere F., Stafoggia M. (2013). African dust outbreaks over the Mediterranean Basin during 2001–2011: PM<sub>10</sub> concentrations, phenomenology and trends, and its relation with synoptic and mesoscale meteorology. *Atmos. Chem. Phys.* 13, 1395–1410.

Salvador P., Pey, J., Pérez, N., Querol, X., Artíñano, B. (2022). Increasing atmospheric dust transport towards the western Mediterranean over 1948–2020. *NPJ Clim. Atmos. Sci.* 5:34.

World Health Organization (2021). WHO global air quality guidelines. Particulate matter (PM<sub>2.5</sub> and PM<sub>10</sub>), ozone, nitrogen dioxide, sulfur dioxide and carbon monoxide. Geneva. Licence: CC BY-NC-SA 3.0 IGO.

## FORMATION AND IMPACT OF A WINTER SHAMAL DUST STORM OVER THE MIDDLE EAST

S. Karbasi<sup>1</sup>, E. Chham<sup>1</sup> and J.A.G. Orza<sup>1</sup>

<sup>1</sup>SCOLab, Department of Applied Physics, Universidad Miguel Hernandez de Elche, Elche, 03202, Spain

Keywords: dust storm, Middle East, air quality, aerosol observations

Presenting author email: skarbasi@umh.es

The Middle East is one of the regions in the world affected by severe dust storms. Dust events are frequent throughout the year but the time of the maximum dust activity is different in different parts of the Middle East. While dust events are more active during winter and spring in the north, their maximum activity with the greater intensity occurs in the summer in the southwest of the region. Middle East is affected by frontal dust storms mainly in winter and by Shamal dust storms mostly in summer.

Surface and satellite observations as well as ERA5 reanalysis data were used to describe the formation and evolution of a winter shamal dust storm that occurred in February 2017. It initiated in central western Iraq and dust was transported southeastward towards the Persian Gulf, impacting all the countries in the region up to the Oman Sea.

The SEVIRI Dust RGB product shows dust mobilization at 07 UTC (10 LT) in several point areas west of the Euphrates River and over Mesopotamia, in Iraq. A dense dust plume is then advected in between the Zagros Mountains to the North and East and the high plains of Saudi Arabia to the South and West, reaching the Persian Gulf in the first hours of February 18. Next day, dust spreads throughout the Persian Gulf and surrounding countries. The dust plume is well seen in the true color MODIS imagery of February 17, 18, and 19. It resulted in the widespread reduction of horizontal visibility and impaired air quality, as reported by the region's Synop/METAR surface observations and air quality stations.

The large-scale upper-level processes leading to this event started days before with a strong amplification of an anticyclonic Rossby wave break in the Polar Jet over the North East Atlantic, with large penetration poleward of subtropical air up to Scandinavia and cold air advection equatorward over Iberia on February 11. At a late dissipative stage and downstream displacement, the RWB resulted in a closed ridge over southeastern Europe and Turkey and in a trough downstream over the study area. A strong pressure gradient was established at low levels between high pressures centered over southeastern Europe and the Black Sea and low pressures over the Persian Gulf with minima over the Arabian Peninsula and over Iran to the north of the Zagros Mountains. On February 17, the location of the trough favored descent associated with transverse circulations on the upstream side of the trough over the mountains in eastern Turkey and northern Iraq, reinforcing the northerly winds imposed

by the pressure gradient. Strong northerly downslope winds on the lee of the mountains in southern Turkey deflated dust in source areas of northern Iraq and Syria. Dust plumes were transported southeastward at heights below 2 km, as shown by CALIPSO profiles in February 18, within the PBL. On February 19, the dust plume was mixed all over the Persian Gulf basin.

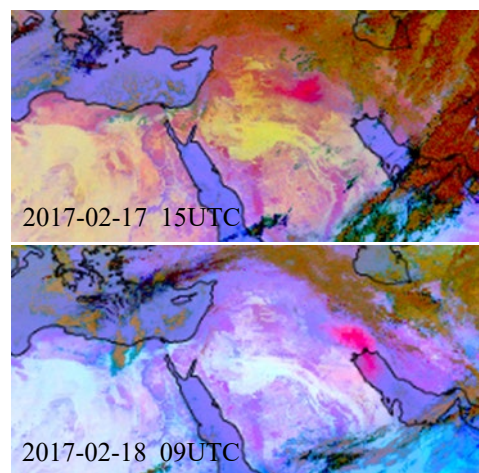


Fig. 1. Displacement of the dust plume through Iraq to the Persian Gulf, from MSG41.5 Dust RGB imagery.

This work was supported by MCIN/AEI/10.13039/501100011033 under Grant PID2020-115153RB-I00 (rROSSETA Project).

## EMERGING EXTREME DUST EVENTS PROMPTS RECORD BEATING PM<sub>10</sub> AND PM<sub>2.5</sub> EPISODES IN SPAIN

S. Rodríguez<sup>1</sup>, J. López Darías<sup>1</sup>

<sup>1</sup>Group of Atmosphere, Aerosols and Climate (GAAC), Consejo Superior de Investigaciones Científicas, IPNA CSIC, La Laguna, Tenerife, Spain

Keywords: Saharan dust, extreme dust events, climate change  
Presenting author email: sergio.rodriguez@csic.es

The influence of climate change on the emissions and transport of desert dust (Kok et al., 2023) is a topic of major interest due to the important socio-economic impacts of the severe dust events (Middleton et al., 2021). Within the frame of the AEROEXTREME project we studied the six extreme Saharan dust episodes occurred between February 2020 and March 2022. This study is based on the analysis of (i) the 2000-2022 PM<sub>10</sub> and PM<sub>2.5</sub> data of the air quality monitoring stations provided by the Ministry for the Ecological Transition and the Demographic Challenge of Spain, (ii) NCEP/NCAR meteorological reanalysis and (iii) MERRA-2 dust modelling reanalysis.

We analysed the data of 330 air quality monitoring stations of Spain, where PM<sub>10</sub> and PM<sub>2.5</sub> concentrations are measured with European EN-standards (12341:2015 and 16450:2017), and found that during the observed six extreme dust events PM<sub>10</sub> concentrations are underestimated due to technical limitations of many PM<sub>10</sub> monitors to properly measure extremely high concentrations (> 1000 µg/m<sup>3</sup>). We assessed the consistency of PM<sub>10</sub> and PM<sub>2.5</sub> data and reconstructed about 1500 PM<sub>10</sub> (1h average) data of ~ 50 air quality monitoring stations by using our novel *duxt-r* method. We processed the PM<sub>10</sub> and PM<sub>2.5</sub> data of the period 2000-2022, and found that these extreme dust events have no precedent in Spain. During these extreme dust events the 1-hour average PM<sub>10</sub> and PM<sub>2.5</sub> concentrations were within the range 1000-6000 µg/m<sup>3</sup> and 400-1200 µg/m<sup>3</sup>, respectively.

The event occurred 22-29 of February 2020 event led to (24h average) PM<sub>10</sub> and PM<sub>2.5</sub> values within the range 600-1850 µg/m<sup>3</sup> and 200-405 µg/m<sup>3</sup> in the Canary Islands and within the range 80-150 µg/m<sup>3</sup> and 50-100 µg/m<sup>3</sup> in the central (Madrid and Castilla La Mancha) and eastern (Comunidad Valenciana) parts of mainland Spain, respectively, being the most intense dust episodes ever recorded in the Canary Islands.

The event occurred 14–20 March 2022 led to (24h average) PM<sub>10</sub> and PM<sub>2.5</sub> values within the range 500-3100 µg/m<sup>3</sup> and 100-700 µg/m<sup>3</sup> in south-eastern (Almería and Granada provinces), 200-1000 µg/m<sup>3</sup> and 60-260 µg/m<sup>3</sup> in central (Castilla La Mancha, Extremadura, Madrid and Castilla León) and 150-500 µg/m<sup>3</sup> and 75-130 µg/m<sup>3</sup> in northern (Galicia and Cantabria) regions of mainland Spain and to 150-430 µg/m<sup>3</sup> and 30-80 µg/m<sup>3</sup> in the Canary Islands, respectively, being the most intense dust episode ever recorded in mainland Spain.

We also analysed the meteorological scenarios in which these extreme dust events occurs and found that they are associated with northern hemisphere meteorological anomalies consistent with the changes in the atmospheric dynamic attributed to the anthropogenic global warming, according to climate projections. The results of this study evidence that the current technical specifications of many PM<sub>10</sub> and PM<sub>2.5</sub> monitors used in air quality monitoring networks is not suitable during these emerging extreme dust events

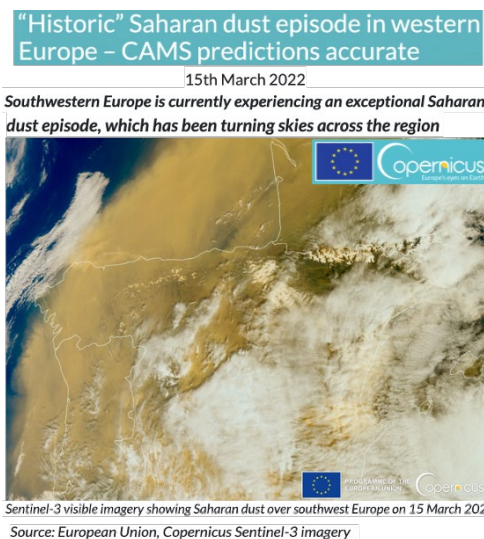


Fig. 1. Satellite image of the extreme dust event occurred 15 March 2022 in the Copernicus platform

This study is part of the project AERO-EXTREME (PID2021-125669NB-I00) funded by the funded by the State Research Agency/Agencia Estatal de Investigación of Spain and the European Regional Development Funds.

Kok et al. (2023). Mineral dust aerosol impacts on global climate and climate change, *Nat. Rev. Earth Environ.*, 4(2), 71–86, doi:10.1038/s43017-022-00379-5, 2023.

Middleton et al. (2021). Synoptic Causes and Socio-Economic Consequences of a Severe Dust Storm in the Middle East, *Atmosphere*, 12(11), 1435, doi:10.3390/atmos12111435, 2021.

*RICTA2024*

**8<sup>th</sup> Iberian Meeting on Aerosol Science and Technology**



**Section 6. Oral Session IV. Thursday,  
June 27<sup>th</sup> 11:45-13:15**

**Chairs: A. Alastuey, J. de la Rosa**

## DEFINING THE MECHANISMS OF AIR PARTICLES TOXICITY USING *IN VIVO* STRESS RESPONSE BIOMARKERS

F. Iñesta Vaquera<sup>1,2</sup>, E.C. Pinilla Gil<sup>3</sup> and C.R. Wolf<sup>2</sup>

<sup>1</sup>Department of Biochemistry and Molecular Biology, University of Extremadura, Badajoz, 06006, Spain.

<sup>2</sup>Division of Systems Medicine, University of Dundee, Dundee, DD1 4HN, U.K.

<sup>3</sup>Department of Analytical Chemistry, University of Extremadura, Badajoz, 06006, Spain.

Keywords: Air pollution; Biomarker; Diesel particles; Mechanism of toxicity

Presenting author email: finestavaquera@unex.es

Air pollution can cause a wide range of serious human diseases. For the informed instigation of interventions which prevent these outcomes there is an urgent need to develop robust *in vivo* biomarkers which provide insights into mechanisms of toxicity and relate air particles to specific adverse outcomes. We propose the application of *in vivo* stress response reporters to establish a hazard ranking and identify toxic mechanisms of air particles and the application of this knowledge in epidemiological studies (Figure 1; Inesta-Vaquera, 2021; 2023).

We demonstrated the utility of reporter mice to understand toxicity mechanisms of air particulate and components thereof. First, we observed that nitro-PAHs (i.e. 3-nitro-fluoranthene and 1-nitro-pyrene, common components of combustion derived particles) induced Hmox1 and CYP1a1 reporters in a time- and dose-dependent, cell- and tissue-specific manner. Using *in vivo* genetic and pharmacological approaches we confirmed that the NRF2 pathway mediated this Hmox1-reporter induction stress reporter activity. In addition, we studied the contribution to compound toxicity of cell metabolism on the activation of nitro-PAHs. We observed that *in vivo* metabolic activation of reporter mice enhanced Hmox1-reporter expression as a response to nitro-PAH exposure.

We also observed the activation of the Hmox1-reporter when mice were exposed to particulate mixtures from different emission scenarios. Reporter mice were subjected to a single oropharyngeal deposition (250 µg/mice), or 5 doses (50µg each, once every 24h) of reference particulate material (PM) PM<sub>10</sub> (SRM1648b), but not PM<sub>2.5</sub> (SRM2975) activated the *in vivo* reporter. In particular, we observed a strong induction in lung immune cells that were in direct contact with particles (Figure 2). We then correlated the activation of stress-reporter models (oxidative stress/inflammation, DNA damage and Ah receptor -AhR- activity) with responses in primary human nasal cells (HPNEpC) exposed to chemicals present in particulate matter (PM<sub>2.5</sub>, PM<sub>10</sub>) or fresh London roadside PM<sub>10</sub>. To exemplify their use in clinical studies, Pneumococcal adhesion was assessed in HPNEpC. The combined use of HPNEpC and *in vivo* reporters demonstrated that London roadside PM<sub>10</sub> particles induced pneumococcal infection in HPNEpC mediated by oxidative stress responses.

The combined use of *in vivo* reporter models with human data thus provides a robust approach to define the relationship between air pollutant exposure and

health risks. Moreover, these models can be used in epidemiological studies to hazard ranking environmental pollutants by considering the complexity of mechanisms of toxicity.

### oxidative stress / inflammation

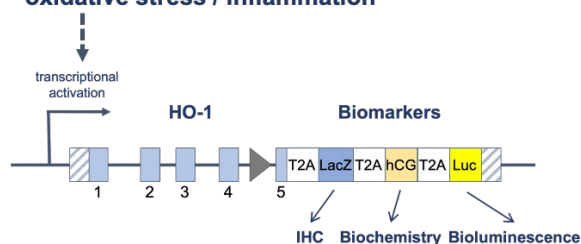


Fig. 1. Schematic representation of *in vivo* Hmox1 reporter. Other models exist for DNA damage (p53-p21 reporter), xenobiotic metabolism (hCAR-hPXR and AhR reporters) or inflammation (AP-1 reporter)

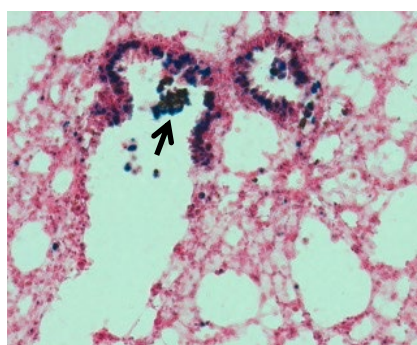


Fig. 2. Hmox1-reporter positive cells (LacZ blue staining; arrow) surround PM<sub>10</sub> (SRM1658b) particles after mouse lung deposition.

This presentation was supported by a Medical Research Council (UK) Project Grant (MR/R009848/1) and a Junta de Extremadura – University of Extremadura partnership (REPICA).

Inesta-Vaquera, F., et al. (2023) Defining the *in vivo* mechanism of air pollutant toxicity using murine stress response biomarkers. *Science of the Total Environment*, 888, 164211.

Inesta-Vaquera, F., et al. (2021) Application of the *in vivo* oxidative stress reporter Hmox1 as mechanistic biomarker of arsenic toxicity. *Environmental Pollution*, 270, 116053.

## AIR PURIFICATION TO MINIMISE OCCUPATIONAL EXPOSURE TO INCIDENTAL NANOPARTICLES IN INDUSTRIAL SETTINGS

V. San Félix<sup>(1)</sup>, E. Monfort<sup>(1)</sup>, D. Bou<sup>(1)</sup>, M. Viana<sup>(2)</sup>, V. Moreno<sup>(2)</sup>, A. Sánchez<sup>(3)</sup>, A.E. Sereno<sup>(3)</sup>

(1) Instituto de Tecnología Cerámica (ITC-AICE). Universitat Jaume I, Castelló, 12006, Spain.

(2) IDAEA-CSIC, Barcelona, 08034, Spain.

(3) ASP-ASEPSIA, Pinto (Madrid), 28320, Spain.

Keywords: incidental nanoparticles, occupational exposure, air purifier, industrial settings

Presenting author email: vicenta.sanfelix@itc.uji.es

Incidental nanoparticles (INPs) can be generated during different high-energy processes, both thermal and mechanical, such as burning fuels, plasma cutting, welding, metal grinding, laser ablation, iron casting, firing, thermal spraying, etc. (vanBroekhuizen, 2017). These industrial processes can be defined as permanent releasers of INPs (up to several millions of NP/cm<sup>3</sup>) which may lead to chronic exposures if these sources are not recognized as such and if control measures are omitted or not adequately designed.

To control and minimise INPs emissions in industrial settings, within the framework of the LIFE NANOHEALTH project, the consortium is working on the development of three technological solutions to minimise the exposure to this type of nanoparticles, one of them being the design and manufacture of a prototype air purifier.

In designing the purifier, the INPs emissions generated in two high-energy thermal processes have been assessed: thermal spraying of ceramic coatings and ceramic tile firing. Both processes have been evaluated in two industrial plants, under real operating conditions, which show a different degree of implementation of corrective measures. INPs emissions near the emission sources and impacts on workers' areas were evaluated (Ostraat et al., 2015).

Table 1. Concentrations and size values obtained in the worker area in the industrial processes evaluated.

Parameter	Thermal spraying	Ceramic tile firing
C <sub>PM10</sub> Average (µg/m <sup>3</sup> )	113	136
C <sub>PM2.5</sub> Average (µg/m <sup>3</sup> )	39	46
C <sub>INP</sub> Average (#/cm <sup>3</sup> )	53 690	251 436
C <sub>INP</sub> Perc90 (#/cm <sup>3</sup> )	115 088	335 122
INP Average size (nm)	56	57

The experimental data showed that INPs were generated inside the thermal spraying booths and kiln combustion chamber but were released to the workers' area due to the presence of openings or leaks, being the INP concentrations in some working areas higher than the proposed Nano Reference Value ( $4 \cdot 10^4$  #/cm<sup>3</sup>) (Table 1) (vanBroekhuizen, 2017). These results confirmed the need to test the air purifier to minimise the occupational exposure to INPs.

To this end, an air purifier prototype has been designed and manufactured. The prototype should be able to respond to these high concentrations in the most unfavourable situations and to achieve an INP removal

efficiency of more than 90% over an area of 600 m<sup>2</sup> in the worker's area.

The main technical specifications of the designed prototype are:

- Airflow: Adjustable airflow with a maximum of 12000 m<sup>3</sup>/h, allowing operational flexibility based on environmental needs and energy efficiency, and achieving a high number of air changes per hour (ACH) in the working area.
- Advanced filtration system: three filtration systems, containing filters for capturing coarser particles down to nanoparticles.
- Control of filters saturation: assessment of particulate matter captured by the filters.
- Online Control: monitoring and control via a web platform.
- Easy mobility: fitted with wheels for positioning in areas with the highest particulate matter concentrations.

The purifier is currently being evaluated for its effectiveness in reducing the concentrations of the micro fraction of particulate matter (PM10 and PM2.5) and INP in the two industrial environments previously evaluated.

### References

- Ostraat, M., Engel, S., Swain, K.A., Kuhlbusch, T.A.J., Asbach, C. (2015). Harmonised Tiered Approach to Measure and Assess the Potential Exposure to Airborne Emissions of Engineered Nano-Objects and their Agglomerates and Aggregates at Workplaces Series on the Safety of Manufactured Nanomaterials.No.55ENV/JM/MONO(2015)19. Paris (France):OECD Environment, Health and Safety Publications.
- Van Broekhuizen, P., 2017. Applicability of provisional NRVs to PGNPs and FCNPs. KLB.DOI:10.13140/RG2.2.18241.25445. BUREAU.

### Acknowledgement

The project LIFE NANOHEALTH is funded by the LIFE Programme of the European Union under the project number LIFE20 ENV/ES/000187 and co-financed by the Generalitat Valenciana, through IVACE

## INDOOR/OUTDOOR MICROPLASTICS ANALYSIS BY THERMOGRAVIMETRIC-BASED TECHNIQUES: THE MADRID'S CITY CASE OF STUDY

J. Cárdenas-Escudero<sup>1\*</sup>, J. Ayuso Haro<sup>1</sup>, S. Deylami<sup>1</sup>, M. López Ochoa<sup>1</sup>, J. Urraca Ruiz<sup>1</sup>, D. Galán- Madruga<sup>2</sup>, J.O. Caceres<sup>1</sup>

<sup>1</sup>Laser Chemistry Research Group, Department of Analytical Chemistry, Faculty of Chemistry, Complutense University of Madrid, 28040 Madrid, Spain

<sup>2</sup>National Centre for Environmental Health, Carlos III Health Institute, Ctra. Majadahonda-Pozuelo km 2.2, 28220 Majadahonda, Madrid, Spain

Keywords: microplastics, atmospheric aerosols, thermogravimetric analysis, infrared spectroscopy

\*Presenting author email: jafetcar@ucm.es

This work was aimed to identify, characterize, and quantify microplastics present in indoor and outdoor environments of the Madrid's City, due to the lack of specialized studies of these emerging contaminants in the big cities (Huang et al. 2020). In recent years, a significant amount of evidence has been collected that has revealed the significant polluting capacity of microplastics in the environment and their special impact on human health (Amato-Lourenço et al. 2020), making this line of research relevant today. To execute the study, aerosol samples were collected from indoor and outdoor environments in the city of Madrid, during an annual campaign (2017-2018).

results obtained will be presented and discussed at the 8<sup>th</sup> edition of the Iberian Meeting on Aerosol Science and Technology (RICTA 2024), in A Coruña, Spain.

This work has been developed with the financial auspices of the Ministry of Science, Innovation and Universities, the State Research Agency and the EU through the European Regional Development Fund (FEDER).

Amato-Lourenço, L. F., L. dos Santos Galvão, L. A. de Weger, P. S. Hiemstra, M. G. Vijver & T. Mauad (2020) An emerging class of air pollutants: Potential effects of microplastics to respiratory human health? *Science of The Total Environment*, 749, 141676.

Huang, Y., X. Qing, W. Wang, G. Han & J. Wang (2020) Mini-review on current studies of airborne microplastics: Analytical methods, occurrence, sources, fate and potential risk to human beings. *TrAC Trends in Analytical Chemistry*, 125, 115821.

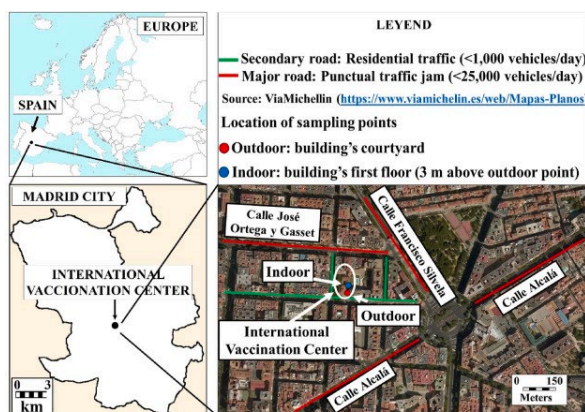


Figure 1. Geographical location of the indoor and outdoor environment sampling points within the City of Madrid, and diagram of the surrounding area.

For subsequent analysis, the samples were directly analyzed using a strategic combination of analytical techniques based on thermogravimetric analysis (TGA) such as Differential Scanning Calorimetry (TGA-DSC) and Fourier Transform Infrared Spectroscopy (TGA-FTIR), depending on the presence of at least one single thermal degradation product for use as a marker in the identification and quantification process. The results emphasize the complementarity of the analytical TGA-based methods, and their potential to play a role as a rapid and simple method that can help improve the resolution of complex aerosol analysis that can guide the chemical identification of microplastics in environmental samples and address the current needs of airborne-microplastics analysis techniques. The

## ASSESSMENT OF MICROPLASTIC PRESENCE IN MADRID'S ATMOSPHERIC ENVIRONMENTS: INDOOR VS. OUTDOOR AIR SAMPLES

S. Deylami<sup>1\*</sup>, J. Ayuso Haro<sup>1</sup>, M. López Ochoa<sup>1</sup>, J. Cárdenas-Escudero<sup>1</sup>, J. Urraca Ruiz<sup>1</sup>, D. Galán- Madruga<sup>2</sup>, J.O. Caceres<sup>1</sup>

<sup>1</sup> Laser Chemistry Research Group, Department of Analytical Chemistry, Faculty of Chemistry, Complutense University of Madrid, Plaza de Ciencias 1, 28040 Madrid, Spain

<sup>2</sup> National Centre for Environmental Health, Carlos III Health Institute, Ctra. Majadahonda-Pozuelo km 2.2, 28220 Majadahonda, Madrid, Spain

Keywords: Airborne microplastics, Outdoor and indoor, Raman spectroscopy, particulate matter.

\*Presenting author email: sdeylami@ucm.es

This study aims to identify, characterize, and quantify microplastics in indoor and outdoor air samples from Madrid City with dynamic diameters below 10 $\mu$ m (PM<sub>10</sub>). Microplastics are small synthetic particles that are found in a variety of ecosystems. However, compared to their counterparts in water and on land, airborne microplastics have not gotten as much attention, and it has been established that Madrid City requires immediate assessment to monitor and identify microplastics to prevent inhalation problems and reduce health problems (Sharaf Din et al., 2024). For this purpose, the work has been carried out using the Fourier transform infrared spectroscopy (FTIR) technique with attenuated total reflectance (ATR) mode (ATR-FTIR) and the  $\mu$ Raman spectroscopy, as in other similar works in big cities (Lin et al., 2018). The findings demonstrate that microplastics are widely distributed in both indoor and outdoor aerosol (PM<sub>10</sub>) samples, with indoor contribution levels being higher than in outdoor, suggesting that textiles and clothing are the main sources. Transparent and black-coloured particles were widespread in both settings, although fibre-shaped microplastics were more common, followed by fragments. ATR-FTIR and  $\mu$ -Raman studies indicated that the primary polymers identified were polyethylene terephthalate (PET), polyethylene (PE), polypropylene (PP), and polystyrene (PS). Particle surfaces showed evidence of weathering from Scanning Electronic Microscopy (SEM) analysis, and Energy Dispersive X-ray spectroscopy detector coupled with SEM (SEM-EDX) identified the essential elements carbon (C) and oxygen (O), interestingly in combination with heavy metals, occasionally. The lack of specialized research on microplastics in urban areas, such as Madrid's City, is filled by these efforts, which is important given the growing evidence about microplastic pollution in the environment and their related human health impact. All these results will be presented in the 8<sup>th</sup> Edition of the Iberian Meeting on Aerosol Science and Technology (RICTA 2024), in A Coruña, Spain.

This work has been developed through the Project CPP2022-009754, with the financial auspices of the Ministry of Science, Innovation and Universities, the State Research Agency, and the EU through the European Regional Development Fund (FEDER).



Figure 1. (A) Geographical location of Madrid city in Spain. (B) localization of the sampling points. (C): Equipment has been installed at the following locations: outdoor: 40° 25' 43.08" N-3° 40' 18.37" W, and indoor: 40° 25' 43.75" N-3° 40' 18.92" W in the international vaccination Center of Madrid city.

Lin L, Zuo L-Z, Peng J-P, Cai L-Q, Fok L, Yan Y, et al. Occurrence and distribution of microplastics in an urban river: A case study in the Pearl River along Guangzhou City, China. *Science of The Total Environment* 2018; 644: 375-381.

Sharaf Din K, Khokhar MF, Butt SI, Qadir A, Younas F. Exploration of microplastic concentration in indoor and outdoor air samples: Morphological, polymeric, and elemental analysis. *Sci Total Environ* 2024; 908: 168398.

## INHALATION/ORAL BIOACCESSIBILITY/BIOAVAILABILITY OF POLLUTANTS ASSOCIATED TO ATMOSPHERIC PARTICULATE MATTER BY USING SIMULATED BODY FLUIDS

J. Sánchez-Piñero, N. Novo-Quiza, J. Moreda-Piñeiro, S. Muniategui-Lorenzo and P. López-Mahía  
University of A Coruña. Grupo Química Analítica Aplicada (QANAP). University Institute of Environment (IUMA).  
Department of Chemistry, Faculty of Sciences, Campus de A Coruña, s/n. 15071 – A Coruña, Spain.

Keywords: Inhalation/oral bioaccessibility, inhalation/oral bioavailability, particulate matter, simulated biological fluids

Presenting author email: joel.sanchez@udc.es

Urbanization and industrialization are accompanied by the emission of significant amounts of pollutants, which have a significant impact on air quality, global climate change, and pose a risk to human health. Atmospheric particulate matter (PM) is a major air pollutant composed of a wide range of solid and liquid particles with different properties (e.g., composition, sizes, shapes, and optical properties) and several epidemiologic studies have associated PM exposure to adverse human health outcomes. Their toxicity is mostly attributed to particle size (i.e., fractions comprising particles  $\leq 10 \mu\text{m}$  of aerodynamic diameter such as  $\text{PM}_{10}$  and  $\text{PM}_{2.5}$ , due to their potential to penetrate and deposit in different regions of respiratory system after inhalation) and to PM-associated pollutants (potential contributors to PM toxicity) (Kastury et al., 2017).

As posing a great risk, target values for several PM metrics and reduction policies were set by governments, which are currently based on the total pollutant content in PM. In the last decades, research on PM and its association to health have been focused on the study of bioaccessibility (i.e., compounds dissolved in human fluids) and bioavailability (i.e., bioaccessible compounds which can also reach to bloodstream by crossing biological membranes) since providing valuable information of how substances may interact with organisms and more realistic health risks assessment (Kastury et al., 2017; Innes et al., 2021). For their assessment, *in vitro* physiologically-based extraction tests (PBETs) have been the most preferred techniques, involving an incubation of samples in simulated biological fluids under conditions similar to human body, whereas a dialysis membrane filled with simulated human plasma (SBF) could be also included to simulate biological membranes for bioavailability assessment (Ren et al., 2020; Lu et al., 2021; Zhao et al., 2021).

In this research, the study of the inhalation and oral bioaccessibility and bioavailability of metal(oid)s and organic pollutants associated with PM was conducted by using *in vitro* PBETs, providing information which could help with understanding PM toxicity mechanisms. Additionally, possible correlations between bioaccessible/bioavailable ratios and PM components (i.e., trace metal(oid)s and major ions), optical properties (i.e., equivalent black carbon (eBC)

and UV-absorbing particulate matter (UVPM)) and oxidative potential will be explored, whereas health risk assessment following USEPA's guidelines using bioaccessible/bioavailable concentrations will be also conducted.

This work was supported by Ministerio de Ciencia e Innovación (MCIN), the Agencia Estatal de Investigación and the European Regional Development Fund (ref: PID2021-125201OB-I00) and the Xunta de Galicia (ref: ED431C 2021/56. N. Novo-Quiza acknowledges the MCIN and the European Union for a predoctoral grant (PRE2019-088744). J. Sánchez-Piñero acknowledges the Xunta de Galicia (Consellería de Cultura, Educación e Universidade) for a postdoctoral grant (ED481B-2022-002). The Laboratorio de Medio Ambiente de Galicia (LMAG) of the Subdirección Xeral de Meteoroloxía e Cambio Climático (Xunta de Galicia) is also acknowledged for providing the samples used in the present research work. The authors would like to thank P. Esperón (MCIU-PTA2018-016005-I).

Kastury, F., Smith, E., Juhasz, A.L. (2017) A critical review of approaches and limitations of inhalation bioavailability and bioaccessibility of metal(loid)s from ambient particulate matter or dust. *Science of the Total Environment*, 574, 1054–1074.

Innes, E., Yiu, H.H.P., McLeaa, P., Brow, W., Boyles, M. (2021) Simulated biological fluids – a systematic review of their biological relevance and use in relation to inhalation toxicology of particles and fibres. *Critical Reviews in Toxicology*, 51, 217–248.

Ren H., Yu Y., An T. (2020) Bioaccessibilities of metal(loid)s and organic contaminants in particulates measured in simulated human lung fluids: A critical review. *Environmental Pollution*, 265, 115070.

Lu, M., Li, G., Yang, Y., Yu, Y. (2021) A review on *in vitro* oral bioaccessibility of organic pollutants and its application in human exposure assessment. *Science of the Total Environment*, 752, 142001.

Zhao, Z., Luo, X-s, Jing, Y., Li, H., Pang, Y., Wu, L., Chen, Q., Jin, L. (2021). *In vitro* assessments of bioaccessibility and bioavailability of  $\text{PM}_{2.5}$  trace metals in respiratory and digestive systems and their oxidative potential. *Journal of Hazardous Materials*, 409, 124638.

## STRUCTURAL FEATURES AND HEALTH EFFECTS OF WATER-SOLUBLE ORGANIC MATTER FROM ATMOSPHERIC FINE AIR PARTICULATES

Antoine S. Almeida<sup>1</sup>, Bruno M. Neves<sup>2</sup>, Regina M. B. O. Duarte<sup>1</sup>

<sup>1</sup>CESAM – Centre for Environmental and Marine Studies, Department of Chemistry, University of Aveiro, 3810-193 Aveiro, Portugal;

<sup>2</sup>Department of Medical Sciences and Institute of Biomedicine - iBiMED, University of Aveiro, 3810-193 Aveiro, Portugal;

Keywords: fine aerosols; water-soluble organic matter; structural characterization, inflammatory effects

Presenting author email: antoinealmeida@ua.pt

Fine atmospheric particulate matter (PM<sub>2.5</sub>, < 2.5 μm) exposure has been recognized as a key public health issue (Murray, C. J. L., 2020). Exposure to atmospheric aerosols has been linked with increased risks of lung cancer, cardiovascular, and respiratory diseases. In addition, PM exposure affects the immune system, leading to an increased susceptibility to infections and pathogens, or exacerbating other pre-existent lung diseases (Buonfiglio, L. G. V., 2020). The main mechanisms through which PM<sub>2.5</sub> can affect the human health, include the induction of reactive oxygen species (ROS), the triggering or exacerbation of an inflammatory response, and PM-related direct cytotoxicity, with these effects mostly affecting lung cells (Feng, S., 2016). These toxicological effects have been associated with PM<sub>2.5</sub> concentration, and its composition in metals and solvent-extractable organics (Casee, F. R., 2013; MohseniBandpi 2017). Although not receiving much attention, the ubiquitous water-soluble organic matter (WSOM) present in PM<sub>2.5</sub> has also been recognized as capable of mediating ROS generation (Almeida, A. S., 2024). Furthermore, WSOM can account for a significant portion of the overall PM<sub>2.5</sub> mass. Hence, it is important to better understand the impacts of the exposure to this PM<sub>2.5</sub> fraction.

In this work, the structural features of daytime and nighttime PM<sub>2.5</sub> WSOM samples from an urban and a rural location will be discussed by means of liquid-state NMR spectroscopy. Furthermore, a brief overview of the effects that these fractions have on a human monocytic cell line (THP-1) will be addressed. Figure 1 shows the percentage distribution of <sup>1</sup>H functional groups of the WSOM samples collected during warm and cold seasons. Some differences can be observed between the two studied environments, for instance, during the daytime of cold seasons the rural sample exhibits a lower percentage of oxygenated aliphatic groups (H-C-O) and increased percentage of saturated aliphatic (H-C) moieties when compared with the urban samples. Furthermore, looking at the night period at the rural site, the relative distribution of saturated aliphatic and saturated oxygenated moieties follow an opposite trend when compared with its daytime counterpart. This inner daily variation might be a result of the increased biomass burning, which is a prevalent practice for household heating in this rural area.

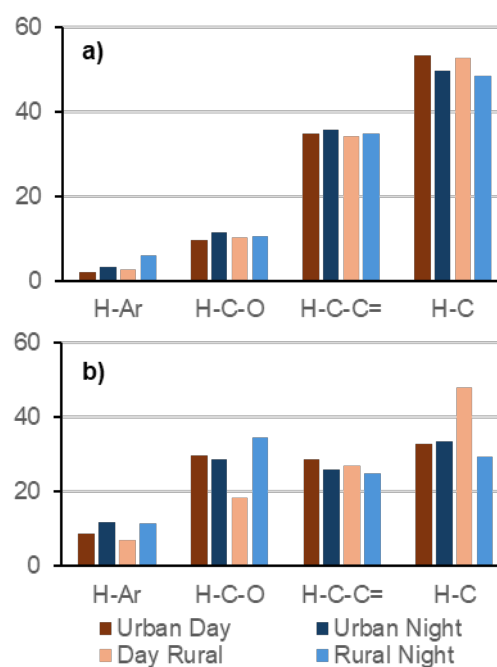


Fig. 1. Percentage distribution of <sup>1</sup>H NMR of aerosol WSOM collected in a) warm and b) cold seasons at an urban and rural location.

Thanks are due to FCT/MCTES for the financial support to CESAM (UIDP/50017/2020 + UIDB/50017/2020 + LAF/0094/2020) and to iBiMED (UIDB/04501/2020) through national funds. FCT/MCTES are also acknowledged for a PhD grant (2020.05804 BD) through national funds and the European Social Fund.

Murray, C. J. L., Aravkin, A. Y., Zheng, P., et al., *Lancet*, 2020, 396, 1223–1249.

Feng, S.; Gao, D.; Liao, F.; Zhou, F.; Wang, X., *Ecotoxicol. Environ. Saf.* 2016, 128, 67–74.

Buonfiglio, L. G. V., Comellas, A. P., *J Thorac Dis*, 2020, 12, 134–136

Cassee, F. R.; Héroux, M.-E.; Gerlofs-Nijland, M. E.; Kelly, F. J., *Inhal. Toxicol.* 2013, 25 (14), 802–812.

MohseniBandpi, A.; Eslami, A.; Shahsavani, A.; Khodaghali, F.; Alinejad, A., *Sci. Total Environ.* 2017, 593–594, 182–190.

Almeida, A. S., Neves, B. M.; Duarte, R. M. B. O., *Environ. Pollut.* 2024, 342, 123121.

*RICTA2024*

**8<sup>th</sup> Iberian Meeting on Aerosol Science and Technology**



**Section 7. Oral Session V. Thursday,  
June 27<sup>th</sup> 14:45-16:45**

**Chairs: C. Alves, M. Piñeiro-Iglesias**

## SOURCES OF DEPOSITED AEROSOLS OVER THE DONAIRE MULTI-SITE NETWORK IN SPAIN

J. Pey<sup>1</sup>, J.C. Larrasoaña<sup>2,3</sup>, I. de la Parra<sup>1</sup>, B.L. Valero-Garcés<sup>1</sup>, N. Pérez<sup>4</sup>, S. Castillo<sup>5</sup>, J. Causapé<sup>2</sup>, M.P. Mata<sup>6</sup>, J. Reyes<sup>6</sup>, J.C. Cerro<sup>7</sup>, and D. Elustondo<sup>8</sup>

<sup>1</sup>Instituto Pirenaico de Ecología, CSIC, Zaragoza, 50059, Spain

<sup>2</sup>Instituto Geológico y Minero de España, CSIC, Zaragoza, 50059, Spain

<sup>3</sup>Dpto. Ciencias & INAMAT, Universidad Pública de Navarra, Pamplona, 31006, Spain

<sup>4</sup>Instituto de Diagnóstico Ambiental y Estudios del Agua, CSIC Barcelona, 08034, Spain

<sup>5</sup>Andalusian Institute for Earth System Research (IISTA-CEAMA), Granada, Spain

<sup>6</sup>Instituto Geológico y Minero de España, CSIC Tres Cantos (Madrid), 28760, Spain

<sup>7</sup>Laboratory of the Atmosphere, Govern Illes Balears, Palma de Mallorca, 07009, Spain

<sup>8</sup>Universidad de Navarra, Instituto de Biodiversidad y Medio Ambiente (BIOMA) Pamplona, 31080, Spain

Keywords: atmospheric deposition, Saharan dust, receptor modelling, source apportionment, global change

Presenting author jorge.pey@ipe.csic.es

This study presents a comprehensive overview of the primary sources of aerosols found in deposited particles across Spain. The DONAIRE network was established in 2016 at 15 locations in eastern and northern Iberia, as well as in the Balearic Islands (Pey *et al.*, 2020; Fig. 1). Upcoming projects allowed for additional monitoring in other locations, all within the same geographical domain. The surveillance sites range from pristine locations to urban areas. The study incorporates data from 2016 to 2023.

To collect deposited aerosols, bulk samples are obtained monthly using homemade devices. Once in the laboratory, samples are filtered onto 47 mm quartz filters using a filtration ramp. Insoluble aerosols (in filters) are quantified by filter mass difference, and soluble aerosols (in aliquots) are counted after chemical determinations of anions and cations by ionic chromatography. Additionally, insoluble particles are analyzed following the procedures outlined by Querol *et al.* (2019). Geochemical databases (more than 300 samples, around 35 variables) organized in geographical domains (Ebro Basin, Mediterranean coast, Northern sites) are employed in Positive Matrix Factorization v5.0 to identify the main sources and contributions.

In each geographical domain, the optimal solution reveals between 5 and 10 factors/sources. Natural sources encompass marine aerosols and 2-3 Saharan dust factors, each with slightly different chemical profiles. Anthropogenic sources are identified at all locations, including road traffic, coal combustion, biomass burning, industrial emissions, shipping, and undefined regional pollution.

Saharan dust sources play a crucial role in regions in the Central Pyrenees, the Balearic Islands and southeastern Iberia, while marine influence dominates, for various reasons, in two of the National Parks included in the network, Picos de Europa and Cabrera. Anthropogenic sources are significantly pronounced in urban areas, yet they vary in typology. It is important to note that remote areas experience a non-negligible contribution of aerosols from anthropogenic sources. Industrial sources are highly relevant in the Picos de

Europa National Park, road traffic emissions have a significant impact in Sierra Nevada, an undefined copper source is crucial in the Balearic Islands, including Cabrera, and unaccounted anthropogenic sources are notable in Ordesa and Monte Perdido.

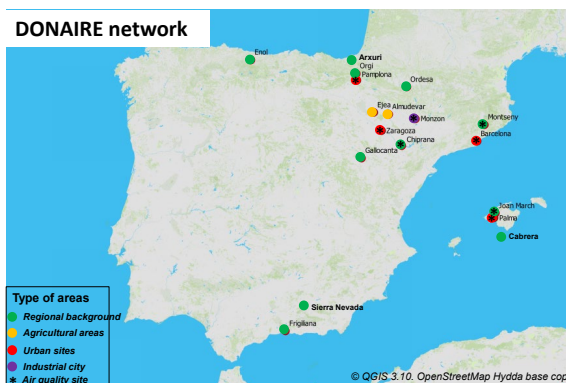


Figure 1 illustrates the DONAIRE network, showcasing the locations of sites and the types of areas they represent.

This research received support from POSAHPI actions (State Research Agency, PID2019-108101RB-I00 and PID2022-143146OB-I00) and ASAH-AS (reference 2799/2021), scientific research projects in the National Parks Network for the year 2021, provided by the Spanish Ministry for the Ecological Transition and the Demographic Challenge.

Pey J., Larrasoaña J.C., Pérez N. *et al.* (2020). Phenomenology and geographical gradients of atmospheric deposition in southwestern Europe: results from a multi-site monitoring network. *Sci. Tot. Environ.*, 744, 140745, <https://doi.org/10.1016/j.scitotenv.2020.140745>.

Querol, X. Pérez N., Reche C. *et al.* (2019). African dust and air quality over Spain: Is it only dust that matters?. *Sci. Tot. Environ.* 686, 737-752. <https://doi.org/10.1016/j.scitotenv.2019.05.349>.

## LEVELS AND ORIGIN OF ULTRAFINE PARTICLES IN A COMPLEX INDUSTRIAL STATES (LA RÁBIDA, SW SPAIN)

P. Pérez Vizcaíno<sup>1</sup>, A.M. Sánchez de la Campa<sup>1</sup>, D.A. Sánchez-Rodas, J.D. de la Rosa<sup>1</sup>

<sup>1</sup>Center for Research in Sustainable Chemistry-CIQSO, Associate Unit CSIC-University of Huelva "Atmospheric Pollution", Campus El Carmen s/n, 21071 Huelva, Spain

Keywords: ultrafine particles, ship events, industrial emissions, photonucleation

Presenting author email: pablo.perez@ciqso.uhu.es

Ultrafine particles (<0.1  $\mu\text{m}$  in diameter), have a great potential to cause harm to health, but their precise role in many illnesses is still unknown. Their high point-source production and rapid redistribution make incidental exposure common for the general population (Schraufnagel, 2020).

A study on how industrial emissions contribute to ultrafine particles concentrations (N) in a complex industrial area is presented. La Rábida is a small historic town situated at the SE of Huelva, crossing the Tinto River, between the industrial areas of Punta del Sebo and Nuevo Puerto.

N and mass of black carbon (BC) data were collected over 8 months (July 2023 – February 2024) with an Ultrafine Condensation Particle Counter (UCPC, TSI-Model 3776) and a Aethalometer (AE33, Magee Scientific), respectively. In order to quantify the process contributing to N, two components (N1 and N2) were segregated following the methodology of Rodríguez and Cuevas (2007). N1 (S1-BC) accounts for vehicle exhaust emissions and may also include compounds nucleating/condensing immediately after emission (incomplete fuel combustion products, condensed trace metals, unburned oil and a fraction of sulphate and organic compounds). N2 (N-N1) is correlated with  $\text{SO}_2$  and accounts for new particle formation due to nucleation and rapid particle growth to detectable sizes (Fernández-Camacho et al., 2010).

Mean hourly values of N during summer are within the range 40k-80k  $\text{cm}^{-3}$  from 10:00 to 13:00 GMT and 10k-30k  $\text{cm}^{-3}$  for the rest of the day in July. For August, these ranges are 30k-60k  $\text{cm}^{-3}$  and 7,500-20k  $\text{cm}^{-3}$ , respectively. In September (16-18th), an ultrafine particle formation event associated with ship emissions and hourly values up to 500k  $\text{cm}^{-3}$  occurred. Mean hourly values of N within the range 15k-30k  $\text{cm}^{-3}$  from 10:00 to 13:00 GMT and 7,500-10,000  $\text{cm}^{-3}$  for the rest of the day are registered in September, October and November (spring months). During winter months, mean hourly values are slightly lower than those of the previous season. They range 10k-25k  $\text{cm}^{-3}$  from 10:00 to 13:00 GMT and 7,500-10,000  $\text{cm}^{-3}$  for the rest of the day. In January, the peak of maximum N ( $\approx 35\text{k}$   $\text{cm}^{-3}$ ) occurs at 15:00 GMT. In the case of BC, the values are relatively constant (300-600  $\text{ng}/\text{m}^3$ ) during July and August. In September and October, a peak of high concentration (800-1000  $\text{ng}/\text{m}^3$ ) from 8:00 to 10:00 GMT is distinguished. For the rest of the day, mean hourly values range between 500-700  $\text{ng}/\text{m}^3$ . From

November to February, a trimodal pattern is observed, with high values (1000-1800  $\text{ng}/\text{m}^3$ ) from 00:00 to 02:00 GMT, from 09:00 to 11:00 and from 21:00 to 23:00 GMT. The lowest mean hourly values range 500-600  $\text{ng}/\text{m}^3$  in this months.

The results of this study show that, in La Rábida, the contribution of the industrial emissions to the ultrafine particles production is clearly much higher than that of the vehicle exhaust emissions (Fig. 1). The production reaches its maximum during daylight, due to the combination of a not necessary very high  $\text{SO}_2$  concentration and solar radiation (photonucleation). The origin of N is related to Cu-smelter and ships emissions from Port of Huelva. Main  $\text{SO}_2$  concentrations are also related to Cu-smelter (Fig. 2).

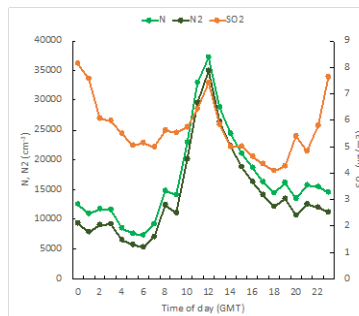


Fig. 1. Hourly averaged values of N, N2 and  $\text{SO}_2$  concentrations in La Rábida during July 2023 – Feb. 2024.

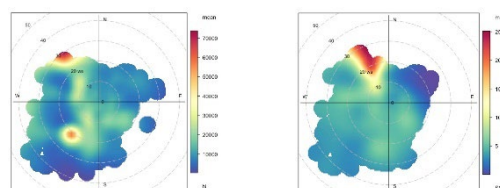


Fig. 2. Polar plot of hourly averaged values of N and  $\text{SO}_2$  concentrations in La Rábida during July 2023 – February 2024.

This work was supported by State Research Agency (AEI) Projects: PID2021-126986OB-I00 and RTI2018-095937-B-I00

Fernández-Camacho, R., et al. (2010) *Atmos. Chem. Phys.* **10**, 9615-9630.

Rodríguez, S., Cuevas, E. (2007) *J. Aerosol Sci.* **38**, 1207-1219.

Schraufnagel, D.E. (2020) *Experimental & molecular medicine* 52(3), 311-317.

## ULTRAFINE PARTICLES IN URBAN EUROPE: RESULTS FROM RI-URBANS

M. Garcia-Marlès<sup>1,2</sup>, R. Lara<sup>1</sup>, A. Alastuey<sup>1</sup>, T. Petäjä<sup>3</sup>, X. Querol<sup>1</sup> and the UFP-RI-URBANS team

<sup>1</sup>Institute of Environmental Assessment and Water Research (IDAEA-CSIC), 08034 Barcelona, Spain

<sup>2</sup>Department of Applied Physics-Meteorology, University of Barcelona, Barcelona, 08028, Spain

<sup>3</sup>Institute for Atmospheric and Earth System Research, Dep. Physics, 00014 University of Helsinki, Finland

Keywords: air quality, particle number concentrations, particle size distribution, source apportionment

Presenting author email: meri.garcia@idaea.csic.es

Ultrafine particles (UFP) are those with a particle size <100 nm, and the concentration is measured in particle number (PNC). The last World Health Organisation Air Quality Guidelines (WHO, 2021) reported that the outputs of studies on health effects associated to the exposure to ambient air UFP are still inconsistent. It was also argued that reasons for this inconsistency might be (at least partially) the scarcity of studies, the lack of harmonisation of measurements and the difficulty of obtaining representative exposure concentrations. Accordingly, these guides recommend the implementation of measurements of UFP in urban areas in a harmonised way to provide data for further epidemiological analyses. Following these recommendations, the European Commission (EC) elaborated a proposal for the new EU Air Quality (AQ) Directive (EC, 2023) requiring measurements of UFP and particle number size distributions (PNSD) in a network of AQ monitoring supersites.

In the framework of the RI-URBANS project (EC, H2020, identified as a major source of support information, in addition to ACTRIS and EMEP, in the base documents of the new AQ Directive), a compilation of existing UFP-PNSD urban datasets was carried out, followed by an evaluation of the quality of datasets and interpretations of i) urban concentrations, spatial and time variability; ii) source apportionment; and iii) inter-annual trends. Here, a summary of the datasets, results and conclusions is reported. Details on locations, measurements, concentrations, time variability and trends are provided by Trechera et al. (2023) and Garcia-Marlès et al. (2024a and b).

This analysis is based on 29 UFP-PNSD datasets provided by AQ research supersites to RI-URBANS, and included 18 urban background (UB), 6 traffic (TR), 4 suburban background (SUB) and 1 regional background (RB) sites. For comparison purposes the period 2017-2019 was selected, and for source apportionment and trend analysis, data from 2009-2019 (when available) were included.

**Measurements:** Only 62% datasets with >70% data availability. The large differences in the lower size detection limit (3 to 20 nm) affected the direct comparison of PNCs.

**Concentrations:** UFP, as BC does, follow a S and E to N Europe and a TR>UB>SUB decreasing trends. In addition to the traffic rush hours UFP concentration peaks, a relevant morning-midday one (coinciding with minimal BC, and caused by Nucleation mode PNC) was evidenced for a number of cities. Cities were classified

into 3 major groups, depending on the time variability of UFP-PNSD: i) Low midday PNC peaks and PNC parallel daily BC (traffic related) patterns, with low spring-summer Nucleation mode PNC; ii) PNC and BC traffic-related daily patterns, but a major midday PNC peak, with inverse seasonal PNC (highest in spring-summer) and BC (highest in autumn-winter) patterns, with high Nucleation mode midday PNC in spring and summer; and iii) dominant traffic-related PNC peaks, but marked midday Nucleation mode peak and no seasonal patterns.

In the **source apportionment analysis**, 4 traffic UFP contributors were identified (diesel and gasoline vehicles, traffic nucleation, and mixed urban traffic). Total traffic reached the highest contribution to UFP in all cities (70-90% of the UB average UFP in 8/12 cities, and 56-62% in 4). Photonucleation (new particle formation mostly at regional scale) reached 24-31% in 2 cities; and domestic heating, 26% in other 2. Much lower contributions were obtained for regional summer, regional winter, urban background, and long-range distance transport.

**Trends:** In most cities a clear abatement of the BC, NO<sub>2</sub>, PM, and the Aitken and Accumulation mode PNCs was obtained, and attributed to the effect of traffic-related policy measures, such as vehicle EURO 5 and 6 standards. The highest declining slopes were obtained at TR sites. The trends in the Nucleation mode PNCs were diverse, and causes were attributed to several factors. Thus, the positive effects of the AQ policies in abating the Aitken and Accumulation mode particles was evidenced, but less for the Nucleation mode.

This work is supported by the European Commission (RI-URBANS contract n. 101036245).

EC. (2023) Proposal for a Directive of The European Parliament and of The Council on ambient air quality and cleaner air for Europe.

WHO (2021) *WHO global air quality guidelines: PM<sub>2.5</sub>, PM<sub>10</sub>, O<sub>3</sub>, NO<sub>2</sub>, SO<sub>2</sub> and CO*, <https://www.who.int/publications/i/item/9789240034228>

Trechera P. et al. (2023) Phenomenology of ultrafine particle concentrations and size distribution across urban Europe. *Environ Int*, 172, 107744.

Garcia-Marlès M. et al. (2024a) Inter-annual trends of ultrafine particles in urban Europe. *Environ Int*, (in press), 108510.

Garcia-Marlès M. et al. (2024b) Source apportionment of ultrafine particles in urban Europe (in prep).

## BIORELEVANT SOLUBLE TRACE METALS IN THE ATMOSPHERIC AEROSOLS TRANSPORTED OBSERVED OVER THE TROPICAL NORTH ATLANTIC AT CAPE VERDE

I. Belbachir<sup>1,\*</sup>, J. López-Darias<sup>1</sup>, S. Rodríguez<sup>1</sup>, G. Villena- Armas<sup>1</sup>, J.H. Ayala<sup>2</sup>, K.W. Fomba<sup>3</sup>, A.C. Fortes<sup>4</sup>, J. de la Rosa<sup>5</sup>, S. Freire<sup>6</sup>, L. Neves<sup>7</sup> and A. M. Sánchez<sup>5</sup>

<sup>1</sup>Consejo Superior de Investigaciones Científicas, IPNA CSIC, La Laguna, Tenerife, Spain

<sup>2</sup>Department of Chemistry, University of La Laguna, E38206, Tenerife, Spain

<sup>3</sup>Leibniz Institute for Tropospheric Research TROPOS, Leipzig, Germany

<sup>4</sup>Ministry of Agriculture and Environment of Cabo Verde, Ribeira Grande, Santo Antão, Cabo Verde

<sup>5</sup>Centre for Research in Sustainable Chemistry - CIQSO, University of Huelva, E21071 Huelva, Spain

<sup>6</sup>University of Cabo Verde, Praia, Cape Verde

<sup>7</sup>Instituto Nacional de Neteorologia y Geofisica, Mindelo, Cabo Verde

Keywords: aerosols, Saharan dust, metals solubility, iron.

Presenting author email: i.b@csic.es

The atmospheric deposition of desert dust aerosols is an important source of nutrients for the marine phytoplankton. Dust deposition influences on sea water composition, by providing dissolved and particulate nutrients as iron, zinc, manganese, copper and nickel, among others. The availability of these nutrients in sea water stimulates the composition and growth of phytoplankton, influencing the marine biodiversity, the CO<sub>2</sub> uptake and climate (Mahowald et al., 2018). The resulting new organic matter is distributed across the trophic web to top predators; off North Africa, the northward migration, from equatorial waters to the Canary Islands, of skipjack tuna tracks the seasonal shift of Saharan dust deposition in the open waters of the Atlantic, evidencing the important role of dust inputs to the marine ecosystems and fisheries (Rodríguez et al., 2023). There is a huge interest in understanding the processes influencing the solubility of the trace metals present in the atmospheric aerosols, due to it is considered that dissolved metals in sea water are more accessible to phytoplankton than the particulate phase.

We present a study focused on the processes affecting the solubility of the iron (Fe), cobalt (Co), copper (Cu) and aluminium (Al) contained in the atmospheric aerosols exported from North Africa and transported over the tropical North Atlantic. From June to August 2022, we collected daily samples of particulate matter smaller than 10 microns (PM<sub>10</sub>) at a mountain site (1400 meters altitude) in Santo Antão Island, Cape Verde. We performed a full chemical characterization of the samples (elemental composition by ICP-MS), ions, cations, organic carbon and elemental carbon. We also determined the soluble fraction of Fe, Co, Cu and Al by dissolution in real sea water (Rodríguez et al., 2021), both in concentration (ng/m<sup>3</sup>) and as soluble fraction (%).

The composition of aerosols experienced significant changes, reflecting the three main transport routes of aerosols from tropical North Africa, Sahara desert and North Atlantic. The solubility of Fe, Co, Cu and Al experienced a significant variability, with low solubilities during dust events and higher solubilities during dust-

free conditions. During dust events, the solubility of Fe and Al is rather narrow, and seems to be linked to the variability of mineralogy and the presence of acid pollutants that may enhance iron solubility, especially for the case of iron. The soluble fraction of copper and cobalt shows signs of anthropogenic industrial influence, as pointed by the correlated variability with sulphate and other pollutants and by the MCAR plots determined with massive back trajectories analysis.

The overall data analysis suggests that anthropogenic industrial activities in North Africa are contributing to increase the solubility of Fe, Co and Cu, with still unknown consequences for the marine ecosystem. The results of our observations may contribute to improve the observational data bases needed to improve climate models for a better understanding on how the chemicals deposited in the ocean influence on climate.

This work was supported by the project AEROEXTREME (PID2021-125669NB-I00), funded by the State Research Agency of Spain, the Ministry of Science, Innovation and Universities of Spain and the European Regional Development Fund.

Mahowald et al. (2018). Aerosol trace metal leaching and impacts on marine microorganisms. *Nat. Commun.* 9 (1), 2614.

Rodríguez et al. (2021). Tracking the changes of iron solubility and air pollutants traces as African dust transits the Atlantic in the Saharan dust outbreaks. *Atmos Environ*, 246, 118092

Rodríguez et al. (2023). African desert dust influences migrations and fisheries of the Atlantic skipjack-tuna, *Atmos Environ*, 312, 120022

## eBC CONCENTRATION IN URBAN EUROPE: RESULTS FROM RI-URBANS

M. Savadkoohi<sup>1</sup>, M. Pandolfi<sup>1</sup>, A. Alastuey<sup>1</sup>, T. Petäjä<sup>2</sup>, X. Querol<sup>1</sup> and eBC-RI-URBANS team

<sup>1</sup>Institute of Environmental Assessment and Water Research (IDAEA-CSIC), 08034 Barcelona, Spain

<sup>2</sup>Institute for Atmospheric and Earth System Research, Dep. Physics, 00014 University of Helsinki, Finland

Keywords: Air quality, Equivalent black carbon, Filter absorption photometer, Source apportionment, Mass absorption cross-section

Presenting author email: andres.alastuey@idaea.csic.es

Equivalent Black Carbon (eBC) has become one of the key targets for current research on air quality (AQ). To incorporate eBC as a new variable in AQ guidelines and to develop effective mitigation strategies, it is crucial to estimate its mass concentration in a consistent way throughout the AQ monitoring networks (AQMNs) with minimal uncertainties. Accordingly, the variability of eBC mass concentrations and their sources in urban Europe were analyzed to provide insights into the use of eBC as an advanced AQ parameter for AQ standards. In the framework of RI-URBANS project (EC, H2020), eBC mass concentration datasets were compiled covering the period between 2006 and 2022 from 50 measurement stations, including 23 urban background (UB), 18 traffic (TR), 7 suburban (SUB), and 2 regional background (RB) sites. eBC mass concentrations were derived from filter absorption photometers (FAPs), mainly aethalometers and MAAPs. The results highlighted the need for the harmonization of eBC measurements to allow for direct comparisons across urban Europe. Here we summarized the results of spatial and temporal variations of eBC and present recommendations for harmonizing its measurements.

**Phenomenology:** The eBC mass concentrations showed a decreasing trend as follows: TR > UB > SUB > RB. Furthermore, a clear decreasing trend was observed in the UB sites moving from Southern to Northern Europe. The eBC exhibited significant spatiotemporal heterogeneity, including marked differences and variable contributions of pollution sources to bulk eBC between different cities. Seasonal patterns in eBC were also evident, with higher winter concentrations observed in a large proportion of cities, especially at UB and SUB sites. The contribution of eBC from liquid fuel combustion, mostly traffic (eBC<sub>LF</sub>) was higher than that of solid sources, mostly biomass burning (eBC<sub>SF</sub>) in all European sites studied. Nevertheless, eBC<sub>SF</sub> still had a substantial contribution to total eBC at a majority of the sites. eBC trend analysis revealed decreasing trends for eBC<sub>LF</sub> over the last decade, while eBC<sub>SF</sub> remained relatively constant or even increased slightly in some cities (Savadkoohi *et al.*, 2023).

**Recommendations:** In order to obtain a reliable determination of eBC mass concentrations derived from FAPs measurements, the mass absorption cross-section (MAC) for converting the absorption coefficient ( $b_{\text{abs}}$ ) to eBC should be quantified appropriately. The spatial-temporal variability of the MAC obtained from simultaneous elemental carbon (EC) and  $b_{\text{abs}}$  measurements performed at 22 sites were studied. Different methodologies for retrieving eBC integrating different options for calculating MAC were investigated

including: locally derived, median value calculated from 22 sites, and site-specific rolling regression MAC. The eBC concentrations that underwent correction using these methods were identified as LeBC (local MAC), MeBC (median MAC), and ReBC (Rolling MAC) respectively. Pronounced differences (up to more than 50 %) were observed between eBC as directly provided by FAPs (NeBC; Nominal instrumental MAC) and ReBC due to the differences observed between the experimental and nominal MAC values. The median MAC was  $7.8 \pm 3.4 \text{ m}^2/\text{g}$  from 12 aethalometers at 880 nm, and  $10.6 \pm 4.7 \text{ m}^2/\text{g}$  from 10 MAAPs at 637 nm. The experimental MAC showed significant site and seasonal dependencies, with heterogeneous patterns between summer and winter in different regions. Long-term trend analysis of eBC, revealed that the trend may be clearly affected by the way eBC is calculated due to the variability of MAC. Thus, NeBC and EC decreasing trends were consistent at sites with no significant trend in experimental MAC. Conversely, where MAC showed s.s. trend, the NeBC and EC trends were not consistent while ReBC concentration followed the same pattern as EC. These results underscore the importance of accounting for MAC variations when deriving eBC measurements from FAPs and emphasize the necessity of incorporating EC observations to constrain the uncertainty associated with eBC. RI-URBANS recommends the use of co-located measurements of  $b_{\text{abs}}$  and EC mass concentrations by expanding monitoring networks to include regular EC sampling and periodically using EC measurements to obtain rolling MAC. However, whenever EC observations are unavailable, we recommend applying the median MAC value of  $10.6 \text{ m}^2/\text{g}$  obtained in this work when  $b_{\text{abs}}$  is provided by MAAP at 637 nm and the MAC value of  $7.8 \text{ m}^2/\text{g}$  when harmonized  $b_{\text{abs}}$  is provided by aethalometers at 880 nm (Savadkoohi *et al.*, 2024).

This work was supported by the RI-URBANS (101036245), CAIAC (PID2019-108990RB-I00), and AIRPHONEMA (PID2022-142160OB-I00) projects EC. (2023) 'Proposal for a Directive of The European Parliament and of The Council on ambient air quality and cleaner air for Europe'.

Savadkoohi, M. *et al.* (2023) 'The variability of mass concentrations and source apportionment analysis of equivalent black carbon across urban Europe', *Environment International Journal*, 178.

Savadkoohi, M. *et al.* (2024) 'Recommendations for reporting equivalent Black Carbon (eBC) mass concentrations based on long-term pan-European in-situ observations', *Environment International Journal*.

*RICTA2024*

**8<sup>th</sup> Iberian Meeting on Aerosol Science and Technology**



**Section 8. Oral Session VI. Friday,  
June 28<sup>th</sup> 10:30-11:30**

**Chairs: V. Cachorro, P. López-Mahía**

## A STUDY OF BLACK CARBON IN MADRID: SOURCES, TRENDS AND CHARACTERISTICS

E. Coz<sup>1</sup>, A. Pons<sup>2</sup>, D. Kolisz<sup>3</sup>, J. Fernández-García<sup>1</sup>, M. Pujadas<sup>1</sup>

<sup>1</sup>Environmental Department, CIEMAT, Madrid, 28040, Spain

<sup>2</sup>ETS Ingenieros Industriales, Universidad Politécnica de Madrid, Madrid, 28006, Spain

<sup>3</sup>Department of Analytical Chemistry, Physical Chemistry and Chemical Engineering, University of Alcalá, Alcalá de Henares, 28802, Spain

Keywords: black carbon (BC), traffic, biomass burning, optical properties, morphology

Presenting author email: esther.coz@ciemat.es

Black carbon (BC) is a short-lived air pollutant that specially impacts on air quality, the climate and human health (Bond et al., 2013). Product of inefficient combustion, and ubiquitous in anthropogenic environments, BC is considered as the second major warming agent, after CO<sub>2</sub>. Its structural characteristics in form of aggregates of several nanometer sized graphitic spherules, make of BC a major threat to our health. Not a chemical component, neither a specific material, BC and co-pollutants become a major challenge in atmospheric studies. How to measure, characterize, classify and legislate BC is on the table for debate (IPCC, 2021).

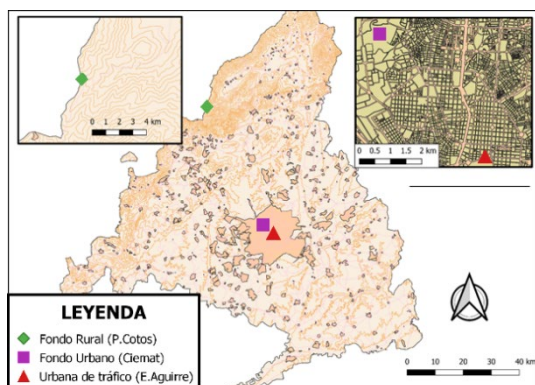


Fig. 1. Location of the BC monitoring stations during the study.

The present study presents the time-evolution of BC and properties in Madrid, one of the most populated cities in Europe, by analyzing concentrations, trends, optical properties, fossil or biomass source apportionment and structural properties for over a decade in a traffic station (Escuelas Aguirre) and in a background urban station (CIEMAT Madrid-ACTRIS) (Fig. 1). Additionally, BC concentrations and optical properties for over a year in a rural background station (Puerto de Cotos) combined with a detailed analysis of the synoptic scenarios has allowed to estimate the local, regional or long-range origin of this BC. To achieve these goals, the data from 3 different 7-wavelength Aethalometers (AE33, Magee Scientific Inc.) has been analyzed in detailed and compared with other pollutants in properties, magnitude and origin.

Major results show that BC concentrations have been evolving decreasing in the last few years in Madrid, as the case of other major European cities. BC

concentrations have been reduced to nearly half of what it were a few years before: from more than 3 to less than 1.5  $\mu\text{g}\cdot\text{m}^{-3}$  in the urban traffic spot, and from over 2 to nearly 1.5  $\mu\text{g}\cdot\text{m}^{-3}$  in the urban background station (Fig.1). Average Absorption Angstrom Exponents (AAE) around 1.2 together with a clear diurnal traffic trend of the BC show a major influence of traffic on BC that corresponds to percentages lower than 20% biomass origin of the BC when applying the Aethalometer model.

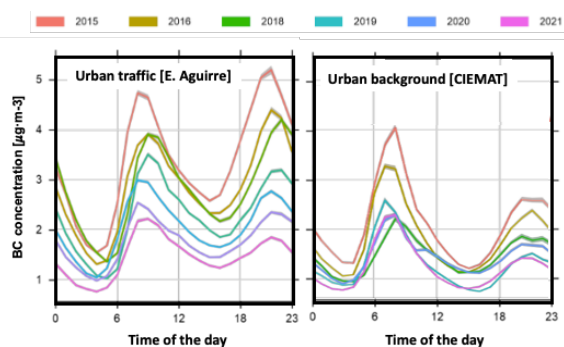


Fig. 2. Diurnal patterns of BC concentrations at the urban traffic (E. Aguirre) and urban background (CIEMAT) stations during the years 2015-2021 respectively.

This work was supported by OASIS (Plan Estatal 2021-PID2021-127885OB-I00) and H2020 programme from the European Union (grant 654109, ACTRIS-2 project). The authors specially acknowledge the readiness of Madrid City and Regional Air Quality Authorities providing the BC data from the urban traffic and rural background stations respectively.

Bond, T.C., S.J. Doherty, D.W. et al. (2013), Bounding the role of black carbon in the climate system: A scientific assessment. *J. Geophys. Res. Atmos.*, **118**, no. 11, 5380-5552, doi:10.1002/jgrd.50171.

IPCC, 2021: Climate Change 2021: The Physical Science Basis. Contribution of Working Group I to the Sixth Assessment Report of the Intergovernmental Panel on Climate Change [Masson-Delmotte, V., P. et al. (eds.)]. Cambridge University Press, Cambridge, United Kingdom and New York, NY, USA, 2391 pp. doi:10.1017/9781009157896.

## EFFECT OF WATER VAPOR ON POLLEN-RICH ATMOSPHERIC LAYERS CHARACTERIZED BY FLUORESCENCE RAMAN LIDAR

F. Molero<sup>1</sup>, R. Barragan<sup>1</sup>, M. Sicard<sup>2</sup> and I. Veselovskii<sup>3</sup>

<sup>1</sup>Department of Environment, (CIEMAT), Madrid, Spain

<sup>2</sup>Laboratoire de l'Atmosphère et des Cyclones (LACy), Université de La Réunion, Saint Denis, France.

<sup>3</sup>Prokhorov General Physics Institute, Russian Academy of Sciences, Moscow, Russia

Keywords: Lidar, pollen, fluorescence, vertical profiles

Presenting author email: f.Molero@ciemat.es

Atmospheric pollen constitutes a substantial fraction of the mass of particulate matter in the air during the flowering season, posing a well-known health threat, irritating the respiratory system and causing asthmatic symptoms (Bousquet et al., 2008). The study of its transport processes is scarce due to the intensive requirements in time and human resources derived from the use ground-level instruments as Hirst-type volumetric air samplers. Better characterization of pollen concentrations and its transport is necessary for prevention of human health effects and the effect of the current climate change in the vegetation.

In recent years, novel techniques have been developed to enable automated pollen monitoring and reduce workload. One of these techniques is the Light detection and ranging (lidar), which has shown potential to investigate the vertical distribution of pollen by both the depolarization ratio and fluorescence signals (Sicard et al., 2016, Veselovskii et al., 2020).

Adding to these capabilities, advanced lidar instruments allow the characterization of multiple atmospheric variables, from aerosol properties to temperature and water vapour concentration. Simultaneous measurements of these variables allow for investigations of interactions among them. The main objective of this work was to study the simultaneous evolution of pollen-rich layers and water vapour with the aim of establishing relevant interactions in order to improve the knowledge of optical properties of pollen in the atmosphere over the CIEMAT site, located north-west of the Madrid metropolitan area. Measurements were performed during the June 2022 – January 2024 period focusing on pollen-rich events using a recently upgraded multiwavelength Raman polarization lidar system (Molero et al 2020). Figure 1 shows an example of the events being studied, with outburst of pollen-rich layers, correlated with changes in the water vapor vertical distribution.

This novel instrumentation will allow a better characterization of the vertical distribution of aerosols, contributing to describe transport events more accurately. The combination with recent developments in automatic measurements at ground-level is expected to produce significant advances in the field in the next years.

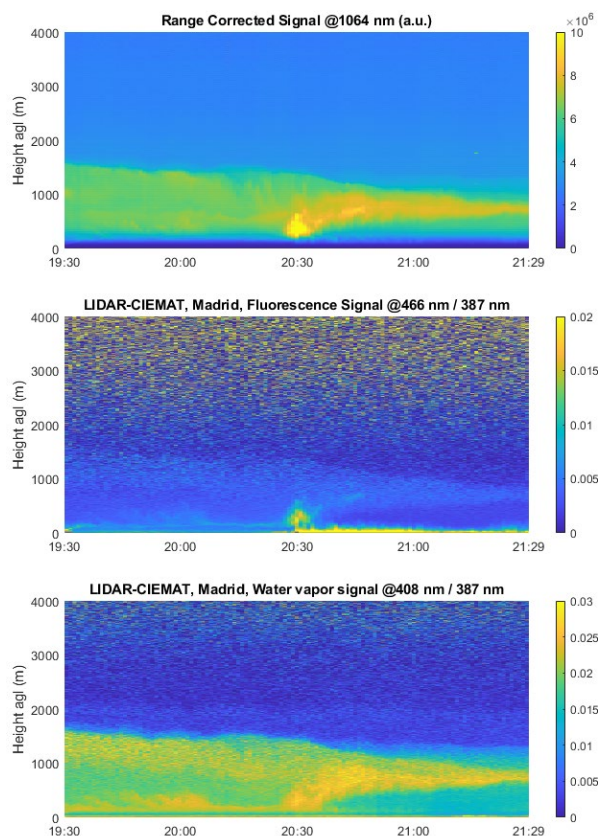


Fig. 1. Height vs time representation of the range corrected signal at 1064 nm, fluorescence and water vapour signals, both normalized by the Raman signal at 387nm.

This work was supported by H2020 programme from the European Union (grant 654109, ACTRIS-2 project), and AtPollenFluo, grant PID2020-117873RB-I00 funded by MCIN/AEI/ 10.13039/501100011033

Bousquet et al. (2008) *Allergy*, 63, 8–160.

Sicard et al. (2016) *Atmos. Chem. Phys.*, 16, 6805–6821.

Veselovskii et al. (2020) *Atmos. Meas. Tech.*, 13, 6691–6701.

Molero et al. (2020) *Remote Sensing*. 12(24):4072.

## INFLUENCE OF DUST AND NPF EVENTS ON CCN CONCENTRATION AND ACTIVATION PROPERTIES USING SIZE-RESOLVED CCN MEASUREMENTS

A. Casans<sup>1</sup>, F. Rejano<sup>1,2</sup>, J.A. Casquero-Vera<sup>1</sup>, H. Lyamani<sup>1,3</sup>, A. Cazorla<sup>1</sup>, S. Castillo<sup>1</sup>, F.J. Olmo<sup>1</sup>, L. Alados-Arboledas<sup>1</sup>, P. Cariñanos<sup>1,4</sup>, M. Gysel-Beer<sup>5</sup> and G. Titos<sup>1</sup>

<sup>1</sup>Andalusian Institute for Earth System Research IISTA, University of Granada, 18006, Granada, Spain

<sup>2</sup>GRASP-SAS, Remote Sensing Developments, LOA/Université de Lille-1, 59655, Villeneuve, D'Ascq, France.

<sup>3</sup>Department of Applied Physics, University of Málaga, 29010, Málaga, Spain

<sup>4</sup>Department of Botany, University of Granada, 18071, Granada, Spain

<sup>5</sup>Paul Scherrer Institute, Laboratory of Atmospheric Chemistry, 5232 Villigen PSI, Switzerland

Keywords: monodisperse, CCN, mineral dust, NPF

Presenting author email: andreacasans@ugr.es

Aerosol particles can be directly emitted to the atmosphere (primary particles) from anthropogenic and natural sources or formed from precursor vapours that could grow by coagulation or condensation processes (secondary particles). When particles reach a diameter of several tens of nanometers, they can activate as cloud condensation nuclei (CCN), playing an important role in the atmosphere since they can change cloud droplet properties and affect the climate. The activation and hygroscopic properties of inorganic particles are well understood. However, the influence of organics, mineral dust and freshly nucleated particles to the overall CCN properties are still poorly investigated. Most CCN measurements in high-altitude remote sites are performed for polydisperse particles, but size-resolved CCN measurements provide additional information about the size-resolved CCN activity, which are important factors for predicting CCN concentrations.

The objective of this work is to study the impact of dust and new particle formation events (NPF) on CCN properties using size-resolved CCN measurements. The BioCloud experimental campaign took place in a high-altitude remote site (Sierra Nevada National Park, SNS, 37.10°N, 3.39°W, 2500 m a.s.l.) during June-July 2021. Due to its location, the site is affected by frequent Saharan dust intrusions as well as by anthropogenic particles, emitted and transported from the nearby urbanized area of Granada (Rejano et al., 2021). During this campaign, the observatory was equipped with a CCN counter (CCN200, DMT) that measured mono- and polydisperse CCN concentrations at different supersaturations. The particle number size distribution was measured by a combination of SMPS and APS (TSI) from 12 nm to 20 µm in diameter. A ToF-ACSM (Aerodyne) was used for the online chemical characterization of sub-micron non-refractory particles and an aethalometer (AE33, Aerosol d.o.o.) for measuring black carbon concentrations.

During the campaign, two Saharan dust intrusions and several NPF events occurred. Fig. 1 shows the size distributions of aerosol particles (CN) and CCN at SS=0.4% for the two dust events and for non-dusty conditions. Remarkable differences are observed between dust events; however, both reduce CN concentration with respect to non-dusty conditions, probably due to the ability of dust particles to act as coagulation sink (Hussein et al., 2011). CCN size distributions during both dust events are similar; with total

CCN concentrations decreasing compared to non-dusty conditions.

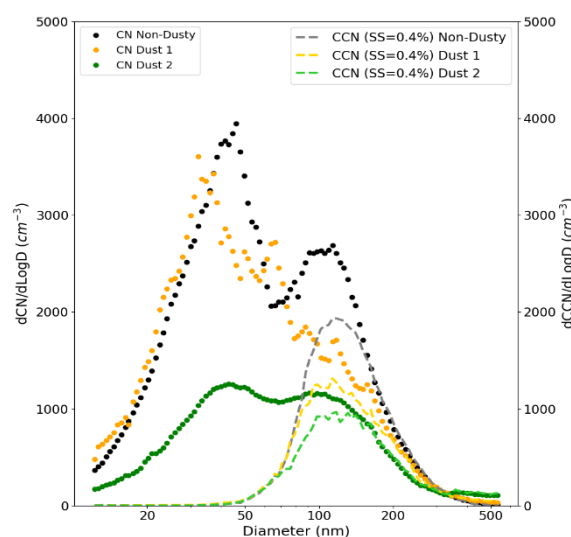


Fig. 1. Mean size distributions of CN and CCN (at SS=0.4%) during dusty and non-dusty conditions.

Concerning NPF events, most events occurred at midday (from 11.00-18.00UTC) and during days when the transport from lower altitudes is more efficient. The particle number concentration in nucleation, Aitken and accumulation modes during event days is higher with respect to non-event days. Newly nucleated particles can grow to sizes up to around 60 nm. Size-resolved CCN measurements showed that particle activation during NPF events is limited to particles larger than this size at SS=0.8%, evidencing low contribution of NPF to CCN budget on the event day. Finally, we have developed a new methodology to estimate more accurately the contribution of NPF to CCN concentration.

This work was supported by NUCLEUS (PID2021-128757OB-I00) and Scientific Unit of Excellence (Earth System UCE-PP2017-02). Andrea Casans is funded by FPI grant PRE2019-090827.

Rejano, F., et al., *Sci. Tot. Envir.*, 762, 143100, 2021.  
Hussein, T., et al., *Aerosol Air Qual. Res.* 11, 109–119, 2011.

## **AFRICAN DUST ABLATION AND TRANSPORT IN THE EXTREME MID-MARCH 2022 CASE**

J.A.G. Orza<sup>1</sup> and M.L. Kaplan<sup>2</sup>

<sup>1</sup>SCOLab, Department of Applied Physics, Universidad Miguel Hernandez de Elche, Elche, 03202 Spain

<sup>2</sup>Division of Atmospheric Science, Desert Research Institute, Reno (NV), U.S.A.

Keywords: dust storms, air quality, large-scale dynamics

Presenting author email: ja.garcia@umh.es

We examine the multiple dust storms that developed in the middle of March 2022 over North Africa by means of multi-level high-resolution reanalysis datasets, and satellite and surface observations. These dust storms ultimately transported a remarkable amount of dust into Europe, and in particular to the Iberian Peninsula.

The analyses show that baroclinic Rossby Wave Breaking (RWB) events over two regions: the eastern North Atlantic and the western Eurasian border, resulted in the creation of a downscale confluence of low-level jets that ablated dust in the Sahara Desert. One of these active baroclinic regions involved multiple wave-breaks over western Russia and the Middle East that transported unseasonably cold air southwestward into Egypt and Sudan. A second active baroclinic region occurred along the North African Atlantic Coast where rapid downstream dispersion of energy was focused in response to very intense cyclogenesis over Labrador. The cold pool which propagated into northwestern Africa and cold air over northeastern Africa effectively sandwiched hot Saharan air in between the Hoggar and Atlas Mountain Ranges. The fronts separating these air masses became juxtaposed with the two mountain ranges creating ideal conditions for blocking and multiple barrier jets' genesis. These barrier jets each combined with larger scale semi-

geostrophic low-level jet formation, resulted in the ablation of dust into two separate large plumes both of which were transported poleward out of North Africa into Europe around an upper-level cutoff-low near Iberia slowly displacing downstream.

The blocked RWB forcing the penetration of cold air over eastern Africa constitutes a substantial difference with respect to other more frequent events where RW trains intensify and penetrate equatorward into North Africa and propagate eastward.

The first dust plume reached southeastern Iberia at noon on March 14 and impacted the surface in the early evening with record particle concentrations. The second plume was registered 24 hours later. They are the result of different processes where complex orography is relevant. The subsequent evolution of the dust plumes in altitude across southern and central Europe is discussed in detail.

This work was funded by MCIN/AEI/10.13039/501100011033 under Grant PID2020-115153RB-I00 (rROSSETA Project).

*RICTA2024*

**8<sup>th</sup> Iberian Meeting on Aerosol Science and Technology**



**Section 9. Oral Session VII. Friday,  
June 28<sup>th</sup> 12:00-13:00**

**Chairs: J. Moreda, S. Muniategui**

## AMMONIA IN URBAN EUROPE: RESULTS FROM RI-URBANS

X. Liu<sup>1</sup>, R. Lara<sup>1</sup>, A. Alastuey<sup>1</sup>, T. Salameh<sup>2</sup>, M. Dufresne<sup>2</sup>, S. Sauvage<sup>2</sup>, X. Querol<sup>1</sup> & the NH<sub>3</sub>-RI-URBANS team

<sup>1</sup>Institute of Environmental Assessment and Water Research (IDAEA-CSIC), 08034 Barcelona, Spain

<sup>2</sup> Centre for Energy and Environment, Institut Mines-Télécom, Université de Lille, 59000, Lille, France

Keywords: air quality, secondary particulate matter, NH<sub>3</sub>, trends

Presenting author email: xavier.querol@idaea.csic.es

Ammonia (NH<sub>3</sub>) is an alkaline gas of high relevance for air quality (AQ). It is a major precursor of secondary inorganic aerosols (SIA) and it negatively impacts on ecosystems. Furthermore, it is the atmospheric pollutant with the lowest decrease in emissions in the last decades (EEA, 2023). In the European urban background a major proportion of ambient PM<sub>2.5</sub> arise from SIA and secondary organic aerosols (SOA). Emitted SO<sub>2</sub> and NO<sub>x</sub> undergo atmospheric oxidation, and with interaction with NH<sub>3</sub> generate ammonium sulphate and nitrate, two major components of PM<sub>2.5</sub>. Thus, the abatement of NH<sub>3</sub> is necessary to reduce PM<sub>2.5</sub>. Furthermore, NH<sub>3</sub> might interact with volatile organic compounds (VOCs) and SOA to produce NH<sub>4</sub><sup>+</sup>-bearing SOA (Paciga et al., 2014). According to EEA (2022), agriculture and farming are the foremost sectors contributing to NH<sub>3</sub> EU-27 emission inventory (94% in 2020), while other sources such as industry, road transportation, and solid waste management contribute with around 1% each. However, in urban areas, traffic and waste management are relevant sources of NH<sub>3</sub> in a high NO<sub>x</sub> environment, which might enhance urban SIA.

In the framework of the RI-URBANS project (EC, H2020), a compilation of urban NH<sub>3</sub> datasets was obtained, followed by interpretations of i) urban concentrations, spatial and time variability; and ii) inter-annual trends (Liu et al., 2024). This analysis is based on 69 datasets of NH<sub>3</sub> concentrations from European regional, suburban and urban background (RB (15 sites), SUB (12) and UB (25), respectively), industrial (IND, 5) and traffic (TR, 12) sites; from Spain (36), France (15), Italy (12), UK (5) and Finland (1). Remote sensing data by Van Damme et al. (2018) was used to identify the sites into farming/agricultural NH<sub>3</sub> hotspot areas (FAHs). Furthermore, arbitrarily, RB sites reaching average concentration >1.5 µg/m<sup>3</sup> identified as RB close to FAHs (RBCHs).

A wide variety of **measurement protocols** were used, limiting the direct comparison of data. There is a need to harmonise online measurements, and to follow CEN and EMEP protocols for offline analysis.

The average **NH<sub>3</sub> concentration** of sites from FAHs was 4-fold higher than that of the non-FAH sites. For non-FAHs sites the concentrations decreased according: IND>TR>UB>SUB>RB, while for FAHs the trend was opposite, with the highest levels being reached at RB close to farming/agricultural sources, and progressively decreasing toward the city as the distance to these sources increases. It is recommended following the directions by Sutton et al. (2022) to abate

the NH<sub>3</sub> emissions from FAHs, and to evaluate current emission inventories to properly account for urban emissions (waste management, traffic and sewage systems, among the main ones).

NH<sub>3</sub> concentrations in the study sites followed a wide range of **seasonal patterns**, probably due to varying combinations of emission and meteorological seasonal patterns. At FAHs, NH<sub>3</sub> tends to be higher in Summer and Autumn. At urban sites seasonal patterns were in many cases affected by the seasonality of emissions from their surrounding environments. **Diel** NH<sub>3</sub> concentrations were influenced by the interplay between daytime high temperatures (causing evaporative emissions from soils and wastes and ammonium nitrate instability), traffic and industrial activities, and diurnal variations of meteorology (wind speed, boundary layer height).

The meta-analysis of **inter-annual trends** of concentrations for RB sites from FAHs yielded a statistically significant (ss) increase. The RB increase of NH<sub>3</sub> has been attributed to its lower consumption to generate SIA following a marked decrease in SO<sub>2</sub> and NO<sub>x</sub>. However, the fact that this ss increase is only found at RBCH sites from FAHs might also imply and increase in emissions. A number of TR, UB and SUB monitoring sites followed a ss NH<sub>3</sub> decrease, which could be attributed to the abatement of emissions from urban sources. A few sites followed increasing trends, pointing to an opposite evolution of these emissions and/or to the decrease of NH<sub>3</sub> by lower SIA formation. This work is supported by the European Commission (RI-URBANS contract no. 101036245).

EEA (2022) *Sources & emissions of air pollutants in Europe*. <https://www.eea.europa.eu/publications/air-quality-in-europe-2022/>

Liu X. et al. (2024) Variability of ambient air ammonia in urban Europe (Finland, France, Italy, Spain, and the UK). *Environ Int* 108519.

Paciga A.L., Riipinen I., Pandis S.N. (2014) Effect of ammonia on the volatility of organic diacids. *Environ Sci Technol*, 48. 13769–13775.

Sutton M. A. et al. (eds.) (2022) *Nitrogen Opportunities for Agriculture, Food & Environment*. UNECE Guidance Document on Integrated Sustainable Nitrogen Management. UK Centre for Ecology & Hydrology, Edinburgh, UK.

Van Damme M. Et al. (2018) Industrial and agricultural ammonia point sources exposed. *Nature*, 564, 99-103.

## MULTI-INSTRUMENTAL OBSERVATIONS FOR THE ANALYSIS OF AEROSOL OPTICAL PROPERTIES AT THE CUMBRE VIEJA VOLCANIC ERUPTION

Celia Herrero del Barrio<sup>1</sup>, Roberto Román<sup>1</sup>, Sara Herrero-Anta<sup>1</sup>, África Barreto<sup>1,2</sup>, Pablo Gonzalez-Sicilia<sup>2</sup>, Daniel González-Fernández<sup>1</sup>, Ramiro González<sup>1</sup>, David Mateos<sup>1</sup>, Abel Calle<sup>1</sup>, Carlos Toledano<sup>1</sup>, Victoria E. Cachorro<sup>1</sup>, and Ángel de Frutos<sup>1</sup>

<sup>1</sup>Group of Atmospheric Optics (GOA-UVA), Universidad de Valladolid, 47011, Valladolid, Spain

<sup>2</sup> Izaña Atmospheric Research Center (IARC), Agencia Estatal de Meteorología (AEMET), 38001 Santa Cruz de Tenerife, Spain

Keywords: Volcanic aerosols, Cumbre Vieja volcan, GRASP, sun/sky photometer, ceilometer, all-sky camera

Presenting author email: celia@goa.uva.es

Between September 19th and December 13th, 2021, the eruption of the Cumbre Vieja volcano took place on the island of La Palma, Spain. During this time, a photometer, ceilometer, and all-sky camera were used to take continuous measurements. They were installed in Fuencaliente, less than 9 km away from the head of the volcano. This work aims to exploit these data to provide a comprehensive study of the volcanic aerosols emitted during the eruption.

The photometer took continuous measurements of aerosol optical depth (AOD) and sky radiance. Nevertheless, the eruption was so violent on some days that cloud-screening algorithms classified some of the most intense emission episodes as contaminated by the presence of clouds. The all-sky camera provides information about the cloud cover, being of great utility for distinguishing the volcano plume. Combining this information with data provided by the ceilometer, some of these episodes have been rescued, which are of great interest given their scarcity and the exceptional conditions of the event.

The GRASP algorithm (Generalized Retrieval of Atmosphere and Surface Properties; Dubovik et al., 2014), has been run using as input AOD and sky radiance measurements from sun-sky photometers, as well as range-corrected signal (RCS) measurements from ceilometers. As a result, the optical and microphysical properties of the emitted aerosols have been obtained both in the atmospheric column and with vertical resolution. The vertical profiles of volume concentration, extinction, scattering, backscattering and absorption coefficients, the size distribution, single scattering albedo and refractive index, are studied in order to characterize the aerosols emitted.

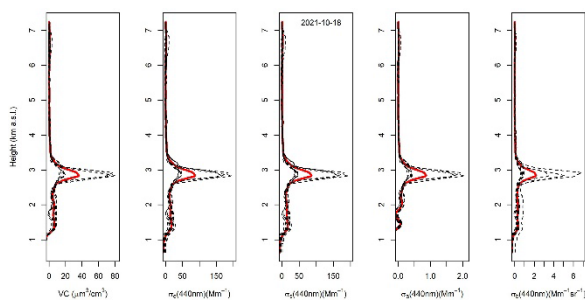


Figure 1. Vertical profiles of volume concentration, extinction, scattering, absorption and backscattering for the 18<sup>th</sup> of October 2021 at La Palma. The red line is the medium value of all the vertical profiles (dashed) for that day.

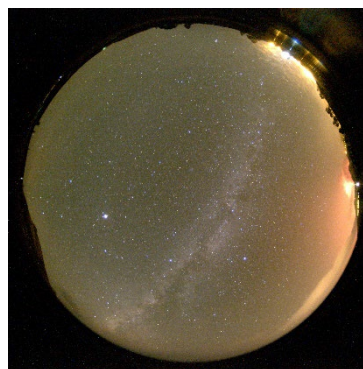


Figure 2. All-sky camera image from the eruption on October 6<sup>th</sup>, 2021. The bright red light on the right is the volcanic eruption.

This research has been supported by the Ministerio de Ciencia e Innovación (grant no. PID2021-127588OB-I00), is part of the TED2021-131211B-I00 project funded by MCIN/AEI/10.13039/501100011033 and European Union "NextGenerationEU"/PRTR, and is based on work from COST Action CA21119 HARMONIA. The authors acknowledge the support of the Spanish Ministry for Science and Innovation to ACTRIS ERIC.

Dubovik, O. et al., GRASP: a versatile algorithm for characterizing the atmosphere, SPIE: Newsroom, 2014.

*RICTA2024*

## **8<sup>th</sup> Iberian Meeting on Aerosol Science and Technology**



## **Section 10. Posters**

## ELECTROSPRAY DEPOSITION OF CATALYST INKS ON POLYMER-ELECTROLYTE MEMBRANES FOR HYDROGEN PEM FUEL-CELLS

A. García-Corral<sup>1,2</sup>, D. García-Sánchez<sup>2</sup>, P. Gazdzicki<sup>2</sup>, S. Martín<sup>1</sup>, K. A. Friedrich<sup>2</sup>, P. L. García-Ybarra<sup>1</sup>, and J.L. Castillo<sup>1</sup>

<sup>1</sup>Dept. Física Matemática y de Fluidos, Facultad de Ciencias, UNED, Las Rozas de Madrid, 28232, Spain

<sup>2</sup>German Aerospace Center (DLR), Institute of Engineering Thermodynamics, Stuttgart, 70569, Germany

Keywords: electrospray, aerosol deposits, low-Pt loading, catalyst-coated membranes.

Presenting author email: pgybarra@ccia.uned.es

The electrohydrodynamic atomization and deposition of inks containing nanoparticle catalysts has proven to be an effective technique for the growth of nanoporous catalytic layers (CLs) during the past decade. By operating an electrospray (ES) deposition under specific conditions, a dry-deposition regime can be achieved, obtaining coatings on the substrate that display a wide-ranged pore-size distribution, down to the nanoscale. The highly nanostructured CLs grown by ES at such dry regime show an enhanced chemical activity, attributed to their large surface-volume ratio, Castillo *et al* (2018).

Polymer-electrolyte-membrane fuel cells (PEMFCs) are considered as a vital technology to reach the EU goals to reduce greenhouse gas emissions to net-zero by 2050. In this context, CLs made by ES have demonstrated the feasibility of this deposition technique to achieve a drastic reduction of Pt loading (catalyst agent), which constitutes a major expenditure of commercial PEMFC systems. Performance losses associated with the reduction of Pt loading are less prominent for electrosprayed CLs than for those made by other deposition methods, Martín *et al* (2013) and Martínez-Vázquez *et al* (2015). Most often, electrosprayed CLs for PEMFCs are deposited on porous conductive carbon-paper substrates, i.e. the gas-diffusion layers (GDLs). Another approach is to deposit the CL directly on the polymer electrolyte membrane (PEM). While the uncompressed GDEs (i.e. the GDL with applied CL) are extremely brittle, hot-pressing catalyst-coated membranes (CCMs) produces a compact CL that is robust, easing its storage, transportation, and manipulation.

This work aims at studying the production and efficiency of compressed CCMs for PEMFCs using the ES technique. This implies to carry out ES depositions on an electrically insulating substrate, i.e., the PEM, which is unfavourable due to large discharging times but can be achieved by employing highly insulating static-dissipative plastic masks fixing the PEM to the collector surface. After ES deposition, the resulting CCMs were compressed with an industrial hot-pressing machine (Fig. 1). Our results show that the PEMFC performance of uncompressed GDEs and compressed CCMs, both made via ES with a reduced Pt loading, are analogous to each other and to commercial (Com) CCMs with high Pt loadings (Fig. 2). Commercial GDEs display the highest performance, yet very similar to the afore mentioned for current densities up to 2 A cm<sup>-2</sup>. SEM images of the electrosprayed CCM revealed that hot-pressing impacts CL structures in the range of microns or above, but a strong nano-structuration remains present below the sub-micron scale.

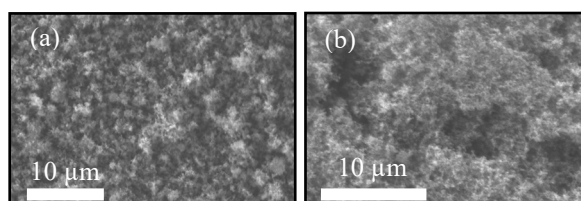


Fig. 1. SEM micrographs of the CL surface of a CCM made via ES on a PEM (a) before and (b) after hot-pressing.

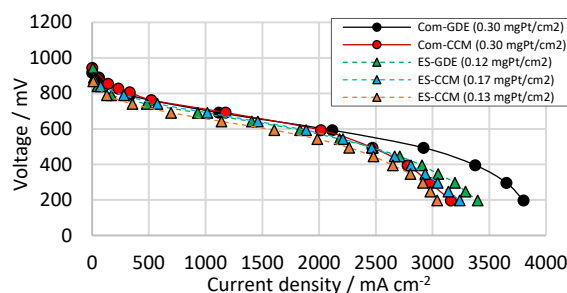


Fig. 2. PEMFC polarization curves of electrosprayed and commercial CCMs (compressed) and GDEs (uncompressed).

AG-C acknowledges the support by a Margarita Salas grant (REGAGE21e00017738309) provided by the Spanish Ministry of Universities in the framework of the Next Generation EU program. Work supported by project PID2022-139082NB-C55 granted by MCIN/AEI/10.13039/501100011033/ FEDER, UE

Castillo J.L., Martín S., Rodríguez-Pérez D., Higuera F.J., García Ybarra P.L. (2018) Nanostructured porous coatings via electrospray atomization and deposition of nanoparticle suspensions. *Journal of aerosol sciences*, 125, 148-163.

Martín S., Martínez-Vázquez B, García Ybarra P.L., Castillo J.L. (2013) Peak utilization of catalyst with ultra-low Pt loaded PEM fuel cell electrodes prepared by the electrospray method. *Journal of Power Sources*, 229, 179-184.

Martínez-Vázquez B., García-Sánchez D., Castillo J.L., Friedrich K. A., García Ybarra P.L. (2015) Scaling-up and characterization of ultralow-loading MEAs made-up by electrospray. *International Journal of Hydrogen Energy*, 40(15), 5384-5389.

# INFLUENCE OF THE AIR MASS ORIGIN ON RADIOACTIVITY LEVELS IN GRANADA (SOUTHERN SPAIN)

I. Berriban<sup>1</sup>, E. Chham<sup>2</sup>, Abdelhamid Nouayti<sup>1</sup>, M. Azahra<sup>1</sup> and J.A.G. Orza<sup>2</sup>

<sup>1</sup>Radiations and Nuclear Systems Group, FS, Abdelmalek Essaadi University, Tetouan, Morocco

<sup>2</sup>SCOLAB, Fisica Aplicada, Miguel Hernandez University, Elche, 03202, Spain

Keywords: Radioactivity, Air masses, Clustering analyses, Gross Alpha and Beta

Presenting author email: echham@umh.es

This work studies the influence of the origin of air masses on the radioactivity levels found in ground-level air in Granada (Southern Spain). To the scope, weekly gross  $\alpha$  and gross  $\beta$  concentration activities measured from 2006 to 2021 by the Radiochemistry and Environmental Radiology Laboratory of the University of Granada were analysed. Aerosol samples were collected weekly on filters and successively analysed by low-level proportional counting. The meteorological database used as input for the trajectory calculation is ERA-Interim, interpolated to 0.5 deg horizontal resolution, from the European Centre for Medium-Range Weather Forecasts (ECMWF). The back-trajectories calculation was performed using the Hybrid Single-Particle Lagrangian Integrated Trajectory (HYSPPLIT) model.

To identify which air masses are associated with the increased radioactivity levels in the atmosphere, the analysis has been carried out by dividing the data set into six activity concentration percentiles of gross  $\alpha$  index (being the same for gross  $\beta$ ) at three different altitudes: 750 m, 1500 m and 3000 m a.s.l. ( $Ac < 10P$ ,  $10P < Ac < 25P$ ,  $25P < Ac < 50P$ ,  $50P < Ac < 75P$ ,  $75P < Ac < 90P$ , and  $Ac > 90P$ ).

The study indicates that the primary air masses affecting the region come from the North (N), Northwest (NW), and West (W), which typically have lower activity concentrations due to their maritime characteristics. However, when activity levels increase, air masses from the South (S) and Mediterranean (Med) regions become more influential, contributing significantly to gross  $\alpha$  and  $\beta$  emitters. The Med air mass cluster prevails at lower altitudes, while the S cluster originates from higher altitudes.

Table 1 shows that air masses residing over the Atlantic have the lowest activity concentrations, while those over the Mediterranean exhibit the highest. While oceanic air has low concentrations of gross  $\alpha$  and  $\beta$ , the Mediterranean behaves more like continental air due to the accumulation of continental-origin compounds. Continental transport to Granada complements marine transport, with a weak association between residence times and activity concentrations. However, air parcels from North Africa reaching higher altitudes show a significant increase in activity concentrations, likely due to dust-laden layers in African air masses that settle and entrain into the boundary layer. A fraction of the air masses reaching Granada from the north (N, NE) has low gross  $\alpha$  and  $\beta$  activity levels despite passing over land, attributed to wet scavenging along their trajectories. Figure 1 illustrates this relationship, showing that air masses with lower activity concentrations are associated with higher humidity levels, indicating efficient removal of radioactive

particles by humidity in the atmosphere. This is observed in both artificial radioactive fallout and naturally occurring radionuclides.

Table 1: Percentage of back trajectories and hours residing over some specific regions by gross  $\alpha$  and gross  $\beta$  activity concentration ranges. The table shows only selected results for 750 and 3000 m.

Activity	Trajectories (%)				Hours (%)			
	Sea	Med	Atlantic	Africa	Sea	Med	Atlantic	Africa
<b><math>\alpha</math></b>								
P10	98.3	26.9	91.8	16.7	60.5	8.6	51.9	5.0
P10/25	96.4	31.9	88.1	24.1	52.9	12.8	40.0	8.8
P25/50	95.6	46.7	75.4	28.9	51.5	22.9	28.6	12.4
P50/75	96.4	58.7	64.8	35.4	54.0	29.8	24.2	15.2
P75/90	97.4	70.4	57.8	38.5	55.0	34.0	21.0	17.8
P90	97.2	83.3	39.3	48.4	59.6	42.8	16.8	23.8
<b><math>\beta</math></b>								
P10	98.4	26.9	91.8	14.8	59.8	7.6	52.2	4.8
P10/25	97.4	31.9	88.1	19.1	53.7	10.6	43.1	6.3
P25/50	96.5	46.7	75.4	28.9	52.9	21.8	31.1	11.5
P50/75	95.3	58.7	64.8	34.4	52.3	29.0	23.3	14.7
P75/90	96.6	70.4	57.8	46.1	55.7	37.4	18.2	23.5
P90	96.8	83.3	39.3	53.3	58.1	47.0	11.1	23.7
Altitude	750m			3000m	750m			3000m

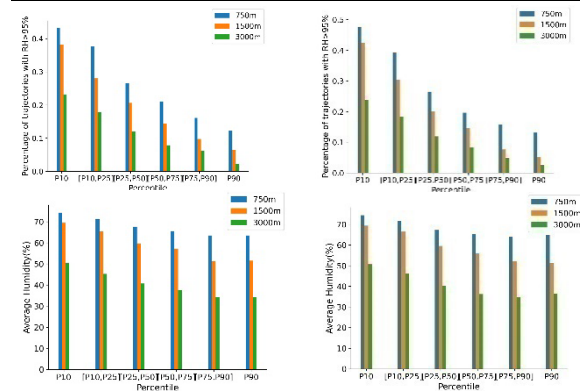


Figure 1: Average Humidity of the back-trajectories (a) for gross Alpha and (b) for gross Beta, Percentage of trajectories which have RH > 95% (c) for gross Alpha and (d) for gross Beta, at three altitudes: 750m, 1500m, and 3000m a.s.l. and for six activity ranges from 2006 to 2021.

In this study, we have successfully identified certain parameters and regions that influence the levels of gross alpha and beta radioactivity in Granada [Berriban et al., 2023].

Berriban I., Chham E., Nouayti A., Azahra M., Orza J.A.G., Ziani H., El Ghalbzouri T., El Bardouni T., Hadouachi M., Milena-Pérez A., Piñero-García F., Tositti L., Brattich E., Ben Maimoun I., Ferro-García M.A. (2023) Influence of synoptic and local parameters on activity concentration of gross Alpha and gross Beta in Granada, Spain. Atmos. Pollut. Res. 14, 101857

## MODELLING THE SECONDARY PARTICLE FORMATION CONTRIBUTION TO PM10 AND PM2.5 CONCENTRATIONS AT THE PORTUGUESE NORTH COAST

C. Gama<sup>1</sup>, D. Luís<sup>1</sup>, V. Rodrigues<sup>1</sup>, and M. Lopes<sup>1</sup>

<sup>1</sup>CESAM, Department of Environment and Planning, University of Aveiro, 3810-193, Portugal

Keywords: air quality, secondary inorganic aerosol, winter episodes

Presenting author email: carlagama@ua.pt

The air quality in the North region of Portugal is marked by periods with concentrations of particulate matter (PM10 and PM2.5) exceeding the limit values and/or guidelines defined for the protection of human health. These pollutants can originate from primary sources (e.g. such as during dust episodes) or form through chemical reactions or physical processes in the atmosphere (secondary aerosols).

This work aims to study the mechanisms of secondary particle formation and assess their contribution to PM10 and PM2.5 concentrations in the North of Portugal, using an atmospheric modelling approach. For this, we ran the CHIMERE chemical transport model, which includes detailed gas-, aerosol- and cloud-phase chemistry, for a one-year period (2021). The selected chemistry mechanism, MELCHIOR2, considers 49 species and 120 chemical reactions. Additionally, seven aerosol species are subdivided into 10 size bins, whose chemistry is also considered. Anthropogenic emission data from the EMEP inventory has been used, temporally and spatially disaggregated using land use, population, and road network as proxies, as well as typical temporal profiles. Biogenic, dust and sea salt emissions have also been considered. Three nested domains were used in the simulations, with horizontal resolutions of 27, 9 and 3 km. Meteorological data was simulated by the Weather Research and Forecast (WRF) model, with boundary conditions from ERA5 reanalysis.

Based on the results of the regional-scale simulations (see Figure 1), particle formation processes were evaluated from reactions between gaseous pollutants such as sulphur dioxide, nitrogen oxides, ammonia, or volatile organic compounds, originating from natural or anthropogenic sources. Seasonal variations, as well as differences between weekdays and weekends, were analysed, considering precursor emission patterns such as the NO<sub>2</sub> weekly cycle depicted in Figure 3.

Overall, this study aims to contribute to understanding the chemical composition and spatial distribution of atmospheric aerosols in the North of Portugal, providing essential information for better air quality management.

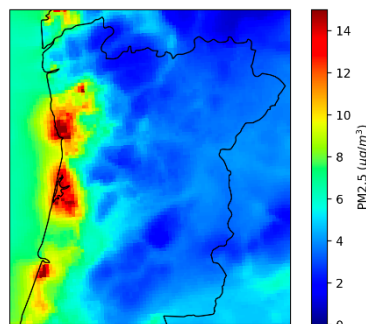


Fig. 1. Mean PM2.5 surface concentrations ( $\mu\text{g}\cdot\text{m}^{-3}$ ) modelled by CHIMERE for January 2021.

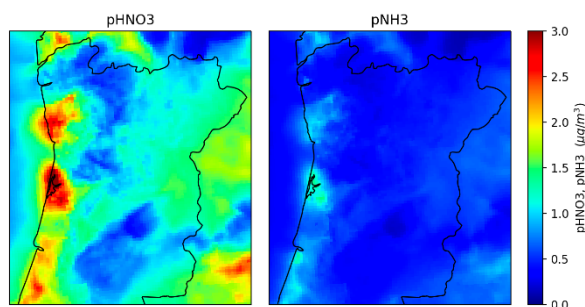


Fig. 2. Mean pNO<sub>3</sub> and pNH<sub>3</sub> surface concentrations ( $\mu\text{g}\cdot\text{m}^{-3}$ ) modelled by CHIMERE for January 2021.

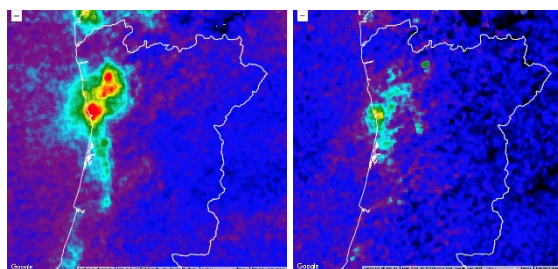


Fig. 3. Mean tropospheric vertical column of NO<sub>2</sub> ( $\text{mol}\cdot\text{m}^{-2}$ ) measured by TROPOMI instrument onboard of Sentinel-5P, during weekdays and weekends in January 2021.

## USE OF PHOTOCATALYTIC MATERIALS IN AN URBAN AREA: ANALYSIS OF POTENTIAL IMPACT ON MORTALITY ATTRIBUTABLE TO NO<sub>2</sub> POLLUTION

J. Fernández-Pampillón<sup>1,2</sup>, M. Palacios<sup>1</sup>, L. Núñez<sup>1</sup> and M. Pujadas<sup>1</sup>

<sup>1</sup>Research Centre for Energy, Environment and Technology (CIEMAT), Madrid, 28040, Spain

<sup>2</sup>The National Distance Education University (UNED), Madrid, 28232, Spain

Keywords: Air pollution, NO<sub>2</sub>, TiO<sub>2</sub>-based photocatalytic materials, mortality

Presenting author email: Jaime.Fernandez-Pampillon@ciemat.es

Road transport sector is the main source of nitrogen oxides (NO<sub>x</sub>=NO+NO<sub>2</sub>) emissions (37 % in the EU-27 in 2020) (EEA, 2022). NO<sub>2</sub> concentrations above the annual limit value (Directive 2008/30/EC) are frequently observed at traffic stations, located in densely populated urban environments. As is known, NO<sub>2</sub> is a species that is additionally relevant as a precursor to both ozone and secondary aerosol.

Within the framework of the LIFE MINOX-STREET project, the use of TiO<sub>2</sub>-based photocatalytic materials, that activated by sunlight (UV-A) allow NO<sub>2</sub> to be eliminated from the air, has been evaluated as an abatement strategy in outdoor conditions. The selected reference scenario was a street in the city of Alcobendas (Community of Madrid, Spain).

First, for three photocatalytic products (selected for application on roads, sidewalks and facades), NO<sub>2</sub> surface deposition velocities were estimated from standard laboratory tests and used to calculate an upper limit of NO<sub>2</sub> photocatalytic degradation in a selected street canyon (300 m long) in the city of Alcobendas (Community of Madrid, Spain). Then, a modelling, considering a first-order kinetics and that the air mass travels longitudinal through, without dilution to the upper atmosphere, was made. The estimated NO<sub>2</sub> reduction for this reference scenario was extrapolated to the entire municipality.

Following, short-term association between NO<sub>2</sub> concentrations and natural cause mortality, named as relative risk (RR=1.009, for Madrid) (Linares et al., 2018), has been used to compute NO<sub>2</sub> attributable mortality, during the period 2001-2019, for the city of Alcobendas, in three different conditions: non-photocatalytic urban surfaces; photocatalytic roads, sidewalks and facades; and NO<sub>2</sub> ambient concentration fixed on 20 µg m<sup>-3</sup> (WHO, 2021).

Finally, the benefit in terms of mortality reduction attributable to NO<sub>2</sub> was derived for the last two cases mentioned above.

For the modelled photocatalytic street, an average NO<sub>2</sub> surface deposition velocity of 5.6 10<sup>-3</sup> ms<sup>-1</sup> was derived, giving a NO<sub>2</sub> uptake coefficient of 6.1 10<sup>-5</sup>. An active surface to air volume above the surface ratio of 0.1 m<sup>-1</sup> was then taken to calculate a NO<sub>2</sub> first-order rate constant, equal to 6.6 10<sup>-4</sup> s<sup>-1</sup>. Taking into account the transport limitations, the referred NO<sub>2</sub> uptake is reduced by more than a factor of two. Furthermore, assuming only half the daytime there is enough UV-A radiation for photocatalysis to take place, an upper

diurnal NO<sub>2</sub> reduction of approximately 3% is finally reached.

Figure 1 shows the annual evolution of the two factors that determine the mortality attributable to NO<sub>2</sub> for the 19-years chosen period in Alcobendas. Until 2008, the average annual concentration of NO<sub>2</sub> increased, but from that year on it stabilized at lower values. Total mortality due to natural causes normalized to 1,000 inhabitants shows an increasing trend throughout the period studied, more pronounced from 2008 onwards, attributable not only to population growth, but also to its progressive aging and other factors.

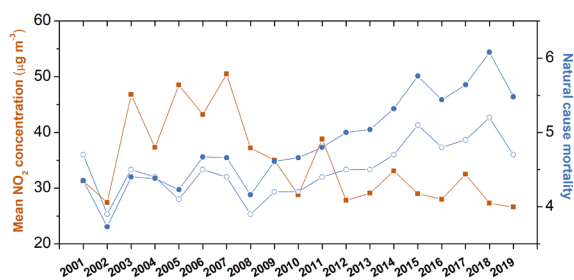


Fig. 1. Annual mean NO<sub>2</sub> concentration (square); total natural cause mortality\*10<sup>-2</sup> (solid circle); total natural cause mortality per 1000 inhabitants (open circle). Data: MITECO and INE.

Considering a reduction of approximately 3% in the average NO<sub>2</sub> concentrations due to the implementation of the selected photoactive products in all roads, sidewalks and facades of Alcobendas, the benefit in saved mortality attributable to NO<sub>2</sub>, regarding the estimate deaths for the reference scenario, would be 9. Furthermore, if the air NO<sub>2</sub> values had respected the threshold of 20 µg m<sup>-3</sup>, the reduction in the total number of deaths would be 57%.

This work was supported by LIFE financial instrument of the European Union (LIFE12/ENV/ES/000280).

European Environment Agency (2022). Air Quality in Europe 2022. Report no. 05/2022. Copenhagen.

Linares C., Falcón I., Ortiz C., Díaz J. (2018). An approach estimating the short-term effect of NO<sub>2</sub> on daily mortality in Spanish cities. *Environment International* 116, 18–28.

World Health Organization (2021). WHO global air quality guidelines: particulate matter (PM<sub>2.5</sub> and PM<sub>10</sub>), ozone, nitrogen dioxide, sulfur dioxide and carbon monoxide. Geneva.

## RELATIONSHIP BETWEEN VOC AND PM IN AMBIENT AIR AT MADRID BARAJAS AIRPORT

R. Pérez-Pastor, J.J. Rodríguez-Maroto, S. García-Alonso, E. Rojas, D. Sanz, I. Ibarra, M. Pujadas.  
Centro de Investigaciones Energéticas Medioambientales y Tecnológicas (CIEMAT), Madrid 28040, Spain  
Keywords: ultrafine particle, BTEX, air quality, airport

Presenting author email: rosa.perez@ciemat.es and enrique.rojas@ciemat.es

BTEX are considered hazardous air pollutants (HAPs) under the US Clean Air Act. They are present in fossil fuels, making the industrial, domestic and transport sectors the main anthropogenic sources of these compounds. Within the transport sector, the presumed increase of the aviation subsector in the coming years and until 2030 (Federal Aviation Agency, FAA, 2010), makes the analysis of its emissions of special interest from different points of view.

Aviation emissions directly affect the atmosphere, both at ground level through the operations of aircraft (Landing-Take-Off Cycles) and ground services, and at higher altitudes (upper troposphere and lower stratosphere) during flights. These pollutants have an impact on public health, the environment and the climate, and are a matter of concern.

In the specific case of VOCs produced at an airport, their direct role as primary pollutants and their implications in the production of other secondary compounds, i.e. secondary organic aerosols (SOA), is considered to be of great interest. BTEX specifically have been reported to account for more than 80% of total SOA formation potential (Kim et al, 2022). Considering this, it is important to evaluate their different relationships in order to define strategies for reducing this kind of pollution. Recently, the concept of VOCs – PM sensitivity coefficients has been established to evaluate how much PM values are affected by the change in VOC ambient concentrations (Han et al., 2017).

In this study, the relation between BTEX and PM measured during a field campaign carried out in 2021 in the vicinity of the runways at Barajas Airport are presented. Based on data obtained a ground level, a study of sensitivity coefficients for BTEX and PM has been carried out.

An off-line automatic sampler (OAS) developed at CIEMAT, with capacity for remote control of the sampling parameters, was used. The equipment allows collecting several samples (simultaneously or sequentially) of both gases and particles for subsequent laboratory analysis. VOC samples were collected in adsorption tubes, then analyzed using thermal desorption coupled to GC/MS. PM was measured by using three different sampling systems for

TSP (OAS), PM<sub>10</sub> (High volume sampler, HVAS) and PM<sub>2.5</sub> (Berner low pressure impactor, BLPI).

Sensitivity coefficients were calculated between BTEX and the three mass fractions, following the method described by Lee et al, (2023). Figure 1 shows the results for the coefficients obtained near runways of Barajas Airport during October 2021.

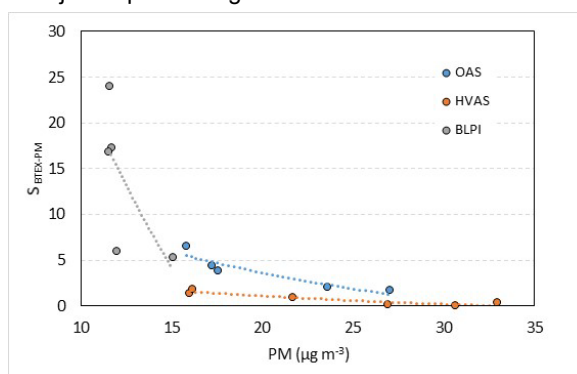


Figure 1. Distribution of BTEX sensitivity coefficients in Barajas during October sampling

As can be seen, higher coefficients were associated to both the lower particulate concentrations and the fine fractions, which indicates that a more change in BTEX concentrations against its background value is required to make a unit change of PM.

This work was supported by the EC (Horizon2020 programme, grant AMD-814801-14), AVIATOR project (Assessing aViation emission Impact on local Air quality at airports: Towards Regulation).

FAA Aerospace Forecast: Fiscal Years 2010-2030. (2010) US Department of Transportation. Federal Aviation Administration. Office of Aviation Policy and Plans;

URL: <https://rosap.ntl.bts.gov/view/dot/59847>

Han, D. Wang, Z., Cheng, J., Wang, Q., Chen, X., Wang, H. (2017) *Environ. Sci. Poll. Res. Int.* 18619-18629

Kim, S.J., Lee, S.J., Lee, H.Y., Son, J.M., Lim, H.B., Kim, H.W., Shin, H.J., Lee, J.Y., Choi, S.D. *Science of the Total Environ.* (2022) 838 156344.

Lee B-K. Choi, S-D., Shin, B. Kim, S.J., Lee, S.I., Kim, D.G., Lee, G., Kang, H.J., Kim, H.S., Park, D.Y. (2023) *Asian Journal of Atmos. Environ* 17(1) 3.

## PM<sub>10</sub>-BOUND-OCPs EVALUATION IN MADRID'S CITY: AIR QUALITY STATUS AND CARCINOGENIC RISK ASSESSMENT

J. Cárdenas-Escudero<sup>1\*</sup>, D. Galán-Madruga<sup>1,2</sup>, S. Deylami<sup>1</sup>, M. López Ochoa<sup>1</sup>, J. Ayuso Haro<sup>1</sup>, J. Urraca Ruiz<sup>1</sup>, J.O. Cáceres<sup>1</sup>

<sup>1</sup> Laser Chemistry Research Group, Department of Analytical Chemistry, Faculty of Chemistry, Complutense University of Madrid, Plaza de Ciencias 1, 28040 Madrid, Spain

<sup>2</sup> National Centre for Environmental Health, Carlos III Health Institute, Ctra. Majadahonda-Pozuelo km 2.2, 28220 Majadahonda, Madrid, Spain

Keywords: Urban air quality, Outdoor and indoor, PM<sub>10</sub>-bound organochlorine pesticides, cancer risk

\*Presenting author email: jafetcar@ucm.es

In this work, organochlorine pesticides (OCPs) bound to particulate matter with an aerodynamic diameter of less than 10  $\mu\text{m}$  (PM<sub>10</sub>), and their associated cancer risk, have been studied for the first time at the European level, as a result of the environmental concerns that have arisen in recent years, about the occurrence of toxic organochlorine pesticides that have been detected as adsorbed components in PM<sub>10</sub> in atmospheric aerosol samples (Galán-Madruga et al. 2023). The research has been carried out to (1) determine qualitatively and quantitatively the indoor/outdoor occurrence of 12 different OCPs in the city of Madrid, (2) delimit the seasonal behaviour of these pollutants and (3) assess the similarity degree between both indoor and outdoor air mixtures, with the aim of (4) estimating the cancer risk associated with human exposure to the detected levels of OCPs. For this purpose, indoor and outdoor PM<sub>10</sub> samples were collected from an urban site in the City of Madrid, Spain, during a one-year period (2017-2018). OCPs were separated from PM<sub>10</sub> by accelerated solvent extraction and subsequently analyzed by Ultra-Trace Gas Chromatography coupled to Dual-Stage-Quadrupole Mass Spectrometry detector (UTGC-DSQ/MS), employing urban dust standard reference material (SRM 1649b NIST). The results obtained showed that the mean annual concentration of  $\Sigma\text{OCPs}$  bound to PM<sub>10</sub> in outdoor and indoor air was 684.81 and 721.72  $\text{pg}/\text{m}^3$ , respectively, with a significant contribution from OCPs of molecular weight less than 400 g/mol. Interestingly, it was obtained that the most representative OCPs within the air mixtures are hexachlorobenzene (outdoor and indoor air), in addition to mirex (outdoor) and 4,4'-DDE (indoor). Finally, the results on the estimation of cancer risk from exposure (inhalation) to the studied OCPs evidenced that the carcinogenic risk is within the acceptable range established by USEPA ( $<10^{-4}$ ) for each target pollutant, except for dieldrin outdoors (winter and spring); and that the cumulative seasonal carcinogenic risk levels are above the acceptable risk outdoors (for all seasons) and indoors (winter and spring). Altogether, these results evidence that PM<sub>10</sub>-bound-OCPs assessment is yet a current problem that needs to be further in-depth studied to delineate more accurately the human exposure to these contaminants and their impact on health for the subsequent adoption of more effective

remediation and regulatory policies. All these results will be presented in the 8<sup>th</sup> Edition of the Iberian Meeting on Aerosol Science and Technology (RICTA 2024), in A Coruña, Spain.

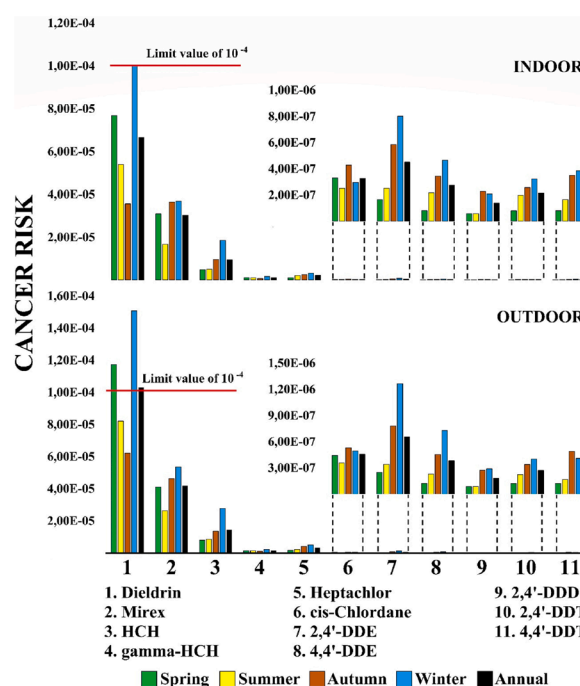


Figure 1. Outcomes reached when estimating seasonal and annual cancer risk associated with the PM<sub>10</sub>-bound-OCPs determined in this work. The annual cancer risk (CR) value corresponds to the seasonal average CR value for each pollutant.

This work was funded by the Carlos III Health Institute, Madrid, Spain (AESI Project: SPY 1357/16). The authors acknowledge to the Municipality of Madrid and the National Centre for Environment Health (Department of Atmospheric Pollution) for their support in this study.

Galán-Madruga, D., J. Cárdenas-Escudero, P. Broomandi, J. O. Cáceres & M. D. C. González (2023) Evaluating urban indoor and outdoor PM<sub>10</sub>-bound organochlorine pesticides. Air quality status and health impact. *Building and Environment*, 228, 109818.

## EXTREME HISTORIC SO<sub>2</sub> LEVELS IN AN INDUSTRIAL CITY (HUELVA, SW SPAIN). AIR QUALITY IMPLICATIONS.

E. Romero Macías<sup>1</sup>, P. Pérez Vizcaino<sup>2</sup>, A.M. Sánchez de la Campa<sup>2</sup>, D.A. Sánchez-Rodas<sup>2</sup>, A. Alastuey<sup>3</sup>, X. Querol<sup>3</sup> and J.D. de la Rosa<sup>2</sup>

<sup>1</sup>Department of Mining and Energy, University of Huelva, 21007 Huelva, Spain

<sup>2</sup> Associate Unit CSIC-UHU "Atmospheric Pollution", University of Huelva, 21007 Huelva, Spain

<sup>3</sup> IDAEA, CSIC, Jordi Girona 18-26, 08034 Barcelona, Spain

Keywords: SO<sub>2</sub>, ultrafine particles, industrial emissions, Air Quality

Presenting author email: .jesus@uhu.es

Sulfur dioxide (SO<sub>2</sub>) is a relevant pollutant in the air due to its adverse effects on human health and ecosystems. Currently, World Health Organization (WHO, 2021) proposes guidelines on ambient air pollution levels, and recommends a 40 µg/m<sup>3</sup> 24-hour mean limit of SO<sub>2</sub> concentrations. Previous WHO Air Quality Guidelines (WHO, 2006) suggested SO<sub>2</sub> concentrations of 20 µg/m<sup>3</sup> 24-hour average and 500 µg/m<sup>3</sup> 10-minute average. The European Union has established two limits for SO<sub>2</sub> (European Directive 2008/50/EC): a) Daily limit: not exceed 125 µg/m<sup>3</sup> more than three times per year; and b) Hourly limit: not exceed 350 µg/m<sup>3</sup> more than 24 times per year. Less than 1% of EU urban population is exposed to SO<sub>2</sub> concentration above EU standards and WHO guidelines in 2021 (WHO, 2021). Since the mid-1960s, several complex industrial estates have been located near the city of Huelva (SW Spain), including Cu smelter, phosphoric acid, oil refinery, petrochemical and paper mills. SO<sub>2</sub> was considered as a major pollutant and related to extreme pollution events in Huelva (Saenz, 2005), exceeding even the peak SO<sub>2</sub> levels of the London smog event in 1952 (Committee on Air Pollution, 1953). Since 1999, the chemical composition and source contribution of particulate matter have been studied in Huelva, demonstrating the relationships between SO<sub>2</sub> and toxic elements (e.g. As, Cu, Zn, Pb, Se and Bi) associated to ultrafine particles (Fernández-Camacho et al. 2012). In this work, we present historical daily levels obtained in 6 stations of Huelva capital between 1976 and 1981. The data were published daily by the Regional Public Health Agency in a local newspaper (ODIEL), which can be consulted as open data in the digital archive of the Huelva Province Government. Sampling was performed by bubblers and SO<sub>2</sub> analysis by spectrophotometry using the thorn method. Daily data availability in a month is 50% in the study period. Table 1 shows the average SO<sub>2</sub> monthly levels in the six monitoring stations of the city of Huelva (1976-1981). Monthly average concentrations exceed the current daily limit (125 µg/m<sup>3</sup>, European Directive 2008/50/EC) in June 1976, December 1977, August and October 1978 and August and September 1979. Maximum concentrations occur during the summer and autumn, favored by the impact of industrial plumes in breezes. During November 5<sup>th</sup> 1978, an extreme concentration exceeding 6 mg/m<sup>3</sup> occurred at the Stella Maris monitoring station. Extreme events of SO<sub>2</sub>

concentrations were frequent due to power supply interruptions and stagnant meteorological conditions. Compared to the studied period, there are currently no exceedances of SO<sub>2</sub> limits in the city of Huelva, although industrial plumes impact in the city 20% of days per year.

Table 1. Average SO<sub>2</sub> (µg/m<sup>3</sup>) monthly levels in the six monitoring stations of the city of Huelva (1976-1981).

SO <sub>2</sub> (µg/m <sup>3</sup> )	1976	1977	1978	1979	1980	1981
January		79	23	54	88	50
February	59	69	82	54	86	70
March	79	60	34	50	57	74
April	63	58	58	58	106	69
May	83	57	75	63	52	56
June	134	64	61	57	90	76
July	90	68	71	69	90	66
August	77	79	153	80	123	67
September	57	96	115	91	121	88
October	46	120	122	86	81	112
November	73	53	118	79	67	68
December	72	146	80	110	45	21
Average	76	79	83	71	84	68

This work was supported by State Research Agency (AEI) Projects: PID2021-126986OB-I00 and RTI2018-095937-B-I00

Committee on Air Pollution (1953) *Interim report, Cmd. 9011*, London: HMSO.

Fernández-Camacho R., et al. (2012) *Source apportionment of ultrafine particles in Huelva industrial city*. Atmospheric Environment 61, 507-517.

Saíenz A. (2005) *El SO<sub>2</sub> en Huelva: La historia de una contaminación*. Junta de Andalucía Ed. . 182 pp.

WHO (2006) *Air Quality Guidelines. Global Update 2005*. 484 pp.

WHO (2021) web link: [bit.ly/3P8LZzk](https://bit.ly/3P8LZzk).

## 2009-2023 TREND IN THE CHEMICAL COMPOSITION OF PM<sub>10</sub> IN A RURAL AREA INFLUENCED BY MINE ACTIVITY IN THE DISTRICT MINING OF RIOTINTO, SPAIN

A.M. Sánchez de la Campa<sup>1,2</sup>, J.D. de la Rosa<sup>1,2</sup>, D. Sánchez-Rodas<sup>1,3</sup> and P. Pérez Vizcaino<sup>2</sup>

<sup>1</sup>Center for Research in Sustainable Chemistry, Robert H. Grubbs Building, University of Huelva, Campus El Carmen, 21071, Huelva

<sup>2</sup>Department of Earth Sciences, Faculty of Experimental Sciences, University of Huelva, Campus El Carmen

<sup>3</sup>Department of Chemistry, Faculty of Experimental Sciences, University of Huelva, Campus El Carmen.

Keywords: PM<sub>10</sub>, metals, arsenic, mine

Presenting author email: ana.sanchez@pi.uhu.es

The Riotinto Mining District is one of the most important polymetallic sulphide mines of the world (Figure 1) (Leistel et al., 1998). In 2015, a new mining project started in the District, with an initial production of 5 Mtn/year in the pre-operational stage, incrementing to 9.5 Mtn/year in the operational stage (2017-21), reaching 15 Mtn/year from 2022 to the present. During the abandoned stage, a minimum impact of the fugitive particles and emissions was registered in the air (Sánchez de la Campa et al., 2011; 2015).

In this work we study the trend in the chemical composition of PM<sub>10</sub> during the abandoned (2009-14), pre-operational (2015-16), operational to 9 Mtn (2017-21) and 15 Mtn (2022-23) stages in Nerva village, belonging to Riotinto Mining District.

observed for As (2.0 ng/m<sup>3</sup>), Sb (1.3 ng/m<sup>3</sup>) and Pb (7.2 ng/m<sup>3</sup>) during 2022-23 (Figure 2).

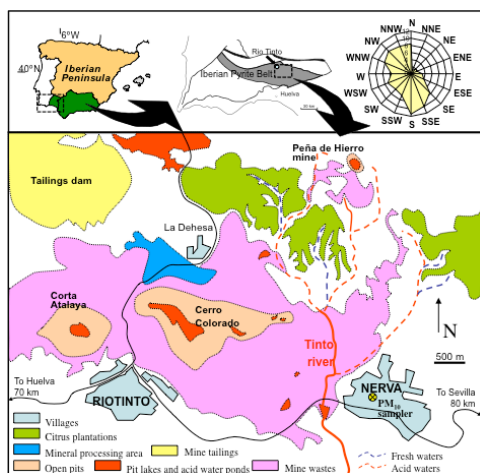


Fig. 1. Map of the Riotinto Mining District and location of the PM<sub>10</sub> sampler in Nerva (Sánchez de la Campa et al., 2011).

Munktell quartz fibre filters were used in high volume captors during 24h on weekly basis, for the PM<sub>10</sub> sampling. The chemical composition of PM<sub>10</sub> was determined using ICP-MS, ICP-OES, IC, LECO and TOT Sunset Laboratory.

The results have reported an increase of the concentrations in some heavy metals during pre-operational period (2015-16), such as: As (3.7 ng/m<sup>3</sup>), Cu (16.5 ng/m<sup>3</sup>), Sb (1.0 ng/m<sup>3</sup>), Pb (9.3 ng/m<sup>3</sup>) and Bi (0.3 ng/m<sup>3</sup>) respect to the abandoned stage; As, 1.1 ng/m<sup>3</sup>; Cu, 6.1 ng/m<sup>3</sup>; Sb, 0.4 ng/m<sup>3</sup>; Pb, 4.7 ng/m<sup>3</sup>; Bi, 0.1 ng/m<sup>3</sup>). However, a new increase has been

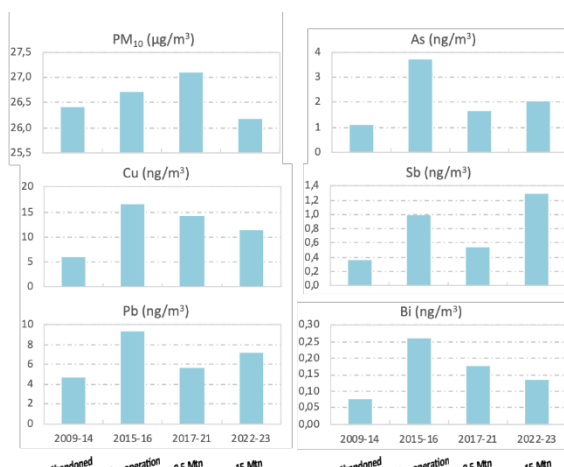


Fig. 2. Annual mean of PM<sub>10</sub>, As, Cu, Sb, Pb and Bi in the different periods considered.

In the case of As and Cu, the concentrations are almost three times higher in pre-operation stage than those obtained during the abandoned stage. In the Figure 2, the overall trend shows an increase of the concentration of the above mentioned elements. The annual mean concentration in PM<sub>10</sub> is relatively constant during all the studied period, reaching its maximum mean concentration in 2017-21.

This work was supported by AEI Project: RTI2018-095937-B-I00.

Leistel, et al. (1998) The volcanic-hosted massive sulphide deposits of the Iberian Pyrite Belt. *Miner. Depos.* 33, 2–30.

Sánchez de la Campa et al. (2011) Impact of abandoned mine wastes on atmospheric respirable particulate matter in the historic mining district of Rio Tinto (Iberian Pyrite Belt). *Environ. Res.* 111, 1018–1023.

Sánchez de la Campa et al. (2015) Geochemical anomalies of toxic elements and arsenic speciation in airborne particles from Cu mining and smelting activities: influence on air quality. *J. Haz. Mat.* 291, 18–27.

## THE COMPOSITION OF THE ATMOSPHERIC AEROSOLS DURING THE 2021 ERUPTION AND POST-ERUPTION PERIODS AT LA PALMA ISLAND

S. Rodríguez<sup>1</sup>, J. López Darías<sup>1</sup>, J. de la Rosa<sup>2</sup>, J. Vilches<sup>3</sup>, T. Boulesteix<sup>1</sup>, N. Taquet<sup>1,4,5</sup>,  
I. Belbachir<sup>1</sup>, O. E. García<sup>4</sup>, Celia Milford<sup>4</sup>, A.M. Sánchez de La Campa<sup>2</sup>

<sup>1</sup>Consejo Superior de Investigaciones Científicas, IPNA CSIC, La Laguna, Tenerife, 38206, Spain

<sup>2</sup>Centre for Research in Sustainable Chemistry - CIQSO, University of Huelva, E21071 Huelva, Spain

<sup>3</sup>Consejería de Transición Ecológica y Energía, Gobierno de Canarias, Las Palmas de Gran Canaria, Spain

<sup>4</sup>Izaña Atmospheric Research Centre, AEMET, Santa Cruz de Tenerife, Spain

<sup>5</sup>TRAGSATEC, Madrid, Spain

Keywords: volcanic aerosols, aerosol chemistry, mass closure, size distribution

Presenting author email: sergio.rodriguez@csic.es

From 19 September to 13 December 2021 a new volcanic eruption occurred in La Palma, the Canary Islands. The volcanic emissions of ashes and sulphur dioxide had a huge impact on the composition of the atmosphere, affecting the navigation air space and air quality. During the eruption up to 35000 persons were called to lockdown because of the adverse air quality conditions which clearly represented a threat for health due to the extremely high concentrations of sulphur dioxide (SO<sub>2</sub>) and particulate matter smaller than 10 microns (PM<sub>10</sub>) (Milford et al., 2023).

We present a study on the chemical composition of PM<sub>10</sub> aerosols during the eruption and post-eruption periods and of the volcanic ashes depositing during the eruption. Our study is based on (i) bulk samples of PM<sub>10</sub> collected every day (24h sampling at 30 m<sup>3</sup>/h) from 24 September 2021 to 24 March 2022, (ii) a set of PM<sub>10</sub> samples segregated by size, from < 10 nm to 10 microns, collected with a DEKATI cascade impactor from October 2021 to ending January 2022, and (iii) falling ashes collected during the eruption. The samples analysis included elemental composition (by IPC-MS & IPC-OES), water soluble salts by ion chromatography (SO<sub>4</sub><sup>2-</sup>, NO<sub>3</sub><sup>-</sup>, Cl<sup>-</sup>, F<sup>-</sup>, Na<sup>+</sup>, Mg<sup>+2</sup>, Ca<sup>+2</sup>) and organic carbon and elemental carbon. Measurements of hydrofluoric (HF) and hydrochloric (HCl) acids columns were performed with a low spectral resolution FTIR spectrometer (Bruker EM27/Sun instrument).

The composition of the PM<sub>10</sub> aerosols was very variable due to (i) the variability of the volcanic aerosols composition, (ii) the occurrence of the Saharan dust events, and (iii) because of the fires caused by the advance of the coladas over the towns that were finally destroyed. During the eruption, the concentrations of PM<sub>10</sub> reached very high values, frequently within the range 100-500 µg/m<sup>3</sup> (24h average), with very high concentrations of sulphate (10-30 µg/m<sup>3</sup>), chloride (10-30 µg/m<sup>3</sup>) and fluoride (1-3 µg/m<sup>3</sup>) linked to the presence of volcanic SO<sub>2</sub> and sulphur, HF and HCl acids. The chemical profile of the volcanic aerosols was very close to that of the volcanic ashes, with most of the mass dominated by the major elements of tephra (Si, Al, Fe, Ca, Mg.); however, the volcanic aerosols were enriched in Ti, Bi, Mo, Pb, Cd, Cu and other trace elements among other elements, with respect to the volcanic ashes, being those elements mainly observed

in the 0.1-1 µm aerosol mode in the cascade impactor samples, indicating that these elements were emitted in the gas phase and then condensed in the ambient air. The chemical profile of the volcanic aerosols was also markedly different to that of the Saharan dust. We provide a detailed comparative analysis of the volcanic versus Saharan dust aerosols, based on the ratios to Al and percentage of the aerosol mass, information of high importance for the climate models that consider the biogeochemical cycles (Wong et al., 2021). The Positive Matrix Factorization (PMF) was unable to segregate the between Saharan and volcanic aerosols, so we developed a source apportionment method based on the elemental ratios that successfully segregated the aerosol mass and chemical profile of the volcanic and Saharan dust aerosols.



Figure 1. Sampler collecting PM<sub>10</sub> samples in La Palma during the 2021 volcanic eruption.

The project AEROEXTREME (PID2021-125669NB-I00) is funded by the State Research Agency of Spain, the Ministry of Science, Innovation and Universities of Spain and the European Regional Development Fund.

Milford et al., 2023. Impact of the 2021 La Palma volcanic eruption on air quality: Insights from a multidisciplinary approach. STOTEN 869, 161652

Wong et al., 2021. Anthropogenic perturbations to the atmospheric molybdenum cycle. Global Biogeochemical Cycles, 35, e2020GB006787.

# IMPACT OF THE SIERRA DE LA CULEBRA WILDFIRE ON THE AIR QUALITY OF THE CITY OF LEÓN: AEROSOL CHARACTERIZATION AND INFLUENCE OF METEOROLOGICAL CONDITIONS

C. Blanco-Alegre<sup>1</sup>, A.I. Calvo<sup>1</sup>, C. Gonçalves<sup>1</sup>, and R. Fraile<sup>1</sup>

<sup>1</sup>Department of Physics, Universidad de León, León, Spain

Keywords: air quality, black carbon, nephelometer, total carbon.

Presenting author email: cmaig@unileon.es

Wildfires and air pollution pose significant challenges in the Mediterranean region, with implications for both human health and the climate, with complex interconnections between them. An instance is the wildfire that occurred in Sierra de la Culebra, Zamora, Spain, from July 15<sup>th</sup> to 20<sup>th</sup>, 2022, affecting approximately 30,000 hectares. During the fire, air masses carried the smoke plume directly towards the city of León, located 100 km away from the fire zone (Fig. 1). The objective of this study is to delineate the principal findings concerning the total number concentration of aerosol particles, their carbonaceous content, and their light-scattering properties in León during this period, taking into account meteorological variables.

The sampling campaign was carried out at the campus of the University of León (Spain) during July 2022. Several sampling instruments were used: i) a Total Carbon Analyzer (TCA08) coupled with an aethalometer AE33 to detect Organic Carbon (OC) and Black Carbon (BC) (and, therefore Total Carbon-TC) in PM<sub>10</sub>; iii) a Scanning Mobility Particle Sizer spectrometer (TSI-SMPS Model 3938) to measure the particle number concentration between 8 and 310 nm in 110 channels; iv) an Ecotech Aurora 3000 nephelometer to measure the forward and backward scattering at three wavelengths (450, 525 and 635 nm) and; v) a weather station to monitor some meteorological variables.

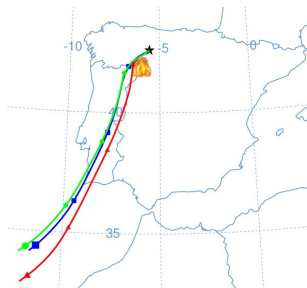


Fig. 1. Backward trajectories of air masses for a 24-hour duration at 100 (red), 300 (blue) and 500 m (green) over León on the 18/07/2022 at 2300 UTC. The point of wildfire is marked with a flame. Source: HYSPLIT model.

All pollutant concentrations increased significantly due to the arrival of the plume the day 18<sup>th</sup> until 20<sup>th</sup> (Fig. 2). Below are the maximum hourly concentrations reached during the fire: i) OC concentration of 61.9  $\mu\text{g m}^{-3}$  on 19/7/2022 at 1900 UTC - it should be noted that the equipment saturated due to high concentration on July 18<sup>th</sup>); ii) BC concentration of 20.2  $\mu\text{g m}^{-3}$  on 18/7/2022

at 2300 UTC; iii) total particle concentration of 21,400 particle  $\text{cm}^{-3}$  with a geometric mean of 20.3 nm on 18/7/2022 at 2300 UTC; iv) a maximum scattering Ångström extinction coefficient ( $\text{SAE}_{525 \text{ nm}/635 \text{ nm}}$ ) of 2.61 on 19/7/2022 at 1700 UTC. It's important to highlight that the temperature presented a decrease in both its maximum and minimum values to 11 and 12 °C, respectively, due to the plume's arrival, the absorption of heat of aerosols in the atmosphere and the inability to reach the Earth's surface radiation (Jiang *et al.*, 2020). However, the relative humidity doubled during the days when the city was covered by smoke.

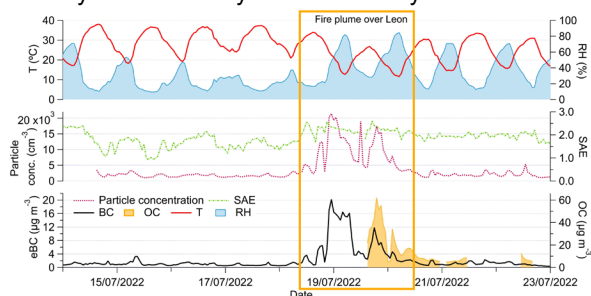


Fig. 2. Evolution of particle concentration, BC, OC,  $\text{SAE}_{525 \text{ nm}/635 \text{ nm}}$  and meteorological conditions between 14 and 23 July 2022 at León.

Given the increase in wildfire frequency in Mediterranean area, the study of "extreme" situations becomes crucial for public health, facilitating the launch of population alerts. The next step in our study will be analyze the influence of such wildfire on radiative forcing.

The authors gratefully acknowledge the NOAA Air Resources Laboratory (ARL) for the provision of the HYSPLIT transport and dispersion model and/or READY website (<http://www.ready.noaa.gov>). This work was partially supported by the Junta de Castilla y Leon co-financed with European FEDER funds (Grant LE025P20). Furthermore, it is part of the project TED2021-132292B-I00, funded by MCIN/AEI/10.13039/501100011033 and by the European Union "NextGenerationEU"/PRTR.

Jiang, Y., Yang, X. Q., Liu, X., Qian, Y., Zhang, K., Wang, M., Li, F., Wang, Y., and Lu, Z. (2020). Impacts of Wildfire Aerosols on Global Energy Budget and Climate: The Role of Climate Feedbacks. *Journal of Climate*, 33(8), 3351–3366.

## PUBLISHED RESEARCH ON AIR QUALITY IN AFRICA: A RESULT OF ENVIRONMENTAL LEGISLATION AND RESEARCH INFRASTRUCTURE

L.B. Osa-Akara, A.I. Calvo, C. Gonçalves, C. Blanco-Alegre, R. Fraile  
 Department of Physics, Universidad de León, Spain

Keywords: Africa, aerosol, bibliometric review, air quality guidelines, air quality monitoring stations  
 E-mail of the presenting author: aicalg@unileon.es

Air pollution is the second leading risk factor for death in Africa, following malnutrition (WHO, 2019). This continent has endured the most severe consequences of air pollution and its global health impacts. Between 1990 and 2017, there was a 60% increase in deaths attributed to air pollution in Africa (Rees et al., 2019). In 2019, this resulted in 1.1 million deaths on the continent (WHO, 2019), with approximately 700,000 premature deaths annually in sub-Saharan Africa (Bauer et al., 2019). The concentration of PM<sub>2.5</sub> in African countries is ten times higher than the WHO recommended levels (WHO, 2021). Air quality studies are limited in Africa (Mahesh et al., 2022). It is crucial to assess the current state of knowledge on air quality in Africa and its evolution over the last decades.

The present study focuses on identifying and quantifying existing research gaps in air quality studies across the five regions that the UN divides the African continent (North Africa, Southern Africa, Central Africa, East Africa, and West Africa). This will allow for the prioritization of areas lacking information for future research.

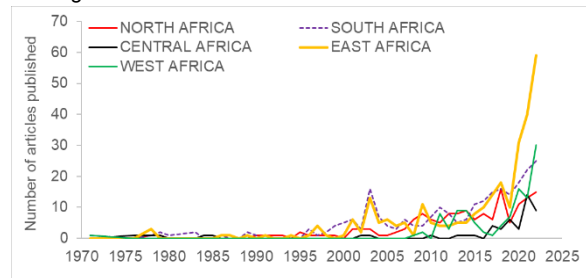
The search was conducted using two digital platforms: Science Direct and Web of Science. It covers records from the earliest available data up to the year 2022. Based on the data obtained, an initial analysis was performed to illustrate the evolution of the number of publications in each region from 1971 to 2022. Subsequently, statistical analyses were carried out to explore the relationship between publications and factors such as the existence of atmospheric monitoring stations, legislation, and universities across different regions.

The regions of Southern Africa and East Africa have the highest volume of publications during the studied period, with a total of 248 and 245 articles, respectively. On the other hand, the Central Africa region has the lowest number of publications (50 articles). West Africa and North Africa have registered a total of 111 and 158 publications, respectively. The first African publications date back to 1971 in Southern Africa and West Africa (Fig. 1). Additionally, in 1978, at least one article was published in each of the five regions. East Africa and Southern Africa have achieved an outstanding number of publications in 2022, with 59 and 30 articles published, respectively.

Among the 54 African countries, only seven have continuous monitoring stations, predominantly located in South Africa, which stands as the sole country in the region with a comprehensive and well-organized air quality monitoring program (Amegah and Agyei-Mensah, 2017). Furthermore, just 19 African nations have implemented legally enforceable standards to improve air quality. Each of the five African regions has seen at least one country adopt air quality-related guidelines. While certain countries have specific regulations like South Africa's Air Quality Act 39 of

2004, others tackle this concern through diverse environmental laws.

Figure 1. Evolution of articles published on air pollution in the five regions of Africa from 1971 to 2022.



This work has been partially supported by the project TED2021-132292B-I00, funded by MCIN/AEI/10.13039/501100011033 and by the European Union "NextGenerationEU"/PRTR. It is also part of the Junta de Castilla y León co-financed with European funds FEDER (Grant LE025P20). L.B.O.A. also thanks the Schlumberger Foundation, the Women for Africa Foundation and the University of León for supporting her PhD studies.

Amegah, A. K., & Agyei-Mensah, S. (2017). Urban air pollution in Sub-Saharan Africa: Time for action. *Environmental Pollution*, 220, 738-743.

Bauer, S. E., Im, U., Mezuman, K., & Gao, C. Y. (2019). Desert dust, industrialization and agricultural fires: Health impacts of outdoor air pollution in Africa. *Nature Communications*, 10(1), 1-121

Mahesh, B., Sivakumar, V., Kulkarni, P., & Sreekanth, V. (2022). Particulate air pollution in Durban: Characteristics and its relationship with 1 km resolution satellite aerosol optical depth. *Advances in Space Research*, 70(2), 371-382.

Rees, N., Wickham, A., Choi Y. (2019) Silent Suffocation in Africa Air Pollution Is a Growing Menace, Affecting the Poorest Children the Most, 2019. <https://www.unicef.org/reports/silent-suffocation-in-africa-air-pollution-2019>.

WHO (2019). Ambient air pollution: training for health care providers (No. WHO/CED/PHE/EPE/19.12.14). World Health Organization.

WHO (2021). WHO's response to COVID-19: 2021 Annual Report.

## REAL-TIME AIR QUALITY MONITORING USING RPAS

S. Filipe-Pozas, A.I. Calvo and R. Fraile  
Department of Physics, Universidad de León, Spain  
Keywords: air quality, Arduino, particulate matter, RPAS  
Presenting author email: aicalg@unileon.es

The expansion of industrial and transportation activities heightens health hazards from urban air pollution (Saini et al., 2020). Drone-assisted systems provide flexibility over traditional monitoring stations. Research has explored drones as a method for detecting environmental air pollution and particulate matter concentrations have been successfully measured (Villa et al., 2016; Chilinski et al., 2018).

This study explores the innovative application of a PM10 and PM2.5 sensor integrated with an Arduino Nano and mounted on a RPAS (Remotely Piloted Aircraft System), specifically the DJI Mini 3 Pro, to assess air quality at various altitudes and locations.

The core objective is to develop a mobile air monitoring system that can provide spatial and temporal data on atmospheric particles concentrations, offering a dynamic complement to stationary air monitoring stations. The specific objectives are:

- Develop a standardized methodology for analyzing atmospheric particles at varying heights, aiming to measure PM10 and PM2.5 concentrations consistently.
- Implement a cost-effective, mobile sampling method to enable monitoring across multiple locations without fixed infrastructure.
- Analyze collected samples to create detailed maps depicting PM10 and PM2.5 concentration distribution, offering insights into pollutant dispersion patterns and high-risk areas.

The methodology includes the selection of equipment, programming of the Arduino Nano for data collection and storage, as well as flight protocols for the DJI Mini 3 Pro drone to ensure broad and representative coverage of the study areas.

The Arduino Nano serves as the central processing unit, managing data collection from the particulate matter sensor. This data is then stored on an SD card module attached to the Arduino, ensuring that information is recorded for subsequent analysis. The mobility of the DJI Mini 3 Pro drone allows for the collection of air quality data in diverse and potentially hard-to-reach environments, presenting a significant advantage over traditional, fixed-location air quality monitoring stations.

This drone (Fig.1) has a weight of 249 g and uses GPS, Galileo, and BeiDou geolocation systems. These will allow for the recording of the coordinates of each sampling point.

Data from this sensor will be compared with those from a fixed air monitoring station.

The integration of the sensor with the RPAS opens new avenues for environmental monitoring, providing a cost-effective and versatile tool for air quality assessment.

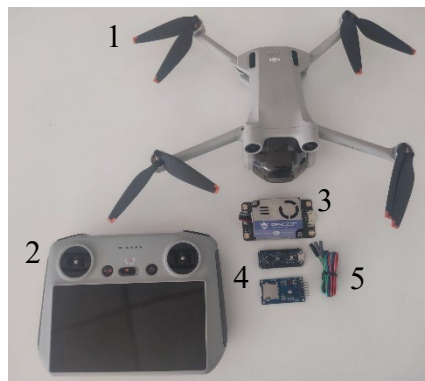


Fig. 1. Elements used for the measurement of atmospheric particles: 1. DJI mini 3 pro drone; 2. DJI RC controller; 3. DFRobot SEN0460 I2C Air Quality Sensor; 4. Kwmobile SD card module; 5. Dupont cables.

This work has been partially supported by the project TED2021-132292B-I00, funded by MCIN/AEI/10.13039/501100011033 and by the European Union "NextGenerationEU"/PRTR. It is also part of the Junta de Castilla y León co-financed with European funds FEDER (Grant LE025P20).

Chilinski, M.T., Markowicz, K.M., Kubicki, M. (2018) UAS as a support for atmospheric aerosols research: case study. *Pure and Applied Geophysics*, 175. 3325-3342.

Saini, J., Dutta, M., Marques, G. (2020) Indoor air quality prediction systems for smart environments: A systematic review. *Journal of Ambient Intelligence and Smart Environments*, 12 (5). 433-453, 4.

Villa, T.F., Gonzalez, F., Miljevic, B., Ristovski Z.D., Morawska, L. (2016) International laboratory. An overview of small unmanned aerial vehicles for air quality measurements: present applications and future perspectives. *Sensors*, 16 (1072) 1-29.

## AIR QUALITY IN LEÓN AND ALMERÍA (SPAIN): IMPACT OF SAHARAN DUST INTRUSIONS IN THE NORTH-SOUTH CONTEXT

M. Fattler, C. Blanco-Alegre, A.I. Calvo and R. Fraile  
Department of Physics, Universidad de León, León, 24071, Spain

Keywords: exceedances, gases, patterns, PM10

Presenting author email: aicalg@unileon.es

Saharan dust intrusions are a recurrent phenomenon that impact air quality in Spain, especially in southern regions and sometimes even in more northerly areas. Saharan dust is transported by air currents from North Africa to southern Europe, and can cover large areas of the country, causing significant repercussions on air quality and public health. When Saharan dust reaches Spain, it can increase the levels of suspended particles in the atmosphere, which has an impact on visibility and air quality. These particles can contain organic compounds, heavy metals and other pollutants that can be harmful to human health, especially for people with respiratory and cardiovascular diseases. For instance, they cause variations in the airborne biological content (Rodríguez-Arias et al., 2023), mainly in south of Iberian Peninsula (Rojo et al., 2021), which leads to an increase in allergies among the population. Saharan dust intrusions can also affect the climate and the environment (Oduber et al., 2019). For example, they can influence precipitation patterns and cloud formation, as well as soil fertility and the health of terrestrial and marine ecosystems.

Although Saharan dust intrusions are a natural phenomenon, their impact on air quality and the environment can be aggravated by factors such as human activity, climate change and local meteorological conditions. This phenomenon has attracted increasing interest in the scientific community due to its potential implications for the environment, economic and public health.

In this context, the present study aims to analyze the air quality in León (NW of Spain) and Almería (SE of Spain), focusing specifically on the impact of Saharan dust intrusions. Over a 10-year period, data on air pollutant concentrations (gases and particles) in both cities will be analyzed. Seasonal, annual, and monthly average values in León and Almería will be determined and compared. These data will be obtained from the air quality networks of Castilla y León and Andalucía (for León and Almería, respectively). The number of exceedances of the limit values established by current legislation (Directive 2008/50/CE) for the various pollutants studied will be determined. The PM10 exceedances will be analyzed in-depth in an attempt to correlate them with the presence of Saharan dust particles in the air.

To achieve these objectives, the Hysplit model will be used to determine the origin of the air masses and other tools, such as the NAAPS and Multimodel models, which provide information on the arrival of Saharan dust to the peninsula. Their presence will be confirmed with

official data from the Ministry for Ecological Transition and the Demographic Challenge. Factors such as geography and meteorology will be examined to understand possible differences between the results obtained for the two cities. Finally, patterns will be established, and the potential environmental and public health implications of Saharan dust intrusions will be analysed.

This work was partially supported by the Junta de Castilla y León co-financed with European FEDER funds (Grant LE025P20). Furthermore, it is part of the project TED2021-132292B-I00, funded by MCIN/AEI/10.13039/501100011033 and by the European Union "NextGenerationEU"/PRTR.

Oduber, F., Calvo, A. I., Blanco-Alegre, C., Castro, A., Nunes, T., Alves, C., Sorribas, M., Fernández-González, D., Vega-Maray, A. M., Valencia-Barrera, R. M., Lucarelli, F., Nava, S., Calzolari, G., Alonso-Blanco, E., Fraile, B., Fialho, P., Coz, E., Prevot, A. S. H., Pont, V., & Fraile, R. (2019) Unusual winter Saharan dust intrusions at Northwest Spain: Air quality, radiative and health impacts. *Science of the Total Environment*, 669, 213–228.

Rodríguez-Arias, R. M., Rojo, J., Fernández-González, F. and Pérez-Badía, R. (2023) Desert dust intrusions and their incidence on airborne biological content. Review and case study in the Iberian Peninsula. *Environmental Pollution*, 316, 120464.

Rojo, J., Moreno, J. M., Romero-Morte, J., Lara, B., Elvira-Rendueles, B., Negral, L., Fernández-González, F., Moreno-Grau, S., and Pérez-Badía, R. (2021) Causes of increased pollen exposure during Saharan-Sahel dust intrusions. *Environmental Pollution*, 284, 117441.

## SAHARAN DUST INTRUSIONS IN SPAIN BETWEEN 2004 AND 2023

A. Herrero, A.I. Calvo, C. Blanco-Alegre, R. Fraile

Department of Physics, Universidad de León, León, 24007, Spain

Keywords: aerosol dispersion, atmospheric dynamics, North–South gradient, PM10

Presenting author email: rfral@unileon.es

Air pollution is a crucial factor in people's quality of life and health. Depending on the concentration and composition of pollutants present in the atmosphere, there are a series of health and environmental issues. Therefore, it is very important to carry out pollution studies to determine the necessary actions to maintain the overall well-being of public health. Atmospheric particulate matter (PM) is defined as a complex mixture of extremely small particles and liquid droplets suspended in the atmosphere that cause serious health effects, influence radiative balance, cloud formation, or modification of albedo. These particles have a wide range of morphological, physical, chemical, and thermodynamic properties. Determining the concentrations of PM in the atmosphere is a key parameter in assessing air quality. PM10 is a magnitude generally used to measure the aerosol amount present in the atmosphere, while PM2.5 refers to particles associated with hazardous effects on human health, as their ability to penetrate the respiratory system is greater than that of bigger particles. Due to the proven influence of this pollutant on human health, climate, and ecosystems, both contributions derived from human activities and those originating from natural sources are regulated in European legislation, although the latter can be evaluated but not controlled (Tahirí, 2021).

Intrusions of African air masses are responsible for increasing the level of mineral particulate matter in areas that may be far away from the continent that is the source of this material (Alonso Pérez, 2007). During dust storms, surface-level events that spread across the troposphere, particles are transported by powerful turbulent winds across extensive distances (Bodenheimer et al., 2019). Due to its strategic position, the Iberian Peninsula receives very often suspended particulate matter from North Africa (Russo et al., 2020).

This study focuses on the temporal trend of natural Saharan dust intrusion events in Spain from 2004 to 2023. Data obtained from the Ministry for Ecological Transition and Demographic Challenge (MITECO) have been analyzed to determine yearly and seasonal trends across nine geographical regions: Canary Islands, Balearic Islands, Southwest peninsula, Southeast peninsula, Centre peninsula, Levante, Northwest peninsula, North peninsula, and Northeast peninsula. Furthermore, the duration of these events has been analyzed. Additionally, the evolution of weather types, following a well-known classification by Lamb (1972), has been studied to assess potential correlations with intrusion events.

Subsequently, a detailed examination was conducted on the unprecedented extreme Saharan dust event that occurred in March 2022. An analysis was carried out using aerosol concentration data from various sampling stations across Spanish territory to delineate the longitudinal and latitudinal dispersion gradient of African dust particles during that episode. The Hysplit model has been employed to determine the origin of air masses, alongside other tools such as the NAAPS and Multimodel models, which provide information on the arrival of Saharan dust to the Peninsula.

This work is part of the project TED2021-132292B-I00, funded by MCIN/AEI/10.13039/501100011033 and by the European Union "NextGenerationEU"/PRTR. Furthermore, it was partially supported by the Junta de Castilla y León, co-financed with European FEDER funds (Grant LE025P20).

Alonso Pérez S. (2007). *Caracterización de las intrusiones de polvo africano en Canarias*. Tesis Doctoral. Universidad de La Laguna. La Laguna, Tenerife, España. Available in: <https://repositorio.aemet.es/handle/20.500.11765/2091> (Consulted: 24/02/24).

Bodenheimer, S., Lensky, I.M., Dayan U. (2019). Characterization of Eastern Mediterranean dust storms by area of origin; North Africa vs. Arabian Peninsula. *Atmos. Environ.* 158-165.

Lamb H. (1972). British Isles Weather types and a register of daily sequence of circulation patterns: 1861–1971. *Geophys. Mem.* 116: 85.

Russo, A., Sousa, P.M., Durão, R.M., Ramos, A.M., Salvador, P., Linares, C., Díaz, J., Trigo, R.M. (2020) Saharan dust intrusions in the Iberian Peninsula: predominant synoptic conditions *Sci. Total Environ.*, 717, 137041.

Tahirí, N. (2021). Impacto de las intrusiones de polvo mineral Sahariano en la calidad del aire de Valladolid durante el periodo 2003-2014. TFM Universidad de Valladolid. Valladolid, España. Available in: <https://uvadoc.uva.es/bitstream/handle/10324/49600/TFM-G1394.pdf?sequence=1&isAllowed=y> (Consulted: 23/02/2024).

## CHARACTERIZATION OF ULTRAFINE PARTICLES: IMPLEMENTATION OF PARTICLE SIZE SPECTROMETER AT AN URBAN BACKGROUND STATION

Pastor-Amat, J. Nicolás, Á. Clemente, N. Galindo, J. Crespo, E. Yubero  
 Department of Physics, University Miguel Hernández, Elche, Alicante, Spain

Keywords: Ultrafine particles, particle number concentration, atmospheric particulate matter.

Presenting author email: eyubero@umh.es

Ultrafine particles (UFP) have the ability to penetrate deeply into the respiratory and cardiovascular systems, posing significant risk to human health. Monitoring of these particles is essential to identify their primary sources and implement effective reduction strategies. Their tiny size poses a challenge to measurement accuracy. In this study, a custom-built TROPOS-type MPSS (mobility particle size spectrometer) was used to collect aerosol particle size distributions (PNSDs) ranging from 10 to 800 nm at a 5-minute time resolution. Following EUSAAR/ACTRIS standards, our closed-loop system maintained a 5:1 sheath to aerosol flow ratio, with sample air drawn in at  $1 \text{ L} \cdot \text{min}^{-1}$  and humidity controlled below 40% using a Nafion dryer. Components included a bipolar diffusion charger (Ni-63), Vienna-type DMA (Differential Mobility Analyzer, 28 cm length), and a TSI 3772 CPC (Condensation Particle Counter, TSI Inc., USA).

This research aims to characterize UFP at an urban background station in southeastern Spain, focusing on the nucleation, Aitken, and accumulation modes. Measurements were carried out in Elche from July 1, 2022, to June 8, 2023.

The average value of the total particle number concentration (PNC) was  $169000 \pm 2000$  while the averages of the different modes were  $68100 \pm 1300$ ,  $78400 \pm 100$  and  $22400 \pm 500$  for the nucleation, Aitken and accumulation modes, respectively.

Figure 1 shows the particle size distribution averaged over the whole period. The maximum values are obtained in the nucleation mode, closely followed by those obtained in the Aitken mode. This characterizes the urban background station, where fresh aerosols emitted close to the station by the surrounding traffic are found at the same time as aerosols that have already started to age since their emission. In comparison, the contribution of aerosols of regional origin does not seem to be very important.

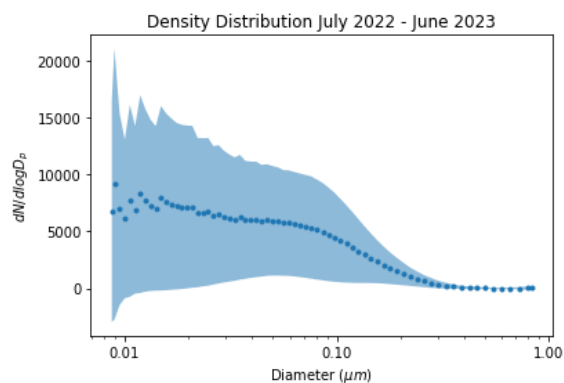


Figure 1. Average particle size distribution during the study period.

The distribution of PNC over the day is shown in figure 2. The maximum is reached in the late hours of the day, related to the reduction of the mixing layer. The minimum is reached in the early morning before traffic starts in the city.

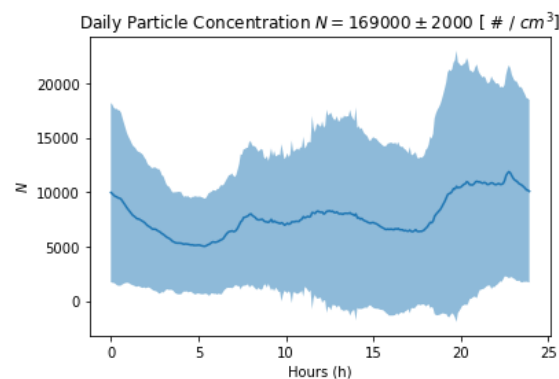


Figure 2. Average daily total particle concentration.

The particle distributions have been compared between different days of the week and for different seasons of the year. A comparison of the results obtained in Elche with other European cities was carried out.

This work was supported by the Valencian Regional Government (Generalitat Valenciana, CIAICO/2021/280 research project) and by MCIN/AEI/10.13039/501100011033 and the “European Union NextGenerationEU/PRTR” (CAMBIO project, ref. TED2021-131336B-I00

## INVESTIGATION ON A NEW BIOMONITOR OF AIR PAHS

F. De Nicola<sup>1,2</sup>, V. Carrieri<sup>1</sup>, J.R. Aboal<sup>3</sup>, J.A. Fernández<sup>3</sup>

<sup>1</sup>Dept. Sciences and Technologies, University of Sannio, 82100 Benevento, Italy

<sup>2</sup>University of A Coruña. Grupo Química Analítica Aplicada (QANAP). University Institute of Environment (IUMA). Department of Chemistry, Faculty of Sciences, Campus de A Coruña, s/n. 15071 – A Coruña, Spain.

<sup>3</sup>Dept. Functional Biology, Faculty of Biology, Universidade de Santiago de Compostela, 15782 Santiago de Compostela, Spain

Keywords: air PAHs, moss, waxes

Presenting author email: fdenicol@unisannio.it

Polycyclic aromatic hydrocarbons (PAHs), formed by two or more condensed benzene rings, are harmful, carcinogenic and persistent pollutants in the environment. Consequently, they represent a high risk for living beings, through the exposure by air inhalation and/or dermal contacts (IARC, 2010), but also for ecosystems (Wright et al., 2018).

Air pollution is one of the major environmental health risk factors, and pollutant levels are conventionally monitored by both active (pumping air through a filter) or passive samplers (which adsorb pollutants on a synthetic polymeric substrate). These methods have high costs, are specific of a single compound and are also time consuming (Aboal et al., 2020). As an alternative, active biomonitoring, by means of moss bags used as passive samplers, overcome most of these limitations. In the last years, the improvement of passive biomonitoring with mosses has taken a qualitative leap in thanks to a new designed type of passive air sampler, the "Mossphere" device. These devices have been found to accurately estimate the atmospheric levels of 4-, 5- and 6-ring PAHs and total PAHs detected in PM10 and even better estimate their levels in bulk deposition (Aboal et al., 2020).

Here, the capability of a moss species, *Physcomitrium patens*, to accumulate air PAHs was tested for the first time. It could be hypothesized that PAH accumulation capacity of mosses is determined by the efficiency to trap particles rather than PAH adsorption directly on cuticular waxes. In order to fill this gap of knowledge, the PAH accumulations in two clones of *Physcomitrium patens* moss, a wild type (WT) and a clone with a deficiency of cuticular waxes (AW), were compared.

At this aim, transplants of the two moss clones were simultaneously exposed (February-July 2020) in 3 sites under anthropic pressure and 1 control site, far from urban or industrial areas, in Benevento (Italy) and Santiago de Compostela (NW Spain).

The two clones were characterized for the concentrations of 26 fatty acids by GC-FID after hexane extraction and trans-esterification, and for the concentrations of 18 PAHs according to the protocols EPA 3550C (2007) and EPA 8270E (2018) for PAH extraction and analyses, respectively.

Overall, the WT clone, with the higher lipid concentration, seemed to better accumulate each single PAH than the AW clone. Medium- and high-molecular weight PAHs were the most present PAHs in both moss clones exposed. It is well known, in fact, that mosses show a strong tendency to accumulate these classes of PAHs (Huang et al., 2018).

The evidence from field exposure seems to corroborate the hypothesis of a "physical" retention of particles, and linked PAHs, rather than a their chemical uptake by adsorption through the cuticle. The *Physcomitrium patens* moss exposed in sites closed to emission sources, i.e. urban and industrial area, showed the highest accumulation of PAHs, both in Italy and Spain. The ability of the selected moss *Physcomitrium patens* to act as a biomonitor of PAHs is undoubted, although the exposure was severely affected by lockdown due to Covid 19.

Table 1. Ranges of total PAH concentrations.

Site	WT ( $\mu\text{g/g d.w.}$ )	AW ( $\mu\text{g/g d.w.}$ )
Benevento	bdl-0.30	bdl-0.16
Santiago	0.02-0.74	0.02-0.19

This research is partially supported by FRA 2020 Unisannio.

Aboal J.R., Concha-Graña E., De Nicola F., Muniategui-Lorenzo S., López-Mahía P., Giordano S., Capozzi F., Di Palma A., Reski R., Zechmeister H., Martínez-Abaigar J., Fernández J.A. (2020) Testing a novel biotechnological passive sampler for monitoring atmospheric PAH pollution. *J. Hazard. Mater.*, 381, 120949.

Environmental Protection Agency (2007). EPA Method 3550C, Ultrasonic extraction, US.

Environmental Protection Agency (2018). EPA Method 8270E, Semivolatile Organic Compounds by Gas Chromatography/Mass Spectrometry (GC-MS), US.

Huang S., Dai C., Zhou Y., Peng H., Yi K., Qin P, Luo S, Zhang X. (2018) Comparisons of three plant species in accumulating polycyclic aromatic hydrocarbons (PAHs) from the atmosphere: a review. *Environ. Sci. Pollut. Res.*, 25(17), 16548–16566.

IARC (2010). Some non-heterocyclic polycyclic aromatic hydrocarbons and some related exposures. *IARC Monogr Eval Carcinog Risks Hum.*, 92, 1–853.

Wright L.P., Zhang L., Cheng I., Aherne J., Wentworth G.R. (2018). Impacts and Effects Indicators of Atmospheric Deposition of Major Pollutants to Various Ecosystems - A Review. *Aerosol Air Qual. Res.*, 18, 1953-1992.

## PM<sub>2.5</sub> AND BIOAEROSOLS EMITTED FROM OLIVE MILL WASTEWATER EVAPORATION PONDS: ASSESSMENT OF TRACE ELEMENTS AND MICROBIAL DIVERSITY

A. Rodríguez<sup>a\*</sup>, G. Viteri<sup>b</sup>, A. Aranda<sup>b</sup>, Y. Díaz de Mera<sup>b</sup>, D. Rodríguez<sup>a</sup>, N. Valiente<sup>c</sup>, N. Rodríguez-Fariñas<sup>a</sup>, S. Seseña<sup>a</sup>.

<sup>a</sup> Faculty of Environmental Sciences and Biochemistry, Toledo, UCLM

<sup>b</sup> Faculty of Chemical Sciences and Technologies, Ciudad Real, UCLM

<sup>c</sup> Department of Science and Agroforestry Technology and Genetics, Albacete, UCLM

Keywords: PM<sub>2.5</sub>, trace elements, airborne microbiota, amplicon sequencing

Presenting author email: anamaria.rodriguez@uclm.es

Olive mill wastewater (OMW) is a pollutant residue from the olive oil industry, usually stored in evaporation ponds as sludge (Kavvadias, 2017). Many of them have become obsolete or abandoned, and the difficulty in handling and eliminating the OMW sludge is linked to serious environmental issues. The suspension of unconsolidated sediments as PM is possible (Li, 2006), which would have a elevated load of associated metals and biological material (bioaerosols), which would play an important role in the geochemical, toxicological and biological processes of the surrounding area.

PM<sub>2.5</sub>, their trace elements (TEs) associated, as well as microbial community (bacteria and fungi) were analysed considering their possible relationship with the biota and metals of the OMW sludge ponds. Additionally, meteorological conditions and back trajectories were assessed to shed light on the sources related to these elements. The polluting effects was assessed by analysis of environmental and health risk indicators.

PM<sub>2.5</sub> presented the highest levels during the warmer months (Fig. 1) with a significant contribution of mineral dust from Saharan intrusions. The total average contribution of TEs to the PM<sub>2.5</sub> mass was 27.8%, with a significant contribution of Hg. The possible sources identified were the OMW sludge stored in the ponds, mineral dust from the area and Sahara intrusions, and traffic. Due to high Hg levels, the ecological risk index (RI) was higher than 720, posing an ecological threat that could affect the ecosystem around the OMW sludge ponds.

Meteorological conditions and dust intrusions from the Sahara influenced the total bioaerosol load, with strong negative correlation between bacteria and fungi (Fig. 1). The microbial diversity of these bioaerosols was analysed and compared to those of the OMW sludge.

The results from this study contribute to a better understanding of the environmental dynamics in the OMW sludge evaporation ponds, and they could aid in the development of effective strategies for its management.

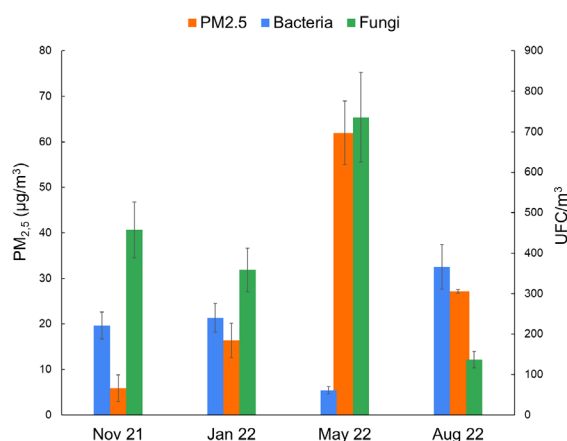


Fig. 1. Temporal evolution of PM<sub>2.5</sub> concentrations (y-axis, left) and microorganism counts (y-axis, right).

This work was supported by JCCM (SBPLY/21/180501/000283).

Kavvadias, V., et al. (2017). Fate of potential contaminants due to disposal of olive mill wastewaters in unprotected evaporation ponds. *Bull. Environ. Contam. Toxicol.* 98, 323–330.

Li, T., et al. (2007) Morphological characterization of suspended particles under wind-induced disturbance in Taihu Lake, China. *Environ Monit Assess* 127, 79–86.

## INDOOR AIR QUALITY IN ELDERLY CARE CENTERS: CHEMICAL AND MICROBIOLOGICAL POLLUTANTS

Susana Seseña<sup>a\*</sup>, María Rodríguez<sup>a</sup>, Nicolas Valiente<sup>b</sup>, Llanos Palop<sup>a</sup>, Ana Rodríguez<sup>a</sup>

<sup>a</sup> Faculty of Environmental Sciences and Biochemistry, Toledo, UCLM

<sup>b</sup> Department of Science and Agroforestry Technology and Genetics, Albacete, UCLM

Keywords: Indoor air quality, bioaerosols, particulate matter, pathogens

Presenting author email: susana.sprieto@uclm.es

The study of indoor air quality in elderly care centers (EECs) has important implications for ensuring the health and safety of residents. EECs are considered places of great relevance because their occupants are elderly people, affected by chronic diseases, with an impaired immune system who, in addition, spend much of their time indoors (Almedia-Silva, 2014). Prolonged exposures of this population to poor indoor air quality (IAQ) could aggravate the most prevalent diseases in the elderly population (Maio, 2015; Bentayeb, 2015). This problem would be exacerbated in the future, as by 2030 Europe will be the most aged continent in the world, with an elderly population (citizens aged >80 years) amounting to 35 million (Betanyeb, 2015). Currently, there are limited studies that have conducted a multidisciplinary analysis of chemical and microbiological parameters, including the assessment of the presence of potential airborne pathogens. Therefore, we measured the concentrations of these parameters in 5 ECCs to determine the origin of the pollutants, the IAQ in the spaces with the longest dwell time (dining room and TV room), and the possible influence of indoor pollution on vulnerable elderly occupants.

In general, the mean values of PM<sub>2.5</sub> and PM<sub>10</sub> were higher in the dining room than in the TV room, most likely due to the proximity of the kitchen to the dining room. The type of food being cooked, the cooking method (i.e., grilling, frying, baking, or sautéing), and the type of cooking fat used will all impact how much PM is produced when cooking. On the other hand, no statistically significant differences were found for ultrafine particles (PM<sub>0.3</sub> and PM<sub>0.5</sub>) attending to the use of the room, so condensation processes from gas-phase compounds could be their main source.

Bacterial counts were higher than those for fungi, and there were statistically significant differences between rooms only for the fungal counts. Kitchens and adjacent spaces, such as the dining room, are of a special interest for fungal growth due to the high moisture content (Pereira, 2021).

In the antibiotic resistant genes quantification by qPCR, we could amplify *bla*TEM and *vanA* in all the locations. In the case of *bla*TEM gene, we do not observe significant differences in the expression of it in any of the sampled places. However we detect significant differences between the TV room before using the PAC with HEPA filter and the rest of the sample's sites in the expression of *vanA* gene (Figure 1).

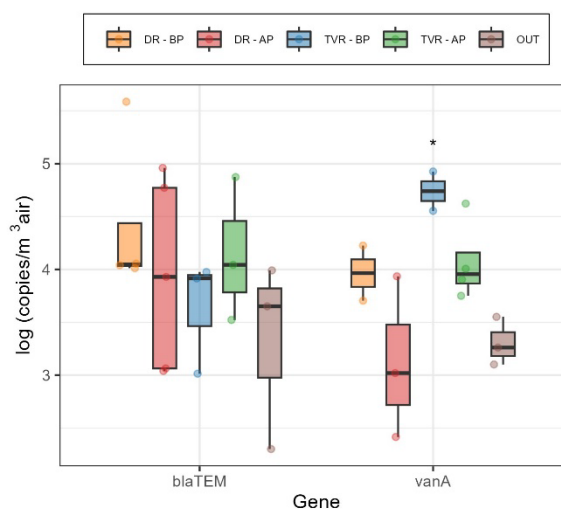


Figure 1. Logarithm of the gene copy number per cubic meter of air of the genes *bla*TEM and *vanA* obtained by qPCR. \* $p < 0.05$  compared to the rest of the values of the expression of this gene

The design of these spaces is very important, since those centres with kitchens open to the dining room presented worse IAQ. In this sense, the revision of the installation of gas cookers to control their emissions, and the design of the spaces to ensure good ventilation, is an essential task in centres with vulnerable elderly occupants.

### References

- Almeida-Silva, H.T. (2014) Elderly exposure to indoor air pollutants, *Atmos. Environ.* 85 54-63.
- Maio, S. (2015) Air quality of nursing homes and its effect on the lung health of elderly residents, *Expert Rev. Respir. Med* 9(6) 671-673.
- Bentayeb, M. (2015) Indoor air quality, ventilation and respiratory health in elderly residents living in nursing homes in Europe, *Eur Respir J* 45(5) 1228-38.
- Pereira, O. (2021) Assessment of indoor air quality in geriatric environments of southwestern Europe, *Aerobiologia* 37(1) 139-153.

## ANALYSIS OF ORGANIC POLLUTANTS RELEASED FROM PM<sub>2.5</sub> IN SIMULATED BIOLOGICAL FLUIDS: *IN-VITRO* INHALATION BIOACCESSIBILITY AND BIOAVAILABILITY ESTIMATION

J. Sánchez-Piñero, N. Novo-Quiza, J. Moreda-Piñeiro, S. Muniategui-Lorenzo and P. López-Mahía  
 University of A Coruña. Grupo Química Analítica Aplicada (QANAP). University Institute of Environment (IUMA).  
 Department of Chemistry, Faculty of Sciences, Campus de A Coruña, s/n. 15071 – A Coruña, Spain.  
 Keywords: Inhalation bioaccessibility, inhalation bioavailability, particulate matter, simulated biological fluids  
 Presenting author email: joel.sanchez@udc.es

In recent decades, there has been a growing interest within the scientific community regarding the study of the fraction that could be released in simulated biological fluids to estimate *in-vitro* bioaccessibility and bioavailability of compounds. In the present study, a methodology for the analysis of 49 organic pollutants, including 18 polycyclic aromatic hydrocarbons (PAHs), 12 phthalate esters (PAEs), 11 organophosphorus flame retardants (OPFRs), 6 synthetic musk compounds (SMCs) and 2 bisphenols released in simulated fluids from PM<sub>2.5</sub> samples was developed. The proposed method consists of a first step of physiologically based extraction test (PBET) by using artificial lysosomal fluid (ALF) and a simulated body fluid (SBF, filling a dialysis membrane) to obtain *in-vitro* inhalation bioaccessible and bioavailable fractions, respectively (Fig.1); followed by a vortex-assisted liquid-liquid microextraction (VALLME) and a final analysis by programmed temperature vaporization-gas chromatography-tandem mass spectrometry (PTV-GC-MS/MS).

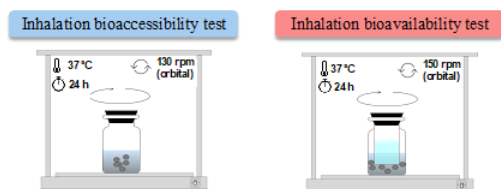


Fig. 1. Scheme of the *in-vitro* procedure to obtain pollutants bioaccessible/bioavailable fractions from PM<sub>2.5</sub> samples.

Successfully validation results were achieved for most of the compounds as a result of using SRM (selected reaction monitoring) mode in MS/MS, matrix-matched calibration and labelled surrogate standards, providing high sensitivity, minimization of matrix effects and recovering losses compensation. Moreover, applicability of the method was demonstrated by analysing 20 PM<sub>2.5</sub> samples, being an *in-vitro* PBET dialyzability approach for assessing organic pollutant's inhalation bioavailability applied to PM<sub>2.5</sub> samples for the first time. As expected, higher concentrations in inhalation bioaccessible with respect to bioavailable fractions were obtained. Among all the compounds, the highest inhalation bioaccessibility and bioavailability ratios were observed for retene (85 % and 71 %, respectively), followed by bisphenol A (76 % and 31 %, respectively). Mean bioaccessibility ratios of the

remaining PAHs, OPFRs and PAEs were 29 %, 48 % and 33 %, respectively, whereas bioavailability ratios could be also estimated for 2 OPFRs, accounting for an average of 18 % (Table 1).

Table 1. Inhalation bioaccessible/bioavailable concentrations (pg m<sup>-3</sup>), bioaccessibility/bioavailability ratios (B<sub>acc</sub> and B<sub>av</sub>, in %) and percentage of samples quantitated (Freq >LOQ, %) found for each compound.

Compound	Inhalation bioaccessibility				Inhalation bioavailability			
	Mean	SD	Freq >LOQ	B <sub>acc</sub> <sup>a</sup>	Mean	SD	Freq >LOQ	B <sub>av</sub> <sup>a</sup>
<b>PAHs</b>								
Phe	13.4	14.3	40	41	<163	— <sup>c</sup>	0	— <sup>c</sup>
Ft	19.3	24.2	95	41	<9.6	— <sup>c</sup>	0	— <sup>c</sup>
Pyr	17.3	29.0	45	20	<66.3	— <sup>c</sup>	0	— <sup>c</sup>
Ret	32.9	17.6	10	85	27.4	21.7	45	71
BaA	17.3	25.2	80	26	<11.2	— <sup>c</sup>	0	— <sup>c</sup>
Chry	33.1	32.4	100	32	<5.4	— <sup>c</sup>	5	— <sup>c</sup>
BbF + BjF	99.8	151	100	31	<13.5	— <sup>c</sup>	5	— <sup>c</sup>
BkF	24.9	32.6	90	24	<25.6	— <sup>c</sup>	0	— <sup>c</sup>
BeP	52.3	73.9	90	32	<15.9	— <sup>c</sup>	0	— <sup>c</sup>
BaP	33.5	42.3	100	30	<9.7	— <sup>c</sup>	0	— <sup>c</sup>
DBahA	9.6	14.7	40	23	<1.9	— <sup>c</sup>	0	— <sup>c</sup>
IP	49.9	69.9	90	24	<17.6	— <sup>c</sup>	0	— <sup>c</sup>
BghiP	74.0	99.2	100	27	<10.0	— <sup>c</sup>	15	— <sup>c</sup>
<b>PAEs</b>								
DNPP	2.8	1.8	25	— <sup>b</sup>	<2.1	— <sup>c</sup>	15	— <sup>c</sup>
DnHP	3.5	2.7	25	41	<4.6	— <sup>c</sup>	0	— <sup>c</sup>
DOP	5.0	4.1	50	24	<74.2	— <sup>c</sup>	0	— <sup>c</sup>
<b>OPFRs</b>								
TiBP	92.9	180	25	57	<20.3	— <sup>c</sup>	5	— <sup>c</sup>
TCPP	292	602	40	63	113	157	15	24
TPPO	166	266	40	25	80.9	114	40	12
<b>Bisphenols</b>								
BPA	7600	8530	85	76	3140	3080	85	31

<sup>a</sup> Calculated as follows: B<sub>acc</sub> or B<sub>av</sub> (%) =  $\frac{C_{Bacc \text{ or } B_{av}}}{C_{total}} \times 100$ ; where C<sub>Bacc</sub> or B<sub>av</sub> are the concentrations found in bioaccessible and bioavailable fractions, respectively, while C<sub>total</sub> corresponds with total concentrations for each compounds.

<sup>b</sup> Not calculated as averaged total concentration were <LOQ (6.7 pg m<sup>-3</sup>);

<sup>c</sup> Not calculated as mean bioavailable mean concentrations were <LOQ.

This work was supported by Ministerio de Ciencia e Innovación (MCIN), the Agencia Estatal de Investigación and the European Regional Development Fund (ref: PID2021-125201OB-I00) and the Xunta de Galicia (ref: ED431C 2021/56). N. Novo-Quiza acknowledges the MCIN and the European Union for a predoctoral grant (PRE2019-088744). J. Sánchez-Piñero acknowledges the Xunta de Galicia (Consellería de Cultura, Educación e Universidade) for a postdoctoral grant (ED481B-2022-002). The Laboratorio de Medio Ambiente de Galicia (LMAG) of the Subdirección Xeral de Meteoroloxía e Cambio Climático (Xunta de Galicia) is also acknowledged for providing the samples used in the present research work. The authors would like to thank P. Esperón (MCIU-PTA2018-016005-I).

## IN-VITRO ORAL BIOAVAILABILITY METHOD FOR ORGANIC TARGET POLLUTANTS IN ATMOSPHERIC PARTICULATE MATTER (PM<sub>10</sub>)

N. Novo-Quiza, J. Sánchez-Piñero, J. Moreda-Piñeiro, S. Muniategui-Lorenzo and P. López-Mahía  
University of A Coruña. Grupo Química Analítica Aplicada (QANAP). University Institute of Environment (IUMA).  
Department of Chemistry, Faculty of Sciences, Campus de A Coruña, s/n. 15071 – A Coruña, Spain.

Keywords: Oral bioavailability, particulate matter, physiologically based extraction, organic pollutants.  
Presenting author email: natalia.novo@udc.es

Recently, scientists have started evaluating the portion of PM-bound pollutants that could potentially be released (bioaccessible fraction) in human fluids and diffused across the gastrointestinal tract and reach the systemic circulation (referred to as the bioavailable fraction). This approach aims to enhance our comprehension of PM risk assessment and toxicological studies. In the present study, an analytical methodology for the determination of 49 organic pollutants, including 18 polycyclic aromatic hydrocarbons (PAHs), 12 phthalate esters (PAEs), 11 organophosphorus flame retardants (OPFRs), 6 synthetic musk compounds (SMCs) and 2 bisphenols (BPs) was validated and applied to characterize the oral bioavailable fraction of PM<sub>10</sub> samples. The proposed method aims to biomimetic complete mouth-gastric-intestinal system basing on an adaptation of the unified bioaccessibility method (UBM) (Wragg et al., 2011). It consists of a combination of the use of simulated gastrointestinal fluids with a physiologically based extraction test (PBET) and novelty inclusion of a dialysis membrane to simulate the intestinal absorption and obtain oral bioavailable fractions (Fig. 1).

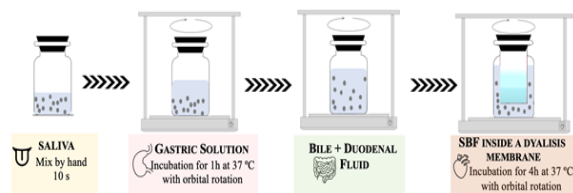


Fig. 1. Scheme of the *in-vitro* procedure to obtain pollutants oral bioavailable fractions from PM<sub>10</sub> samples.

Then, a vortex-assisted liquid-liquid extraction (VALLE) and a final analysis by programmed temperature vaporization-gas chromatography-tandem mass spectrometry (PTV-GC-MS/MS) were used for bioavailable pollutant quantification. The quantification procedure were effectively validated by employing SRM (selected reaction monitoring) mode in MS/MS, matrix-matched calibration, and deuterium-labelled surrogate standards. This approach ensured heightened sensitivity, minimized matrix effects, and compensated for any losses during the process. The validated methodology allowed the quantification of 48 organic pollutants in the oral bioavailable fraction of PM<sub>10</sub> samples, obtaining successful validation parameters in terms of linearity, precision, recovery, LODs and LOQs for the majority of the compounds.

After application to real samples collected from an urban background area of A Coruña city, most of the the target compounds content in the bioavailable fraction belong to PAHs family, mainly during the months of July, March and May, with almost no presence of the rest of the compounds in this urban background area (Fig. 2). Considering the total concentration of target compounds, PAHs were almost the only compounds that have been able to be quantified, reinforcing the idea that the sampling area is a poorly contaminated site.

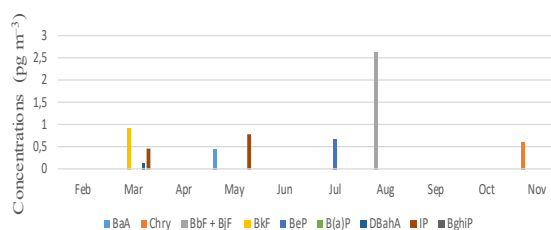


Fig. 1. PAHs' oral bioavailable concentrations found in PM<sub>10</sub> samples.

This work was supported by Ministerio de Ciencia e Innovación (MCIN), the Agencia Estatal de Investigación and the European Regional Development Fund (ref: PID2021-125201OB-I00) and the Xunta de Galicia (ref: ED431C 2021/56). N. Novo-Quiza acknowledges the MCIN and the European Union for a predoctoral grant (PRE2019-088744). J. Sánchez-Piñero acknowledges the Xunta de Galicia (Consellería de Cultura, Educación e Universidade) for a posdoctoral grant (ED481B-2022-002). The Laboratorio de Medio Ambiente de Galicia (LMAG) of the Subdirección Xeral de Meteoroloxía e Cambio Climático (Xunta de Galicia) is also acknowledged for providing the samples used in the present research work. The authors would like to thank P. Esperón (MCIU-PTA2018-016005-I).

Wragg, J., Cave, M., Basta, N., Brandon, E., Casteel, S., Denys, S., Gron, C., Oomen, A., Reimer, K., Tack, K., Van De Wiele, T. (2011) An inter-laboratory trial of the unified BARGE bioaccessibility method for arsenic, cadmium and lead in soil. *Science of The Total Environment*, 409, 4016–4030.

## OXIDATIVE POTENTIAL OF THE INHALATION BIOACCESSIBLE FRACTION OF PM<sub>10</sub> SAMPLES

N. Novo-Quiza, J. Sánchez-Piñero, J. Moreda-Piñero, I. Turnes-Carou, S. Muniategui-Lorenzo and P. López-Mahía

University of A Coruña. Grupo Química Analítica Aplicada (QANAP). University Institute of Environment (IUMA).

Department of Chemistry, Faculty of Sciences, Campus de A Coruña, s/n. 15071 – A Coruña, Spain.

Keywords: Oxidative potential, physiologically based extraction, bioaccessible fraction, dithiothreitol and ascorbic acid assays

Presenting author email: natalia.novo@udc.es

Atmospheric particulate matter (PM) has been related to numerous adverse health effects in humans. Nowadays, it is believed that one of the possible mechanism of toxicity could be the oxidative stress, which involves the development of reactive oxygen species (ROS) (Cigánková et al., 2021). Different assays have been proposed to characterize oxidative stress, such as dithiothreitol (DTT) and ascorbic acid (AA) acellular assays ( $OP^{DTT_V}$  and  $OP^{AA_V}$ ), as a metric more relevant than PM mass measurement for PM toxicity. This study evaluates the OP of the bioaccessible fraction of 65 PM<sub>10</sub> samples collected at an Atlantic Coastal European urban site using DTT and AA assays. A physiologically based extraction (PBET) using Gamble's solution (GS) as a simulated lung fluid was used for the assessment of the bioaccessible fraction of PM<sub>10</sub>. The use of the bioaccessible fraction, instead of the fraction assessed using conventional phosphate buffer and ultrasounds assisted extraction (UAE), was compared for OP assessment. Correlations between  $OP^{DTT_V}$  and  $OP^{AA_V}$ , as well as total and bioaccessible concentrations of polycyclic aromatic hydrocarbons (PAHs) and metal(oid)s, were investigated to explore the association between those compounds and OP. OP values obtained at this site (Fig. 1) were lower than those reported in most other sites in Spain and Europe. This could be due to the low the low surface tension of GS, the presence of chelating agents in GS composition, and the avoidance of ultrasounds during extraction process, which may reduce the solubilisation of induced ROS activity compounds from PM<sub>10</sub> samples. The clean Atlantic air masses arriving at sampling site, which improve the air quality in this region, may also contribute to the reduction in oxidative stress of samples.

In general, no statistically significant seasonal changes were found in  $OP^{DTT_V}$  and  $OP^{AA_V}$  (as well as major ions, metal(oid)s and PAHs). Data from univariate and multivariate approaches suggest a that  $OP^{DTT_V}$  and  $OP^{AA_V}$  are correlated with major ions ( $K^+$ ,  $NO_3^-$  and  $SO_4^{2-}$ ) and concentrations of equivalent black carbon (eBC) and UV-absorbing particulate matter (UVP). They are also correlated with the total and bioaccessible concentrations of metal(oid)s (such as As, Bi, Cd, Cu, Cr, Fe, Mn, Ni, V and Zn) and  $\Sigma 12$ PAHs. Furthermore, inhalation bioaccessibility ratios for Cr, V, phenanthrene, fluoranthene and pyrene were found to vary from 40 to 70% (Fig. 2), indicating that these

species might enter the circulation through alveolar absorption. Additionally, *in-vitro* bioaccessible ratios lower than 25% were observed for Al, Cu, Fe, Mn, Ni, Se, Zn and PAHs with 6 condensed rings.

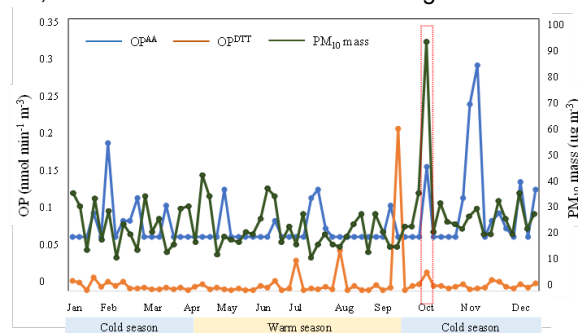


Fig. 1. Temporal variation of  $OP^{AA_V}$  and  $OP^{DTT_V}$  ( $\text{nmol min}^{-1} \text{m}^{-3}$ ) and PM<sub>10</sub> mass ( $\mu\text{g m}^{-3}$ ) during the study period.

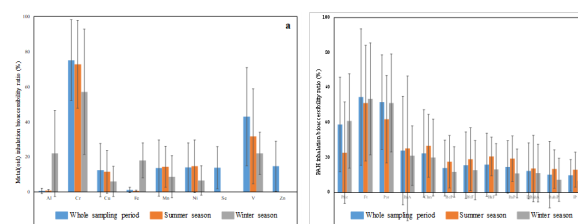


Fig. 2. Metal(oid)s (a) and PAHs (b) *in-vitro* inhalation bioaccessibility ratios (%) obtained for PM<sub>10</sub> samples.

This work was supported by Ministerio de Ciencia e Innovación (MCIN), the Agencia Estatal de Investigación and the European Regional Development Fund (ref: PID2021-125201OB-I00) and the Xunta de Galicia (ref: ED431C 2021/56). N. Novo-Quiza acknowledges the MCIN and the European Union for a predoctoral grant (PRE2019-088744). J. Sánchez-Piñero acknowledges the Xunta de Galicia (Consellería de Cultura, Educación e Universidade) for a postdoctoral grant (ED481B-2022-002). The council of A Coruña is acknowledged for its assistance (collaboration agreement for PM<sub>10</sub> sampling). The authors would like to thank P. Esperón (MCIU-PTA2018-016005-I).

Cigánková, H., Mikuška, P., Hegrová, J., Krajčovič, J. (2021) Comparison of oxidative potential of PM<sub>1</sub> and PM<sub>2.5</sub> urban aerosol and bioaccessibility of associated elements in three simulated lung fluids. *Science of the Total Environment*, 800, 149502.

## TREND ANALYSIS OF IN-SITU AND COLUMN-INTEGRATED AEROSOL RADIATIVE PROPERTIES IN SPAIN

J.J. Fernández<sup>1</sup>, G. Titos<sup>1,2</sup>, H. Lyamani<sup>1,3</sup>, E. Bazo<sup>1,2</sup>, M. Sorribas<sup>4</sup>, M. Pandolfi<sup>5</sup>, A. Barreto<sup>6</sup>, S. Rodríguez<sup>7</sup>, Y. González<sup>6,8</sup>, F.J. Olmo<sup>1,2</sup>, L. Alados-Arboledas<sup>1,2</sup> and A. Cazorla<sup>1,2</sup>.

<sup>1</sup>Andalusian Institute for Earth System Research (IISTA-CEAMA), Granada 18006, Spain

<sup>2</sup>Department of Applied Physics, University of Granada, Granada 18071, Spain

<sup>3</sup>Department of Applied Physics, University of Málaga, 29010, Málaga, Spain

<sup>4</sup>Atmospheric Sounding Station 'El Arenosillo', INTA, Mazagón-Huelva, Spain

<sup>5</sup>Institute of Environmental Assessment and Water Research (IDAEA-CSIC), Barcelona, Spain

<sup>6</sup>Izaña Atmospheric Research Centre, (IARC/CIAI), AEMet, Santa Cruz de Tenerife, Spain

<sup>7</sup>Consejo Superior de Investigaciones Científicas, IPNA CSIC, La Laguna, E38206, Tenerife, Spain

<sup>8</sup>Scientific department, CIMEL Electronique, Paris, 75011, France

Keywords: Atmospheric aerosol, Remote sensing, In-situ, Radiative balance, Trends

Presenting author email: ebazo@ugr.es

Atmospheric aerosol particles alter Earth's radiative balance through processes involving absorption and scattering of solar radiation. Long-term measurements allow to quantify the temporal trends in aerosol radiative properties, which are necessary to address the climate impact of aerosol particles as well as the effect of pollution mitigation strategies. In-situ (IS) and remote sensing (RS) techniques are commonly used to measure aerosol optical properties worldwide, although there are large differences between these techniques as well as in the measurement frequency and measured atmospheric volume. Despite the abundance of studies using these methods, few of them combine both techniques and explore potential differences in long-term temporal trends of aerosol optical properties. This study aims to investigate the overall temporal trend of aerosol optical properties obtained by in-situ and remote sensing techniques over an extended period of time at four different sites in Spain. The sites include the rural station of El Arenosillo (ARN, 37.104 °N, 6.734 °W, 41 m a.s.l.; 2012-2022), two mountain stations: Montsec (MSA, 42.051 °N, 0.730 °E, 1572 m a.s.l.; 2013-2021) and Izaña (IZO, 28.309 °N, 16.499 °W, 2364 m a.s.l.; 2008-2022), and an urban station at Granada (UGR, 37.164 °N, 3.605 °W, 680 m a.s.l.; 2006-2021). For in-situ measurements, the WDCA database of scattering and absorption coefficients are used, while for passive remote sensing, atmospheric columnar aerosol data from AERONET are employed. For the temporal trend analysis, a monthly and annual study of the data distribution is conducted based on the technique of Collaud Coen *et al.* (2020a). Mann-Kendall statistical test with variance-corrected trend-free pre-whitening procedure (VCTFPW) (Yue and Wang, 2004) is employed as the criterion for defining the statistical significance of the trend. The Theil-Sen estimator is utilized to characterize and infer the trend's slopes (Collaud Coen *et al.*, 2020b).

Table 1 shows the mean intensive columnar and in-situ aerosol optical properties obtained in the different sites. The aerosol population in Granada (UGR) is characterized by a predominance of fine and more absorbing particles compared to ARN, IZO and MSA,

both in the entire atmospheric column and near the surface. Significant difference is found between the near-surface and the entire atmospheric column aerosol properties at UGR, due to a higher proportion of fine-sized, absorbing anthropogenic aerosols (primarily black carbon) emitted near the surface by local sources (road traffic), while the other sites show a better agreement between the in-situ and remote sensing intensive properties.

Table 1. Mean±std values of aerosol intensive optical properties obtained by in-situ (IS) and remote sensing (RS) methods. SSA = Single Scattering Albedo, AE = Angström Exponent, SAE = Scattering Angström Exponent

	UGR	ARN	IZO	MSA
SSA <sub>RS</sub>	0.9±0.1	0.94±0.07	0.97±0.04	0.93±0.11
SSA <sub>IS</sub>	0.7±0.1	0.91±0.06	0.92±0.07	0.90±0.12
AE <sub>RS</sub>	1.2±0.5	1.1±0.4	1.0±0.6	1.3±0.4
SAE <sub>IS</sub>	1.6±0.5	1.3±0.5	0.8±0.7	1.2±0.9

At UGR station, the trend analysis of in-situ and remote sensing aerosol properties for both the entire dataset, as well as for simultaneous data (not shown here), shows a consistent decreasing trend of aerosol load both in surface and column over the study period. However, at ARN station, discrepancies between the aerosol trends in surface and column were observed. In contrast, for IZO and MSA stations, statistically significant trends are not observed, except for AOD (Aerosol Optical Depth) in MSA. This implies absence of significant temporal changes in aerosol optical properties both near the surface and in the atmospheric column at all sites investigated except UGR.

This work was supported by NUCLEUS (PID2021-128757OB-I00) funded by MCIN/AEI/10.13039/501100011033 and NextGenerationEU/PRTR and the Scientific Unit of Excellence: Earth System (UCE-PP2017-02).

Collaud Coen M. *et al.* (2020a) *Atmos. Chem. Phys.*, 20, 14, 8867-8908.

Collaud Coen M. *et al.* (2020b) *Atmos. Chem. Phys.*, 13, 12, 6945-6964.

Yue S. and Wang C. (2004) *Water Resources Management*, 18, 201-218.

## AFRICAN DESERT DUST INFLUENCES ON THE ATLANTIC - SAHARAN MIGRATION OF THE SKIPJACK AND OTHER TROPICAL TUNA

S. Rodríguez<sup>1</sup>, R. Riera<sup>2</sup>, A. Fonteneau<sup>3</sup>, S. Alonso-Pérez<sup>4</sup>, J. López-Darias<sup>1</sup>

<sup>1</sup>Group of Atmosphere, Aerosols and Climate (GAAC), Consejo Superior de Investigaciones Científicas, IPNA CSIC, La Laguna, Tenerife, Spain

<sup>2</sup>IU-ECOQUA, Grupo en Biodiversidad y Conservación, Universidad de Las Palmas de Gran Canaria, Spain

<sup>3</sup>Institut pour la Recherche et le Développement, Marseille, France

<sup>4</sup>Departamento de Ingeniería Industrial, Universidad de La Laguna, Tenerife, Spain

Keywords: Saharan dust, dust deposition, dust fertilization, fisheries, skipjack tuna

Presenting author email: sergio.rodriguez@csic.es

Marine phytoplankton is a primary producer of the Earth System that uses carbon dioxide and sunlight to produce organic carbon and oxygen. The growth of marine phytoplankton requires key nutrients, as nitrogen (N) to produce proteins and nucleic acids, phosphorus (P) to produce phospholipids needed in the cell membranes, silicon (Si) to produce the (exo)skeletons of the diatoms and calcium (Ca) to produce shells. Of special relevance are the limiting/co-limiting macronutrients nutrients, as N and P, and micronutrients such as iron (Fe), manganese (Mn), cobalt (Co), zinc (Zn) or nickel (Ni), needed in a set of functions of the metabolism (Mahowald et al., 2018). Because desert dust composition includes key nutrients (~18% Si, 4% Ca, 4% Fe, 0.8‰ P, 5‰ Mn, 0.8‰ Zn, 0.8‰ Co and 0.2‰ Ni, as average of dust mass) the atmospheric deposition of desert dust aerosols fuels the growth of phytoplankton, especially in the oligotrophic open ocean, where nutrients are scarce. After massive dust deposition events, a number of studies have reported blooms of chlorophyll associated with increases in the growth rate and primary production (Mahowald et al., 2018). Dust deposition influence on sea water composition and may also modify the composition of phytoplankton, thus affecting the marine microbial biodiversity. Although this process has an impact on upper trophic levels and fisheries, direct evidence is lacking (Rodríguez et al., 2023). We focused on studying the influence on desert dust deposition on the migration and fisheries of other tropical tuna, including skipjack (*Katsuwonus pelamis*) which is the most abundant and commercially important tuna in the Atlantic, whose main stocks occur in the tropical and subtropical North-East Atlantic. For this purpose, we analysed the data of captures of the International Commission for the Conservation of Atlantic Tuna (ICCAT) by using the MERRA-2 dust reanalysis and the NASA Ocean Biogeochemical Model water composition.

We found that the skipjack and other tropical tuna performs a seasonal migration tracking the seasonal shift of Saharan dust deposition in the Atlantic, to which we have called *Atlantic-Saharan* migration. From boreal winter to summer, skipjack migrates from equatorial (0-5°N) to subtropical waters of the North-East Atlantic (regularly reaching open waters off Mauritania ~20°N and the Canary Islands ~28°N), tracking the seasonal

shift of dust deposition in the North-East Atlantic. The observed long-term associations of skipjack catches with the seasonal cycles, anomalies and meridional variability of dust over the North-East Atlantic, shows that along the year skipjack catches mainly occur in waters affected by massive dust deposition. These results have important implications on our understanding on the influence of atmospheric dust on marine ecosystems and on the management of fisheries.

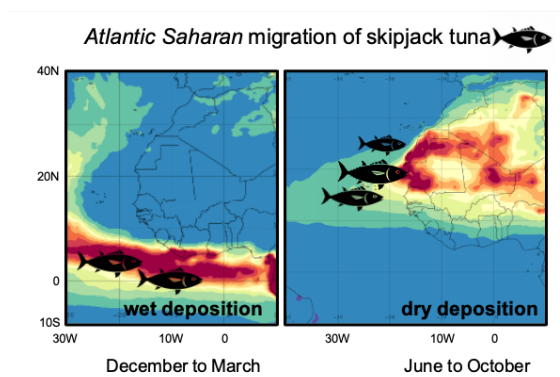


Fig. 1. Atlantic Saharan migration of skipjack tuna indicating the fishing regions of skipjack tuna (black fish) and the dust deposition field obtained with MERRA-2 model.

This study is part of the project VARDUSTSAL (PGC2018-099166-B- I00), funded by the Agencia Estatal de Investigación/State Research Agency of Spain, the Ministry of Science, Innovation and Universities of Spain and the European Regional Development Fund (ERDF)

Mahowald et al. (2018). Aerosol trace metal leaching and impacts on marine microorganisms. *Nat. Commun.* 9 (1), 2614. <https://doi.org/10.1038/s41467-018-04970-7>.

Rodríguez et al. (2023). African desert dust influences migrations and fisheries of the Atlantic skipjack-tuna, *Atmos Environ*, 312, 120022 <https://doi.org/10.1016/j.atmosenv.2023.120022>.

## IMPLEMENTATION OF A SYNERGY STRATEGY OF GROUND-BASED PHOTOMETER AND SPECTROMETER OBSERVATIONS USING GRASP ALGORITHM FOR SATELLITE PRODUCTS VALIDATION

F. Rejano<sup>1,2</sup>, M. Herreras-Giralda<sup>1</sup>, D. Pérez-Ramírez<sup>2</sup>, O. Dubovik<sup>3</sup>, A. Cede<sup>5</sup>, and D. Fuertes<sup>1</sup>, J. Fischer<sup>6</sup>, R. Preusker<sup>6</sup>

<sup>1</sup> GRASP-SAS, Remote Sensing developments, LOA/Université de Lille-1, Villeneuve D'Ascq, France

<sup>2</sup> Andalusian Institute for Earth System Research, IISTA-CEAMA, University of Granada, Granada, Spain

<sup>3</sup> Laboratoire d'Optique Atmosphérique, UMR8518, CNRS–Université de Lille 1, Villeneuve d'Ascq, France

<sup>5</sup> LuftBlick, Innsbruck, Austria

<sup>6</sup> Institute for Space Science, Free University of Berlin, Berlin, Germany

Keywords: remote sensing, satellites validation, inversion algorithms

Presenting author email: fernando.rejano@grasp-earth.com

Earth observation by satellites provides global data coverage and allows us to advance in our understanding of aerosol and gases spatial distribution (e.g., Chen et al., 2019). However, aerosol and gas products obtained from satellite sensors need to be validated with respect to ground-based instruments to ensure the accuracy of satellite data products. Thus, remote sensing measurements from ground-based instruments provide continuum validation datasets from a wide variety of sites.

The Aeronet network of sun-sky photometers and Pandonia network of spectrometers, both with a high number of stations worldwide, represent the ideal infrastructures to validate the aerosol and gases products obtained by satellites, respectively. However, Aeronet and Pandonia networks mainly focused to retrieve one product type (aerosol properties for Aeronet and gases species for Pandonia) and, therefore, each inversion algorithm must assume the lack of information correspondingly: gases for Aeronet and aerosol for Pandonia. For that reason, a scientific challenge of great interest is to develop a unique inversion algorithm that combines sun-photometer and spectrometer measurement to retrieve aerosol and gases at the same time without a priori assumptions.

In this sense, the Generalized Retrieval of Atmosphere and Surface Properties (GRASP) algorithm is the first unified algorithm to be developed for characterizing atmospheric properties gathered from a variety of remote sensing observations (Dubovik *et al.*, 2021). Adapting GRASP configuration to invert photometer and spectrometer measurements will involve a better quality of aerosol and gas products for satellite validation tasks.

The objective of this work is to optimize the GRASP configuration to retrieve aerosol and gases products using the synergic observations of ground-based photometer and spectrometer. Firstly, we simulated synthetic data of both instruments using GRASP forward model, and we performed validation tests for different products to find out the optimal configuration of GRASP algorithm to retrieve aerosol and gases products from the synthetic data. Results showed that retrievals of aerosol optical depth (AOD), single scattering albedo (SSA), H<sub>2</sub>O, NO<sub>2</sub> and O<sub>3</sub> column

concentrations can be accurately inverted when using Aeronet and Pandonia data as input for GRASP. As an example, Figure 1 shows satisfactory results for the synthetic validation test of O<sub>3</sub> column concentration assuming different atmospheric conditions.

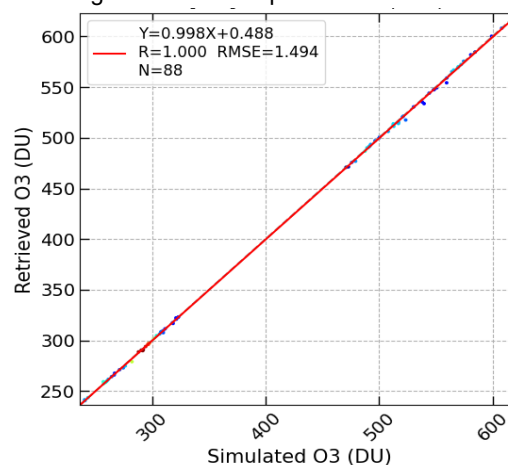


Fig. 1. Synthetic test of O<sub>3</sub> column concentration retrieval from GRASP algorithm. the validation of the retrieved and simulated parameter.

Further research will consist of inverting real data from both instruments with the new optimized GRASP configuration and, in turn, using these new products for the validation task of the upcoming satellite missions.

This work was supported by the European Space Agency (ESA) through project DIVA and IDEAS-QA4EO CCN09 projects.

Chen, C. *et al.* (2019) 'Constraining global aerosol emissions using POLDER/PARASOL satellite remote sensing observations', *Atmospheric Chemistry and Physics*, 19(23), pp. 14585–14606. Available at: <https://doi.org/10.5194/acp-19-14585-2019>.

Dubovik, O. *et al.* (2021) 'A Comprehensive Description of Multi-Term LSM for Applying Multiple a Priori Constraints in Problems of Atmospheric Remote Sensing: GRASP Algorithm, Concept, and Applications', *Frontiers in Remote Sensing*, 2. Available at: <https://doi.org/10.3389/frsen.2021.706851>.

# FLUXES AND GEOCHEMICAL CHARACTERISATION OF SAHARAN DUST DEPOSITED IN HIGH-MOUNTAIN NATIONAL PARKS OF THE IBERIAN PENINSULA

Sonia Castillo<sup>1,2</sup>, Alberto Cazorla<sup>1,2</sup>, Blas L. Valero-Garcés<sup>3</sup>, Lucas Alados-Arboledas<sup>1,2</sup>, Jorge Pey<sup>3</sup>

<sup>1</sup> Andalusian Institute for Earth System Research (IISTA-CEAMA), Granada, Spain

<sup>2</sup> Dpt. Applied Physics, University of Granada, Granada, Spain

<sup>3</sup> Instituto Pirenaico de Ecología (CSIC), Zaragoza, Spain

Keywords: atmospheric deposition, Saharan dust, atmospheric geochemistry, National Parks

Presenting author email: jorge.pey@ipe.csic.es

High mountain regions often serve as receptors for air pollution emanating from both nearby and distant areas. The deposition of aerosols in these elevated landscapes can exert both positive and negative influences on ecosystems, prompting protective regulations owing to their considerable geological and biological richness. Notably, the deposition of specific aerosols, such as mineral dust or soot, significantly impacts the optical properties of snow. This alteration leads to reduced albedo, hastened snowmelt, and a consequent decrease in snow cover.

This study undertakes a comparative analysis of three high-mountain National Parks (NPs) in the Iberian Peninsula, each situated in distinct climatic contexts and at different distances from the Sahara Desert (Figure 1): Picos de Europa (Cantabrian Mountains), Ordesa-Monte Perdido (Pyrenees), and Sierra Nevada (Betic Mountains). Spanning the period 2017-2021, the research examines total aerosol deposition fluxes, identifies Saharan dust events (SAH), and local pollution events (LPE), meticulously quantifying their respective contributions.

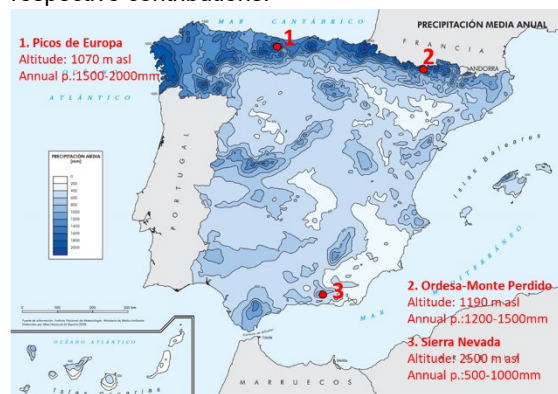


Figure 1 Locations of the three study sites.

To gather deposited aerosols, monthly bulk samples are obtained and subsequently filtered onto 47 mm quartz filters using a filtration ramp. Insoluble aerosols within the filters are quantified through filter mass differences, while soluble aerosols in aliquots are enumerated after chemical determinations of anions and cations through ionic chromatography. Additionally, insoluble particles are analyzed following procedures outlined by Querol et al. (2019).

The climatic differences among the three NPs manifest in the deposition phenomenon. In Picos de Europa

NP, where only 10% of days are influenced by SAH events, the contribution of such particles to the total annual deposited fluxes stands at a mere 10%. During these events, the dominant fraction comprises soluble particles, constituting 90% of the total mass. In Ordesa-Monte Perdido NP, where 16-20% of days are influenced by SAH events, the contribution of these particles to the total annual deposited fluxes rises to 60%, with both fractions nearly evenly distributed. Finally, in the Sierra Nevada NP, experiencing 36-42% of days under SAH influence, the contribution of these particles to the total annual deposited mass increases to 70%. Here, the dominant fraction during these events is the insoluble fraction, comprising over 60% of the total mass.

Table 1. Annual mean deposition fluxes.

Insoluble fraction	Soluble fraction	TOTAL	% Insoluble	% Soluble	Precip. mm
<b>PICOS DE EUROPA</b>					
3.5	40	44	10	90	1600
<b>ORDESA-MONTE PERDIDO</b>					
14	16	30	47	53	1200
<b>SIERRA NEVADA</b>					
8.5	5.5	14	64	35	650

This research received support from POSAHPI actions (State Research Agency, PID2019-108101RB-I00 and PID2022-143146OB-I00) and ASAH-AS (OAPN 2021, reference 2799/2021). This research is part of the project "LifeWatch -2019-10-UGR-01, co-funded by the Ministry of Science & Innovation through the FEDER funds (POPE) 2014-2020.

Pey J., Larrasoaña J.C., Pérez N. *et al.* (2020). Phenomenology and geographical gradients of atmospheric deposition in southwestern Europe: results from a multi-site monitoring network. *Sci. Tot. Environ.*, 744, 140745, <https://doi.org/10.1016/j.scitotenv.2020.140745>.

Querol, X. Pérez N., Reche C. *et al.* (2019). African dust and air quality over Spain: Is it only dust that matters?. *Sci. Tot. Environ.* 686, 737-752. <https://doi.org/10.1016/j.scitotenv.2019.05.349>.

## THE NORTH AFRICAN REGIONS INDUCING VARIABILITY OF DUST COMPOSITION IN THE SAHARAN AIR LAYER IDENTIFIED DURING THE VARDUSTSAL CAMPAIGN AT HIGH ALTITUDE IN CAPE VERDE

S. Rodríguez<sup>1</sup>, F. Giardi<sup>2</sup>, J. López-Darias<sup>1</sup>, F. Lucarelli<sup>2</sup>, A. Carlos Fortes<sup>3</sup>, S. Nava<sup>2</sup>, M. Chiari<sup>2</sup>, G. Calzonai<sup>2</sup>, S. Alonso Pérez<sup>4</sup>, M.I. García<sup>1</sup> and I. Belbachir<sup>1</sup>

<sup>1</sup>Consejo Superior de Investigaciones Científicas, IPNA CSIC, La Laguna, Tenerife, 38206, Spain

<sup>2</sup>Istituto Nazionale di Fisica Nucleare, Firenze, 50019, Italy

<sup>3</sup>Ministry of Agriculture and Environment, Ribeira Grande, Santo Antão, 1110, Cabo Verde

<sup>4</sup>Departamento de Ingeniería Industrial, Universidad de La Laguna, Tenerife, Spain

Keywords: Saharan dust, source regions, variability dust composition, high resolution

Presenting author email: sergio.rodriguez@csic.es

North Africa is the largest and most active dust sources of the Earth System. Dust plumes occur along thousands of kilometres over the Atlantic and Europe influencing on radiative fluxes, cloud formation, nutrients supply to ecosystems and human health. Dust is a mixing of tens of minerals with different physicochemical properties modulating dust impacts, thus, feldspars act as ice nuclei, hematite absorb UV radiation, carbonates neutralize acid pollutants, whereas iron bearing clays and oxides provide iron to ecosystems. Models including such mineral are still under development. Experimental methods still have limitations for quantifying the variability of dust mineralogy, thus complementary elemental composition data are being used.

We present the results of the campaign VARDUSTSAL-2 (Variability of dust composition in the central path of the Saharan Air Layer), developed in Cape Verde from May to August 2022, when we collected 1200 1h-resolution aerosol samples ( $< 10\mu\text{m}$ ) in Santo Antão island by using a STRAS sampler (Lucarelli, 2020). VARDUSTSAL-1 was previously developed in Tenerife, Canary Islands (Rodríguez et al., 2020). This new campaign was also developed during the North African monsoon period, when dust is exported to the Atlantic at high altitude. The samples were collected in a mountain site at 1400 meters altitude with the objective of identifying the North African source regions that induce variability in the composition of dust in the Saharan Air Layer. The samples were analysed (for 26 elements) by PIXE (Lucarelli, 2020). For the data analysis we determined the Median Concentrations At Receptor sites (MCAR) (Rodríguez et al., 2020).

We found that dust composition experiences an important variability, the content (%) in some elements (as Ca, Mg, Mn, S or K, among others) changes in a factor 2 in just a few (5 to 8) hours linked to the changes in the meteorology and its influence on dust emissions and transport from the different source regions. The analysis of the MCAR plots allowed identifying the geographical location of the dust sources inducing variability of dust composition in the Saharan Air Layer.

We also detected the presence of air pollutants (e.g. S, V, Cr, Pb and other heavy metals) mixed with dust. The

MCAR and meteorological analysis shows that these pollutants are associated with industrial emissions in specific regions of tropical North Africa, including manufacturing fertilizing plants, oil refineries, metallurgic heavy industry. The overall dataset allows identifying the source regions that induce variability of dust composition, a topic of major interest for the validation of the next generation of models and satellite observations of dust meteorological observations.

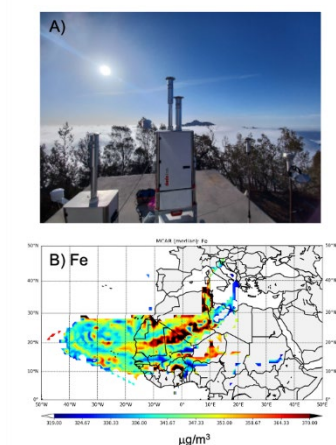


Figure 1. A) Picture of the sampler in Santo Antão islands during the campaign. B) MCAR plot for iron.

The project VARDUSTSAL (PGC2018-099166-B- I00) is funded by the State Research Agency of Spain, the Ministry of Science, Innovation and Universities of Spain and the European Regional Development Fund.

Rodríguez et al. (2020) Rapid changes of dust geochemistry in the Saharan Air Layer linked to sources and meteorology. *Atmos. Environ.* 223, 117186.

Lucarelli F., How a small accelerator can be useful for interdisciplinary applications: the study of air pollution, *The European Physical Journal plus* 135, (2020), 538.

## DEVELOPMENT OF THE GRANADA ICE NUCLEATING SPECTROMETER GRAINS

E. Bazo<sup>1,2</sup>, G. Titos<sup>1,2</sup>, G. Pérez-Fogwill<sup>3</sup>, A. A. Piedehierro<sup>3</sup>, A. Welti<sup>3</sup>, F.J. Olmo<sup>1,2</sup>, L. Alados-Arboledas<sup>1,2</sup>, and A. Cazorla<sup>1,2</sup>

<sup>1</sup>Andalusian Institute for Earth System Research (IISTA-CEAMA), Granada 18006, Spain

<sup>2</sup>Department of Applied Physics, University of Granada, Granada 18071, Spain

<sup>3</sup>Finnish Meteorological Institute (FMI), 00560 Helsinki, Finland

Keywords: ice nucleating particles, droplet freezing assay, immersion freezing

Presenting author email: ebazo@ugr.es

Atmospheric aerosol particles can form ice crystals in clouds by acting as ice nucleating particles (INPs) in heterogeneous freezing processes. These ice crystals affect the Earth's radiative budget and the hydrological cycle since they affect the cloud optical and microphysical properties. Their impact is directly related to changes in the concentration, morphology, and type of aerosol particles acting as INP. Aerosol-cloud interactions (ACI) have large uncertainties in climate change estimations (Forster et al., 2021), which is partly due to a lack of knowledge of particle sources and how aerosol particles evolve to become effective INP. Therefore, it is crucial to study the INP ability of different aerosol types and under different atmospheric conditions.

In this work we present the GRANADA Ice Nucleating particle Spectrometer (GRAINS), developed at the AGORA Observatory. The instrument's design is based on INSEKT (Schiebel, 2017) from the Karlsruhe Institute of Technology (KIT). GRAINS allows to characterize INP concentration in a broad temperature range with the use of immersion freezing techniques. The instrument consists of an aluminium block that fits two 96-well PCR (polymerase chain reaction) plates, with a volume of 0.2 ml per well (Fig. 1). The aluminium block is connected to a thermostat (LAUDA RP 250 E) that uses ethanol as a working fluid and cools the block and the PCR plates at a controlled cooling rate. The temperature is measured with a Pt100 sonde placed inside the aluminium block, between both PCR plates. Additionally, there is a camera (ELP USB8MP02G-SFV (5-50)) placed perpendicular to the wells that takes frames every 5 seconds. In a typical freezing experiment, the particle-containing suspension to analyse is dosed in equal volume aliquots into the PCR wells and cooled down using GRAINS until all wells are frozen. The freezing events are monitored through images and identified from them as a brightness change. As a result, the fraction of frozen well as a function of the temperature is obtained. The INP concentration is calculated from the frozen fraction through normalization (Vali, 1971). A background correction is applied to each measurement based on the ability of ultrapure water, used to create the solutions, to freeze in the temperature range of the experiments.

Since the heat transfer from the aluminium block to the PCR plates may differ depending on the location of

different wells, the temperature of each well is characterized to correct for this feature. To do so, the PCR wells are filled with ethanol and various cooling rates are tested to study the response of the temperature inside the wells with the use of ancillary Pt100 sensors that are fully immersed in the liquid. Additionally, the use of well-known INPs serves as a performance validation of the instrument.

In this study, we focus on temperature determination of the different wells in the GRAINS instrument and its validation with the use of commercial particles that are effective INPs, such as Feldspar, Illite or Snomax®.

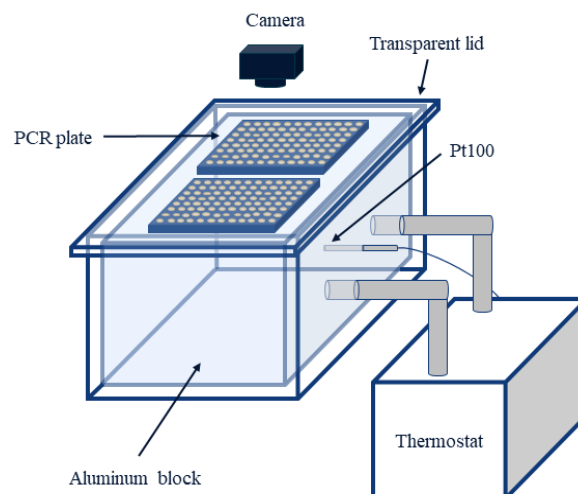


Fig. 1. Scheme of GRAINS.

E. Bazo received funding by MCIN/AEI/10.13039/501100011033 and the FSE + (ref. PRE2022-101272). This work was supported by NUCLEUS project (PID2021-128757OB-I00) funded by MCIN/AEI/10.13039/501100011033 and NextGenerationEU/PRTR, ACTRIS-IMP, ATMO\_ACCESS (grant agreement No 101008004) and the Scientific Unit of Excellence: Earth System (UCE-PP2017-02).

Forster et al., (2021). *Climate Change 2021: The Physical Science Basis*, Cambridge University Press.

Schiebel, (2017). Karlsruhe Institute of Technology.

Vali, G., (1971). *J. Atmos. Sci.*, 28, 402–409.

## STUDY OF THE EFFECT OF SYNOPTIC METEOROLOGICAL PATTERNS ON AEROSOL CONCENTRATION DUE TO BOUNDARY LAYER HEIGHT VARIATIONS OVER MADRID FROM 2020 TO 2023

F. Molero<sup>1</sup>, P. Salvador<sup>1</sup>, R. Barragán<sup>1</sup> & M. Pujadas<sup>1</sup>

<sup>1</sup>CIEMAT, Avda Complutense, 40, Madrid, 28040, Spain

Keywords: Aerosols, boundary layer, ceilometer, long-range transport

Presenting author email: f.Molero@ciemat.es

Anthropogenic aerosols are mostly concentrated within the planetary boundary layer (PBL), with heights ranging from hundreds of meters to a few kilometers. The PBL height is mainly determined by solar radiation and weather conditions, limiting the vertical mixing of the air pollutants generated near the surface.

Lidars have demonstrated their capabilities to study the aerosol vertical distribution and their spatio-temporal evolution can provide very complete information on both aerosol spatial distribution and their characterization. A particular type of lidars, ceilometers are capable of providing continuous aerosol vertical profiles with good spatial resolution and a large vertical range. The ceilometer used in this work is a Lufft CHM15k-Nimbus, which operates at 1064nm providing data related to atmospheric aerosols, with a repetition frequency of 6.5 kHz and a maximum height of 15.36 km a.g.l. It belongs to the MDR-CIEMAT ACTRIS station (40.4565°N, 3.7257°W, 669 m a.s.l.) (Molero et al., 2014), which is located in the North-West outskirts of the city of Madrid. This city is located in the center of the Iberian Peninsula and its metropolitan area has a population of nearly 6 million inhabitants and a car fleet of almost 3 million vehicles.

The worst pollution episodes over Madrid are characterised by relatively low PBL height at midday, light synoptic winds, and the development of mountain breezes along the slopes of the nearby Guadarrama Mountain Range.

Advanced methods are required to estimate the PBL height due to difficulties with low clouds or residual layers. One recently developed, the STRATfinder algorithm (Kotthaus et al., 2020) is used in the present work. The algorithm tracks PBL heights to provide values every 10 minutes during a 24-hour period. The main objective of this research is the assessment of the PBL by means of the STRATfinder algorithm using ceilometer signals, along four years period 2020-2023 in order to establish the influence of synoptic meteorological patterns. The database of PBL heights of continuous measurements have been classified regarding the most frequent patterns of synoptic circulation. Six synoptic meteorological patterns were identified through cluster analysis of sea level pressure fields (Salvador et al., 2021) as the main responsible of the weather conditions in the Iberian Peninsula.

The results shows the effect of high stability and air-mass blockage, frequent scenarios in winter, with the algorithm difficulties due to the presence of low clouds

coupled to the PBL. Special synoptic situation, such as long-range transport of aerosols, Saharan dust intrusions and clean-atmosphere situations, have been purposely studied. For instance, a systematic reduction of the PBL height has been detected during the occurrence of Saharan dust intrusions. On average, the PBL height daily profile decreased as a function of the desert dust contribution. This effect illustrates the strong direct radiative forcing by desert dust plumes on atmospheric stability within the lower troposphere and consequently on air quality. A robust relationship between the occurrence of specific synoptic meteorological patterns and characteristic daily evolution of the PBL have been established.

This work was supported by Madrid Regional Government (TIGAS-CM, Y2018/EMT-5177), H2020 programme from the European Union (grant 654109, ACTRIS-2 project) and the Spanish Ministry of Economy and Competitiveness (Grant PID2020-117873RB-I00 funded by MCIN/AEI/10.13039/501100011033). The authors would like to acknowledge the STRATfinder software developers

Molero, F. et al, (2014). *Int. J. Rem Sensing* 35(6), 2311-2326.  
<http://dx.doi.org/10.1080/01431161.2014.894664>.  
2014.

Kotthaus, S. et al, (2020). *Remote Sens.* 12, 3259.  
<https://doi.org/10.3390/rs12193259>.

Salvador, P. et al, (2021) *Atmos. Environ.* 245,  
<https://doi.org/10.1016/j.atmosenv.2020.118016>.

## CHANGES IN THE AEROSOL OPTICAL PROPERTIES DURING COVID-19 LOCKDOWN IN SPAIN

M.A. Obregón<sup>1</sup>, B. Martín<sup>1</sup> and A. Serrano<sup>1</sup>

<sup>1</sup>Departamento de Física, Universidad de Extremadura, Badajoz, 06006, Spain

Presenting author email: nines@unex.es

The sudden emergence of the 2019 coronavirus disease (COVID-19) in December 2019 in Wuhan, China, evolved into a global pandemic. In response to the rapid spread of the virus, numerous countries implemented stringent measures to limit human movement, resulting in a marked reduction in gas and aerosol emissions. Specifically, this situation led to a significant cut in the emission of aerosols produced by road traffic and industry, leaving the aerosol load predominantly sourced from natural sources. The unexpected situation provides unique conditions to investigate the human contribution to the overall aerosol load. Distinguishing between anthropogenic and natural origins of aerosols is of paramount scientific importance, given the significant role aerosols play in climate change.

Numerous studies have investigated the impact of the pandemic on air quality, revealing a significant reduction in primary air pollutants, particularly in PM<sub>2.5</sub>. The scarcer studies of column aerosols have obtained different results. For example, an increase in aerosol optical depth has been observed in most areas of Europe, except for its western part. This disparity in aerosol behavior between near the ground and column underscores the importance of studying both types of measurements.

Within Europe, Spain is an area of particular interest due to its location, as it is affected by a large variety of natural and anthropogenic sources of aerosols. However, little research has been conducted on the impact of the lockdown on column aerosol measurements in this region. Therefore, this study aims to detect changes in column aerosol properties in Spain due to the COVID-19 lockdown. High-quality AERosol RObotic NETwork (AERONET) measurements of aerosol optical depth (AOD), Ångström exponent (AE), and single scattering albedo (SSA) spanning from 2012 to 2020 are used for this purpose. Ten AERONET stations located throughout Spain with extensive data records were selected to assess changes during the lockdown and post-lockdown periods. The study proposes a comprehensive methodology based on three statistical analyses to evaluate changes in the dataset's general characteristics, central tendency, and extreme values for each parameter. Daily data from 2020 were compared with measurements from the same calendar days in 2012–2019.

Results show a general increase in AOD during the lockdown and a decrease post-lockdown. This observed increase in AOD during the lockdown period appears to contradict the reported decrease in PM documented by other authors in various locations

across Spain. These high AOD values could be due to the increase in days affected by desert dust intrusions coming from the Sahara during the 2020 lockdown.

While AE shows no general trend, SSA shows a general and significant increase at most sites during the 2020 lockdown and post-lockdown periods. Figure 1 shows a decrease in the number of low-SSA cases and almost all of them also showed an increase in the number of high-SSA cases during the lockdown period. Similarly, during the post-lockdown period, the number of low-SSA cases decreased at nine stations, and the number of high-SSA cases increased at eight stations. The increase observed in SSA can be attributed to two potential causes: the removal of absorbing aerosols or the addition of predominantly scattering aerosols. This study contributes to understanding the impact of COVID-19 lockdown measures on aerosol levels and provides methodologies for detecting such effects.

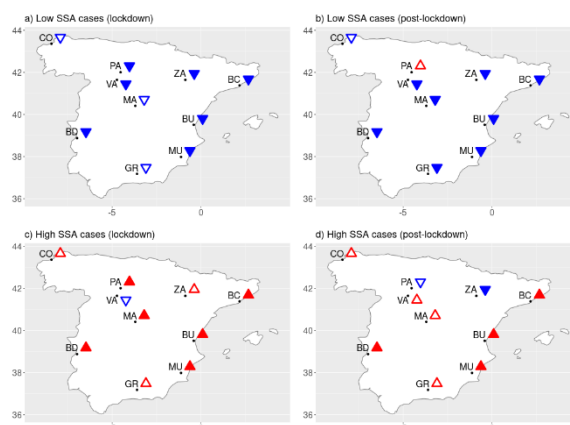


Fig. 1. Sign of the change in the proportion of low/high SSA cases during the 2020 lockdown (a,c) and post-lockdown (b,d) periods compared to the 2012–2019 reference period. An increase in the proportion is indicated by upward-pointing red triangles and a decrease is indicated by downward-pointing blue triangles. Closed and open symbols represent statistically significant and non-significant results, respectively.

This work was supported by the Grant TED2021-130532A-I00 funded by MCIN/AEI/10.13039/501100011033 and by the “European Union NextGenerationEU/PRTR”.

## IS THERE A RELATIONSHIP BETWEEN SURFACE AND COLUMN AEROSOL PROPERTIES?

M.A. Obregón<sup>1</sup>, A. Quirós<sup>1</sup> and A. Serrano<sup>1</sup>

<sup>1</sup>Departamento de Física, Universidad de Extremadura, Badajoz, 06006, Spain

Presenting author email: nines@unex.es

Aerosols play a crucial role in processes as fundamental as the Earth's radiative balance and the planet's hydrological cycle, as well as influencing ecosystems. Its presence in the air also significantly affects the health of people and can cause serious diseases. The measurement and analysis of aerosols is therefore very important and necessary both on the earth's surface and throughout the atmospheric column. This study analyzed the relationship between two surface aerosol parameters (particulate matter with diameter less than 10  $\mu\text{m}$ , PM<sub>10</sub>, or 2.5  $\mu\text{m}$ , PM<sub>2.5</sub>) and one column aerosol parameter (aerosol optical depth, AOD) in the city of Badajoz during the common period of databases (July 2012 - September 2020). For this purpose, the measurements recorded by the high volume sampler DIGITEL DH80 belonging to the REPICA network (Red Extremeña de Protección e Investigación de la Calidad del Aire) and by the solar photometer CIMEL belonging to the AERONET network (Aerosol RObotic NETwork) managed by NASA have been used. The measuring stations of these networks in Badajoz are less than one kilometre distant (Figure 1), allowing a precise study to be made of the relationship between the above parameters since it depends on local conditions.



Fig. 1. Location of the two aerosol measurement stations. The yellow line indicates the distance between them.

To analyze the relationship between surface and column aerosol parameters, the Pearson correlation coefficient between aerosol parameters has been calculated. In addition, the annual cycles presented by the different aerosol parameters have been studied. As a result, it is found a similar general behavior, with peaks occurring during the warmest months and additional spikes in spring (see Figure 2). Notably, elevated PM<sub>2.5</sub> levels are particularly prominent in

October and the winter months, likely attributed to agricultural stubble burning and increased fuel burning for heating purposes. These seasonal peaks underscore the dependence of the study parameters with local conditions.

The correlation between AOD<sub>440</sub> and PM<sub>10</sub> is 0.61 for daily measurements and 0.47 for monthly averages, consistent with findings in various studies. These values suggest a relationship between the two parameters, but they also indicate the influence of other factors that affect them differently at the surface and at higher altitudes. The correlation between AOD<sub>440</sub> and PM<sub>2.5</sub> is lower, with values of 0.39 for daily measurements and 0.27 for monthly averages. This discrepancy is attributed to the fact that PM<sub>2.5</sub> only considers particles with diameters less than 2.5  $\mu\text{m}$ , unlike PM<sub>10</sub>, which includes larger particles in addition to smaller ones.

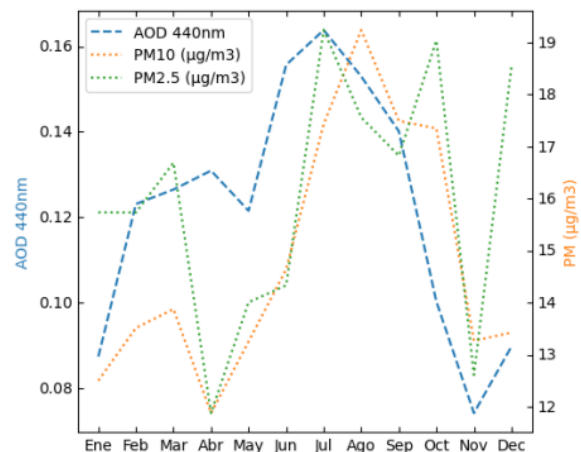


Fig. 2. Monthly average values of AOD<sub>440</sub>, PM<sub>10</sub> and PM<sub>2.5</sub> in Badajoz.

In conclusion, a moderate correlation between the AOD, PM<sub>10</sub> and PM<sub>2.5</sub> parameters of aerosols is found, probably due to the mixture that occurs between different aerosol contributions at different heights. Iberian Peninsula is affected by a large variety of sources of aerosols.

This work was supported by the Grant TED2021-130532A-I00 funded by MCIN/AEI/10.13039/501100011033 and by the "European Union NextGenerationEU/PRTR".

## IS THE LORENZ-MIE THEORY VALID FOR QUASI-SPHERICAL PARTICLES?

A. Valenzuela<sup>1,2</sup>, G. Sánchez-Jiménez<sup>1,2</sup>, D. Pérez-Ramírez<sup>1,2</sup>, J.L. Guerrero-Rascado<sup>1,2</sup>, L. Alados-Arboledas<sup>1,2</sup> and F.J. Olmo-Reyes<sup>1,2</sup>

<sup>1</sup>Andalusian Institute for Earth System Research (IIISTA-CEAMA), Granada 18006, Spain

<sup>2</sup>Department of Applied Physics, University of Granada, Granada 18071, Spain

Keywords: single particles, microphysical properties, non-sphericity

Presenting author email: gemasj@ugr.es

Experimental measurements of light scattering and extinction caused by individual aerosol particles are crucial for evaluating the effect of geometry and validating models that take into account non-sphericity. The Atmospheric Physics Group at the University of Granada has a number of capabilities, including a single particle electrodynamic trap coupled to a double cavity ring down spectroscopy setup (CRDS), which allows for a variety of analyses to be carried out in the characterisation of physicochemical properties at the fundamental single particle level (Valenzuela et al., 2024). Any material, whether spherical or non-spherical, which scatters or absorbs radiation and falls within the nanometre to micrometre size range, can be suspended and confined in the electrodynamic trap.

In this work we present measurements of extinction cross sections ( $\sigma_{\text{ext}}$ ) as well as the size estimated from phase function fitting of an individual ammonium sulphate (( $\text{NH}_4$ )<sub>2</sub>SO<sub>4</sub>) particle in two different phases: firstly, when the particle is spherical and continuously evaporates, and secondly, when efflorescence occurs and drastically loses water and mass.

Ring-down time measurements and experimental phase functions are recorded continuously throughout the experiment, covering both phases of the particle. Two different codes (one based on Lorenz-Mie theory, which considers spherical particles, and a spheroids model based on the T-matrix) are used to fit the experimental data. Figure 1a shows the  $\sigma_{\text{ext}}$  at 532 nm of a ( $\text{NH}_4$ )<sub>2</sub>SO<sub>4</sub> particle during the evaporation process. For each external relative humidity to which the particle is exposed, it evaporates or condenses water to thermodynamically equilibrate with the water vapour pressure. ( $\text{NH}_4$ )<sub>2</sub>SO<sub>4</sub> is a salt with hysteresis in its hygroscopic cycle. This property is perfectly reflected in our data for both the  $\sigma_{\text{ext}}$  (Figure 1a) and the radius fit from the phase functions (Figure 1b). There is an abrupt jump in these two variables because of the rapid loss of water and mass of the particle. The relevance of our results is that the adjustment of phase functions by Lorenz-Mie theory still works after efflorescence has occurred. This indicates that the particle remains with a quasi-sphere shape. Our findings are confirmed by the experimental  $\sigma_{\text{ext}}$  data from the cavity ring down spectroscopy setup, whose mean value agrees well with that of Lorenz-Mie theory (Figure 1c). The experimental phase functions were also fitted with a T-matrix model based on a spheroidal particle geometry. The code was run for different aspect ratios (h) of the spheroid shape (i.e. the ratio of the equatorial axis to

the polar one). The values of h chosen were close to 1, as the particle shape is unlikely to deviate much from sphericity. The values obtained are within the experimental values of the CRDS and agree well with those predicted by the Lorenz-Mie theory. Therefore, although further lab-experiments will be necessary, we can use Lorenz-Mie theory as a first approximation to fit experimental phase functions of quasi-spherical solid particles of ( $\text{NH}_4$ )<sub>2</sub>SO<sub>4</sub>.

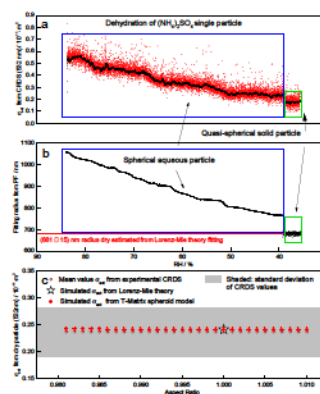


Fig. 1a)  $\sigma_{\text{ext}}$  at 532 nm from CRDS, b) fitting radius from phase functions, and c) experimental and simulated (Lorenz-Mie and T-Matrix code)  $\sigma_{\text{ext}}$  at 532 nm of a ( $\text{NH}_4$ )<sub>2</sub>SO<sub>4</sub> particle during an evaporation process.

This work was supported by the Spanish Ministry of Science and Innovation through projects ELPIS (PID2020-12001-5RB-I00), PID2020-117825GB-C21 and PID2020-117825GB-C22, the European Union's Horizon 2020 research, ATMO-ACCESS (grant agreement No 101008004) and ACTRIS-España (RED2022-134824-E).

Valenzuela et al. (2024) Electrodynamic single-particle trap integrated into double-cavity ring-down spectroscopy for light extinction. *Journal of Aerosol Science*. Elsevier. 175-106292.

## PASSIVE MONITORING OF AIRBORNE MICROPLASTICS IN NORTHWEST OF SPAIN USING QC-LDIR AND COMPARISON OF BULK SAMPLERS

A. López-Rosales<sup>1</sup>, B. Ferreiro<sup>1</sup>, M. Fernández-Amado<sup>1</sup>, P. Esperón, J.M. Andrade<sup>1</sup>, M. González-Pleiter<sup>2</sup>, P. López-Mahía<sup>1</sup>, R. Rosal<sup>3</sup>, S. Muniategui-Lorenzo<sup>1</sup>

<sup>1</sup>Group of Applied Analytical Chemistry, University Institute of Environment, Universidade da Coruña, Campus da Zapateira s/n, E-15071 A Coruña, Spain

<sup>2</sup>Department of Biology, Faculty of Science, Universidad Autónoma de Madrid, E-28049, Madrid, Spain

<sup>3</sup>Department of Chemical Engineering, Universidad de Alcalá, E-28871 Alcalá de Henares, Madrid, Spain

Keywords: airborne microplastics, LDIR, Bulk sampler, Atmospheric pollution

Presenting author email: adrian.lopez.rosales@udc.es

The number of studies on airborne microplastics (AMPs) is increasing, but sampling methods and handling procedures are still not standardised enough.

A rapid and reliable method to characterise AMPs has been developed. In addition, two passive sampling devices for the collection of bulk atmospheric deposition were compared: the EnviroPlaNet prototype of the Spanish Plastic Pollution Research Network ([www.enviroplanet.net](http://www.enviroplanet.net)) and the commercial Depobulk<sup>®</sup> system. In addition, certain operational parameters of a high-throughput quantum cascade laser-based infrared (LDIR) instrument were optimised: an effective automatic approach for distinguishing fibres from particles (with over 90% success) and a criterion for confirming matches when comparing an unknown spectrum with a spectral database (proposed match index > 0.9 and manual verification of the spectra with a 0.85-0.9 match index). In addition, two transference protocols were validated and compared (using a reflective slide and a gold-coated filter).

The amount and type of microplastics (MPs) deposited in a suburban area NW Spain were assessed. All samples were collected during different seasons between 2021 and 2023 and processed at the University of A Coruña using a mild digestion protocol based on SDS and H<sub>2</sub>O<sub>2</sub> (surfactant+oxidative method).

To summarise the results, it can be said that the EnviroPlaNet system tended to present higher deposition rates than the other system, although this was only statistically significant in the sample of autumn 2021. On the contrary, the Depobulk<sup>®</sup> system lead to less data scattering, probably due to its design.

The most common polymers found in the airborne samples were polypropylene (PP), polyethylene terephthalate (PET), polyamide (PA) and polyethylene (PE), in that order. The total number of AMPs in this area ranged from 50 MPs/m<sup>2</sup>/day to 490 MPs/m<sup>2</sup>/day, depending on the sampler and the season. Particles between 20 and 50 µm predominated, accounting for more than 60% of the particles.

### Acknowledgements

This work was supported by the following projects: EU-H2020 “LAnd-Based Solutions for PLAstics in the Sea Project (LABPLAS, Grant 101003954); Programa de Ciencias Mariñas de Galicia (ThinkInAzul), Ministerio de Ciencia e Innovación-Xunta de Galicia, NextGenerationEU (PRTR-C17.11) and “European Maritime and Fisheries Fund”. The Galician Government (Grant ED431C 2021/56) is also acknowledged. M. Fernández-Amado appreciates MCIU (PTA2022-021336-I) support. P. Esperón thanks a MCIU-PTA 2018-016005-I grant.

## EXPERIMENTAL EVIDENCE OF INHIBITED DEHYDRATION OF AN INORGANIC COMPOUND CAUSED BY AN ORGANIC COATING

G. Sánchez-Jiménez<sup>1,2</sup>, D. Pérez-Ramírez<sup>1,2</sup>, J.L. Guerrero-Rascado<sup>1,2</sup>, L. Alados-Arboledas<sup>1,2</sup>, F.J. Olmo-Reyes<sup>1,2</sup> and A. Valenzuela<sup>1,2</sup>

<sup>1</sup>Andalusian Institute for Earth System Research (IISTA-CEAMA), Granada 18006, Spain

<sup>2</sup>Department of Applied Physics, University of Granada, Granada 18071, Spain

Keywords: single particles, microphysical properties, non-sphericity

Presenting author email: gemasj@ugr.es

Atmospheric particles can interact directly or indirectly with sunlight, altering the Earth-atmosphere energy balance. The process of water uptake has a significant effect on the aerosol particles optical properties and their ability to act as cloud condensation nuclei (CCNs), which in turn affects their climate properties.

Hygroscopicity is a crucial aspect for characterising the water uptake ability of the particles. The hygroscopic tandem differential mobility analyser (HTDMA) is a commonly used technique for investigating the aerosol particles hygroscopic growth in different environments. The HTDMA has significantly enhanced our understanding of the hygroscopicity of ambient aerosol particles. However, it only provides an average growth factor for size-resolved aerosol populations. Thus, the hygroscopicity variation among particles in the aerosol population cannot be distinguished. To tackle this issue, a cavity ring down spectroscopy setup coupled to a Paul electrodynamic trap involving single particles has been employed to study hygroscopicity (Valenzuela et al., 2024). This helps to understand the mixing state and hygroscopicity of individual particles.

Figure 1 (a), (b), and (c) show three separate aqueous droplets that were trapped and confined in three distinct experiments. The ring down time measurements of an aqueous droplet of NaCl during an evaporation process are presented in Figure 1a. NaCl is an inorganic salt that exhibits hysteresis in its hygroscopic curve. The optical cavity ring down times measurements accurately captures this characteristic during the efflorescence process, where the droplet experiences a significant loss of water and mass. When a 1:1 mass ratio of organic (1,2,6-hexanetriol) and inorganic (NaCl) mixtures is present, the hysteresis effect disappears during the NaCl evaporation process (Figure 1b). Finally, the experiment showed in Figure 1c demonstrates that increasing the concentration of the organic component over the inorganic component at a mass mixing ratio of 3:1, while suppressing the hysteresis effect in the salt, reduces the evaporation rate of the water in the aqueous droplet.

Preliminary results indicate that the organic shell (1,2,6-hexanetriol) acts as a barrier to water vapor exchange with inorganic core particulate NaCl during liquid-liquid phase separation. The presence of organic species on the particle surface also influences the surface tension and the water activity, leading to changes in the equilibrium vapor pressure of water over these solution droplets. To improve air quality predictions and

understand aerosol-climate interactions, it is essential to integrate information on aerosol physical-chemical properties, hygroscopicity, and particle growth into atmospheric modelling, including phase-separated particle data.

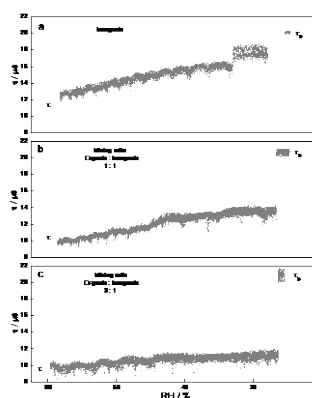


Fig. 1. Illustrates the evaporation processes of individual aqueous droplets containing a) NaCl, b) 1:1 mixing ratio of 1,2,6-hexanetriol and NaCl, and c) 3:1 mixing ratio of 1,2,6-hexanetriol and NaCl.

This work was supported by the Spanish Ministry of Science and Innovation through projects ELPIS (PID2020-12001-5RB-I00), INTEGRATYON<sup>3</sup> (PID2020-117825GB-C21 and PID2020-117825GB-C22), ATMO-ACCESS (grant agreement No 101008004) and ACTRIS-España (RED2022-134824-E).

Valenzuela A. et al. (2024) Optical properties from extinction cross-section of single pollen particles under laboratory-controlled relative humidity. *Journal of Aerosol Science*, 177, 106311.

## CHARACTERISATION OF THE WET AND DRY ATMOSPHERIC DEPOSITION OVER LEÓN - NW SPAIN

C. Gonçalves<sup>1</sup>, E.D. Vicente<sup>2</sup>, C. Alonso-Rodríguez<sup>1</sup>, P. Rodríguez-Rodríguez<sup>1</sup>, C. Blanco-Alegre<sup>1</sup>, L.B. Osa-Akara<sup>1</sup>, A.I. Calvo<sup>1</sup>, A. Rodríguez-Fernández<sup>3</sup>, A. Sánchez de la Campa<sup>4</sup>, M. Cerqueira<sup>2</sup> and R. Fraile<sup>1</sup>

<sup>1</sup>Department of Physics, Universidad de León, Campus de Vegazana, 24071, León, Spain; <sup>2</sup>Department of Environment and Planning, Centre for Environmental and Marine Studies, University of Aveiro, 3810-193, Aveiro, Portugal; <sup>3</sup>Department of Biodiversity and Environmental Management, Universidad de León, León, Spain;

<sup>4</sup>Centre for Research in Sustainable Chemistry, University of Huelva, Huelva, E21071, Spain.

Keywords: atmospheric particles, deposition fluxes, physical-chemical characterisation, source contribution  
Presenting author email: cmaig@unileon.es

Aerosol atmospheric deposition is the ultimate path by which particles and trace gases are removed from the atmosphere. This process can occur through precipitation scavenging (wet deposition), or by direct sedimentation during periods without rain (dry deposition) (Seinfeld and Pandis, 2016).

The chemical composition of the wet and dry deposition can offer insights into local pollutant emission sources, and also the effects of emissions transported over long distances (like those from Saharan dust intrusions or forest fires events).

Based on a long monitoring campaign, the goal of this research is to characterise atmospheric particulate matter deposition in León city in terms of aerosol fluxes, chemical composition and sources with a special focus on origin of the air mass.

Sampling was carried out in León city, Spain, at NW of the Iberian Peninsula. Two sampling sites with different characteristics were selected: 1) the top of a public building located in downtown León, at a height of around 20 m above street level (42°35'59.5"N, 5°34'34.3"W), classified as roadside, and 2) the top of the Faculty Veterinary Medicine building at the University of León (42°36'47.4"N 5°33'27.3"W), at a height of around 12 m above street level, located in a suburban area at NE of the city center of León. This second site is characterised by the absence of large emitting industries and classified as an urban background site. The sampling took place simultaneously at the two places (for most of the campaign time). Daily rainwater samples were collected between January 2022 and May 2023 with two Eigenbrodt model UNS130/E automatic collectors, both equipped with an dry sample container unit. The dry deposition samples were collected during the same period, on a weekly basis. The meteorological parameters (temperature, wind and relative humidity) were continuously recorded by an automatic weather station. The physical characteristics of rain (drop size distribution, rain intensity, falling velocity, etc.) were measured with a laser precipitation monitor on a 1-minute basis. Air mass trajectories were also analysed using HYSPLIT-model. To segregate the soluble substances from the insoluble ones, the samples were passed through quartz fiber filters, which was previously calcinated at 600 °C for 6 hours. Quartz filters of water insoluble fraction of rain and dry

deposition samples were used for the determination of the carbon content (EC, WIOC – water insoluble organic carbon and WITC - water insoluble total carbon), by a thermal-optical method. Whereas the particulate WIOC fraction can be investigated by examining filterable OC of rain, the dominant fraction of particulate OC which is water soluble (WSOC) cannot be directly determined in rain. The ratio between the concentrations of WSOC and WIOC in aerosols (data from other research work) has been used to estimate the contribution of organic particles to the global pool of dissolved organic carbon (DOC) in rainwater. DOC was determined by a total organic carbon analyser. The filtrate was also used for analysing inorganic ions (by ionic chromatography) such as F<sup>-</sup>, Cl<sup>-</sup>, NO<sub>2</sub><sup>-</sup>, Br<sup>-</sup>, NO<sub>3</sub><sup>-</sup>, PO<sub>4</sub><sup>3-</sup>, SO<sub>4</sub><sup>2-</sup>, Na<sup>+</sup>, NH<sub>4</sub><sup>+</sup>, K<sup>+</sup>, Ca<sup>2+</sup>, Mg<sup>2+</sup>. Dry deposition fluxes were calculated based on dry deposition velocities found in existing literature and concentration levels observed in our research.

Table 1. Summary with dry and wet days and number of samples collected during the period studied. \*until May

Year	Roadside		Urban background	
	Dry days	Wet days	Dry dep. samples	Wet dep. samples
2022	240	125	48	84
2023*	102	49	24	31

This work was partially supported by the Junta de Castilla y Leon co-financed with European FEDER funds (Grant LE025P20). Furthermore, it is part of the project TED2021-132292B-I00, funded by MCIN/AEI/10.13039/501100011033 and by the European Union "NextGenerationEU"/PRTR. The authors thank to Dr. Mário Cerqueira (Dep. of Environment and Planning, University of Aveiro, Portugal) for providing one of the automatic rain collectors used in this work.

Seinfeld, J.H. et al. (2016) Atmospheric Chemistry and Physics: From Air Pollution to Climate Change, 3rd Ed. John Wiley & Son, NewJersey.

## ASSESSING THE INFLUENCE OF BIOMASS BURNING ON AEROSOL OPTICAL PROPERTIES IN A RURAL ENVIRONMENT

M. Alfosea-Simón<sup>1</sup>, E. Borrás<sup>2</sup>, N. Galindo<sup>1\*</sup>, E. Yubero<sup>1</sup>, J.F. Nicolás<sup>1</sup>, T. Vera<sup>2</sup>, T. Gómez<sup>2</sup>, M. Martínez<sup>2</sup>, R. Soler<sup>2</sup>, M. Ródenas<sup>2</sup>, E. Mantilla<sup>2</sup>, B. Domínguez<sup>2</sup>, A. Muñoz<sup>2</sup>, J. Crespo<sup>1</sup>

<sup>1</sup>Department of Applied Physics, Miguel Hernández University of Elche, Elche, 03202, Spain

<sup>2</sup>Fundación CEAM. EUPHORE Laboratories, C/ Charles R. Darwin 14, 46980, Paterna, Spain

Keywords: biomass burning, aerosol composition, elemental carbon

Presenting author email: ngalindo@umh.es

Biomass burning (BB), especially wood and agricultural waste, constitutes a significant source of air pollution associated with adverse environmental and health effects. Wood combustion generates significant amounts of carbonaceous species such as organic carbon (OC) and black carbon (BC) (Jiang et al. 2023). BC strongly absorbs solar radiation from ultraviolet (UV) to near-infrared, being the most efficient absorber among atmospheric aerosols. On the other hand, several organic carbon species (denoted as brown carbon, BrC) can absorb strongly in the UV and visible spectral ranges (Laskin et al. 2015).

The main objective of this study was to assess the impact of BB on PM<sub>2.5</sub> levels and absorption optical properties in a rural environment (Beneixama, Southeastern Spain). During winter, this area is characterized by wood burning for domestic heating and open burning of pruning residues. For this, daily PM<sub>2.5</sub> samples were collected from December 2023 to February 2024 using a high-volume sampler (30 l/min). Furthermore, a simultaneous study on the optical properties of aerosols was carried out. Minute-by-minute measurements of  $\sigma_{ap}$  (absorption coefficient) were performed using an aethalometer (AE33 model, Magee Scientific, USA). The aethalometer provided the absorption coefficient at seven wavelengths (370, 470, 520, 590, 660, 880, and 950 nm), as well as values of BC, and the percentage of Biomass Burning (BB%). The Absorption Angstrom Exponent (AAE) was derived from the aethalometer measurements. AAE characterizes the variation of light absorption with wavelength. Those days under the influence of mineral dust from North Africa were excluded from the analysis. Table 1 presents various statistical parameters of PM<sub>2.5</sub> and optical absorption properties obtained during the measurement period. Absorption values recorded in this study were those expected for a rural station. The significant difference between the mean and median values of the absorption coefficients is noteworthy. This could be due to the impact of BB episodes at the monitoring site. The average value of AAE (1.50) suggests a significant contribution from BrC to the absorption process. In fact, the P95 value of AAE (1.91) indicates that, in certain cases, BrC is strongly involved in the process. These assumptions are reinforced by the high percentage of BB obtained (37.7%).

Table 1. Summarized statistics of BC, BB (%), absorption optical properties and PM<sub>2.5</sub> concentration.  $\sigma_{ap}$  is given in Mm<sup>-1</sup>, BC in ng·m<sup>-3</sup>, BB in % and PM concentrations in  $\mu\text{g}\cdot\text{m}^{-3}$ . AAE is dimensionless.

Parameter	Mean	P5	Median	P95
$\sigma_{ap,370\text{ nm}}$	14.3	1.3	8.7	43.8
$\sigma_{ap,440\text{ nm}}$	10.5	1.1	6.4	30.9
$\sigma_{ap,520\text{ nm}}$	8.2	0.9	5.0	24.0
$\sigma_{ap,590\text{ nm}}$	6.7	0.7	4.1	19.5
$\sigma_{ap,660\text{ nm}}$	5.6	0.4	3.4	16.2
$\sigma_{ap,880\text{ nm}}$	4.0	0.4	2.4	11.4
$\sigma_{ap,950\text{ nm}}$	3.6	0.4	2.2	10.4
AAE	1.50	1.08	1.47	1.91
BC	879	86	523	2532
BB (%)	37.7	8.1	35.2	77.1
PM <sub>2.5</sub>	9.0	4.8	9.1	13.3

P5: 5<sup>th</sup> Percentil; P95: 95<sup>th</sup> Percentil.

The MAE (Mass Absorption Efficiency) value for PM<sub>2.5</sub> at 370 nm obtained was 1.59 m<sup>2</sup>g<sup>-1</sup>.

This work was supported by MCIN/AEI/10.13039/501100011033 and the "European Union NextGenerationEU/PRTR" (CAMBIO project, ref. TED2021-131336B-I00), by MCIN/AEI/10.13039/501100011033 and by "ERDF A way of making Europe" (ATMOBE project, ref. PID2022-1423660B-I00), and by the Valencian Regional Government (Generalitat Valenciana, CIAICO/2021/280 research project). The authors would like to thank the ACTRIS-Spain network (RED2022-134824-E).

Jiang K., Xing R., Luo Z., Huang W., Yi F., Men Y., Zhao N., Chang Z., Zhao J., Pan, B. and Shen, G. (2023) Pollutant emissions from biomass burning: A review on emission characteristics, environmental impacts, and research perspectives. *Particuology*. 85:296-309.

Laskin A., Laskin J. and Nizkorodov S.A. (2015) Chemistry of atmospheric brown carbon. *Chem. Rev.* 115, 4335–4382.

## METHANOL AND WATER-SOLUBLE ORGANIC CARBON IN PM<sub>10</sub> IN THE IBERIAN PENINSULA

N. Gómez-Sánchez<sup>1</sup>, N. Galindo<sup>1</sup>, J.F. Nicolás<sup>1</sup>, M. Alfosea-Simón<sup>1</sup>, J. Crespo<sup>1</sup> and E. Yubero<sup>1</sup>

<sup>1</sup>Department of Applied Physics, Miguel Hernández University of Elche, Elche, Spain.

Keywords: Brown carbon, water-soluble, methanol-soluble.

Presenting author email: eyubero@umh.es

Biomass burning is a major source of brown carbon (BrC), contributing significantly to radiative forcing (Ramanathan *et al.* 2001). In climate change-sensitive urban areas of south-western Europe, where strong emissions from residential wood burning (RWB) occur, the radiative impact of carbonaceous aerosols remains mainly unknown.

This study examines the absorption properties of methanol-soluble organic carbon (MSOC) and water-soluble organic carbon (WSOC) in a small village in southeastern Spain (Benejama, Alicante), where the use of RWB is very common during winter months. Measurements were conducted between late winter and early spring of 2023 (22 February – 4 April). A total of 38 daily PM<sub>10</sub> samples were collected onto quartz fibre filters. Sample extracts were analysed using UV-Vis spectrophotometry to determine the absorption of methanol and water-soluble organic carbon. MSOC concentrations, used as a proxy for BrC, were determined using an indirect quantification protocol (Cheng *et al.* 2016). For this, samples were analysed by the thermal-optical method to quantify the OC content before and after their extraction with methanol. The concentration of MSOC was determined by subtracting the OC mass concentration after methanol extraction from the total OC concentration. WSOC were quantified using a Total Organic Carbon analyser.

The mean concentration of MSOC during the study period was  $1.96 \pm 0.31 \mu\text{g}/\text{m}^3$  contributing 63% to the total OC, while the mean concentration of WSOC was  $1.33 \pm 0.31 \mu\text{g}/\text{m}^3$ , contributing 43% to the total OC.

The winter average absorptions of MSOC\_BrC and WSOC\_BrC at 365 nm were  $0.69 \pm 0.39 \text{ Mm}^{-1}$  and  $0.56 \pm 0.37 \text{ Mm}^{-1}$  respectively. Normalizing the absorption coefficient measured at 365 nm to the extractable OC mass resulted in an average mass absorption efficiency (MAE) of  $0.35 \pm 0.16 \text{ m}^2/\text{g}$  for water-soluble extracts and  $0.84 \pm 0.2 \text{ m}^2/\text{g}$  for methanol-soluble extracts.

Furthermore, we found a robust linear correlation between methanol and water extract at 365 nm and the levoglucosan ( $R^2 = 0.66$ ;  $R^2 = 64$ ), a tracer of biomass burning, indicating that this source significantly contributed to brown carbon concentrations during the study period (Figure 2).

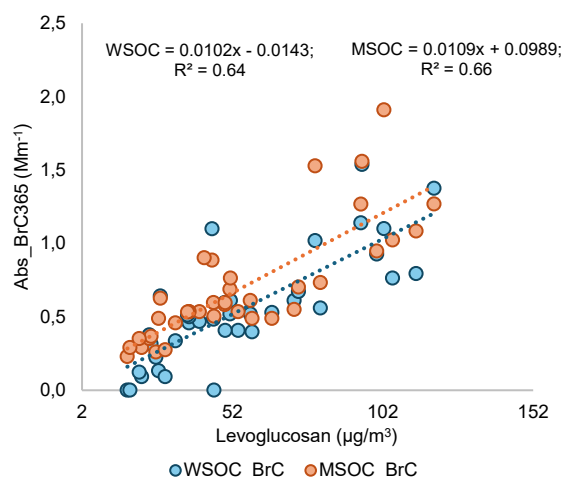


Figure 2. Correlations between methanol and water extract at 365 nm and levoglucosan concentrations.

This work has been funded by the Generalitat Valenciana (Generalitat Valenciana, research project CIAICO/2021/280) and the Spanish Ministry of Science and Innovation (Ministerio de Ciencia e Innovación MCIN/AEI/10.13039/501100011033). The authors would like to thank the ACTRIS-Spain network (CGL2017-90884-REDT).

Cheng, Y., He, K., Du, Z., Engling, G., Liu, J, Ma, Y., Zheng, M., Weber, R.J. (2016) The characteristics of brown carbon aerosol during winter in Beijing, *Atmos. Environ.*, 127, 355-364.

Ramanathan, V., Crutzen, P.J., Kiehl, J.T., Rosenfeld, D. (2001) Aerosols, climate, and the hydrological cycle, *Science*, 294, 2119-2124.

## FIRST HIGH-TIME-RESOLUTION CARBONACEOUS AEROSOL SPECIATION USING AN ADVANCED TC-BC( $\lambda$ ) METHOD IN A CORUÑA, SPAIN

M. Fernández-Amado<sup>1</sup>, M. Piñeiro-Iglesias<sup>1</sup>, A. Gregorič<sup>2,3</sup>, M. Ivančič<sup>2</sup>, M. Rigler<sup>2</sup>, J. Moreda-Piñeiro<sup>1</sup>, P. López-Mahía<sup>1</sup> and S. Muniategui-Lorenzo<sup>1</sup>

<sup>1</sup>Grupo de Química Analítica Aplicada (QANAP), Instituto Universitario de Medio Ambiente (IUMA), Universidade da Coruña, Pazo de Lóngora, Liáns, 15179 A Coruña, Spain

<sup>2</sup>Aerosol d.o.o., Research & Development Department, Ljubljana, SI-1000, Slovenia, EU

<sup>3</sup>Centre for Atmospheric Research, University of Nova Gorica, Nova Gorica, SI-5000, Slovenia, EU

Keywords: carbonaceous aerosols, brown carbon, primary and secondary organic aerosols

Presenting author email: maria.fernandez.amado@udc.es

Carbonaceous aerosols (CA) can have significant impacts on climate, air quality, and human health. For example, they can absorb or scatter sunlight, which can affect the Earth's radiation balance and contribute to regional and global warming. Additionally, these aerosols can influence cloud formation and properties, leading to changes in precipitation patterns. In terms of human health, exposure to carbonaceous aerosols has been associated with respiratory and cardiovascular problems.

Understanding the sources, composition, and behaviour of carbonaceous aerosols is important for developing effective strategies to mitigate their impacts on the environment and public health.

In this study, we used the Carbonaceous Aerosol Speciation System (CASS, Aerosol Magee Scientific), comprised of two instruments, a Total Carbon Analyzer TCA08 (Rigler *et al.*, 2020) in tandem with an Aethalometer AE33 (Drinovec *et al.*, 2015), which allows us to perform high-time-resolution measurements of total carbon (TC) and black carbon (BC). CASS can provide valuable insights into the sources, transport, and impact of carbonaceous aerosols on air quality and climate.

The sampling was carried out in a suburban area located in Oleiros, close to A Coruña (5 km), in the northwest of Spain. It is a residential zone with moderate traffic density, and very close to the sea (<1 km). There are also 3 industrial sites, an airport and a harbour in the surroundings (within a radius of 13 km). The site is characterized by an Atlantic climate.

Due to the characteristics of the aerosol in the sampling site, the quartz fibre filters (used in the TCA08) get loaded with inorganic salts in a few days. To prolong the filter's lifetime, the use of a PM<sub>1</sub> size selective inlet instead of default PM<sub>2.5</sub> is recommended.

The advanced method to apportion CA into six components based on their optical absorption properties and their primary or secondary origin developed by Ivančič *et al.* (2022) was applied to high-time resolution measurements with CASS (Fig. 1).

Primary organic carbon (POC) has a diurnal profile comparable to BC, while secondary organic carbon (SOC) has afternoon and nocturnal peaks.

BrC contribution was almost negligible which is consistent with previous analyses.

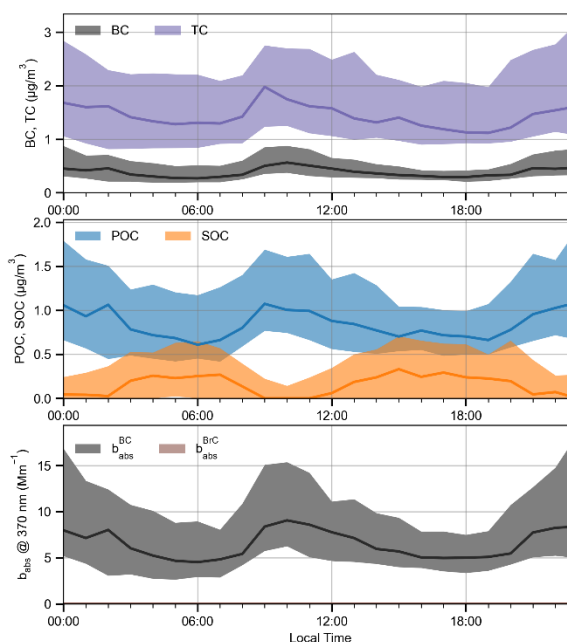


Fig. 1. Diurnal profiles of CA in A Coruña.

This work was supported by FEDER-MINECO-Xunta de Galicia (UNLC15-DE-3097), Xunta de Galicia (GRC2017-28, ED431C2021/56) and MCIU/MCIN-AEI-FEDER (PID2021-125201OB-I00). M. Fernández-Amado appreciate MCIU (PTA2022-021336-I) support. The authors would like to thank P. Esperón.

Drinovec L. *et al.* (2015) The "dual-spot" Aethalometer: an improved measurement of aerosol black carbon with real-time loading compensation. *Atmos. Meas. Tech.*, 8, 1965.

Ivančič M. *et al.* (2022) Two-year-long high-time-resolution apportionment of primary and secondary carbonaceous aerosols in the Los Angeles Basin using an advanced total carbon-black carbon (TC-BC( $\lambda$ )) method. *Sci. Total Environ.*, 848, 157606.

Rigler M. *et al.* (2020) The new instrument using a TC-BC (total carbon-black carbon) method for the online measurement of carbonaceous aerosols. *Atmos. Meas. Tech.*, 13, 4333.

## CAECENET: CONTINUOUS AND AUTOMATIC COLUMNAR AND VERTICAL AEROSOL PROPERTIES

Celia Herrero del Barrio<sup>1</sup>, Roberto Román<sup>1</sup>, Ramiro González<sup>1</sup>, Alberto Cazorla<sup>2,3</sup>, Marcos Herreras-Giralda<sup>4</sup>, Juan Carlos Antuña-Sánchez<sup>1,4</sup>, Francisco Molero<sup>5</sup>, Francisco Navas-Guzmán<sup>2,3</sup>, Antonio Serrano<sup>6</sup>, María de los Ángeles Obregon<sup>6</sup>, Yolanda Sola<sup>7</sup>, Marco Pandolfi<sup>8</sup>, Sara Herrero-Anta<sup>1</sup>, Daniel González-Fernández<sup>1</sup>, Jorge Muñoz-Rosado<sup>2,3</sup>, David Mateos<sup>1</sup>, Abel Calle<sup>1</sup>, Carlos Toledano<sup>1</sup>, Victoria E. Cachorro<sup>1</sup>, and Ángel de Frutos<sup>1</sup>

<sup>1</sup>Group of Atmospheric Optics (GOA-UVA), Universidad de Valladolid, 47011, Valladolid, Spain

<sup>2</sup>Department of Applied Physics, Universidad de Granada, 18071, Granada, Spain

<sup>3</sup>Andalusian Institute for Earth System Research, IISTA-CEAMA, Granada, Spain

<sup>4</sup>GRASP-SAS, Remote Sensing Developments, Villeneuve D'Ascq, France

<sup>5</sup>Departamento de Medio Ambiente, Centro de Investigaciones Energéticas, Medioambientales y Tecnológicas (CIEMAT), 28040 Madrid, Spain

<sup>6</sup>Departamento de Física, Universidad de Extremadura, Badajoz, Spain

<sup>7</sup>Group of Meteorology, Department of Applied Physics, Faculty of Physics, University of Barcelona, Barcelona, Spain

<sup>8</sup>Institute of Environmental Assessment and Water Research (IDAEA-CSIC), Barcelona, Spain

Keywords: Aerosols, CAECENET, GRASP, photometry, ceilometer.

Presenting author email: celia@goa.uva.es

This study presents CAECENET, a novel system designed to automatically retrieve columnar and vertically resolved aerosol properties. The system employs the GRASP algorithm (Generalized Retrieval of Atmosphere and Surface Properties; Dubovik et al., 2014), utilizing as input aerosol optical depth (AOD) and sky radiance measurements from sun-sky photometers, as well as range-corrected signal (RCS) measurements from ceilometers. The implementation of this approach, known as GRASP<sub>pac</sub> (Román et al., 2018), is integrated into CAECENET system. This system assimilates sun-sky photometer data from the CÆLIS database (Fuertes et al., 2018) and ceilometer data from the ICENET database (Iberian Ceilometer Network; Cazorla et al., 2017).

an example of CAECENET's data at Valladolid (Spain), for the 27<sup>th</sup> of June 2023, when a biomass burning aerosol, originated in Canada wildfires, reached the Iberian Peninsula.

The future goal is configuring CAECENET to assimilate data from other types of lidar systems, such as Micropulse Lidars (MPL), or from other ceilometer networks, like E-PROFILE, to provide the GRASP<sub>pac</sub> products in a greater number of locations. This could be a useful and powerful tool that may serve to monitor, characterize and quantify the vertically-resolved aerosol properties of arctic aerosols. Moreover, this could be used in the computation of aerosol vertical radiative forcing, in order to study the climate and environmental impacts of aerosols.

This research has been supported by the Ministerio de Ciencia e Innovación (grant no. PID2021-127588OB-I00), is part of the TED2021-131211B-I00 project funded by MCIN/AEI/10.13039/501100011033 and European Union "NextGenerationEU"/PRTR, and is based on work from COST Action CA21119 HARMONIA. The authors acknowledge the support of the Spanish Ministry for Science and Innovation to ACTRIS ERIC.

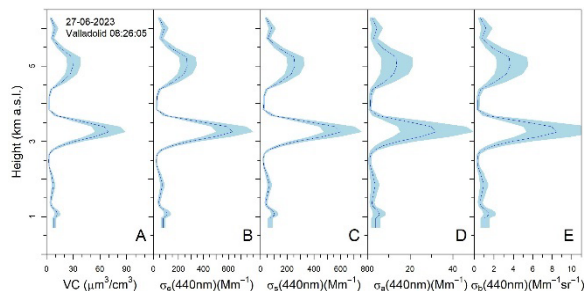


Figure 1. Vertical profiles of volume concentration (A), extinction (B), scattering (C), absorption (D) and backscattering (E) for the 27<sup>th</sup> of June 2023 at Valladolid. Shadowband represents the uncertainty of the retrieved values.

The arrangement of measurement stations, for now across the Iberian Peninsula, allows the near-real-time aerosol 3D monitoring. This approach allows for the collection of data regarding the speed of event dissemination, variations in aerosol altitude, potential impediments or external factors influencing its concentration, and the resulting impacts on aerosol optical properties. This information is valuable for both scientific research on aerosols and for the general public due to its contribution to monitor events that can impact aviation traffic or public health. Figure 1 shows

Cazorla, A., et al., Near-real-time processing of a ceilometer network assisted with sun-photometer data: monitoring a dust outbreak over the Iberian Peninsula, *Atmospheric Chemistry and Physics*, 17, 11 861–11 876, 2017.

Dubovik, O. et al., GRASP: a versatile algorithm for characterizing the atmosphere, *SPIE: Newsroom*, 2014.

Fuertes, D., et al., CÆLIS: software for assimilation, management and processing data of an atmospheric measurement network, *Geoscientific Instrumentation, Methods and Data Systems*, 7, 67–81, 2018.

Román, R., et al.: Retrieval of aerosol profiles combining sunphotometer and ceilometer measurements in GRASP code, *Atmospheric Research*, 204, 161–177, 2018.

## ANALYSIS OF MINERAL DUST EPISODES DURING A-LIFE EXPERIMENT IN CYPRUS

D. Mateos<sup>1</sup>, C. Toledano<sup>1</sup>, A. Calle<sup>1</sup>, R. Román<sup>1</sup>, R. González<sup>1</sup>, S. Herrero-Anta<sup>1</sup>, D. González-Fernández<sup>1</sup>, C. Herrero-del Barrio<sup>1</sup>, A. Nisantzi<sup>2</sup>, V. E. Cachorro<sup>1</sup>, Ángel M. de Frutos<sup>1</sup>

<sup>1</sup>Grupo de Óptica Atmosférica, Universidad de Valladolid, Paseo Belén 7 47011, Spain

<sup>2</sup>Eratosthenes Center of Excellence, Limassol, Cyprus

Keywords: mineral dust; AERONET; absorbing properties; Saharan and Arabian dust

Presenting author email: mateos@goa.uva.es

The field experiment conducted in Cyprus in April 2017 as part of the A-LIFE (Absorbing aerosol layers in a changing climate: aging, lifetime, and dynamics) project featured the utilization of a diverse set of instruments from various measurement disciplines, both ground-based and airborne and both remote sensing (passive and active) and in-situ techniques. Further details about this experiment were given by Groß et al. (2024).

This study presents the columnar records obtained by sun photometry throughout the experiment. Two sun/sky/lunar photometers, operating within AERONET framework, were strategically positioned at two distinct sites: Pafos and Limassol, which were 40 kilometers apart. Optical and microphysical aerosol properties, derived from direct sun and sky radiance measurements (level 2.0 data), were analyzed to establish an inventory of aerosol event days throughout the experiment, highlighting mineral dust as the predominant type. A total of 12 days out of 35 presented only (or strongly predominant) mineral dust in the atmosphere being 4 days from Saharan desert, 3 days from Arabian desert, and 5 days occurring a mixture of these two types in greater or lesser extent. Mixtures of fine and coarse aerosols occurred in 14 days, but with different intensity regimes.

Identifying dust sources is crucial to assess size distribution and absorption capabilities. Saharan dust comprises smaller and less absorbing particles compared to Arabian dust. The columnar volume efficiency factor, established through a linear fit between aerosol optical depth and total volume concentration, emerged as a dependable proxy for identifying dust origin, as Arabian and Saharan dusts exhibited distinct slopes: 1.28 and 1.68  $\mu\text{m}^2/\mu\text{m}^3$ , respectively. The study also addressed the role of mixtures, both comprising mineral dust from various sources and consisting of fine and coarse aerosols concurrently. Results indicated that cases involving mixtures of mineral dust were primarily influenced by Arabian dust, whereas for other types of mixtures, there was no clear evidence regarding dust origin. Moreover, there were no distinct indications of black carbon-rich aerosols throughout the column, as absorption Ångström exponent values ranged between 1.6 and 3 for the different aerosol categories identified via sun photometry.

This work was supported by the Ministerio de Ciencia e Innovación (MICINN), with the grant no. PID2021-127588OB-I00. This work is part of the project TED2021-131211B-I00375 funded by MCIN/AEI/10.13039/501100011033 and European Union, "NextGenerationEU"/PRTR. The A-LIFE field experiment was mainly funded by an ERC Starting Grant (A-LIFE) with support of the Deutsches Zentrum für Luft- und Raumfahrt (DLR). The authors acknowledge the support of the Spanish Ministry for Science and Innovation to ACTRIS ERIC.

Groß, S., et al (2024). Characterization of aerosol over the Eastern Mediterranean by polarization sensitive Raman lidar measurements during A-LIFE – aerosol type classification and type separation, EGUsphere [preprint], <https://doi.org/10.5194/egusphere-2024-140>.

## CARBONACEOUS FINE AEROSOL IN AN URBAN-INDUSTRIAL SITE NEAR LISBON, BEFORE AND AFTER THE COVID-19 LOCKDOWN

C. Gamelas<sup>1,2\*</sup>, N. Canha<sup>1,3</sup>, S.M. Almeida<sup>1</sup>, A. Vicente<sup>4</sup>, C. Alves<sup>4</sup>, Z. Kertesz<sup>5</sup>, M.R. Guascito<sup>6,7</sup>, E. Merico<sup>7</sup>, D. Contini<sup>7</sup>

<sup>1</sup>Centro de Ciências e Tecnologias Nucleares (C<sub>2</sub>TN), Instituto Superior Técnico, Universidade de Lisboa, 2695-066 Bobadela, Portugal,

<sup>2</sup>Instituto Politécnico de Setúbal (IPS), Escola Superior de Tecnologia de Setúbal, 2914-508 Setúbal, Portugal

<sup>3</sup>Hylab - Green Hydrogen Collaborative Laboratory, Estrada Nacional 120-1 Central Termoelétrica, Sines 7520-089, Portugal

<sup>4</sup>CESAM—Centre for Environmental and Marine Studies, University of Aveiro, 3810-193 Aveiro, Portugal

<sup>5</sup>Laboratory for Heritage Science, Institute for Nuclear Research, Debrecen, Hungary

<sup>6</sup>Department of Environmental and Biological Sciences and Technologies (DISTEBA), University of Salento, Lecce 73100, Italy

<sup>7</sup>Institute of Atmospheric Sciences and Climate, ISAC-CNR, Str. Prv. Lecce-Monteroni km 1.2, 73100 Lecce, Italy

Keywords: particulate matter, organic carbon, elemental carbon, secondary organic carbon, fossil fuel

Presenting author email: carla.gamelas@ctn.tecnico.ulisboa.pt

Carbonaceous aerosols, including elemental carbon (EC) and organic carbon (OC), have significant effects on the global climate and human health (Paisi et al., 2024). EC results from the incomplete combustion of biomass and fossil fuels. OC includes primary organic carbon (POC), directly emitted from natural and anthropogenic sources, and secondary organic carbon (SOC), formed through photochemical reactions.

Seixal municipality comprises an industrial park and is crossed by highways with intense commuting traffic to Lisbon. Previously, PM<sub>2.5</sub> was chemically characterized (by PIXE and ion chromatography) and source apportionment was performed (Gamelas et al., 2023). Here we aim to study for the first time the source of carbonaceous aerosols in this urban-industrial site, before and after the COVID-19 lockdown.

PM<sub>2.5</sub> samples were collected in 128 sampling days, in winter (December 2019-March 2020), summer (June-August 2020) and autumn (September-November 2020), spanning from the pre-pandemic to the pandemic context. OC and EC were determined in each sampled quartz filter, using a carbon analyzer (Sunset Laboratory Inc., USA) and the EUSAAR2 protocol (Cavalli et al., 2010).

A chemical mass balance was performed, including the contributions of organic matter, elemental matter, non-sea salt sulfate, mineral dust, sea salt, NO<sub>3</sub><sup>-</sup>, NH<sub>4</sub><sup>+</sup>, trace elements, to the PM<sub>2.5</sub> mass.

The mean concentrations of PM<sub>2.5</sub>, OC and EC are presented in Table 1. OC, EC and total carbonaceous aerosol (TCA) contributed on average 21.4%, 6.3% and 44.7% to PM<sub>2.5</sub> concentrations, respectively.

Table 1. Mean concentrations (± s.d.) of OC, EC and OC/EC.

Month	PM <sub>2.5</sub> (µg.m <sup>-3</sup> )	OC (µg/m <sup>3</sup> )	EC (µg/m <sup>3</sup> )	OC/EC
<b>Pre-confinement</b>				
Winter	17.3±14.2	4.8±7.2	1.2±1.4	3.7±1.4
<b>Post-confinement</b>				
Summer	9.3±5.2	1.8±1.2	0.4±0.3	4.5±1.5
Autumn	9.3±6.8	2.3±1.9	0.8±0.7	3.3±1.2
<b>Whole period</b>	12.6±10.9	3.2±4.9	0.8±1.0	3.8±1.4

From the pre- to the post-confinement period, there was a reduction of 46.1% in PM<sub>2.5</sub>, 57.3% in OC and 50.6% in EC, attributed to the impact of the pandemic and

seasonality. The mean OC/EC ratio for the whole period ( $3.8 \pm 1.4$ ) suggests that the study area was mainly affected by fossil fuel combustion and vehicle emissions (Salameh et al., 2015). A strong positive correlation ( $r^2=0.80$ ) was found between EC and OC in the whole period (Fig. 1), demonstrating common sources of emission. SOC was estimated using the EC tracer method (Turpin and Huntzicker, 1995):

$$\text{SOC} = \text{OC} - \text{POC} = \text{OC} - \text{EC} \times (\text{OC}/\text{EC})_{\text{primary}}$$

where  $(\text{OC}/\text{EC})_{\text{primary}}$  is the observed minimum ratio value. The mean SOC concentration during the whole sampling period was  $1.78 \pm 3.40 \mu\text{g.m}^{-3}$ , accounting for 50.4% of OC.

This study shows the relevance of organic matter, namely of secondary origin, in the fine aerosol in Seixal, data that must be taken into consideration when proposing more effective local air pollution control measures.

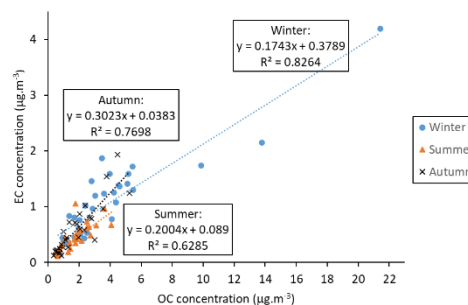


Fig. 1. Relation between OC and EC.

FCT is acknowledged for PTDC/CTAAMB/3263/2021, 2021.00088.CEECIND and UIDB/04349/2020+UIDP/04349/2020.

Paisi N., et al. (2024) *Sci. Reports* 14, 1530.

Gamelas C., et al. (2023) *Urban Clim.* 49, 101446.

Cavalli F., et al. (2010) *Atmos. Meas. Tech.* 3, 79.

Salameh D., et al. (2015) *Atmos. Res.* 155, 102.

Turpin B., Huntzicker J. (1995) *Atmos. Environ.* 29, 3527.

## SOURCE APPORTIONMENT OF PM<sub>2.5</sub> AT MULTIPLE SITES IN ALGERIA

Yago Alonso Cipoli<sup>1,2,3\*</sup>, Sidali Khedidji<sup>4,5</sup>, Selma Said<sup>4</sup>, Célia Alves<sup>1\*</sup>

<sup>1</sup>Centre for Environmental and Marine Studies (CESAM), Department of Environment, University of Aveiro, 3810-193 Aveiro, Portugal

<sup>2</sup>Centro de Investigação de Montanha (CIMO), Instituto Politécnico de Bragança, 5300-253, Bragança, Portugal

<sup>3</sup>Laboratório Associado para a Sustentabilidade e Tecnologia em Regiões de Montanha (SusTEC), Instituto Politécnico de Bragança, 5300-253, Bragança, Portugal

<sup>4</sup>Departments of Chemistry, University of Akli Mohand Oulhadj, Bouira, 10000, Algeria

<sup>5</sup>Faculty of Chemistry, University of Sciences and Technology Houari Boumediene (USTHB), BP 32 El-Alia, Bab-Ezzouar, 16111, Algiers, Algeria

Keywords: PM<sub>2.5</sub>, PMF, Algeria

Presenting author email: celia.alves@ua.pt

Air pollution in African countries varies widely due to diverse geographical, economic, and industrial factors. In Algeria, several studies have been conducted to characterise the chemical composition of particulate matter (PM) (Yassaa et al. 1999; Terrouche et al. 2016; Talbi et al. 2018; Khedidji et al., 2020). Characterising in detail the PM chemical composition and source contributions is an essential prerequisite for implementing effective regulations and policies to reduce the particulate pollution levels. Positive matrix factorisation (PMF) is the most widely used multivariate receptor model to estimate the contributions of emission sources. With the aim of chemically characterising PM<sub>2.5</sub> and applying PMF, a medium-volume sampler (DDA-PLOB-PD) was equipped with a PM<sub>2.5</sub> size-selective inlet using 47 mm quartz filters (Munktel, Sweden) at five locations in Algeria: University of Bouira, Tikjda forest, suburban park Errich in Bouira, bus station (transportation services) and surroundings of a cement plant in Bouira region. Sampling was carried out for 24-h over 10-20 days in each site. PM<sub>2.5</sub> samples were analysed for organic and elemental carbon (OC and EC) by a thermo-optical transmission system, elements using total reflection X-ray fluorescence spectroscopy (TXRF) and organic compounds by CPP-GC/MS. After careful inspection of the dataset, 65 samples and 35 species were selected to run the PMF model. The 7-factors solution showed very good agreement between the predicted and the measured PM<sub>2.5</sub> ( $r^2 = 0.98$  and slope of 0.94). The chemical profiles and their contributions to the PMF solution are detailed in Fig. 1.

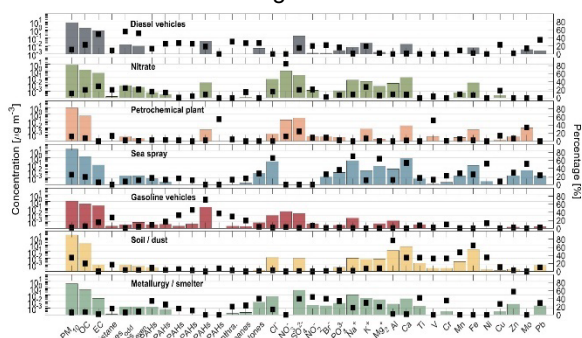


Fig. 1. Profiles for seven sources identified using PMF.

Source contributions to PM<sub>2.5</sub> were as follows: soil / dust (34%) > sea spray (24%) > petrochemical plant (12%) > diesel vehicles (11%) > nitrate (11%) > metallurgy / smelter (6%) > gasoline vehicles (2%). The vehicle emissions profile was characterised by n-alkanes, EC, PAHs and Pb. The profile named as petrochemical plant presented high loading for 7-ring PAHs, V and Mo, while the metallurgical/smelter profile showed a great contribution from Ti, Cu, Cr, and Zn. The soil/dust had high loadings of crustal elements such as Al, Ca, Cr, Mn, and Fe, while the sea spray factor presented the typical ions Na<sup>+</sup>, Cl<sup>-</sup> and Mg<sup>+</sup>. These results show a significant contribution from anthropogenic sources to PM<sub>2.5</sub>, which can be potentially harmful to the population health.

An acknowledgement is given to FCT for its support through national funds FCT/MCTES (PIDDAC) to CIMO (UIDB/00690/2020 and UIDP/00690/2020), SusTEC (LAP/0007/2020), CESAM (UIDP/50017/2020 + UIDB/50017/2020 + LAP/0094/2020) and Cipoli's PhD scholarship (SFRH/BD/04992/2021). This work was developed within APAM, a project supported by national funds (OE), through FCT/MCTES (<https://doi.org/10.54499/2022.04240.PTDC>).

Yassaa N., Meklati B. Y., Cecinato A. (1999) Analysis of volatile organic compounds in the ambient air of Algiers by gas chromatography with a  $\beta$ -cyclodextrin capillary column. *J Chromatogr A* 846:287-293.

Talbi A., et al. (2018). Assessment of annual air pollution levels with PM<sub>1</sub>, PM<sub>2.5</sub>, PM<sub>10</sub> and associated heavy metals in Algiers, Algeria. *Environ Pollut* 232:252–263.

Terrouche A., et al. (2016). Identification of sources of atmospheric particulate matter and trace metals in Constantine, Algeria. *Air Qual Atmos Heal* 9:69–82.

Khedidji S., et al. (2020). Chemical Characterization of Marine Aerosols in a South Mediterranean Coastal Area Located in Bou Ismail, Algeria. *Aerosol Air Qual Res* 20:2448-2473.

## FINE AEROSOL EUROPEAN OVERVIEW IN THE FRAME OF RI-URBANS

M. Via<sup>1</sup>, B. Chazeau<sup>2</sup>, A. Prévôt<sup>3</sup>, X. Querol<sup>3</sup>, K. R. Daellenbach<sup>2</sup>, and A. Alastuey<sup>3</sup> and the RI-Urbans team

<sup>1</sup>Centre for Atmospheric Research, University of Nova Gorica, Ajdovščina, 5270, Slovenia

<sup>2</sup>Paul Scherrer Institute, Villigen, Switzerland 5232

<sup>3</sup>Institute of Environmental Assessment and Water Research, Barcelona, 08034, Spain

Keywords: NR-PM<sub>1</sub>, organic aerosol, source apportionment

Presenting author email: martaviagonzalez@gmail.com

There is ample evidence that Particulate Matter (PM) negatively impacts both the climate and human health (Shrivastava et al. 2019, WHO, 2021a), however, the effects are different depending on PM composition and origin. The recognition that the epidemiological and toxicological consequences depend more on PM composition than on PM levels was a turning step in the prior paradigm of measuring PM effects on health (Daellenbach et al., 2024). Likewise, climate effects, mainly driven by the modification of the atmospheric scattering and absorption capability, are compound and source-dependent (Laj et al., 2020). For these reasons, monitoring PM composition and origin is of crucial interest for climate and human health effects prevention.

PM can both be measured through offline and online, this is, with or without a time lag between sampling and concentration determination, respectively. Online PM measurements usually provide higher time resolution and/or time span measurements. Hence, online instrumentation is regarded as more suitable for impact assessment, especially for source-based studies. Source apportionment of the organic aerosol (OA), the major non-refractory PM<sub>1</sub> (NR-PM<sub>1</sub>) component, has been performed from the release of the first online spectrometry instruments, and European overviews have been already published (Chen et al. 2022).

The objective of this work is the extension of the intercomparison including more sites and for a longer period. The intercomparison of the NR-PM<sub>1</sub> compounds has included data ranging from 2009 to 2023 provided by air quality monitoring networks (such as those from ACTRIS) to RI-URBANS, including urban background, regional background, traffic, rural, suburban, coastal, mountain, and arctic sites. Instrumentation used for such measurements are the quadrupole (Q) or the time of flight (ToF) aerosol chemical speciation monitor (ACSM), or aerosol mass spectrometers, with Capture ToF or Q standard vaporisers depending on the size (PM<sub>2.5</sub>, PM<sub>1</sub>, respectively).

Preliminary results show that the mean NR-PM<sub>1</sub> concentration at these sites was  $(10.67 \pm 6.9) \mu\text{g}\cdot\text{m}^{-3}$  and that suburban sites present the highest concentrations in average. The region of higher concentrations is the Po Valley, due to the frequent stagnation episodes given the orographic situation. In the broader European frame, it has been found that the

majority of the high-concentration episodes happen during winter stagnation conditions.

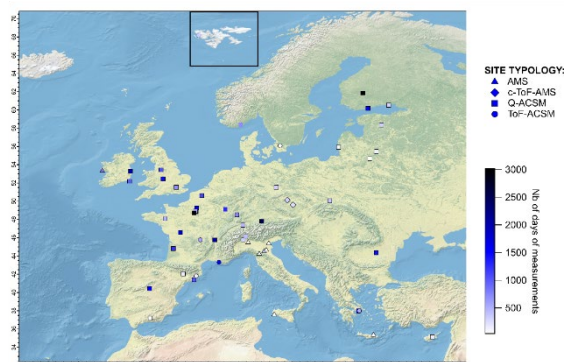


Fig. 1. Location of the sites participating in the European intercomparison coloured by the number of days of measurements and marker-coded by the instrument used for measurement.

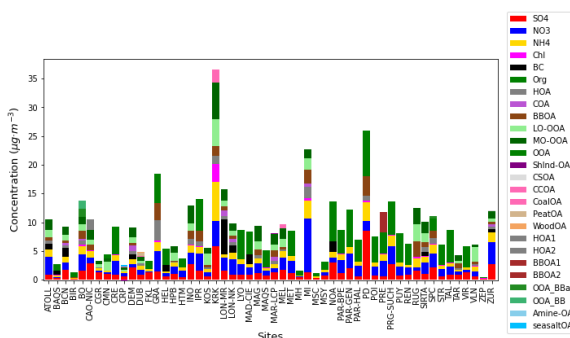


Fig. 2. Non-normalised concentration of the NR-PM<sub>1</sub> compounds and OA sources per all sites.

This work was supported by the European Union's Horizon 2020 research and innovation programme (101036245, RI-URBANS).

Chen, G., et al. (2022). *Environment international*, 166, 107325.

Daellenbach, K. R., et al, (2020). *Nature*, 587(7834), 414-419.

Laj, P. *Atmospheric Measurement Techniques*, 13(8), 4353-4392.

Srivastava, D., et al. *Science of The Total Environment* 690 (2019): 944-955.

WHO global air quality guidelines. World Health Organization; 2021.

## SPATIO-TEMPORAL DISTRIBUTION OF PM<sub>2.5</sub> EMISSIONS IN MOZAMBIQUE

F.A. Júnior<sup>1</sup>, M. Machanguana<sup>1</sup>, S. Chilaulé<sup>1</sup> and M.C. Marques<sup>1,2</sup>

<sup>1</sup> School of Life and Environmental Sciences (ECVA), University of Trás-os-Montes e Alto Douro (UTAD), Quinta de Prados, 5000-801 Vila Real, Portugal

<sup>2</sup> Centre for the Research and Technology of Agro-Environmental and Biological Sciences (CITAB), UTAD, Quinta de Prados, 5000-801 Vila Real, Portugal

Keywords: Africa, air pollution, emission source, COVID-19 pandemic

Presenting author email: mcm@utad.pt

In 2019, around 4.14 million premature deaths were attributed to fine particulate air pollution (PM<sub>2.5</sub>), 91% of which occurred in low- and middle-income countries (Health Effects Institute, 2020). Air pollution in Africa remains understudied despite its significant impact on human health (Kirago *et al.*, 2022). In Mozambique, it was estimated that 95% of the population used unclean fuels for cooking, in 2010, and that the result of household air pollution is responsible for approximately 18,000 premature deaths, in 2015 (Forouzanfar *et al.*, 2016). The aim of this study was to assess the spatio-temporal variation of PM<sub>2.5</sub> concentrations in Mozambique, using satellite images, in the period between 2019 and 2023 (before, during and after the COVID-19 pandemic).

Mozambique has an area of 799,380 km<sup>2</sup> and is located in the south-eastern region of Africa. It is bordered to the north by Tanzania; to the west by Malawi, Zambia, Zimbabwe and Swaziland; and to the south by South Africa. To the east, it is bathed by the Indian Ocean. Satellite data was obtained from the Giovanni application, provided by the Goddard Earth Sciences (GES) Data and Information Services Centre (DISC) (<http://disc.sci.gsfc.nasa.gov/giovanni>). The Merra-2 reanalysis was selected and the temporal resolution of 2019-2023 and spatial resolution of 0.5 x 0.625° were defined.

Figure 1 shows the spatio-temporal distribution of PM<sub>2.5</sub> emissions in Mozambique. It can be seen that during the period under analysis there was a notable increase in PM<sub>2.5</sub> pollution throughout most of the country, especially in the central region. It should be noted that this region has the highest mining activity in Mozambique, as well as being the most affected by extreme events (e.g. Cyclone Idai in 2019). Other sources of PM<sub>2.5</sub> in Mozambique are related to: i) climatic conditions; ii) burning biomass and coal as fuel; iii) frequent use of old vehicles; iv) uncontrolled industrial emissions. These results are corroborated by research by Kalisa *et al.* (2023) into the main sources of PM<sub>2.5</sub> emissions in Africa. It should be noted that during the COVID-19 pandemic, PM<sub>2.5</sub> emissions intensified. It is plausible that this is due, on the one hand, to the fact that industries in Mozambique did not close during the pandemic and, on the other, to the common practice of incinerating household waste. After the pandemic, there was a reduction in emissions in the northern region compared to the central and southern regions of the country, which may also be a

consequence of the ongoing conflict, which has led to population mobility and the closure of extractive industries.

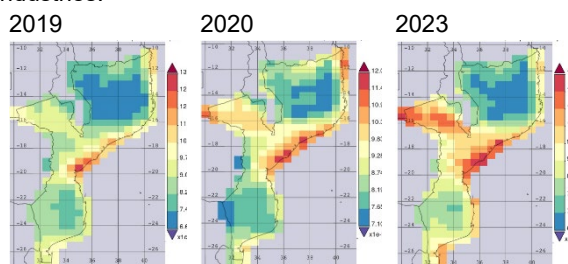


Figure 1: Spatio-temporal evolution of PM<sub>2.5</sub> emissions in Mozambique.

PM<sub>2.5</sub> pollution in Mozambique, despite its significant impact on human health and the regional climate, continues to be ignored. A significant increase in pollution has been observed, especially in the central region of the country, attributed to industrial activities, the burning of biomass and coal, local climatic conditions and the use of old vehicles.

This work is financially supported by National Funds through FCT - Portuguese Foundation for Science and Technology, under the project UIDB/04033/2020.

Forouzanfar, H. *et al.* (2016) Global, regional, and national comparative risk assessment of 79 behavioural, environmental and occupational, and metabolic risks or clusters of risks, 1990–2015: a systematic analysis for the Global Burden of Disease Study 2015. *The Lancet*, 388(10053), 1659-1724, [https://doi.org/10.1016/S0140-6736\(16\)31679-8](https://doi.org/10.1016/S0140-6736(16)31679-8)

Health Effects Institute (2020) *State of Global Air 2020*. Special Report, Boston.

Kalisa, W., Zhang, J., Igabawua, T., Henchiri, M., Mulinga, N., Nibagwire, D., Umuhoza, M. (2023) Spatial and temporal heterogeneity of air pollution in East Africa. *Science of The Total Environment*, 886, <http://dx.doi.org/10.1016/j.scitotenv.2023.163734>.

Kirago, L., Gatari, M.J., Gustafsson, O., Andersson, A. (2022) Black carbon emissions from traffic contribute substantially to air pollution in Nairobi, Kenya. *Commun Earth Environ*, 3, 74, <https://doi.org/10.1038/s43247-022-00400-1>.

## EVOLUTION OF THE NUMBER OF NUCLEATION EVENTS IN AN URBAN BACKGROUND SITE

F.J. Gómez-Moreno, E. Alonso-Blanco, P. Mediavilla and M. Pujadas  
Department of Environment, CIEMAT, 28040 Madrid, Spain

Keywords: Atmospheric aerosol, Particle nucleation, New particle formation

Presenting author email: fj.gomez@ciemat.es

New particle formation (NPF) in the atmosphere is one of their main generation mechanisms and, at the same time, the least understood process related to the presence and distribution of aerosols. It is characterized by a sudden burst of high concentrations of nanometer particles followed by their growth. Kulmala et al. (2004) determined that NPF (nucleation) via gas-to-particle conversion is the largest global source of atmospheric particles (in number) and it is thought to contribute up to a half of the global Cloud Condensation Nuclei (CCN) inventory (Yu et al. 2009). CIEMAT site (40° 27' 23.49' N and 3° 43' 31.77' W, ~650 m a.s.l.) has been operating for more than 15 years and is focused on the characterization of particles and gaseous pollutants in Madrid. This site is located approximately 9 km north northwest of the Madrid city centre, being considered a priori a representative urban background site (UB), as it is not directly affected by any local pollution source. The particle size distribution is measured by a TSI SMPS (DMA3081+CPC3775), which belongs to the ACTRIS European Network ([www.actris.eu](http://www.actris.eu)). Other variables are also measured, including other particle properties, pollutant gas concentrations and meteorology parameters.

NPF is a frequent phenomenon in Madrid. Gómez-Moreno et al. (2011) carried out a detailed study for two years of data (2005-2006) for the first time in Madrid. In most recent studies at this site, in addition to identifying frequent NPF events, associated shrinkages were observed (Alonso-Blanco et al., 2017), both occurring at the regional level in the Madrid basin (Carnerero et al., 2018). These findings make Madrid an exceptional site for the NPF study as highlighted by Garcia-Marlès et al (2024). To this end, this work aims to extend the atmospheric NPF study to the period 2007-2020, completing previous studies at the site. Thus, attending to the characteristics of each case, it is possible to classify the NPF events into three classes: Ia, Ib and II according to Dal Maso et al. (2005). In Class Ia, the typical banana shape is clearly visible. In Class Ib, the banana shape is not clear, but the particle growth can be observed. Finally, Class II corresponds to a situation in which particle growth determination is not possible. The main results can be found in Figure 1, including the NPF classification per month. Data for August were not available. The event number shows a slight decrease over time, although in an irregular way. Most of the events correspond with class I, and very few with class II. Class Ia events used to occur during spring and summer, when there were biogenic emissions and high photochemical activity. They were mainly characterized

by starting at noon, when the insolation is highest, there was a low wind speed and air masses came from sparsely populated areas, mainly parks and forests. These air masses together with those from the urban area produced a mix of conditions with high BVOC and AVOC concentrations, which can participate in the NPF events and the particle growth (Gómez-Moreno et al., 2022).

Class Ib events occurred during all the year, although in winter they had a low frequency. The oscillations in the wind speed and that the wind direction was rotating in the typical clockwise sense from northeast to west could be the reason why a complete banana-shaped growth was not observed.

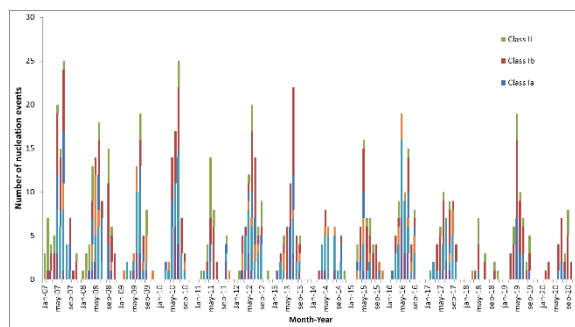


Fig. 1. Temporal evolution of the number of NPF events. It includes the nucleation classification per month.

This research has been partially funded by the OASIS project (PID2021-127885OB-I00 fund by MCIN/AEI/10.13039/501100011033 and by 'ERDF A way of making Europe')

Alonso-Blanco et al (2017) *Atmos. Environ.* 160, 154.  
Carnerero et al (2018) *Atmos. Chem. Phys.* 18, 16601.  
Dal Maso et al. (2005) *Boreal Environ. Res.* 10, 323.  
Garcia-Marlès et al (2024) *Environ. Inter.* In Press, Corrected Proof, Available online 16 February 2024.  
Gómez-Moreno et al (2011) *Atmos. Environ.* 45, 3169.  
Gómez-Moreno et al. (2022) *Environ. Res. Commun*, 4, 125010.  
Kulmala et al. (2004) *J. Aerosol Sci.* 35, 143.  
Yu et al. (2009) *J. Geophys. Res.* 114, D10206.

## NUCLEATION AND ULTRAFINE PARTICLES OBSERVED DURING THE 2021 VOLCANIC ERUPTION IN LA PALMA ISLAND

J. López Darias<sup>1</sup>, S. Rodríguez<sup>1</sup>, I. Belbachir<sup>1</sup>, J. Vilches<sup>2</sup>, J.H. Ayala<sup>3</sup>, M.I. García Álvarez<sup>1</sup>, Gorka Villena<sup>1</sup>, J. de la Rosa<sup>4</sup>, T. Boulesteix<sup>1</sup>, N. Taquet<sup>1</sup>, Y. González<sup>5,6</sup>, Á. Barreto<sup>6</sup>, A.M. Sánchez de la Campa<sup>4</sup> y C.J. Torres<sup>6</sup>

<sup>1</sup>Consejo Superior de Investigaciones Científicas, IPNA CSIC, La Laguna, Tenerife, 38206, Spain

<sup>2</sup>Consejería de Transición Ecológica y Energía, Gobierno de Canarias, Las Palmas de Gran Canaria, Spain

<sup>3</sup>Department of Chemistry, University of La Laguna, E38206, Tenerife, Spain

<sup>4</sup>Centre for Research in Sustainable Chemistry - CIQSO, University of Huelva, E21071 Huelva, Spain

<sup>5</sup>Scientific department, CIMEL Electronique, Paris, 75011, France

<sup>6</sup>Izaña Atmospheric Research Center, Santa Cruz de Tenerife, Spain

Keywords: volcanic aerosols, nucleation, condensation, sulphuric acid

Presenting author email: j.lopez.darias@csic.es

Volcanoes are a natural component of the Earth System that release huge amounts of gases and aerosols that influence on climate and ecosystem. Eruptions near populated areas also represent a threat to human health due to the poor air quality conditions linked to the presence of harmful gases, aerosols and ashes. We present a study on nucleation and ultrafine particles during the 2021 volcanic eruption of Tajogaite volcano, which occurred from 19 September to 13 December 2021 in La Palma, the Canary Islands.

At La Palma Island we performed a continuous monitoring (28 Sep 2021 to 11 Apr 2022) of the particle size distribution (10-400nm) by using a TSI SMPS NanoScan Sizer 3910 at two sites: Los Llanos de Aridane (28 Sep 2021 to 19 Jan 2022) and El Paso (19 Jan to 11 Apr 2022). At Los Llanos we also monitored black carbon (AE33 aethalometer Magee), SO<sub>2</sub>, NO<sub>x</sub>, PM<sub>10</sub>, PM<sub>2.5</sub> and studied the chemical size distribution of aerosols with a DEKATI cascade impactor and subsequent laboratory analysis. At Izaña Observatory (Tenerife Island) we also performed a continuous monitoring of the particle size distribution by using a TSI SMPS 3080 connected to a 3772 CPC and number concentrations with a 3010 and 30776 CPCs.

At La Palma, the particle number concentration (N)(10-400 nm) showed a high variability: low background levels ( $< 10^3 \text{ cm}^{-3}$ ) alternated with extremely high concentrations within the range (1h averages) 20-100·10<sup>3</sup> cm<sup>-3</sup>. During the 5 first weeks of eruption, the advance of the volcanic coladas over the towns and banana crop cultivations caused fires that prompted high concentrations of black carbon and of 50-120 nm particles (up to 60·10<sup>3</sup> cm<sup>-3</sup>). The concentration of 10-20 nm particles remained low during the first 6 weeks of eruption, subsequently it experienced an important increase (with values of up to 30 – 100 ·10<sup>3</sup> cm<sup>-3</sup>) associated with high SO<sub>2</sub> concentrations near ground due to the loose of the ejection for of the eruption which resulted in SO<sub>2</sub> plumes near ground (Milford et al., 2023).

The cascade impactor samples shows that the ultrafine particles mass is dominated by sulphuric acid, sulphate, chloride and tephra linked to the volcanic sulphuric and hydrochloric acids and nano-tephra particles. During no nucleation periods the particle size distribution tend to

show a predominant mode at about 100 nm, a feature observed in La Palma and at Izaña Observatory (Tenerife) during the impacts of the volcanic plume. After the end of the eruption, SO<sub>2</sub> and the particle number concentration experience a rapid decrease and showed clear evidences of being associated with vehicle exhaust emissions.

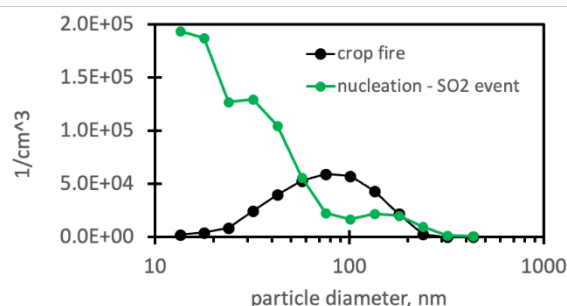


Figure 1. Particle size distribution at Los Llanos de Aridane during a nucleation & SO<sub>2</sub> event and during the fire event due to the advance of the coladas over the crops.

The project AEROEXTREME (PID2021-125669NB-I00) is funded by the State Research Agency of Spain, the Ministry of Science, Innovation and Universities of Spain and the European Regional Development Fund.

Milford et al., 2023. Impact of the 2021 La Palma volcanic eruption on air quality: Insights from a multidisciplinary approach. STOTEN 869, 161652.

## INTERCOMPARISON BETWEEN A LOW-COST MICROSTATION AND REFERENCE EQUIPMENT

A.V. Silva<sup>1,2</sup>, Y.A. Cipoli<sup>1,2</sup>, L.C. Furst<sup>1,2</sup>, M.J.S. Feliciano<sup>2</sup>, C.A. Alves<sup>1</sup>

<sup>1</sup>Department of Environment and Planning, CESAM — Centre for Environmental and Marine Studies, University of Aveiro, 3810-193 Aveiro, Portugal

<sup>2</sup>Higher Agricultural School, CIMO – Mountain Research Centre, Polytechnic University of Bragança, Bragança, 5300-253, Portugal

Keywords: Optical Sensor, Gravimetric Method, Beta Attenuation

Presenting author email: celia.alves@ua.pt

The Gravimetric Method (GM) for Particulate Matter (PM) monitoring has been the reference in Europe for over a decade (CEN, 2014). However, high cost, complexity, and limitations of Reference-Grade Equipment (RGE) hinder real-time and spatial monitoring, requiring parallel methods for short response times. This has spurred the development of low-cost sensors (LCS), which offer potential solutions for these limitations, though concerns about their reliability and accuracy remain (Chojer et al., 2020). Therefore, this study assesses a BettAir<sup>®</sup> Low-Cost MicroStation (LCMS), which uses electrochemical sensors for multi-pollutant air monitoring and a sensor based on an Optical Method (OM) for PM monitoring. The study compares LCMS against RGEs: Tecora<sup>®</sup> EchoPM (TCR) and AMS<sup>®</sup> High-Volume Sampler (HVS) that use GM, DURAG<sup>®</sup> Verewa F-701 (BM) that uses the Beta Radiation Attenuation Method (BRAM), and TSI<sup>®</sup> DustTrak (DT) and OPS 3330 both based on OM. Sample collection was conducted in two distinct locations: Luanda, the capital of Angola, a megacity with lack of air quality research, and a smaller city in inland Portugal, offering varied urban contexts for sensor assessment. In Portugal, the assessment utilized only the TSI<sup>®</sup> OPS device, whereas in Angola, all equipment were used, except TSI<sup>®</sup> OPS. Python was used for data processing, including the Coefficient of Determination ( $R^2$ ), Pearson Correlation Coefficient ( $r$ ), Root Mean Square Error (RMSE), Linear Regression and Bland-Altman plots. The PM<sub>10</sub> daily results showed that the LCMS exhibited strong linear correlation ( $r > 0.79$ , RMSE 55.1  $\mu\text{g}/\text{m}^3$ ) with GM (TCR and HVS), slightly less than with the DT ( $r > 0.88$ , RMSE=27.2  $\mu\text{g}/\text{m}^3$ ), but with higher RMSE values. For PM<sub>2.5</sub> LCMS had a weaker linear correlation but reasonable daily mean agreement with TCR ( $r=0.64$ , RMSE=21.6  $\mu\text{g}/\text{m}^3$ ) and a slightly stronger correlation with BM ( $r=0.74$ , RMSE=12.6  $\mu\text{g}/\text{m}^3$ ). LCMS also showed a strong correlation with DT ( $r=0.93$ ), despite a high RMSE (80.7  $\mu\text{g}/\text{m}^3$ ). It showed slightly higher correlation with BM ( $r=0.74$ , RMSE=12.6  $\mu\text{g}/\text{m}^3$ ), while BM had the best match with TCR. LCMS also demonstrated strong linear correlation with DT, despite notable RMSE differences ( $r=0.93$  and RMSE=80.7  $\mu\text{g}/\text{m}^3$ ). The hourly values of LCMS correlated well with DT across all sizes ( $r > 0.90$ ) and less with OPS ( $r > 0.65$ ), despite varied RMSE scales (with DT 75.3–85.7  $\mu\text{g}/\text{m}^3$  and OPS 0.9–2.0  $\mu\text{g}/\text{m}^3$ ). The study suggests

systematic biases in OM's values, although the daily means present reasonable agreement. In contrast, such systematic errors were not observed among LCMS, TCR and BM for PM<sub>2.5</sub>. Therefore, the LCMS presents reliable performance compared to OM equipment on the market, especially for PM<sub>2.5</sub>, showing even better correlations than the DT.

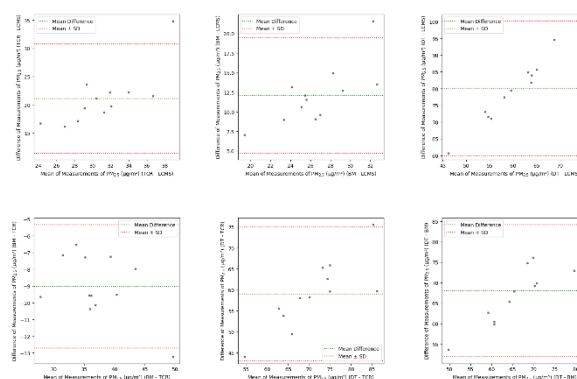


Fig. 1. Bland-Altman analysis of PM<sub>2.5</sub> monitoring data of equipment with different operation principles.

This work was supported by the Portuguese Foundation for Science and Technology (FCT) through the PhD fellowships 2023.02059.BD, SFRH/BD/04992/2021 and SFRH/BD/08461/2020. The research was performed in the frame of the project APAM, financially supported by national funds (OE), through FCT/MCTES (DOI: 10.54499/2022.04240.PTDC). The financial support to CESAM by FCT/MCTES (UIDP/50017/2020+UIDB/50017/2020+LA/P/0094/2020), through national funds, is acknowledged.

CEN (2014). *Ambient air - Standard gravimetric measurement method for the determination of the PM<sub>10</sub> or PM<sub>2.5</sub> mass concentration of suspended particulate matter*. EN 12341:2014, Brussels, Belgium.

Chojer H., Branco P. T.B.S., Martins F. G., Alvim-Ferraz M. C.M., Sousa S. I.V. (2020) Development of low-cost indoor air quality monitoring devices: Recent advancements. *Science of the Total Environment*, 727.

## ATMOSPHERIC MONITORING WITH A HIGH-PERFORMANCE RAMAN LIDAR: ALHAMBRA

S. Fernández-Carvelo<sup>1,2</sup>, J.A. Bravo-Aranda<sup>1,2</sup>, A. del Águila<sup>1,2</sup>, A. Díaz-Zurita<sup>1,2</sup>, A. Casans<sup>1,2</sup>, J.L. Guerrero-Rascado<sup>1,2</sup>, M.J. Granados-Muñoz<sup>1,2</sup>, F. Navas-Guzmán<sup>1,2</sup>, D. Pérez-Ramírez<sup>1,2</sup> and L. Alados-Arboledas<sup>1,2</sup>

<sup>1</sup>Andalusian Institute for Earth System Research (IISTA), University of Granada, Granada, 18006, Spain

<sup>2</sup>Department of Applied Physics, University of Granada, Granada, 18071, Spain

Keywords: lidar, spectral fluorescence, aerosol typing.

Presenting author email: andreacasans@ugr.es

Aerosol particles significantly influence on the estimation of the atmospheric energy balance, playing a key role in cloud formation and evolution. Obtaining accurate aerosol measurements can be challenging due to the high variability of aerosol characteristics, such as type, concentration, size, and chemical composition, being a key contributor to the primary uncertainty in estimating total radiative forcing. (Quaas et al., 2022).

The ALHAMBRA system, operational at the UGR urban station in Granada, Spain, as part of the AGORA (Andalusian Global Observatory of the Atmosphere) ACTRIS National Facility, consists of two sub-systems. The near-field sub-system focuses on the atmospheric boundary layer (ABL) and includes elastic detection at 1064 (1064.2 nm), 532 (532.1 nm), and 355 (354.7 nm), along with N<sub>2</sub> vibrational Raman (VR) detection at 532 (607.4 nm) and 355 (386.7 nm). The far-field sub-system extends to the low stratosphere, covering elastic detection at 1064 (1064.2 nm), 532 (532.1 nm), and 355 (354.7 nm), as well as N<sub>2</sub> rotational Raman (RR) detection at 1064 (1058 nm), 532 (530.2 nm), and 355 (353.9 nm). Each subsystem includes water vapor detection ( $\omega$ ) at 355 (407.5 nm).

The linear particle depolarization ratio ( $\delta$ ) can be determined at 532 and 355 nm, is proven to be valuable for studying atmospheric aerosol and aerosol-cloud interactions (Bravo-Aranda et al., 2013; Granados-Muñoz et al., 2015; Ansmann et al., 2019).

Detecting pure rotational energy states of molecules (RR) extends independent extinction ( $\alpha$ ) and backscattering ( $\beta$ ) profiles to nearly the entire day, overcoming VR limitations and reliably improving signal-to-noise ratio (SNR) (Ortiz-Amezcuca et al., 2020).

The system also integrates fluorescence capabilities ( $\varphi$ ) for both subsystems through two approaches: integrated signal detection in the 420-520 nm range using a broadband interferential filter (Veselovskii et al., 2022) and spectral signal detection via optical fiber to a HORIBA 1250M imaging spectrometer (Tatarov et al., 2021; Reichardt et al., 2023).

By having the near-field subsystem, the total overlap height can be significantly reduced to approximately 180 metres above ground level, improving characterisation at lower atmospheric levels, where are found the highest concentration of primary biological aerosol particles, such as pollen grains. Figure 1 illustrates an example of range-corrected signal at 532

nm derived from Alhambra once the Canadian wildfire smoke outbreak was detected in Granada on June 27, 2023.

The synergistic combination of  $3\beta+3\alpha+2\delta+\omega+2\varphi$  within the vertical column from the lowermost layers is expected to offer a significant opportunity to enhance the exploration of atmospheric processes.

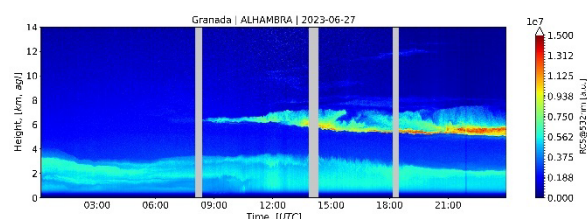


Figure 1. Range-corrected signal at 532nm over the whole day for 27<sup>th</sup> June 2023 at UGR station (AGORA).

This work is part of the Spanish national projects PID2020-120015RB-100, PID2020-117825GB-C21/C22, PID2021-128008OB-100, PID2022-142708NA-100 and Strategic network RED2022-134824-E and infrastructure grants EQC2019-006192-P and EQC2019-006423-P founded by MCIN/AEI /10.13039/501100011033, ATMO-ACCESS grant agreement No 101008004, ACTRIS-IMP grant agreement No 871115, and Scientific Unit of Excellence: Earth System (UCE-PP2017-02). Sol Fernández-Carvelo received funding from the Spanish Ministry of Research and Innovation (Agencia Estatal de Investigación), grant PRE2021-098351 (co-funded by the European Social Fund Plus).

Quaas et al. (2022) *Atmos. Chem. Phys.*, 22, 12221–12239.

Bravo-Aranda, J. A. et al. (2013) *Atmospheric chemistry and physics*, 17(11), 6839–6851.

Granados-Muñoz et al., 2015. *Atmospheric Measurement Techniques*, 8(2), 705–718.

Ansmann et al. (2019) *Atmospheric Measurement Techniques*, 12(9), 4849–4865.

Ortiz-Amezcuca, P. et al (2020) *Optics Express*, 28(6), 8156–8168.

Veselovskii et al. (2022) *Atmos. Meas. Tech.*, 15, 4881–4900.

Tatarov et al., (2021). *Optics Letters*, 46(20), 5173–5176.

Reichardt et al. (2023) *Atmos. Meas. Tech.*, 16, 1–13.

## EVALUATION OF A LOW-COST SENSOR FOR eBC MONITORING IN A SUBURBAN AREA WITH LOW CONCENTRATIONS

M. Fernández-Amado, M. Piñeiro-Iglesias, J. Moreda-Piñeiro, P. López-Mahía and S. Muniategui-Lorenzo  
 Grupo de Química Analítica Aplicada (QANAP), Instituto Universitario de Medio Ambiente (IUMA), Universidade da Coruña, Pazo de Lóngora, Liáns, 15179 A Coruña, Spain

Keywords: equivalent black carbon, low-cost sensors, portable devices  
 Presenting author email: maria.fernandez.amado@udc.es

In recent years, new metrics of emerging concern are being introduced to control air quality, including black carbon (BC, named equivalent black carbon, eBC, when it is derived from optical methods). Due to the health risks associated and its part in climate change, this parameter is included in the draft of the new European Commission Directive on ambient air quality (EC, 2022), and the World Health Organization guidelines recommend its monitoring among good practice statements (WHO, 2021).

For real-time monitoring of eBC, the aethalometer is the most used instrument, but there are as well some portable and low-cost sensors to measure this parameter. Although they do not include artifacts' corrections as sophisticated as the aethalometer nor the measurements at different wavelengths that are further used for source apportionment, low-cost sensors still can be useful in some applications, like for example, to carry out simultaneous measurements in many sampling points.

In this work, monitoring of eBC using an AE33 aethalometer (Magee) has been carried out at the suburban air quality station of IUMA (near to A Coruña city, NW Spain) in Dec 2021-Jul 2023. During approx. 300 days in this period, an ObservAir BC sensor (dst, USA) was also measuring at the same location.

The sampling site is characterised by low levels of pollutants, including eBC (average concentration of 0.67  $\mu\text{g}/\text{m}^3$  in the studied period). The sampling location is in a residential zone, so in the cold period (Sep-Feb) biomass burning for domestic heating increases the levels of eBC. The Sandradewi *et al.* (2008) model has been applied to estimate contributions of biomass (eBCbb) and fossil fuel (eBCff) burning, which confirm a higher prevalence of eBCbb during the cold period (Fig. 1).

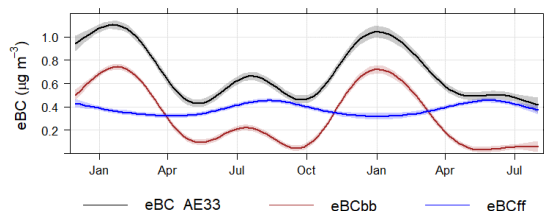


Fig. 1. Smoothed evolution of eBC, eBCff and eBCbb values. Openair package in R was used for data treatment.

A comparison between eBC data (hourly averages) from the aethalometer and the ObservAir sensor shows a relatively good correlation ( $R^2 = 0.74$ ), with slightly

lower values for the sensor when compared to the aethalometer (Fig. 2). Splitting data into warm and cold periods, a much better correlation ( $R^2 = 0.84$ ) is found for the colder seasons, maybe due to the higher values obtained in this period. On the contrary, the warm period shows a poorer correlation ( $R^2 = 0.68$ ).

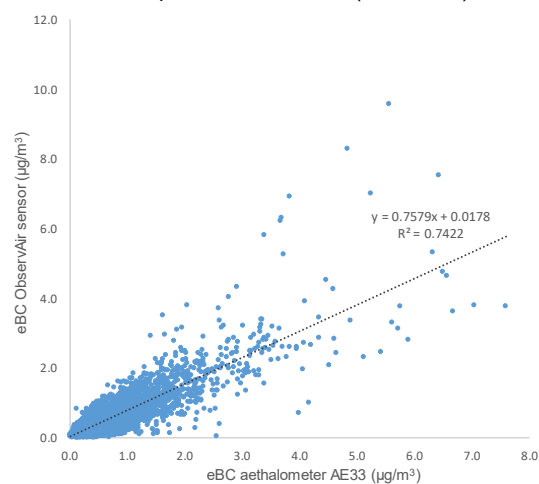


Fig. 2. Correlation between eBC measurements with aethalometer and sensor.

The effect of relative humidity and ATN values (filter loading effect) have also been evaluated, but no significant differences were found. The temporal evolution of eBC concentrations with the two instruments is similar, thus the sensor can be useful to found high level peaks or changes in trends.

This work was supported by FEDER-MINECO-Xunta de Galicia (UNLC15-DE-3097), Xunta de Galicia (GRC2017-28, ED431C2021/56) and MCIU/MCIN-AEI-FEDER (PID2021-125201OB-I00). M. Fernández-Amado appreciates MCIU (PTA2022-021336-I) support. The authors would like to thank P. Esperón.

EC (2022) *Proposal for a Directive of the European Parliament and of the Council on ambient air quality and cleaner air for Europe*, 26.10.2022

Sandradewi J. *et al.* (2008). *Environ. Sci. Technol.*, 42, 3316-3323.

WHO (2021) *WHO global air quality guidelines. Particulate matter (PM<sub>2.5</sub> and PM<sub>10</sub>), ozone, nitrogen dioxide, sulfur dioxide and carbon monoxide*. Geneva: World Health Organization; 2021. Licence: CC BY-NC-SA 3.0 IGO.

## TRENDS OF AIRBORNE POLLEN CONCENTRATIONS IN MADRID (SPAIN) OVER 2001-2020. INFLUENCE OF SYNOPTIC METEOROLOGICAL PATTERNS

P. Salvador<sup>1</sup>, F. Molero<sup>1</sup>, Z. Ferencova<sup>2</sup>, P. Cervigón<sup>2</sup> and A.M. Gutierrez<sup>2</sup>

<sup>1</sup>Department of Environment, CIEMAT, Madrid, 28040, Spain

<sup>2</sup>Departamento de Farmacología, Farmacognosia y Botánica, Facultad de Farmacia UCM, Madrid, 28040, Spain

Keywords: Pollen, Trend analysis, Synoptic meteorological patterns

Presenting author email: pedro.salvador@ciemat.es

Time series of airborne pollen concentration and meteorological parameters in the city of Madrid, central Spain, have been analyzed in the period 2001-2020 with the aim to elucidate two main questions: 1: What has been the temporal evolution of the concentrations of the main pollen types in this region in the last decades?; 2: Is synoptic meteorology a driving mechanism of airborne pollen dynamics in the central region of the Iberian Peninsula?

Time series of daily pollen concentrations (pollen counts per cubic metre of air -  $p/m^3$ ) of selected pollen types were produced by the aerobiological network of Madrid (PALINOCAM). Airborne daily samples were obtained from a Hirst sampler located in "Ciudad Universitaria" in the NW sector of the city and analysed using the standardized method (Thibaudon *et al.*, 2017). Eight pollen types (*Castanae*, *Cupressaceae*, *Olea*, *Platanus*, *Pinaceae*, *Fraxinus*, *Poaceae* and *Quercus*) were selected due to their abundance in Madrid air during different seasons of the year and their high allergenic effect in sensitive people as well. Trend estimates of the pollen concentration were undertaken, using the Theil-Sen method and the OpenAir data analysis tools (Carslaw and Ropkins, 2012). It also estimates the magnitude of the trend as a positive or negative slope, indicating the increase or decrease of the analysed magnitude in units per year. A robust classification of the 6 main synoptic meteorological patterns (SMP) that occurred during the period of study over the Iberian Peninsula has been used to interpret trends. The classification process of sea level pressure daily data fields used to generate these patterns, as well as the validation of this process, has been previously published (Salvador *et al.*, 2021).

Statistically significant positive trends were obtained for the whole period for *Cupressaceae*, *Platanus*, *Pinaceae* and *Quercus* (0.11, 0.02, 0.09 and 0.03 ( $p/m^3$ )/year, respectively). These pollen taxa registered the highest daily mean concentrations in 2001-2020 (51.5, 35.0, 28.7 and 9.9  $p/m^3$  for *Platanus*, *Cupressaceae*, *Quercus* and *Pinaceae*, respectively) with specific pollination periods. Thus, the highest mean levels of *Platanus*, *Quercus* and *Pinaceae* were registered in spring (205.8, 101.0 and 25.4  $p/m^3$ , respectively) and of *Cupressaceae* in winter (105.2  $p/m^3$ ). When trends were computed only for days when specific SMPs happened, statistically significant positive trends were obtained for *Cupressaceae* and *Platanus*, during SMP-1 (7.46 and 3.84 ( $p/m^3$ )/year, respectively) and for *Quercus* and *Pinaceae*, during

SMP-2 (0.18 and 0.19 ( $p/m^3$ )/year, respectively). In this case, a seasonal-trend decomposition procedure based on loess was applied to remove the seasonal cycle.

SMP-2 was characterized by the presence of the Azores high pressure system and by a low-surface pressure gradient at the synoptic scale. It was the most frequently produced meteorological situation (32% of the days), mainly in the summer and spring seasons and under high levels of surface temperature and solar irradiance and moderate levels of wind speed. This synoptic situation generates the most favorable meteorological conditions for pollination. On the contrary, SMP-1 represented a synoptic situation of high atmospheric stability, where the stationary high pressure system over the Iberian Peninsula caused a blockage of the entrance of air masses from marine or continental regions. It was produced only 4% of all days, mainly in the winter period, under high levels of surface pressure and low values of wind speed, temperature and solar irradiance in Madrid. In this case, the high associated concentrations of *Cupressaceae* and *Platanus* could be explained by the atmospheric stagnation conditions that favoured the accumulation of the emissions of air pollutants from road traffic in Madrid, such as  $NO_2$  and ultrafine particles (Salvador *et al.*, 2021).

Surface temperatures in Madrid have increased in the period 1948-2021 under SMP-1 and SMP-2 (increasing trends of 0.03 °C/year in "Retiro" meteorological station for both meteorological situations). The frequency of stagnation events under SMP-1 have also risen along this period (0.02 days/year). It points to an exacerbation of the impact of these SMPs on pollen concentrations in Madrid.

This work was supported by research project AtPollenFluo, grant PID2020-117873RB-I00 funded by MCIN/AEI/ 10.13039/501100011033.

Carslaw D.C. and Ropkins K. (2012). *Environ. Model. Softw.* 27-28, 52-61.

Salvador P., Barreiro M., Gómez-Moreno F.J., Alonso-Blanco E. and Artífano B. (2021) *Atmos. Environ.* 245, 118016.

Thibaudon M., Monnier S., Galán C., Bonini M., Röseler S. and Fernández González D. (2017). *Rev. Salud Ambient.* 17, 40-43.

## INHALED PARTICLE DOSIMETRY MODELLING IN KINDERGARTEN AND SCHOOL ROOMS: MPPD VERSUS EXDOM2

Isabella Charres<sup>1,2</sup>, Yago Cipoli<sup>1,2</sup>, Leonardo C. Furst<sup>1,2</sup>, Estela Vicente<sup>1</sup>, Ismael Casotti Rienda<sup>1</sup>, Mihalis Lazaridis<sup>3</sup>, Manuel Feliciano<sup>2</sup>, Celia Alves<sup>1</sup>

<sup>1</sup>Centre for Environmental and Marine Studies (CESAM), Department of Environment, University of Aveiro, Aveiro, 3810-193, Portugal

<sup>2</sup>Centro de Investigação de Montanha (CIMO), Instituto Politécnico de Bragança, Bragança, 5300-253, Portugal

<sup>3</sup>Department of Environmental Engineering, Technical University of Crete, Polytechnioulpolis, Chania, 73100, Greece

Keywords: Schoolchildren, Particulate Matter, MPPD, ExDoM2

Presenting author email: celia.alves@ua.pt

The school environment is fundamental to the health, learning and psychosocial development of students since children spend a considerable part of their time in educational environments. In Portugal, some studies have investigated potential sources of particulate matter (PM) in classrooms (Madureira *et al.*, 2016), the relationship between allergy symptoms and indoor air quality in schools (Szabados *et al.*, 2022), and inhaled doses of PM (Faria *et al.*, 2020). Despite this, there is still no information on the doses of size-segregated PM deposited in the various regions of the children's respiratory tract during the school period. Therefore, this study aimed to assess the hourly and seasonal variations of the total and regional deposition fractions and doses of PM. This research was carried out in a school near a chemical industrial complex in Portugal. The school is attended by children aged 3–12 years. Indoor particulate matter (PM<sub>10</sub>, PM<sub>2.5</sub>, PM<sub>1</sub>) was measured in two seasons in 3 classrooms of different buildings. Particle deposition in the respiratory tract of pupils in classrooms during the school day was calculated using two models: Multiple-Path Particle Dosimetry Model (MPPD) and Exposure Dose Model (ExDoM2). In general, a greater variability in PM<sub>2.5</sub> and PM<sub>1</sub> concentrations was observed in winter than in spring when classrooms were not occupied, while PM<sub>10</sub> concentrations varied more during school hours in both seasons. Regardless of the dosimetry model and season, the highest deposition of PM<sub>10</sub> and PM<sub>2.5</sub> was in the upper region of the respiratory tract while the lowest was in the tracheobronchial (TB) region. The highest doses of PM<sub>10</sub> and PM<sub>2.5</sub> during school hours were in the spring, ranging from 54.2 to 128 µg and from 83.9 to 186 µg with MPPD and ExDoM2, respectively, while PM<sub>2.5</sub> varied from 9.1 to 21.5 µg and from 12.3 to 17.3 µg, with MPPD and ExDoM2, respectively. Some differences between the models were observed (Fig.1). On the one hand the deposited dose of PM<sub>10</sub> during the school day was higher by up to 58% when calculated with ExDoM2, while the dose of PM<sub>1</sub> was higher by up to 69% when estimated with MPPD. On the other hand, regardless of the age, season and size of the PM, the fraction deposited in the TB and lung regions was always higher when calculated with MPPD, but the doses deposited did not follow this pattern, being in some cases higher when

estimated with ExDoM2. These results indicate that particle dose and deposition in spring may be more harmful to pupils' health than in winter.

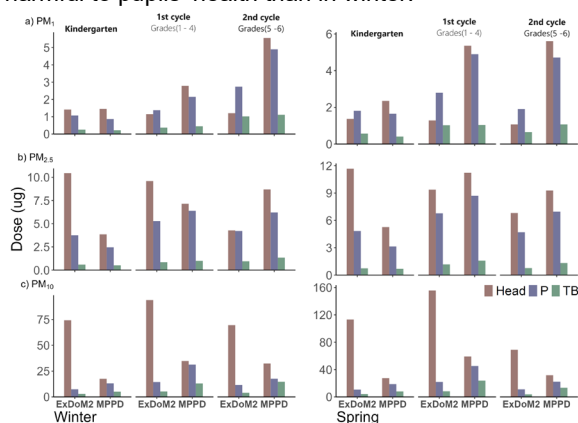


Fig. 1. Deposited dose of PM for each group during the school day in winter and spring. P: pulmonary; TB: tracheobronchial.

This work was supported by the LabEx-DRIIHM-OHM programme (CNRS – INEE, France). The financial support of the Portuguese Foundation for Science and Technology to CESAM (UIDP/50017/2020 + UIDB/50017/2020 + LA/P/0094/2020), through national funds, and to the PhD fellows I. Charres, Y. Cipoli and L. Furst (SFRH/BD/2022.12142, SFRH/BD/04992/2021 and SRFH/BD/08461/2020, respectively) is acknowledged.

Madureira, J., Slezakova, K., Silva, A. I. (2020) Assessment of indoor air exposure at residential homes: inhalation dose and lung deposition of PM<sub>10</sub>, PM<sub>2.5</sub> and ultrafine particles among newborn children and their mothers. *Science of The Total Environment*, 717, 137293.

Szabados, M., Kakucs, R., Páldy, A. (2022) Association of parent-reported health symptoms with indoor air quality in primary school buildings–The InAirQ study. *Building and Environment*, 221, 109339.

Faria, T., Martins, V., Correia, C. (2020) Children's exposure and dose assessment to particulate matter in Lisbon. *Building and Environment*, 171, 106666.

## STATISTICAL QUANTIFICATION OF PM10-BOUND POLYCYCLIC AROMATIC HYDROCARBONS IN AMBIENT AIR NEAR THE RIO TINTO MINE (SOUTHWEST SPAIN)

Erica Lorenzo<sup>1</sup>, Antonio Morato<sup>1</sup>, Carlos Boente<sup>2</sup> and Gonzalo Márquez<sup>1</sup>

<sup>1</sup>Department of Mining, Mechanical, Energetic and Civil Engineering, Universidad de Huelva, 21819 Huelva, Spain

<sup>2</sup>Laboratorio de Estratigrafía Biomolecular, E.T.S.I. Minas y Energía, Universidad Politécnica de Madrid, 28003 Madrid, Spain

Keywords: polycyclic aromatic hydrocarbons, PM10, OC/EC, K+, Río Tinto mine

Presenting author email: erica.lorenzo@dimme.uhu.es

We report the statistical results from a 4 month-long study of the organic compounds associated to PM10 samples collected near the Río Tinto mine (7 samples per month) in southwest Spain (Fig. 1). Sampling campaign was done from November 2020 to February 2021. Concentrations of particulate polycyclic aromatic hydrocarbons (PAHs) were measured using gas chromatography-mass spectrometry (GC-MS). The average abundances of PM10-bound benzo[a]pyrene (BaP) are 0.016 at La Dehesa monitoring station. Temporal variations are observed for concentrations of  $\Sigma$ PAHs. For PAHs, the highest concentrations averaging c.a. 0.466 are reported during January 2021, coinciding with the minimal temperatures in the Río Tinto district. According to a Principal Component Analysis (Table 1), PAHs are present in PM10 principally as result of motor vehicle exhausts (Guzmán et al. 2023). Potassium ion, a tracer for biomass burning, peaked in February 2021, during the high residential wood-burning season. In addition, multivariate analysis was used to assess the origin of organic components of PM10 samples. The two principal components are characterized by the grouping of heavy PAHs associated to vehicular traffic, and potassium ion indicating mining activity or biomass burning emissions, respectively.

In conclusion, the highest  $\Sigma$ PAH concentrations during the sampling period were recorded during winter, coincident with climate factors such as low rainfall, dry soils favouring resuspension and/or high photodegradation in the Río Tinto district (Boente et al., 2023). Diagnostic ratios and multivariate analysis suggest contributions from the road traffic emissions, shipping oil combustion and industrial estate, along with a definite influence of biomass burning.



Fig. 1. Panoramic view of the Río Tinto mine.

Table 1. Average aerosol mass concentrations.

PAH	PC1	PC2	PC3
Benzo(b)fluoranthene	<b>0.997</b>	0.060	-0.044
Benzo(k)fluoranthene	<b>0.989</b>	0.092	-0.113
Dibenz(a,h)anthracene	<b>0.988</b>	0.142	-0.068
Benzo(a)pyrene	<b>0.984</b>	0.054	0.171
Chrysene	<b>0.982</b>	0.064	0.178
Fluoranthene	<b>0.979</b>	-0.019	0.201
Indeno(123-cd)pyrene	<b>0.955</b>	-0.217	0.204
Pyrene	<b>0.894</b>	0.445	0.054
Benzo(ghi)perylene	<b>0.830</b>	0.385	-0.403
Phenanthrene	<b>0.810</b>	0.576	-0.110
Anthracene	<b>0.756</b>	0.502	0.421
Benzo(a)anthracene	<b>0.693</b>	0.666	-0.275
PM10	0.082	<b>-0.970</b>	0.227
K+	-0.116	<b>-0.912</b>	-0.394
OC	-0.101	0.233	<b>0.967</b>
EC	0.246	-0.304	<b>0.921</b>
Eigenvalues	10.7	2.9	2.4
% Variance explained	66.8	18.3	14.9
% Cumulative variance	66.8	85.1	100.0

Boente, C., Zafra-Pérez, A., Fernández-Caliani, J.C., Sánchez de la Campa, A., Sánchez-Roas, D., de la Rosa, J., (2023) Source apportionment of potentially toxic PM10 near a vast metallic ore mine and health risk assessment for residents exposed. *Atmos. Environ.* 301, 119696.

Guzmán, M.A., Fernández, A.J., Boente, C., Márquez, G., Sánchez de la Campa, A.M., Lorenzo, E., (2023). Study of PM2.5-bound polycyclic aromatic hydrocarbons and anhydro-sugars in ambient air near two Spanish oil refineries: Covid-19 effects. *Atm. Pollut. Res.* 14, 101694.

## PM<sub>10</sub>-BACTERIAL INFECTION INTERACTION IN A-549 CELLS: A ONE HEALTH PERSPECTIVE

P. Rodríguez-Rodríguez<sup>1</sup>, C. Alonso-Rodríguez<sup>1</sup>, B. Lorente-Torres<sup>2</sup>, M. Letek<sup>2</sup>, C. Gonçalves<sup>1</sup>, E. Vicente<sup>4</sup>, F.J. Pereira<sup>3</sup>, R. Fraile<sup>1</sup> and A.I. Calvo<sup>1</sup>

<sup>1</sup>Department of Physics, University of León, Campus de Vegazana, 24071, León, Spain;

<sup>2</sup>Department of Molecular Biology, University of León, Campus de Vegazana, 24071, León, Spain;

<sup>3</sup>Department of Chemistry, University of León, Campus de Vegazana, 24071, León, Spain;

<sup>4</sup>Department of Environment and Planning, Centre for Environmental and Marine Studies (CESAM), University of Aveiro, 3810-193, Aveiro, Portugal.

Keywords: antibiotic resistant bacteria, domestic coal combustion, *Staphylococcus aureus*, viability.

Presenting author email: aicalg@unileon.es

Despite efforts to promote decarbonization, there remains a heavy reliance on coal for domestic heating, especially in colder regions such as León (Castilla y León, Spain) (Vicente et al., 2021). Of the compounds derived from its combustion, there is growing concern about atmospheric particulate matter (PM<sub>10</sub>). *In vivo* and *in vitro* studies show that this exposure can lead to serious pulmonary and cardiovascular conditions (Inesta-Vaquera et al., 2023). However, the potential consequences with antibiotic-resistant bacteria are yet to be studied. In this context, the synergistic presence of PM<sub>10</sub> and *Staphylococcus aureus* (USA300), a facultative intracellular superbug that is the leading cause of death in more than 135 countries (Ikuta et al., 2022), represents an additional challenge.

Therefore, in this study, we start from the One Health approach, which recognises the interconnection between pollution and impacts on human and environmental health. The aim is to understand how tumour cells of basal alveolar epithelium (A-549) respond to two of the main environmental conditions to which humans are usually exposed: atmospheric pollution and bacterial infection.

PM<sub>10</sub> samples were collected on quartz filters using a high-volume sampler (CAV-A) located in a public building in the centre of León (Spain). This is an area with a high number of homes that use coal in their heating systems. The samples were extracted using a flow of dichloromethane followed by filtration with methanol, to be subsequently evaporated under a flow of nitrogen. The final extract was diluted in dimethyl sulfoxide (DMSO) at a concentration below 1% (v/v).

As for the cells, they were cultured in 96-well plates, each with 4x10<sup>4</sup> cells, and were maintained at 37 °C in a 5% CO<sub>2</sub> atmosphere in Dulbecco's Modified Eagle Medium (DMEM) supplemented with 10% (v/v) Fetal Bovine Serum (FBS) and 5% penicillin-streptomycin, until reaching 70-80% confluence. Subsequently, the effect on cell viability resulting from exposure to increasing concentrations of PM<sub>10</sub> samples from 0.05 to 200 µg/mL at 24 and 48 h was analysed.

Subsequently, the cells, previously contaminated, were infected for one hour from aliquots of USA300 prepared at an optical density of 0.8 and with a MOI (Multiplicity of Infection) of 5 bacteria per cell. Finally, the infection was stopped using a 1:10 ratio of vancomycin-

gentamicin in DMEM. The readings of this assay were performed at 24 h in a fluorescence reader (VICTOR Nivo™, PerkinElmer).

It is important to mention that the cell line used is transfected with m-Cherry, which allows direct analysis of the results over time without the need to add additional reagents. However, in order to establish a comparison, the same studies have been carried out using the MTT (3-[4,5-dimethylthiazol-2-yl]-2,5 diphenyl tetrazolium bromide) assay.

The preliminary results indicate an upward trend in cell viability as the concentration of PM<sub>10</sub> increases, referred exclusively to exposure to this particulate matter. This finding contrasts with what was obtained after the infection, where a slight decrease in viability is observed at the highest concentrations of the pollutant.

This study is part of the project TED2021-132292B-I00, funded by MCIN/AEI/10.13039/501100011033 and by the European Union "NextGenerationEU"/PRTR. Furthermore, it was partially supported by the Junta de Castilla y Leon co-financed with European FEDER funds (Grant LE025P20).

Ikuta, K. S., Swetschinski, L. R., Aguilar, G. R., Sharara, F., Mestrovic, T., Gray, A. P., Weaver, N. D., Wool, E. E., Han, C., Hayoon, A. G., Aali, A., Abate, S. M., Abbasi-Kangevari, M., Abbasi-Kangevari, Z., Abd-Elsalam, S., Abebe, G., Abedi, A., Abhari, A. P., Abidi, H., ... Naghavi, M. (2022). Global mortality associated with 33 bacterial pathogens in 2019: a systematic analysis for the Global Burden of Disease Study 2019. *The Lancet*, 400(10369), 2221–2248.

Inesta-Vaquera, F., Miyashita, L., Grigg, J., Henderson, C. J., & Wolf, C. R. (2023). Defining the *in vivo* mechanism of air pollutant toxicity using murine stress response biomarkers. *Science of the Total Environment*, 888, 164211.

Vicente, E. D., Figueiredo, D., Gonçalves, C., Lopes, I., Oliveira, H., Kováts, N., Pinheiro, T., & Alves, C. A. (2021). *In vitro* toxicity of indoor and outdoor PM<sub>10</sub> from residential wood combustion. *Science of the Total Environment*, 782, 146820.

## EXPOSURE ASSESSMENT OF 3D PRINTING OF PLA WITH GRAPHENE FILAMENTS UNDER EN-17058:2018

M. Domat<sup>1</sup>, C. Salcines<sup>2</sup>, L. Castañón<sup>3</sup>, E. Blanco<sup>3</sup>, J. Ruiz<sup>4</sup>, R. Valiente<sup>5</sup>

<sup>1</sup>Department of Physics, University of Oviedo, Oviedo, 33007, Spain.

<sup>2</sup>Health and Safety Unit. Infrastructure Service. University of Cantabria, Santander, 39005, Spain.

<sup>3</sup> GITECO Research Group, University of Cantabria, Santander, 39005, Spain.

<sup>4</sup> Prevention Area, FREMAP, Majadahonda, 28222, Spain

<sup>5</sup>Department of Applied Physics, University of Cantabria, Santander, 39005, Spain.

Keywords: Exposure assessment, Graphene, 3D print, Indoor Aerosols

Presenting author email: domatmaida@uniovi.es

The use of 3D printing raises concerns about potential risk of respiratory exposure, as fine particles released during the process may be inhaled. And is of particular concern when the filament has Nano-Objects and their Aggregates and Agglomerates (NOAA) embed to enhance their properties. Addressing safety measures is crucial to mitigate potential health risks.

In this research, it was studied the presence in of graphene oxide (GO) nanoparticles from 3D printing of a PLA filament additivated with GO. To assess exposure, a tiered approach as proposed by the EN 17058:2018 was followed.

In first place, an initial assessment (Tier 1) was conducted, gathering info about the potential release of NOAA. Since in this case, emission cannot be excluded, a basic assessment (Tier 2) was evaluated, in which some measurement campaigns took place. Different particle and gas monitoring instruments were placed in the near field, close to the breathing zone of the operator of the printer, and far field (Fig. 1), including particle counters, sample collectors, cascade impactor to apply characterization techniques like Raman spectroscopy and Scanning Electron Microscopy (SEM-EDX). Also, Volatile Organic Compounds (VOCs) were evaluated as short-term exposure, where an acceptable exposure assessment has been obtained based on the corresponding Exposure Indexes (INSST, 2022).

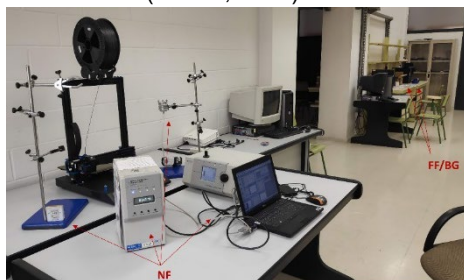


Fig. 1. Exposure scenario and location of instruments.

Despite of the decreasing and low particle concentrations in the breathing zone, having an average of around 2000 part/cm<sup>3</sup> (Fig. 2), offline analysis of samples detected carbon exclusively originated from the added graphene, comparing the samples before and after printing and including a graphene-free control.

Following the decision logic from the EN 17058:2018, statistical and the decision rule methods as shown in Klein et al (2011) were applied to interpret the online monitoring results and ensure that, despite the release of the GO from the sample, the exposure to the investigated NOAA was not significant and can be controlled by implementing risk management measures in place as an alternative to the Tier 3 assessment.

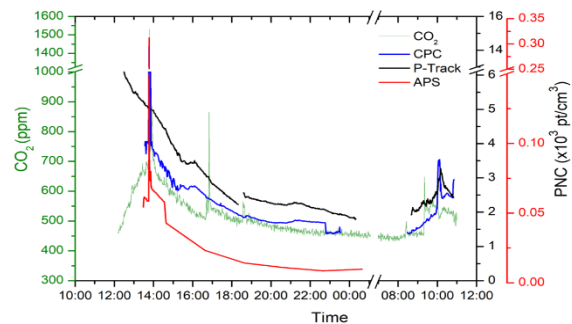


Fig. 2. CO<sub>2</sub> and Particle Number concentrations during 3D printing.

This work was supported by the Spanish Ministry of Science and Innovation and by the European Commission through three grants:

- “Fostering the circular economy and low CO2 technologies through the additive manufacturing - 3DCircle-” (Ref: PID2020-112851RA-I00).
- “Enhancing biodiversity in the Atlantic area through sustainable artificial reefs -EBASAR-” (Ref: TED2021-129532B-I00).
- “Artificial Reef 3D Printing for Atlantic Area - 3DPARE-” (Ref: EAPA\_174/2016).

EN 17058:20218 (2018), *Workplace exposure – Assessment of exposure by inhalation of nano-objects and their aggregates and agglomerates.*

INSST, Instituto Nacional de Seguridad y Salud en el Trabajo (2022), *Límites de Exposición Profesional para Agentes Químicos en España*, INSST, Spain.

Klein E., R. H., Fransman, W., & Brouwer, D. H. (2011). *How to statistically analyze nano exposure measurement results: Using an ARIMA time series approach.* J. Nanopart. Res. 2011, 13 (12) pp. 6991–7004.

## CHARACTERIZATION OF PERSONAL EXPOSURE TO PARTICULATE MATTER OXIDATIVE POTENTIAL IN THE SANTANDER BAY (NORTHERN SPAIN)

A. Expósito<sup>1</sup>, M. Santibáñez<sup>2</sup> and I. Fernández-Olmo<sup>1,\*</sup>

<sup>1</sup>Department of Chemical and Biomolecular Engineering, Universidad de Cantabria, Santander, 39005, Spain

<sup>2</sup>Global Health Research Group, Department of Nursing, Universidad de Cantabria, Santander, 39008, Spain

Keywords: particulate matter, oxidative potential, personal exposure,

\*Presenting author email: fernandi@unican.es

Exposure to particulate matter (PM) negatively affects human health. The PM toxicity mechanisms seem to be related to the ability of certain PM components to modify the balance between oxidants and antioxidants and to generate reactive oxygen species (ROS), triggering inflammatory responses in the organisms. A metric that can represent this toxicity mechanism has been developed in recent years, the so-called PM oxidative potential (PM OP). Although many OP studies have been recently published, most of these assess the PM OP exposure by stationary samplers. A better characterization of PM exposure may be made by personal samplers, which account for indoor/outdoor activities (Expósito et al., 2021). Personal sampling can be incorporated into epidemiological studies to assess the impact of PM OP exposure on health, mainly in vulnerable groups such as people having respiratory diseases.

With this aim, the ASTHMA-FENOP project was planned. Asthmatic (n=44) and control (n=37) subjects living in the Santander bay (northern Spain) were recruited to wear PM personal samplers (SKC PMI coarse) for 24 h and to determine systemic (interleukin 6 and 10) and respiratory (fractional exhaled nitric oxide (FENO)) inflammatory biomarkers. Santander bay was selected for this study because previous studies reported relatively high levels of some transition metals active in OP assays, such as Mn and Fe (Hernández-Pellón and Fernández-Olmo, 2019).

PM10-2.5 and PM2.5 filters were collected from each volunteer and delivered to the laboratory for freezing until OP analysis. Two OP assays were carried out, measuring the depletion of two antioxidants; dithiothreitol (DTT), and ascorbic acid (AA). The OP-DTT and OP-AA values were calculated from the slope of AA/DTT concentration vs time curves, and were expressed per m<sup>3</sup> of inhaled air (nmol/min/m<sup>3</sup>). In this work, only PM OP results are presented.

Overall, 81 volunteers participated in the study. The PM OP results are shown in Table 1 for both size fractions.

Table 1. PM OP of personal samples (nmol/min/m<sup>3</sup>): arithmetic mean of asthmatic/control subjects

OP-DTTv	OP-AAv	OP-DTTv	OP-AAv
PM10-2.5	PM10-2.5	PM2.5	PM2.5
0.21/0.13	0.80/0.17	0.33/0.17	0.99/0.34

The order of magnitude of personal OP values were similar to that found in a previous study, where two

stationary PM samplers were used, one near the main metal industrial emitter (a Mn alloy production plant) and the other one in an urban background site (University campus at Santander). However, although the former study showed higher OP values in the urban-industrial site respect to the urban site, the personal sampling campaign did not show site differences, as depicted in Figure 1.

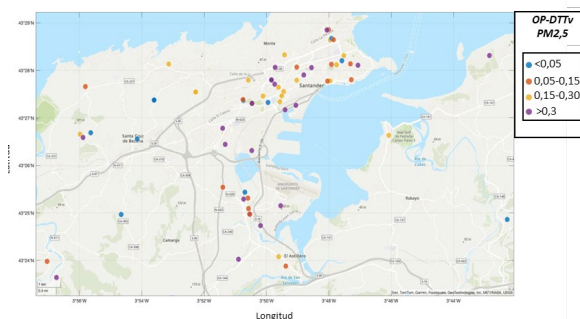


Fig. 1. Map of PM OP (nmol/min/m<sup>3</sup>) and residence of volunteers.

To conclude, personal exposure did not show a spatial pattern of PM OP, probably due to the contribution of indoor and occupational exposure to personal OP values, contrary to OP studies with stationary samplers, which only account for outdoor exposure.

This work was supported by the Spanish Ministry of Science and Innovation (Project PID2020-114787RB-I00, funded by MCIN/AEI/10.13039/501100011033 and “ERDF A way of making Europe”).

Hernández-Pellón, A., Fernández-Olmo, I. (2019). Using multi-site data to apportion PM-bound metal(loid)s: Impact of a manganese alloy plant in an urban area. *Science of the Total Environment*, 651, 1476–1488.

Expósito, A., Markiv, B., Ruiz-Azcona, L., Santibáñez, M., Fernández-Olmo, I. (2021). Personal inhalation exposure to manganese and other trace metals in an environmentally exposed population: Bioaccessibility in size-segregated particulate matter samples. *Atmospheric Pollution Research*, 12(8), 101123..

## THE IMPACT OF PM<sub>10</sub> COMPONENTS ON THE OXIDATIVE POTENTIAL AT A RURAL BACKGROUND SITE IN SOUTHEASTERN SPAIN

N. Gómez-Sánchez<sup>1</sup>, E. Yubero<sup>1</sup>, M. Alfosea-Simón<sup>1</sup>, J.F. Nicolás<sup>1</sup>, J. Crespo<sup>1</sup> and N. Galindo<sup>1</sup>

<sup>1</sup>Department of Applied Physics, Miguel Hernández University of Elche, Elche, Spain.

Keywords: oxidative potential, OP<sup>DTT</sup>, OP<sup>AA</sup>

Presenting author email: ngalindo@umh.es

Exposure to airborne particulate matter (PM) is strongly associated with various adverse health effects such as respiratory, cardiovascular and cerebrovascular diseases (Contini *et al.* 2021). The severity of these effects depends on the size and chemical composition of the particles. Most of the particulate mass consists of low toxicity components such as sulphate, ammonium nitrate, sodium chloride and mineral dust. However, low levels of transition metals and water-soluble organic compounds can have significant health effects, acting as strong oxidants capable of generating reactive oxygen species (ROS) (Borm *et al.* 2007). In this context, oxidative potential (OP) emerges as a more sensitive measure of PM toxicity than PM mass by itself, as it reflects the ability to oxidise target molecules (Lionetto *et al.* 2019).

In this study, a total of 38 PM<sub>10</sub> daily samples were collected in a small village in southeastern Spain (Benejama, Alicante), during late winter and early spring of 2023 (22 February – 4 April) using a high-volume sampler (30 l/min) onto quartz fibre filters. PM mass concentrations were determined gravimetrically. Samples were analysed for organic carbon (OC), elemental carbon (EC), water-soluble ions, water-soluble organic carbon (WSOC), trace metals and levoglucosan, a tracer of biomass burning. Finally, the OP assays used in this work were the acellular dithiothreitol (OP<sup>DTT</sup>) and ascorbic acid (OP<sup>AA</sup>) tests.

The mean values of PM<sub>10</sub>, OP<sup>AA</sup> and OP<sup>DTT</sup> during the study period were  $20.2 \pm 10.8 \mu\text{g}/\text{m}^3$ ,  $0.11 \pm 0.06 \text{ nmol}/\text{min}\cdot\text{m}^3$  and  $0.32 \pm 0.09 \text{ nmol}/\text{min}\cdot\text{m}^3$ , respectively. Low correlations of PM<sub>10</sub> with OP<sup>AA</sup> ( $r = 0.40$ ) and OP<sup>DTT</sup> ( $r = 0.20$ ) were found, which suggest that PM mass alone cannot adequately assess aerosol toxicity. Regarding the correlation between the two OP methods, we found a moderately good correlation ( $r = 0.66$ ), as shown in Figure 1.

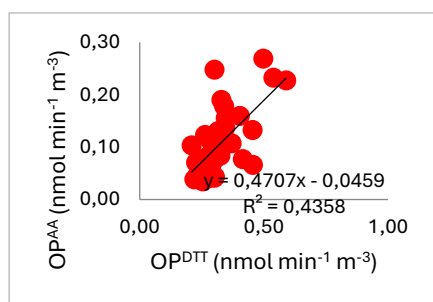


Figure 1. Correlation between OP<sup>AA</sup> and OP<sup>DTT</sup>.

In order to evaluate the sources for OP<sup>AA</sup> and OP<sup>DTT</sup>, a correlation analysis was conducted between both assays and the components of PM<sub>10</sub> (Table 1). A significant correlation was found between secondary species and both methods. Unexpectedly, both methods presented a strong correlation with EC concentrations, although the impact of traffic emissions in the study area was low, as evidenced by the low correlation with Cu. The OP<sup>DTT</sup> was also strongly correlated with WSOC, as shown in previous studies (Hakimzadeh *et al.* 2020). On the other hand, a statistically significant correlation between OP<sup>DTT</sup> and levoglucosan and K<sup>+</sup> was observed, which suggest that biomass burning is an important source for OP<sup>DTT</sup>.

Table 1. Pearson correlation coefficients among OP measurements and PM<sub>10</sub> organic components.

	OP <sup>AA</sup>	OP <sup>DTT</sup>
NO <sub>3</sub> <sup>-</sup>	0.69	0.59
SO <sub>4</sub> <sup>-</sup>	0.6	0.66
OC	0.33	0.43
EC	<b>0.75</b>	<b>0.74</b>
WSOC	0.58	<b>0.84</b>
Levo	0.27	0.59
K <sup>+</sup>	0.65	<b>0.81</b>
Cu	0.16	0.37

This work was supported by MCIN/AEI/10.13039/501100011033 and the “European Union NextGenerationEU/PRTR” (CAMBIO project, ref. TED2021-131336B397 I00) and by the Valencian Regional Government (Generalitat Valenciana, CIAICO/2021/280 research project).

Contini D, Lin YH, Hänninen O, Viana M. (2021) Contribution of aerosol sources to health impacts. *Atmosphere*. 12:730.

Lionetto MG, Guascito MR, Caricato R, Giordano MR, De Bartolomeo AR, Romano MP, Conte M, Dinioi A, Contini D. (2019) Correlation of oxidative potential with ecotoxicological and cytotoxicological potential of PM<sub>10</sub> at an urban background site in Italy. *Atmosphere*. 10:733.

Borm PJA, Kelly F, Kunzli N, Schins RPF, Donalson K. (2007) Oxidant generation by particulate matter: from biologically effective dose to a promising, novel metric. *Occup Environ Med*. 64:73–74.

Hakimzadeh M, Soleimanian E, Mousavi A, Borgini, A, De Marco C, Ruprecht A.A, Sioutas C (2020) The impact of biomass burning on the oxidative potential of PM<sub>2.5</sub> in the metropolitan area of Milan. *Atmos. Environ.*, 224, 117328.

## CHEMICAL PROFILES OF PM<sub>10</sub> IN INDOOR AND OUTDOOR AIR OF A CHARCOAL-GRILLED CHICKEN RESTAURANT

M. Evtyugina<sup>1</sup>, E.D. Vicente<sup>1</sup>, D. Figueiredo<sup>1</sup> and C. Alves<sup>1</sup>

<sup>1</sup>Department of Environment and Planning, CESAM, University of Aveiro, Aveiro, 3810-193, Portugal

Keywords: PM<sub>10</sub>, organic compounds, charcoal, grilled chicken

Presenting author email: celia.alves@ua.pt

Charcoal grilling is traditionally a popular option for domestic barbecues or restaurants due to the characteristic smoky flavour and smell of grilled food. However, it releases significant amounts of various air pollutants associated with adverse effects on human health and indoor/outdoor air quality (Mencarelli et al., 2023; Wu et al., 2015). Cooking aerosol is a significant component of indoor/outdoor particulate matter (PM). The amounts, chemical composition and toxicological properties of cooking-related PM emissions depend greatly on the cooking method and food ingredients. Considering the fact that charcoal-grilled chicken restaurants are widespread throughout the world, it is important to evaluate the resulting environmental and health impacts. Thus, the detailed characterisation of the chemical composition of the cooking-related aerosol is a fundamental requirement. Accordingly, the main goal of the present study was the chemical speciation of PM<sub>10</sub> in indoor and outdoor air of a charcoal-grilled chicken restaurant.

One-week sampling campaign was performed in a charcoal-grilled chicken restaurant located in Aveiro, Portugal. PM<sub>10</sub> samples were collected inside of the restaurant and outdoors using high-volume samplers. Background indoor/outdoor measurements were carried out when the restaurant was closed. Samples were primarily extracted with dichloromethane and methanol with subsequent separation of the dry extracts into five different organic fractions by flash chromatography, which were then analysed by gas chromatography–mass spectrometry (GC–MS). The fractions containing polar organic compounds were derivatised to trimethylsilyl ethers prior to GC-MS analysis.

A wide range of organic compounds, including acids, saccharides, plasticisers, alcohols, phenolics, among others, were found in the PM<sub>10</sub> extracts (Fig. 1). Extremely high indoor/outdoor (I/O) ratios for the average concentrations of alkanolic, hydroxy and carboxylic acids suggest strong indoor sources. Fatty acids are basic components of plant oils and meat fats and can be released during heating in unchanged form or undergo oxidative processes. Saccharides were also one of the dominant classes in PM<sub>10</sub>-bound organics. Levoglucosan/mannosan and levoglucosan/(mannosan + galactosan) ratios were  $13.8 \pm 3.8$  and  $11.3 \pm 3.5$  for indoors and  $9.9 \pm 1.4$  and  $7.0 \pm 1.3$  for outdoors, respectively. Total concentrations of non-alkylated polycyclic aromatic compounds (PAHs) were higher in the restaurant when compared to outdoors, revealing I/O ratios between 1.2

and 15.6. In conclusion, charcoal grilling was found to be a source of various PM<sub>10</sub>-bound organics, including hazardous species such as PAHs and phenolics, which can potentially affect indoor air quality and health.

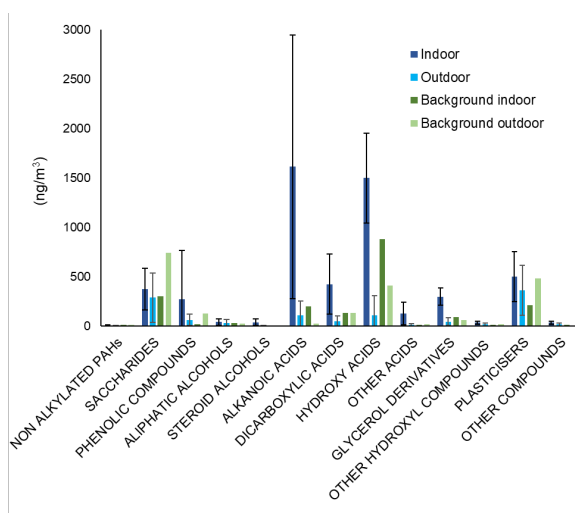


Fig. 1. Average concentrations (ng m<sup>-3</sup>) of different classes of PM<sub>10</sub>-bound organic compounds.

This work was supported by the project APAM – Air Pollution in an African Megacity: Source Apportionment and Health Implications (DOI: 10.54499/2022.04240.PTDC). The financial support to CESAM by FCT/MCTES (UIDP/50017/2020 + UIDB/50017/2020 + LA/P/0094/2020), is also acknowledged. The research contract under Scientific Employment Stimulus to E. D. Vicente (DOI: 10.54499/2022.00399.CEECIND/CP1720/CT0012) and the fellowship contract to D. Figueiredo (2020.06414.BD) were funded by FCT.

Mencarelli A., Greco R., Balzan S., Grigolato S., Cavalli R. Charcoal-based products combustion: Emission profiles, health exposure, and mitigation strategies. (2023) *Environ. Adv.* 13, 2666–7657.

Wu C.C., Bao L.J., Guo Y., Li S.M., Zeng E.Y., 2015. Barbecue fumes: an overlooked source of health hazards in outdoor settings? *Environ. Sci. Technol.* 49, 10607–10615.

## ASSESSMENT OF BLACK CARBON EXPOSURE AND SOURCE APPORTIONMENT IN SLEEPING ENVIRONMENTS OF LISBON DWELLINGS

C. Gamelas<sup>1,2\*</sup>, S. Mendez<sup>1</sup>, J. Lage<sup>1</sup>, S.M. Almeida<sup>1</sup>, N. Canha<sup>1</sup>

<sup>1</sup>Centro de Ciências e Tecnologias Nucleares (C<sub>2</sub>TN), Instituto Superior Técnico, Universidade de Lisboa, 2695-066 Bobadela, Portugal,

<sup>2</sup>Escola Superior de Tecnologia de Setúbal, Instituto Politécnico de Setúbal (IPS), 2914-508 Setúbal, Portugal

Keywords: particulate matter, Black Carbon, fossil fuel, biomass burning, indoor air, bedroom

Presenting author email: carla.gamelas@ctn.tecnico.ulisboa.pt

Black Carbon (BC) is emitted from the incomplete combustion of fossil fuels and biomass burning, its main sources being traffic, residential heating, industry, and forest fires. As BC absorbs light from the ultraviolet to the infrared spectrum, it has been recognized as the third most important climate-changing agent (Bond et al., 2013). Furthermore, exposure to PM<sub>2.5</sub> and BC has a detrimental impact on human health, with elevated morbidity and mortality, especially within high-risk groups, namely those with cardio-respiratory disease (WHO, 2012).

Given that individuals dedicate a significant portion of their lives to sleep, the characterization of sleeping microenvironments is of the utmost importance for an accurate evaluation of individuals' overall daily exposure to PM. Nevertheless, the characterization of indoor air during sleep encounters numerous challenges, namely the disruptive noise generated by the sampling equipment, and for these reasons, there is a limited characterization of this microenvironment (Canha et al., 2021).

The HypnosAir project aims to address this challenge by chemically characterizing PM<sub>2.5</sub> sampled (both indoor and outdoor) during the sleep period, in bedrooms of dwellings in the Lisbon metropolitan area. The sampling campaign took place in 2023/2024, during 4 consecutive weeknights, in 30 bedrooms occupied by one or two non-smoking adults.

In each setting, the gravimetric collection of PM<sub>2.5</sub> in Teflon filters was performed in parallel by SILENT Sequential Air Samplers (FAI Instruments, Italy) and medium volume Leckel sampler (MVS6, Sven Leckel, Germany), respectively in the indoor and outdoor.

Real-time BC concentrations were measured with a portable micro-aethalometer (microAeth® Model AE51, AethLabs, USA). The determination is based on the Beer-Lambert law, by measuring the changes of light absorption by the aerosol continuously collected on a Teflon-coated borosilicate glass fiber filter, at 880 nm. The obtained data was post-processed with the Optimised Noise-reduction Averaging (ONA) algorithm (Hagler et al., 2011).

BC concentrations were also determined using a Multi-wavelength Absorption Black Carbon Instrument (MABI, ANSTO). The light transmission is measured through unexposed ( $I_0$ ) and sampled ( $I$ ) Teflon filters, for seven wavelengths, and these values are used to determine the mass absorption coefficients ( $\epsilon$ ) and the BC concentrations at each wavelength, allowing the differentiation of the contributions from biomass burning (BC<sub>bb</sub>) and fossil fuel combustion (BC<sub>ff</sub>) (Manohar et al., 2021). The smoke indicator ( $B_{405-BC_{1050\text{ nm}}}$ ) is used for this purpose, since for BC<sub>ff</sub> the module of this indicator

is  $\leq 50\text{ ng.m}^{-3}$ , and when the indicator is  $>500\text{ ng.m}^{-3}$ , BC<sub>bb</sub> is present (Manohar et al., 2021).

This study presents:

- an overview of the BC concentrations assessed in the bedrooms (and outdoors), both by the filter-based method and real-time monitoring, and the correlation between both;
- the analysis of the temporal variability of PM and BC concentrations based on real-time monitoring;
- the correlation between BC and PM<sub>2.5</sub> mean concentrations;
- the assessment of the BC exposure during sleep (product of the BC concentration measured in the bedroom and the time spent in it) and potential inhaled dose;
- the BC source apportionment and the BC<sub>ff</sub> and BC<sub>bb</sub> contributions, in bedrooms and outdoors.

The results show that the impact on personal exposure can be significant, considering the time individuals spend in the sleeping environments. BC dominated by fossil fuel has been identified in the PM<sub>2.5</sub> sampled in most of the bedrooms and respective outdoors, probably because the locations of the dwellings in the Lisbon metropolitan area are generally exposed to traffic.

This work was supported by FCT through PTDC/CTAAMB/3263/2021, 2021.00088.CEECIND (N. Canha) and UIDB/04349/2020+UIDP/04349/2020. C. Gamelas acknowledges IPS for a RAADRI grant.

Bond T.C., et al. (2013) Bounding the role of black carbon in the climate system: a scientific assessment. *J. Geophys. Res.-Atmos.* 118, 5380.

Canha N., et al. (2021) How is indoor air quality during sleep? A review of field studies. *Atmosphere* 12(1), 110.

Hagler G.S.W., et al. (2011) Post-processing Method to Reduce Noise while Preserving High Time Resolution in Aethalometer Real-time Black Carbon Data. *Aerosol and Air Quality Research*, 11, 539.

Manohar et al. (2021) MABI - A multi-wavelength absorption black carbon instrument for the measurement of fine light absorbing carbon particles. *Atmos. Pollut. Res.*, 12(4), 133.

WHO (2012) *Health Effects of Black Carbon*, WHO Regional Office for Europe.

## ASSESSMENT OF FINE AEROSOL EXPOSURE IN SLEEPING ENVIRONMENTS OF LISBON DWELLINGS

S. Mendez<sup>1\*</sup>, C. Gamelas<sup>1,2</sup>, J. Lage<sup>1</sup>, S.M. Almeida<sup>1</sup>, N. Canha<sup>1</sup>

<sup>1</sup>Centro de Ciências e Tecnologias Nucleares (C2TN), Instituto Superior Técnico, Universidade de Lisboa, 2695-066 Bobadela, Portugal,

<sup>2</sup>Escola Superior de Tecnologia de Setúbal, Instituto Politécnico de Setúbal (IPS), 2914-508 Setúbal, Portugal

Keywords: particulate matter, indoor air, bedroom, sleep

Presenting author email: carla.gamelas@ctn.tecnico.ulisboa.pt

Given that individuals dedicate a significant portion of their lives to sleep, and its pivotal role in well-being, performance, and health, a growing scientific interest has surged in recent years in assessing air quality in sleep environments and its potential impact on sleep quality, a question that remains unanswered. Nevertheless, the characterization of indoor air during sleep encounters numerous challenges, namely the disruptive noise generated by the sampling equipment. Most studies concentrate on comfort factors (temperature and humidity) and carbon dioxide, and particulate matter assessment is usually carried out using real-time monitoring equipment which does not allow the PM chemical characterization. For these reasons, there is a limited characterization of this microenvironment (Canha et al., 2021), resulting in imprecise evaluations of individuals' overall daily exposure to PM.

The HypnosAir project ([www.hypnosair.com](http://www.hypnosair.com)) aims to address this challenge, by assessing air quality during sleep in bedrooms of 30 residences across the Lisbon metropolitan area (both indoor and outdoor), sampling and subsequently performing the chemical characterization of PM<sub>2.5</sub>, to apportion the contribution of emission sources.

The sampling campaign took place in 2023/2024, during 4 consecutive weeknights, in 30 bedrooms occupied by one or two non-smoking adults. In each setting, the gravimetric collection of PM<sub>2.5</sub> was performed in two filter materials (Teflon and quartz), by two SILENT Sequential Air Samplers (FAI Instruments, Italy) in the indoor. PM<sub>2.5</sub> was sampled concurrently in the outdoor, by two medium volume Leckel samplers (MVS6, Sven Leckel, Germany).

Continuous monitoring of size-segregated mass fraction concentrations (PM<sub>1</sub>, PM<sub>2.5</sub>, respirable, PM<sub>10</sub>, and total PM) was performed indoors with the photometric instrument DustTrak, DRX 8533 model (TSI, USA). Since the response of optical instruments varies for different types of aerosols, PM<sub>2.5</sub> and PM<sub>10</sub> measurements of DustTrak were rectified using correction factors obtained from an intercomparison study using this instrument and Leckel reference gravimetric equipment.

This study presents an overview of the PM levels, determined both by the gravimetric method and real-time monitoring (as well as the IAQ assessment) in the bedrooms. Real-time monitoring will allow the analysis of the temporal variability of PM (and IAQ parameters). Most bedrooms presented mean PM<sub>2.5</sub> concentrations during the sleeping period above the international World Health Organization guideline value of 5 µg.m<sup>-3</sup> (WHO, 2021), but the PM<sub>2.5</sub> means were below the limit value of 25 µg.m<sup>-3</sup> established by the Portuguese Ordinance no. 138-G/2021 (Figure 1). In a previous

study in 10 bedrooms in Lisbon, a mean PM<sub>2.5</sub> concentration of 15.3 ± 9.1 µg.m<sup>-3</sup> was found (Canha et al., 2020).

PM exposure (defined as the product of the PM concentration measured in the microenvironment and the time spent in it) and the potential inhaled dose were assessed for the bedrooms of the present study, indicating that despite the relatively low mean levels, their impact on personal exposure is not negligible, considering the time individuals spend in their bedrooms.

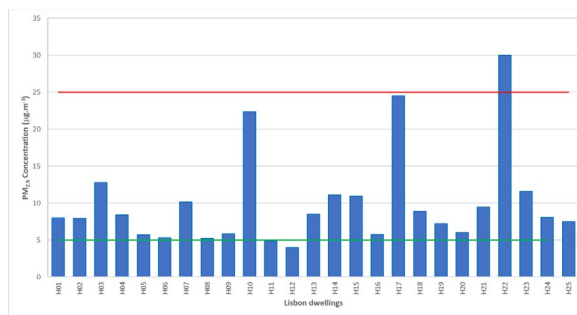


Fig. 1. PM<sub>2.5</sub> mean concentrations in bedrooms; red line – Limit Value established by the Portuguese legislation; green line – WHO guideline value.

This work was supported by the Portuguese Foundation for Science and Technology (FCT, Portugal) through the project HypnosAir (PTDC/CTAAMB/3263/2021), the contract 2021.00088.CEECIND (N. Canha), 2023.03202.BD (S. Mendez) and the financial support to C2TN/IST (UIDB/04349/2020+UIDP/04349/2020).

Canha N., Teixeira C., Figueira M., Correia C. (2021) How Is Indoor Air Quality during Sleep? A Review of Field Studies. *Atmosphere* 12(1), 110.

Canha N., Alves A.C., Marta C.S., Lage J., Belo J., Faria T., Cabo Verde S., Viegas C., Alves C., Almeida S.M. (2020) *Environmental Pollution* 264, 114619.

WHO (2021) *WHO global air quality guidelines: particulate matter (PM<sub>2.5</sub> and PM<sub>10</sub>), ozone, nitrogen dioxide, sulfur dioxide and carbon monoxide.*

## LEVELS OF PM-BOUND ORGANIC COMPOUNDS FROM RESIDENTIAL COAL COMBUSTION

E.D. Vicente<sup>1,2</sup>, A.I. Calvo<sup>2</sup>, M. Evtuygina<sup>1</sup>, A. Vicente<sup>1</sup>, R. Fraile<sup>2</sup> and C. Alves<sup>1</sup>

<sup>1</sup>Country Department of Environment and Planning, CESAM, University of Aveiro, Aveiro, 3810-193, Portugal

<sup>2</sup> Department of Physics, University of León, León, 24071, Spain

Keywords: coal, PM-bound organics, residential combustion

Presenting author email: aicalg@unileon.es

According to estimates, household air pollution from solid fuel combustion was responsible for 3.2 million deaths in 2020, due to health-damaging pollutants such as particulate matter (WHO, 2022). The majority of deaths associated with indoor air pollution, caused by the use of solid fuels, affect children under the age of five (resulting in low birth weight, acute lower respiratory tract infections, anemia, and premature mortality) and women (leading to chronic obstructive pulmonary disease and cardiovascular disorders) (Ali et al., 2021). Among the variety of solid fuels available, coal continues to be widely used for heating and cooking all over the world (Kerimray et al., 2017). Although emissions from indoor coal burning are a major public health concern in developing areas, little is known about indoor air quality in households equipped with coal burning appliances in higher income countries. To fill this gap in knowledge the present study aimed to evaluate the impact of residential coal combustion on indoor particulate organic composition. Indoor air quality was assessed in an empty rural house with a coal-burning stove. Four combustion experiments were performed, during which no other indoor activities occurred, ensuring unbiased data under real environmental conditions. Every day, the stove was ignited using wood chips and newspaper sheets, followed by the burning of six coal batches. Each experiment lasted approximately 6 hours and 40 minutes, with consistent refill intervals and coal amounts on different burn days. Additionally, two days of no burning were included for background measurements. The collection of PM<sub>10</sub> samples was performed with high-volume samplers positioned centrally in the open kitchen/living area and outdoors, on the front porch. These samples underwent extraction using dichloromethane/methanol, with subsequent injection of the dried extracts into a gas chromatograph-mass spectrometer (GC-MS). For the analysis of anhydrosugars and acid compounds, the extracts were silylated before injection. The study targeted twenty PAH compounds, revealing higher average PAH concentrations indoors during coal burning ( $33.4 \pm 20.9 \text{ ng m}^{-3}$ ) compared to outdoors ( $3.18 \text{ ng m}^{-3}$ ) and indoors without stove operation ( $4.07 \text{ ng m}^{-3}$ ). PAHs with higher molecular weights (more than four rings) constituted the largest portion (77-91%) of indoor PM<sub>10</sub> samples.

The PM<sub>10</sub> samples contained a diverse range of oxygenated organic compounds, including saccharides, phenolics, acids, alcohols, and glyceric

constituents. Levoglucosan showed significantly higher concentrations during coal burning days (averaging 8.4 times higher than background air). Several compounds like phenyl compounds, aromatic dicarboxylic acids, and fatty acids exhibited significantly lower concentrations or were absent in outdoor/background air but were prevalent during coal burning, suggesting emissions linked to coal combustion or stove materials. Even-numbered homologs dominated the series of n-alkanols and n-alkanoic acids, with high indoor concentrations during burning days compared to outdoors, indicating their association with coal combustion. Similarly, compounds such as dehydroabietic acid, glyceryl esters of long chain fatty acids, cholesterol, phthalimide, and oxidized Irgafos 168 were only present during combustion experiments. Some compounds' presence, like phthalimide and oxidized Irgafos 168, may suggest contamination from plastic packaging or coal interaction, warranting deeper research into their sources and impacts.

This work was partially supported by the Junta de Castilla y Leon co-financed with European FEDER funds (Grant LE025P20). It was also in part supported by the AEROHEALTH project (Ministry of Science and Innovation, co-financed with European FEDER funds, Grant PID2019-106164RBI00). Furthermore, it is part of the project TED2021-132292B-I00, funded by MCIN/AEI/10.13039/501100011033 and by the European Union "NextGenerationEU"/PRTR. The financial support to CESAM by FCT/MCTES (UIDP/50017/2020 + UIDB/50017/2020 + LA/P/0094/2020), through national funds, is also acknowledged. FCT is acknowledged for the research contract under Scientific Employment Stimulus to Estela D. Vicente (DOI: 10.54499/2022.00399.CEECIND/CP1720/CT0012).

Ali M.U., Yu Y., Yousaf B., Munir, M.A.M. Ullah S., Zheng C., Kuang X., Wong M.H. (2021) Health impacts of indoor air pollution from household solid fuel on children and women. *J. Hazard. Mater.* 416, 126127.

Kerimray A., Rojas-solórzano L., Amouei M., Hopke P.K., Gallachóir B.P.Ó. (2017) Coal use for residential heating: Patterns, health implications and lessons learned. *Energy Sustain. Dev.* 40, 19–30.

WHO, 2022. Fact Sheets: Household Air Pollution. <https://www.who.int/news-room/fact-sheets/detail/household-air-pollution-and-health>.



# RICTA

8<sup>th</sup> Iberian Meeting on  
Aerosol Science and Technology  
A Coruña · June 26<sup>th</sup>-28<sup>th</sup> 2024

## ORGANIZERS:



UNIVERSIDADE DA CORUÑA



## IN COOPERATION WITH:



Fundación  
UNIVERSIDADE DA CORUÑA



## SPONSORS (alphabetical order):

Aerospec

Cambustion



Grupo Álava



## COLLABORATORS (alphabetical order):



Concello da Coruña



Deputación  
DA CORUÑA



XUNTA  
DE GALICIA

Congress co-funded by the Vice-rectorate for Research and Transference of the University of A Coruña (UDC).

The Scientific and Organising committees would like to thank the HIGHER TECHNICAL UNIVERSITY COLLEGE OF MARITIME AND NAVAL MACHINES, UNIVERSITY OF A CORUÑA for providing its facilities for the meeting.